Spring 2016

Impact of Silo Storage Time and Specimen Fabrication Methods on Hot Mix Asphalt Mixtures

Christopher Daniel Jacques
University of New Hampshire, Durham

IMPACT OF SILO STORAGE TIME AND SPECIMEN FABRICATION METHODS ON HOT MIX ASPHALT MIXTURES

BY

CHRISTOPHER JACQUES

B.S. Civil Engineering, University of New Hampshire, 2014

THESIS

Submitted to the University of New Hampshire

in Partial Fulfillment of

the Requirements for the Degree of

Master of Science

in

Civil Engineering

May, 2016

This thesis has been examined and approved in partial fulfillment of the requirements for the degree of Master of Science in Civil Engineering by:

Thesis Director, Dr. Jo Sias Daniel, Professor of Civil and Environmental Engineering

Dr. Eshan Dave, Assistant Professor of Civil and Environmental Engineering

Dr. Ricardo Medina, Associate Professor of Civil and Environmental Engineering

On February 11, 2016

Original approval signatures are on file with the University of New Hampshire Graduate School.

ACKNOWLEDGEMENTS

This research was made possible through funding from the participating agencies in Transportation Pooled Fund 5(230) "Evaluation of Plant-Produced High-Percentage RAP Mixtures in the Northeast": FHWA, NH, MD, NJ, NY, PA, RI, and VA. Funding was also provided by NHDOT for the "Performance of High RAP Pavement Sections in New Hampshire" project.

I would also like to express my profound gratitude to the individuals who have personally provided guidance and encouragement throughout my undergraduate and graduate years at the University of New Hampshire. I would first like to sincerely thank my advisor Dr. Jo Sias Daniel for her continued support and guidance. Your mentorship over the past several years was very valuable and I am extremely grateful for your encouragement and patience as an advisor. Thank you also to Dr. Eshan Dave, who has always been available to provide support and valuable knowledge. You have acted as another advisor to me and I appreciate the guidance you provided.

Thank you very much to the past and present members of the asphalt research group at the University of New Hampshire: Dave Mensching, Mirkat Oshone, Reyhaneh Rahbar-Rastegar, Saman Salari, Mohamed Elshaer, Chris DeCarlo, Sonja Pape, Jayne Knott, Saeid Salehi, Katie Haslett, Bob Moore, Yuefeng Zhu, Rasool Nemati, and Ashton Congalton. Your friendship and generosity have made my time at UNH memorable. I enjoyed working with you all and wish you the best for the future. Thank you also to the undergraduate students I had the pleasure to teach the past two years. My time as a TA for the Engineering Materials class was perhaps the most enjoyable aspect of my academic career and I enjoyed getting to know all of you. Finally, thank you very much to Michelle Mancini and Kristen Parenteau in the Department of Civil and Environmental Engineering and Kelly Shaw in the CEPS Business Center.

TABLE OF CONTENTS

LIST OF FIGURES

LIST OF TABLES

LIST OF EQUATIONS

ABSTRACT

IMPACT OF SILO STORAGE TIME AND SPECIMEN FABRICATION METHODS ON HOT MIX ASPHALT MIXTURES

by

Christopher Jacques

University of New Hampshire, May 2016

Performance of asphalt as a pavement material depends on a variety of factors such as mixture properties, the mix design process, and the way in which the materials are produced and placed. There are also different methods and practices in hot mix asphalt construction, such as the way in which specimens are fabricated for laboratory testing and the time that hot mix asphalt is stored at plants following production. There is currently a lack of understanding within the asphalt industry on the potential performance impacts of these variations. This thesis involves two projects that explored variations in the production and placement aspects of hot mix asphalt construction.

One study that is included in this document aims to characterize the impact of silo storage time on asphalt mixtures. Many hot mix asphalt plants store material in heated silos before they are ready to be transported to construction sites. As the material is exposed to elevated temperatures, aging of the mixtures could increase susceptibility to cracking in the field. Through extensive binder and mixture testing, the results indicated that silo storage time has a significant impact on mixture performance, and RAP materials experienced a greater effect. Another study included in this thesis compares four different methods of producing specimens for laboratory testing: plant mixed, plant compacted; plant mixed, lab compacted; lab mixed, lab compacted; and small geometry specimens from field cores. Mixture testing showed that variations exist in stiffness characterization among the fabrication methods.

CHAPTER 1: INTRODUCTION

Civil engineers have an important societal duty to maintain the safety and satisfactory performance of transportation infrastructure. Given the large economic deficit in transportation infrastructure in the US, researchers must actively seek methods to reduce costs while maintaining or improving performance so that funds can be allocated elsewhere (e.g. rehabilitating damaged roads). It is also critical for researchers and practitioners to gain a better understanding of the properties of the material being placed in a pavement system. The focus of this thesis is to explore areas that can help better characterize the properties of what is actually being placed in the field. Performance of asphalt mixtures depends on a variety of factors such as properties of the materials, the mixture design process, and the way in which the materials are produced and placed. The production and placement aspects are of particular importance to the research in this thesis. One study that is included in this document, as part of *Transportation Pooled Fund 5(230): Evaluation of Plant Produced RAP Mixtures in the Northeast*, aims to characterize the impact of storing mixtures in silos following production at asphalt plants. Any potential variations on mixture performance caused by silo storage time are not currently considered because this parameter is not controlled at production plants. Another study included in this thesis, as part of *Performance of High RAP Pavement Sections in New Hampshire* funded by New Hampshire Department of Transportation (NHDOT), compares different methods of producing specimens for laboratory testing. Variations in fabrication methods can lead to inaccurate characterization of mixtures that are to be placed in a pavement structure. Both projects emphasize the need to better understand the properties of what is being placed in the field because current procedures contain variations that may not be considered for mixtures that are to be used in transportation infrastructure.

Following the production process at hot mix asphalt (HMA) plants, asphalt mixtures are often stored in steel silos before being loaded into trucks and transported to the construction site. The asphalt materials are stored at or near mixing temperatures to maintain sufficient workability and fluidity of the asphalt cement such that the material can be appropriately discharged from the silo. However, exposure to elevated temperatures has a potential to cause short-term aging in the binder due to volatilization as the lighter constituents of the binder evaporate, which causes the asphalt to become stiffer and more brittle. This embrittlement of the binder can have a significant effect on the pavement service life and performance, especially in terms of susceptibility to cracking in the field. As the material is exposed to elevated temperatures for longer periods of time in the silo, the short-term aging process that is experienced during typical production stages could potentially continue. Silo storage time is typically not a parameter that is strictly controlled, or even documented, at asphalt plants. It should be noted, though, that practitioners are wary of storing mixes for very long durations because of the threat of stalling production and potential changes to the binder properties. The time that a material stays in the silo can vary widely based on a number of variables such as construction region, weather, silo type and specifications, silo temperature, plant operation schedules, mixture size, mixture qualities, and construction and truck schedules. If there is indeed a significant impact on pavement performance, the wide variability in storage practices and lack of strict limits on silo storage time would be problematic in terms of accurately characterizing how mixtures would perform in the field.

Production parameters such as silo storage time and haul time, among others, are important to consider. Mix designers do not have control over these parameters, and the potential effects on mixture performance are not currently taken into account. The objective of this research is to gain a better understanding of the effect of silo storage time, a key production parameter, as it relates

to asphalt binder and mixture performance. Silo storage time is evaluated for virgin (no recycled materials) mixtures and reclaimed asphalt pavement (RAP) mixtures to measure the short-term aging effect and determine if blending/diffusion occurs in the silo with the RAP mixture. This interaction between aged RAP binder and the virgin binder at elevated temperatures must be considered, and a literature review on this subject is explored further in Section 1.3.2 Blending of RAP and Virgin Binders.

In addition to silo storage time, the way in which specimens are fabricated for laboratory testing is an important area of asphalt production that should be considered. Researchers and practitioners have always recognized that differences in the methods used to produce asphalt concrete specimens for laboratory testing can impact the measured material properties and performance. As agencies move towards performance-based design and using performance tests for acceptance, it is increasingly important to understand the impact of specimen preparation on the measured laboratory parameters. Material handling, mixing temperatures and equipment, and compaction methods vary with different specimen preparation methods and can all impact the measured material properties. Four of the most common methods used to prepare asphalt mixture test specimens were evaluated in this study:

1. **Plant mixed, plant compacted (PMPC):** the specimens are compacted in a laboratory at the plant immediately following production without reheating of the loose mixture.
2. **Plant mixed, laboratory compacted (PMLC):** the specimens are fabricated in the laboratory by reheating and compacting the loose mix produced at the plant.
3. **Laboratory mixed, laboratory compacted (LMLC):** the specimens are mixed and compacted in the laboratory using conditioning methods that are intended to simulate what happens in the plant and are generally used for mix design purposes.

4. **Field cores (FC):** the specimens are taken from the asphalt pavement and are the best representation of in-place mixture conditions but may be limited to use in tests that use certain geometries due to available lift thickness.

1.1 RESEARCH OBJECTIVES

The main objective of this thesis is to explore two particular areas that can help better characterize the properties of materials placed in the field. The objectives of each individual study are outlined below.

It should be noted that the primary focus of the silo storage study is to gain a better general understanding of the relation between production parameters, particularly silo storage time, and field performance. Recommendations on silo storage length and other quantitative determinations are not necessarily within the scope of this study. The main objectives of the silo storage study include the following:

1. Determine if silo storage time has a significant impact on the properties of virgin and RAP mixtures.
2. Determine if any changes from silo storage time are due to aging within the silo and/or blending between RAP and virgin binders.
3. Provide further understanding of the blending that occurs between RAP and virgin binder in plant-produced mixtures.

Four specimen fabrication methods were evaluated as part of the specimen fabrication methods study: small geometry specimens obtained from field cores, specimens compacted from loose mix sampled at the plant with and without reheating, and specimens fabricated from raw materials in the laboratory. The scope of this thesis focuses on the field cores, but comparison to

other fabrication methods is also explored. The objectives of this document in relation to the specimen fabrication methods study include the following:

1. Explore the use of small geometry specimens obtained from field cores as a method for laboratory testing.
2. Compare the asphalt mixture properties measured from the four different fabrication types.
3. Evaluate the impact of RAP content and virgin binder grade on the properties of the different mixtures.

1.2 OVERVIEW OF PROJECTS

The silo storage study is officially an Additional Task of the *Transportation Pooled Fund (TPF) 5(230): Evaluation of Plant Produced RAP Mixtures in the Northeast*. The lead agency for this project is NHDOT and the additional states participating in this study include: Maryland, New York, New Jersey, Pennsylvania, Rhode Island, and Virginia. The Federal Highway Agency (FHWA) has also contributed funds to this project. Phase I of the TPF 5(230) project began in 2010 to evaluate the impact of various mixture properties and production parameters on performance of RAP mixtures. A variety of information (e.g. discharge temperature, silo storage time, plant type) was gathered from three asphalt plants for 18 mixtures with differing RAP contents, PG grades, and compaction methods, among other variables. Analysis of the data from the 2010 testing seemed to indicate that there was an impact of silo storage time on the measured properties. Based on these findings, a controlled silo storage study was conducted as part of TPF 5(230) Phase II in 2011.

The controlled silo storage study in 2011 included a virgin and 25% RAP mixture with PG 64-22 binder that were produced, stored in a silo, and then sampled at various time increments up to 10 hours. Analysis of these mixtures showed that the RAP mixture experienced stiffening with

longer durations of storage time, but the virgin mixture showed unexpected trends. It was discovered that the virgin mixture had been contaminated during plant production. A polymer-modified PG 76-22 asphalt binder had been bled in by the plant operator at the beginning of production for the virgin mixture. Therefore, the results of the contaminated virgin mixture could not be compared to the RAP mixture. A replacement virgin mixture with similar properties was produced in December 2013. The results presented in this thesis detail the findings from the 2011 RAP mixture and the new virgin material. A paper from this research has also been submitted for publication in the 2016 Transportation Research Record, Journal of the Transportation Research Board. This paper is included in its entirety in Appendix C: "Effect of Silo Storage Time on the Characteristics of Virgin and RAP Asphalt Mixtures" by Jacques et al.

The project exploring specimen fabrication methods is part of *Performance of High RAP Pavement Sections in New Hampshire,* funded by NHDOT. The use of RAP in HMA is routine in New Hampshire. However, the amount of RAP has typically been limited to the 15-20% range due to a lack of experience with, and understanding of, mixtures containing higher amounts of RAP. For a variety of reasons, NHDOT and local contractors are interested in pursuing the use of higher percentages of RAP in state projects. Additional research and study is needed to establish the best practices and procedures necessary to produce high RAP mixtures that have equal or better performance than the mixtures currently used in New Hampshire. As part of this study, four different specimen fabrication methods were compared: laboratory mixed, laboratory compacted; plant mixed, plant compacted; plant mixed, laboratory compacted; and field cores.

1.3 LITERATURE REVIEW

1.3.1 High RAP Content

Hot mix asphalt (HMA) mixtures are comprised of coarse and fine aggregates, asphalt binder, possibly various modifiers or additives (such as polymers or rejuvenators), and recycled materials. Recycled materials have been used extensively in asphalt paving materials in recent years primarily due to the cost savings. Reclaimed asphalt pavement (RAP) and recycled asphalt shingles (RAS) are common recycled materials in HMA mixtures, and these recycled materials, particularly RAP, have economic and environmental benefits mainly due to the savings of replacing new materials such as binder and aggregate. However, RAP contains asphalt binder that has undergone aging in the field. Asphalt goes through an oxidative aging process over the long-term, which essentially changes its mechanical properties through stiffening and embrittlement of the asphalt, making it more prone to cracking. Many agencies have become comfortable using RAP percentages up to 15-20% RAP (by total mass) and observed satisfactory field performance. However, the amount of RAP has typically been limited to the 15-20% range due to a lack of experience with, and understanding of, mixtures containing higher amounts of RAP. The main difference between RAP mixtures and their virgin (i.e. mixtures with 0% RAP) counterparts is the increased stiffness from the aged material. Also, it has been shown that the stiffening effect from long-term oven aging on RAP mixtures is less than that of virgin mixtures, most likely due to the already-aged binder that stiffens at a slower rate (Daniel et al., 2013, Tarbox and Daniel, 2012). Due to the stiffened properties of RAP, there are concerns about low temperature and fatigue performance at the higher RAP contents.

It has been shown that the low temperature performance does change with increasing RAP content. In research utilizing up to 40% RAP, critical cracking temperatures were shown to get

warmer with more RAP perhaps due to a decreased ability of the binder to relax (Mensching et al., 2014, McDaniel et al., 2012). Sabouri et al. (2015) showed that using a soft base binder and maintaining the optimum asphalt binder content and/or increasing the asphalt layer thickness are effective strategies in producing a high RAP mixture that performs well and is economical. Diefenderfer and Nair (2007) found that mixtures containing up to 45% RAP can be successfully constructed if proper procedures are followed.

In recent years, agencies have shown an interest in using higher amounts of RAP, prompting several studies to explore the performance of plant- and lab-produced high RAP mixtures. Most studies conducted on plant- and lab-produced mixtures show that lab-produced specimens are stiffer than plant-produced specimens. Johnson et al. (2010) evaluated asphalt mixtures containing RAP and RAS and showed that the dynamic modulus of plant-produced specimens are lower than those of lab-produced mixtures. Mogawer et al. (2012) showed that reheating mixtures in the laboratory (PMLC) caused a significant increase in stiffness among RAP mixtures compared to those that were not reheated (PMPC). Results also showed that while lab compacted methods were stiffer than plant compacted, the plant compacted mixtures saw a larger increase in modulus with an increase in RAP content. Xiao et al. (2014) evaluated plant-foamed asphalt mixtures containing RAP and found that the measured rut depth of PMLC specimens were lower than PMPC specimens and that warmer failure temperatures were measured on the binders recovered from the plant produced materials. Various aging methods were also tested through beam fatigue tests by Islam and Tarefder (2014). In this study, loose mixture appeared to have more aging compared to the compacted samples.

1.3.2 Blending of RAP and Virgin Binders

At elevated temperatures in a silo, the interaction of virgin and RAP binders needs to be considered in addition to the potential short-term aging effect. Mixtures containing recycled materials include already-aged, stiffer, and more brittle RAP binder that is combined with the unaged virgin binder. In a silo at high temperatures, the aged binder that coats the RAP aggregates may become more fluid and blend with the virgin binder. Several recent studies have attempted to characterize the interaction that occurs between virgin and RAP binders, which is a complex process that some have hypothesized to be diffusion, mobilization, and/or mechanical processes. Many current research projects involve measuring the degree of blending or characterizing the interaction process that occurs. It is important to understand this blending/diffusion process in order to separate the effects of silo storage time on virgin and RAP binders.

The two major processes that occur in the virgin-RAP binder interaction are mixing, or contact between the binders, and blending/diffusion after contact (Kriz et al., 2014). In a study by Huang et al. (2005), it was concluded that mechanical blending affected only a small portion of the aged RAP binder. Instead of blending with the virgin asphalt, a composite layered system was formed when the aged asphalt in RAP coated the RAP aggregate particles. Another study by Zhao et al. (2015) attempted to characterize blending in mixtures with high amounts of RAP. It was concluded that the fatigue and cracking resistance of HMA containing >30% RAP was reduced not just because of the high stiffness of the already-aged RAP binder, but also due to its lower mobilization rate which potentially caused heterogeneous blending or an under-asphalted mixture.

The key mechanism in the RAP-virgin binder interaction is the diffusion process, according to Kriz et al. Whether the interaction can be characterized as diffusion or not has been recently debated, but it was clear in the research by Kriz et al. that there is some type of interaction occurring

between RAP and virgin binders. The research included dynamic shear rheometer (DSR) simulations to understand the diffusion process and degree of blending in thick and thin binder layers. It was concluded that the diffusion process is completed (100% blending) within minutes of mixing for thinner binder layers and only about 90% degree of blending completed after typical production stages for thicker binder layers. The degree of blending was analyzed using typical mixing, storage, transportation, and placement times. Figure 1 presents results from this study in which the ideal blend viscosity fraction is used as a measure of degree of blending. It is interesting to note that the assumed storage time was 60 minutes and the majority of blending in thick binder layers occurred during the storage stage. As the storage time continues past one hour, it is hypothesized that the diffusion or blending could continue between the binders and that this phenomenon may have an appreciable impact on mixture performance. The storage time could have an effect on the short-term aging of the overall mixture and/or an effect on the blending between RAP and virgin binders.

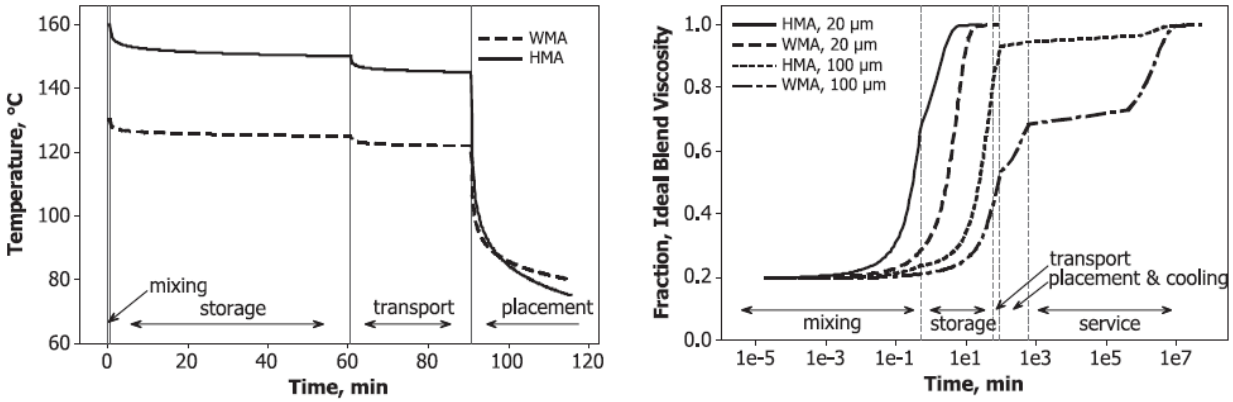

Figure 1: Time-Temperature Profile (Left) and Degree of Blending Simulation (Right) During Typical Production Stages
Source: Kriz et al. (2014)

Achieving good blending or diffusion between RAP and virgin binders is important because the rheological properties of the blended binders can then assume properties of a homogeneous blend (Kriz et al.). It is hypothesized in this thesis that RAP could undergo stiffening

at a greater rate with longer durations in the silo, even though the mixture contains already-aged RAP binder. As blending continues within the mixture, more of the RAP binder that was not previously accessible to the mixture may be blended with the virgin binder. The RAP mixture may potentially undergo aging as a result of the silo, but may also experience further stiffening, resulting from the composite system progressing towards a homogeneous blend as it takes on the properties of the RAP binder.

1.3.3 Small Specimen Geometry

The main objective of laboratory testing, whether compaction was done in the laboratory or at the plant, is to accurately characterize field performance. Field-compaction would be ideal because that is what actually occurs (i.e. it is not a simulation). Typical dynamic modulus testing is performed on 100 mm diameter by 150 mm tall specimens, which is larger than the thickness of most pavement layers. Therefore, mixtures must be fabricated and compacted with laboratory equipment, such as a gyratory compactor, to simulate field compaction. Recent research has been done to explore the feasibility of using smaller geometry specimens cored from field cores to assess stiffness and fatigue characteristics of in-place pavements. Using field cores to characterize mixtures would provide significant benefits because the real properties of the mixture can be captured rather than a laboratory or plant simulation that may not factor in a number of variables (e.g. mixture discharge temperature, silo storage time, field compaction method). Forensic analysis of in-place pavements could also be performed using field cores.

Li and Gibson (2013) proposed using small-scale specimens obtained from field cores to characterize the stiffness and fatigue characteristics. In this study, dynamic modulus and fatigue characterization testing was performed on small geometry specimens cored from gyratory-compacted materials and field cores. The small specimens were compared to their full-scale

counterparts to assess the feasibility and reliability of the small-scale geometry. A diameter of 38 mm was chosen for these specimens based on previous research from Kim et al. (2004) that showed that test specimens could be as thin as 38 mm when performing IDT testing. Final dimensions used for the small specimens were 38 mm in diameter by 110 mm, as the alternative 38 mm x 140 mm samples showed more variability due to the slenderness.

The main concern with the small geometry specimens is whether the specimens are large enough to be a representative sample of the asphalt mixture. However, Li and Gibson showed that the small scale approach is very promising, and the modulus and fatigue results of small-scale specimens can be quite similar to the full-size specimens. It was noticed that the stiffness of the small specimens were slightly softer at higher temperatures/ lower frequencies and occasionally stiffer than the full-size samples, but the difference in dynamic modulus was generally less than 20% between small- and full-size specimens. Diefenderfer et al. (2015) also showed that small-scale specimens can be used when full-scale specimens cannot be fabricated. In this study, it was shown that any of the four dimensions (38 x 135 mm, 38 x 110, 50 x 135, and 50 x 110) were suitable alternatives to the full-sized specimens for nominal maximum aggregate sizes of 9.5 and 12 mm. Using small-scale specimens would allow field-compacted characteristics of mixtures to be assessed, among other benefits.

CHAPTER 2: MATERIALS AND MIXTURES

2.1 MATERIALS FOR SILO STORAGE STUDY

2.1.1 Mixture Production

A virgin (0% RAP) and 25% RAP hot mix asphalt mixture was evaluated in this study at incremental silo storage times. The materials were produced at the King Road Materials facility of Callanan Industries in Schenectady, New York. The asphalt plant is a counter-flow drum plant, originally rated at 550 tons per hour. The RAP mixture was produced on November 7, 2011, and the virgin mixture was produced on December 5, 2013. Gyratory specimens were produced by sampling mixture discharged from the silo and compacting immediately at the plant's quality assurance/ quality control laboratory without reheating. Loose mix was also provided for potential reheating in the laboratory if extra material was needed. Tank binder was provided for the virgin mixture and used for RTFO-conditioning.

The virgin mixture used a PG 64-22 binder, 12.5 mm nominal maximum aggregate size (NMAS), and included material sampled from the silo after approximate storage lengths of 0 hours, 2.5 hours, 5 hours, and 7.5 hours. The RAP mixture included 25% RAP by total weight, used a PG 64-22 binder, 12.5 mm NMAS, and included material sampled at approximately 0 hours, 2.5 hours, 5 hours, 7.5 hours, and 10 hours. The RAP mixture achieved the silo storage times by sampling mix from the silo as it was being filled because it was an active paving job. The virgin mixture accomplished the storage times by sampling mix from the silo at the various increments. For the virgin and RAP mixture, the silo times are approximate, but the higher storage times are certainly greater than the lower storage times.

The aggregate gradation for the virgin mixture can be seen in Table 1 and this information is plotted in a 0.45 Power Chart in Figure 2. The sieve analysis was performed on aggregates extracted from the mix that was collected from the silo at various storage times. This information was not available for the RAP mixture.

Table 1: Aggregate Gradation for Virgin Silo Mixture

Sieve Size	% Passing					
	0 hours	2.5 hours	5 hours	7.5 hours	Target	Range
1"	100.0%	100.0%	100.0%	100.0%		
3/4"	100.0%	100.0%	100.0%	100.0%	100	100
1/2"	100.0%	100.0%	99.9%	99.9%	99	95-100
3/8"	94.9%	94.1%	93.4%	93.9%		
1/4"	83.4%	82.3%	82.5%	82.3%	85	78-92
#4	71.2%	68.9%	69.9%	68.6%		
1/8"	56.5%	55.0%	55.1%	54.0%	58	51-65
#8	43.9%	42.9%	42.8%	41.6%		
#16	25.5%	25.2%	24.6%	24.0%		
#20	20.6%	20.5%	19.8%	19.4%	23	16-30
#30	16.6%	16.5%	15.8%	15.5%		
#40	12.9%	12.7%	12.0%	11.7%	15	8-22
#50	9.8%	9.6%	8.9%	8.6%		
#80	7.0%	6.7%	6.2%	5.9%	6	2-10
#100	6.3%	6.0%	5.5%	5.2%		
#200	4.2%	4.0%	3.6%	3.4%	3	1-5

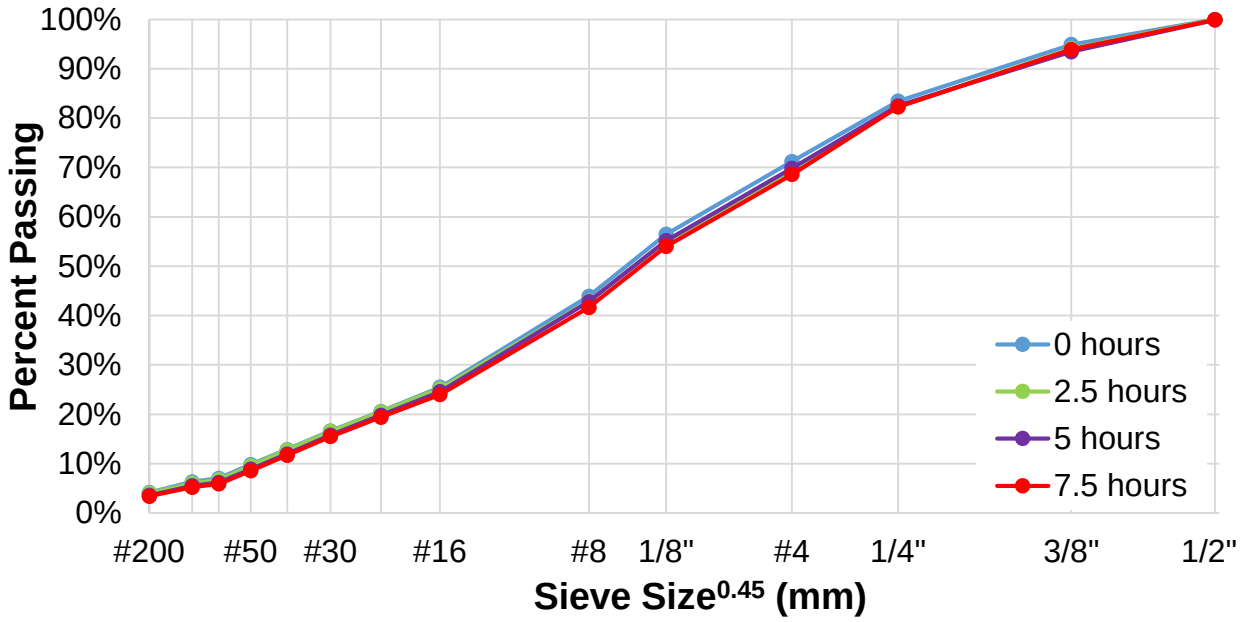

Figure 2: 0.45 Power Chart for Virgin Silo Mixture

Selected production and volumetric information is shown in Table 2 for the virgin and 25% RAP mixtures. Some properties of the RAP mixture were not available. The mixture discharge temperatures should be noted, as the temperatures are high for typical hot mix asphalt production. Production plants typically operate at around 300° F, but this can vary depending on the region and season. It is not unreasonable for plants to operate at higher temperatures near the end of the construction season in the northeast, especially if the material will be stored in a silo for extended periods of time during cold weather. Excessive temperatures may cause a higher degree of oxidation or volatilization in the binder during production. While the temperatures are notably high, they are consistently high, so any conclusions regarding silo storage time are not influenced by the high temperatures.

Table 2: Production and Volumetric Properties for Virgin and RAP Silo Mixtures

Production/ Volumetric Property	Virgin Mixture				25% RAP Mixture				
	0 hrs	2.5 hrs	5 hrs	7.5 hrs	0 hrs	2.5 hrs	5 hrs	7.5 hrs	10 hrs
Mixture Discharge Temperature	325° F	360° F	350° F	360° F	340° F	310° F	350° F	350° F	350° F
Target AC Content	5.4%	5.4%	5.4%	5.4%	5.4%	5.4%	5.4%	5.4%	5.4%
Final AC Content	5.8%	5.8%	5.9%	5.8%	-	-	-	-	-
Gyrations (N_{des})	75	75	75	75	75	75	75	75	75
Gmm	2.528	2.534	2.540	2.541	2.558	2.565	2.553	2.554	2.546
Gmb	2.400	2.379	2.378	2.361	2.468	2.460	2.482	2.462	2.469
VMA	15.27	15.99	16.04	16.63	-	-	-	-	-
VFA	66.76	61.81	60.04	57.49	-	-	-	-	-
Aggregate Gsb	2.679	2.679	2.679	2.679	-	-	-	-	-
Ps	94.6	94.6	94.6	94.6	-	-	-	-	-

Information that was not available is indicated with "-"

2.1.2 Typical Silo Storage Practices

A brief overview and background of general silo storage operations are provided in this section for the reader to better understand this process. It should be noted that the information and images in this section do not necessarily reflect the silo storage practices involved in this study. The specifications for the silos involved in this study were not readily available.

The manufacture of hot mix asphalt occurs at two different types of plants, batch and drum plants. The key difference between the two processes is that batch plants produce mixtures in batches while drum plants produce mix continuously. Drum plants are able to produce higher volumes of mix, alleviate maintenance costs, and use higher amounts of RAP product. Batch plants are able to produce a wide variety of mixes due to the batch-size manufacturing. Drum plants have a clear need to store materials because mix is being produced continuously and must be stored in order for operations to proceed. Many drum plants have several silos due to the need for storing different mixtures or loading multiple trucks simultaneously with the same mixture. Batch plants also typically have storage capabilities due to the benefits of increased production capacity.

Following production of mixtures at asphalt plants, HMA is passed through conveyor belts to the top of steel silos for storage. Material flows by gravity to the bottom of the silo, where most silo designs have a conical section to allow for sufficient mass flow. Material within the silo is discharged to trucks that enter under the silos when a gate below the conical section is opened. The mixtures may be immediately released to the vehicles for transport or held within the silo until the time for delivery to the project site is appropriate. Typical silos can hold up to 250 tons of material, and many drum plants have several silos depending on the plant capacity and variety of mixes being made. An example of silo storage at a drum plant can be seen in Figure 3. Shown in the image is a group of six storage silos, the conveying mechanism that deposits material into the

silo at the top, and the entrance for trucks beneath the silo. Figure 4 shows two examples of trucks collecting material that is discharged from beneath the silo. A common practice is for material to be loaded to the truck bed in three small batches to avoid aggregate segregation that would occur if the material was loaded in one large mass.

Figure 3: Example of Storage Silos

Figure 4: Example of Material Being Discharged from Silos to Trucks

It is very important for storage silos to maintain complete air tightness so that the HMA does not have access to oxygen. If the asphalt was exposed to oxygen, an oxidative aging process would occur, and this chemical reaction is amplified at elevated temperatures. Oxidation, among other causes for age hardening in asphalt, causes the mixture to become stiffer, more brittle, and more prone to cracking in the field. Short-term aging also occurs during the production stages, but this is taken into account when designing mixtures and producing laboratory samples. Any potential aging effects within a silo are not considered. It is assumed that silos are 100% air tight, but there is a possibility for structural deficiencies that could allow oxygen access to the mixtures.

Asphalt materials within the silo are stored at or near mixing temperatures to maintain sufficient workability of the asphalt cement. These elevated temperatures are achieved by keeping the silos heated or well-insulated. Maintaining temperature within the silo is dependent upon the design of the structure; some silos provide heat through ceramic tiles, others may have the cone section heated only, and many designs do not provide heat but keep the silo well-insulated so that the material stays at elevated temperatures and heat is not lost. Even if there is no access to oxygen, there still remains a concern for aging through volatilization because of the high temperatures. Volatilization is another cause for age hardening and occurs as the lighter constituents of the asphalt binder evaporate. Maintaining high temperatures of the mixture is important because the HMA is more fluid at higher temperatures and can be discharged successfully from the silos. Also, heat loss or repeated thermal changes affect the mixture characteristics and cause a thermal distribution of the mixture within the truck bed. While the importance of keeping mix at high temperatures is realized, it should also be noted that as materials are exposed to elevated temperatures for longer durations, volatilization or other aging effects may significantly alter the properties of the mixture. Silo storage time is a variable that is not closely controlled and any

changes due to the storage duration are not considered in the final product under current specifications.

2.1.3 Binder Specimen Preparation

Binder testing for the virgin and RAP mixtures in this study was performed by Rutgers University in New Jersey. This includes binder extraction and recovery, Rolling Thin Film Oven (RTFO) conditioning, and testing. The asphalt binder testing was conducted on two sets of liquid asphalt binders: 1) binders sampled from the storage tank at the asphalt binder plant and 2) binders extracted and recovered from mixtures. The binders were extracted and recovered in accordance with AASHTO T164: *Procedure for Asphalt Extraction and Recovery Process* and ASTM D5404, *Recovery of Asphalt from Solution from Solution Using the Rotatory Evaporator*, using tri-chlorethylene (TCE) as the extracting solvent. The rotary evaporator system at Rutgers University is shown in Figure 5. The recovered asphalt binder was treated as an RTFO-aged asphalt binder, assuming that the aging that occurred during specimen fabrication was equivalent to what occurs during RTFO aging. Binder extraction for the virgin mixture was from the outer gyratory cores following coring of the dynamic modulus samples, and binder extraction for the 25% RAP mixture was from gyratory samples compacted at the plant.

Figure 5: Rotary Evaporator System at Rutgers University for Asphalt Binder Recovery

All asphalt binders were performance graded (PG) in accordance with AASHTO M320: *Standard Specification for Performance-Graded Asphalt Binder*. RTFO conditioning was performed at various conditioning times, including 45, 85, 135, 170, and 300 minutes, on virgin PG 64-22 tank binder to compare plant production practices to laboratory methods. There was no available binder from the 25% RAP mixture for this analysis. PG grading, RTFO conditioning, and other binder analyses performed in the silo storage study are further detailed in Section 3.1 Binder Testing and Analysis.

2.1.4 Mixture Specimen Preparation

Mixture testing included dynamic modulus and cyclic fatigue using the simplified viscoelastic continuum damage (S-VECD) model developed by Underwood and Kim (2010). A viscoelastic pavement life evaluation model, the Layered Viscoelastic Critical Distresses (LVECD) software, was performed using data obtained from the dynamic modulus and S-VECD fatigue results. Low temperature cracking performance testing was also performed by the University of Massachusetts at Dartmouth using the Thermal Stress Restrained Specimen Test (TSRST). Those results are not within the scope of this thesis but are included in the paper "Effect of Silo Storage Time on the Characteristics of Virgin and RAP Asphalt Mixtures" by Jacques et al., which can be found in the Appendix.

Dynamic modulus tests were performed on gyratory samples compacted at the plant without reheating for both virgin and RAP mixtures. Gyratory samples obtained from the plant were 150 mm diameter by 180 mm height. Testing was also performed on loose mix samples that were compacted at the plant and reheated in the laboratory at compaction temperature for the RAP mixture only. The loose mix was then compacted with a gyratory compactor to dimensions of 150 mm diameter by 180 mm height.

Specimen preparation involved coring through the center of the gyratory samples and cutting material off the two ends so that the final specimen dimensions were 100 mm diameter by 150 mm height. Studs were then attached to the specimen with Devcon® 10240 five-minute steel epoxy using the gluing jig apparatus shown in Figure 6. This apparatus was used to ensure that the studs were attached with sufficient pressure, appropriately aligned, centered vertically, and precisely 70 mm apart (i.e. 70 mm gauge length). Three replicate specimens were tested for each silo storage time. Specimens were placed in a separate environmental conditioning chamber until appropriate temperatures were achieved within the specimen.

Figure 6: Gluing Jig Apparatus for Applying Studs

Cyclic fatigue testing was performed in uniaxial tension, in accordance with AASHTO TP107: *Determining the Damage Characteristic Curve of Asphalt Concrete from Direct Tension Cyclic Fatigue Tests*, on virgin mixtures obtained from gyratory samples compacted at the plant. Testing was not performed on the 25% RAP mixtures due to a lack of available specimens. The gyratory specimens (150 mm diameter by 180 mm tall) were cut and cored to dimensions of 100 mm diameter by 130 mm tall. Affixing of the studs for LVDT placement was then completed. The

ends of the specimen were also glued to end platens, which connect to fixtures in the AMPT, with approximately 120 g total of Devcon® 10110 steel epoxy. The gluing jig shown in Figure 7 was used to accurately align the end plates and ensure strong bonding between the specimen and end plates. The epoxy was allowed four hours to cure before the specimen was removed from the jig. Specimens were then placed in a separate environmental chamber until the appropriate test temperature was achieved.

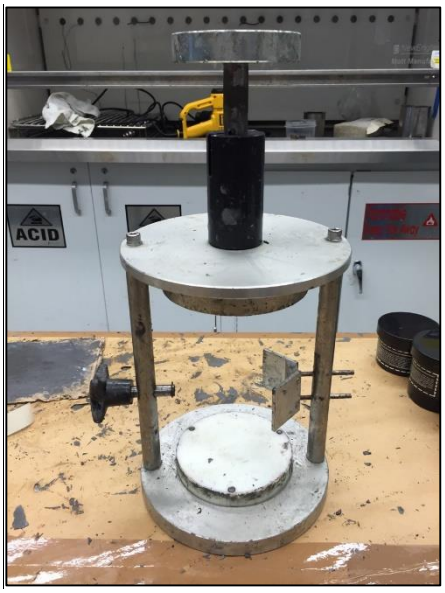

Figure 7: Fatigue Gluing Jig

Properties of each dynamic modulus and S-VECD fatigue replicate specimen were obtained for the gyratory and final cut specimen, including air void content and bulk specific gravity (G_{mb}); these values, along with the maximum theoretical specific gravity (G_{mm}) which was obtained at each sampling increment at the plant, are reported for the virgin mixture in Table 3 and Table 4. Bulk specific gravity was calculated using Equation 1 from measurements made in accordance with AASTHO T166: *Bulk Specific Gravity of Compacted Bituminous Mixtures Using Saturated Surface-Dry Specimens*. Air void content was calculated using Equation 2 given the individual weight measurements, which are tabulated in the Appendix. The average air void

content among various tests for both virgin and RAP mixture are summarized in Table 5. The air void content from mix design verification samples is also reported in this table.

Equation 1: Bulk Specific Gravity by AASHTO T166

$$G_{mb} = \frac{Dry\ Weight}{SSD\ Weight - Wet\ Weight}$$

Equation 2: Air Void Content by AASHTO T166

$$Air\ Voids\ (\%) = \left(1 - \frac{G_{mm}}{G_{mb}}\right) \times 100$$

Table 3: Properties of Dynamic Modulus Test Specimens for Virgin Silo Mixture

Silo Time	Replicate	Final Cut Specimen			Gyratory Specimen		
		Gmb	Gmm	Air Voids	Gmb	Gmm	Air Voids
0 hrs	1	2.343	2.528	7.3%	2.313	2.528	8.5%
0 hrs	2	2.355	2.528	6.8%	2.318	2.528	8.3%
0 hrs	3	2.330	2.528	7.8%	2.305	2.528	8.8%
2.5 hrs	1	2.353	2.534	7.2%	2.320	2.534	8.5%
2.5 hrs	2	2.365	2.534	6.7%	2.329	2.534	8.1%
2.5 hrs	3	2.352	2.534	7.2%	2.313	2.534	8.7%
5 hrs	1	2.354	2.540	7.3%	2.316	2.540	8.8%
5 hrs	2	2.350	2.540	7.5%	2.320	2.540	8.7%
5 hrs	3	2.352	2.540	7.4%	2.331	2.540	8.2%
7.5 hrs	1	2.360	2.541	7.1%	2.331	2.541	8.3%
7.5 hrs	2	2.357	2.541	7.2%	2.328	2.541	8.4%
7.5 hrs	3	2.361	2.541	7.1%	2.329	2.541	8.3%

Table 4: Properties of S-VECD Fatigue Test Specimens for Virgin Silo Mixture

Silo Time	Replicate	Final Cut Specimen			Gyratory Specimen		
		Gmb	Gmm	Air Voids	Gmb	Gmm	Air Voids
0 hrs	1	2.351	2.528	7.0%	2.316	2.528	8.4%
0 hrs	2	2.379	2.528	5.9%	2.331	2.528	7.8%
0 hrs	3	2.337	2.528	7.6%	2.299	2.528	9.1%
0 hrs	4	2.355	2.528	6.8%	2.321	2.528	8.2%
2.5 hrs	1	2.360	2.534	6.8%	2.322	2.534	8.4%
2.5 hrs	2	2.361	2.534	6.8%	2.320	2.534	8.5%
2.5 hrs	3	2.352	2.534	7.2%	2.320	2.534	8.4%
2.5 hrs	4	2.369	2.534	6.5%	2.323	2.534	8.3%
5 hrs	1	2.346	2.540	7.6%	2.318	2.540	8.8%
5 hrs	2	2.341	2.540	7.9%	2.302	2.540	9.4%
5 hrs	3	2.365	2.540	6.9%	2.331	2.540	8.2%
5 hrs	4	2.351	2.540	7.4%	2.308	2.540	9.1%
7.5 hrs	1	2.384	2.541	6.2%	2.337	2.541	8.0%
7.5 hrs	2	2.373	2.541	6.6%	2.330	2.541	8.3%
7.5 hrs	3	2.374	2.541	6.6%	2.333	2.541	8.2%
7.5 hrs	4	2.371	2.541	6.7%	2.330	2.541	8.3%

Table 5: Average Air Void Content of Virgin and RAP Silo Mixtures for Various Tests

Silo Storage Time	Mix Design Samples	Dynamic Modulus	S-VECD Fatigue
Virgin Mixture			
0 hours	5.1%	7.3%	6.8%
2.5 hours	6.1%	7.0%	6.8%
5 hours	6.4%	7.4%	7.5%
7.5 hours	7.1%	7.1%	6.5%
25% RAP Mixture			
0 hours	3.5%	6.6%	N/A
2.5 hours	4.1%	6.5%	N/A
5 hours	2.8%	6.0%	N/A
7.5 hours	3.6%	5.8%	N/A
10 hours	3.0%	5.5%	N/A

2.2 MATERIALS FOR SPECIMEN FABRICATION METHODS STUDY

2.2.1 Mixture Production

The mixtures were produced at an H&B batch plant with 250-300 tons per hour capacity owned by Pike Industries, Inc. and located in Northfield, New Hampshire. The mixtures had a nominal maximum aggregate size of 12.5 mm with an optimum asphalt content of 5.8%. Six different mixtures were produced using two different virgin binder grades and different RAP contents:

- Virgin PG 58-28
- 15% RAP with PG 58-28 binder
- 25% RAP with PG 58-28 binder
- 25% RAP with PG 52-34 binder
- 30% RAP with PG 52-34 binder
- 40% RAP with PG 52-34 binder

For each of the six mixture types, four different fabrication methods were used to prepare test specimens. Raw materials were collected to replicate the mix design and evaluate the properties of laboratory mixed, laboratory compacted (LMLC) specimens. Loose mix was sampled during production and specimens were compacted without reheating (plant mixed, plant compacted: PMPC) for testing. Loose mix was also collected and brought back to the laboratory and reheated to fabricate specimens (plant mixed, laboratory compacted: PMLC). Finally, field cores were taken from the six test sections that were constructed along I-93 southbound between Lincoln and Littleton, New Hampshire.

Test strip locations, constructed in June 2011, were placed between mile markers 95.1 to 101.1 along I-93 southbound. Approximate locations for the test sections are shown in Figure 8.

There were six total test sections (one for each mixture), each approximately one mile long. Field cores were extracted with a coring drill from each of the test sections, and the cores measured 140-150 mm in diameter and ranged from approximately 30-85 mm in thickness. Approximately ten field cores were obtained for each mixture, but several had significant damage from transport to the laboratory while others were too thin for extraction of test specimens. The field core specimens can be seen in Figure 9.

Figure 8: Field Core and Test Strip Locations Along I-93 Southbound
Source: Google Maps

Figure 9: Ten Field Cores from Each Test Section

The aggregate gradation for the mixtures can be seen in Table 6 and this information is plotted in a 0.45 Power Chart in Figure 10. The RAP used in the mixtures had a continuous PG grade of 82.3-19.7. Table 7 shows the mixture design volumetric information and the production volumetric information for each mixture. During production, the asphalt content for all mixtures was higher than the optimum, with the largest difference of 0.4% in the 30% and 40% RAP PG 52-34 mixtures.

Table 6: Aggregate Gradation for Mixtures in Specimen Fabrication Methods Study

Sieve Size	% Passing					
	Virgin PG 58-28	**15% RAP PG 58-28**	**25% RAP PG 58-28**	**25% RAP PG 52-34**	**30% RAP PG 52-34**	**40% RAP PG 52-34**
3/4"	100.0%	100.0%	100.0%	100.0%	100.0%	100.0%
1/2"	97.7%	97.6%	97.2%	97.4%	97.8%	97.2%
3/8"	85.3%	85.3%	86.1%	83.6%	88.1%	86.8%
#4	59.3%	57.3%	55.6%	52.9%	64.1%	61.4%
#8	44.3%	43.1%	40.7%	38.4%	48.9%	46.5%
#16	34.1%	33.6%	31.6%	30.3%	38.0%	35.9%
#30	25.7%	24.7%	23.4%	21.4%	26.4%	24.7%
#50	17.3%	16.1%	14.6%	12.7%	15.8%	13.1%
#100	8.7%	8.3%	7.7%	6.4%	8.3%	6.4%
#200	4.1%	4.3%	4.1%	3.1%	4.3%	3.9%

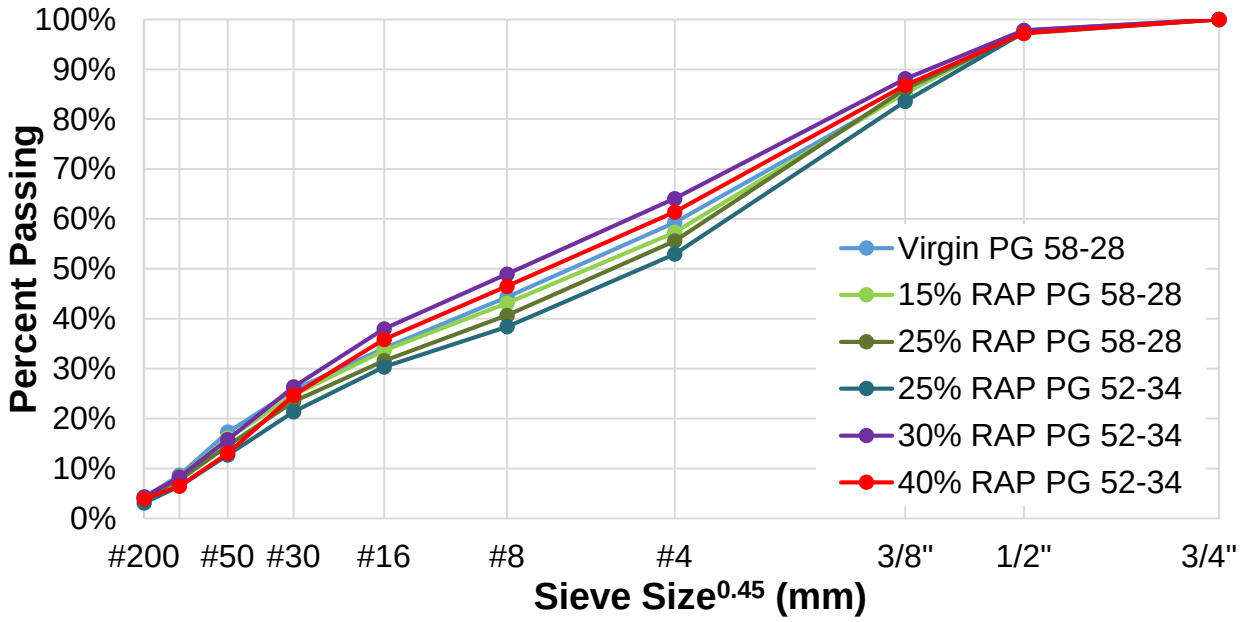

Figure 10: 0.45 Power Chart for Mixtures in Specimen Fabrication Methods Study

Table 7: Mixture Design and Production Volumetric Data for Mixtures in Specimen Fabrication Methods Study

Mixture Design						
Mix	**Virgin PG 58-28**	**15% RAP PG 58-28**	**25% RAP PG 58-28**	**25% RAP PG 52-34**	**30% RAP PG 52-34**	**40% RAP PG 52-34**
Mixture Discharge Temperature (° F)	295-305	295-305	295-305	280-290	280-290	280-290
AC Content	5.90	5.80	5.80	5.80	5.80	5.80
Gmm	2.494	2.479	2.479	2.467	2.469	2.471
Va	4.4	4.3	4.1	3.5	3.6	4.2
VMA	16.8	16.9	16.7	16.5	16.4	17.0
VFA	74.0	74.2	75.3	79.0	78.1	75.2
DP	0.9	0.8	0.8	0.8	0.8	0.8
% Gmm @ Nini	89.3	89.2	89.2	90.1	90.4	89.5
Gsa	2.756	N/A	N/A	N/A	N/A	N/A
Gse	2.739	2.715	2.715	2.703	2.706	2.708
Gsb	2.697	2.687	2.687	2.687	2.682	2.687
Production						
Mix	**Virgin PG 58-28**	**15% RAP PG 58-28**	**25% RAP PG 58-28**	**25% RAP PG 52-34**	**30% RAP PG 52-34**	**40% RAP PG 52-34**
Mixture Discharge Temperature (° F)	305	290	295	295	295	295
AC Content	5.96	6.11	5.98	5.91	6.23	6.19
Gmm	2.472	2.471	2.463	2.454	2.466	2.447
Va	3.5	2.5	2.2	2.5	3.7	3.4
VMA	16.9	15.6	15.2	15.8	16.4	16.7
VFA	79.5	84.2	85.9	84.1	77.7	79.7
DP	0.7	0.8	0.7	0.5	0.8	0.7
% Gmm @ Nini	90.2	91.1	91.4	91.1	90.3	90.7
Gsa	2.735	2.716	2.709	2.709	2.701	2.701
Gse	2.714	2.719	2.703	2.692	2.723	2.696
Gsb	2.701	2.680	2.672	2.673	2.664	2.664

2.2.2 Specimen Preparation for PMPC, PMLC, and LMLC Materials

Loose mix was sampled at the plant and then compacted immediately without reheating to produce the plant mixed, plant compacted (PMPC) specimens. The specimens measured 150 mm

in diameter and approximately 170 mm tall, with a target air void content of 7 ± 0.5%. Specimens were wrapped and placed in plastic bags to avoid oxidative aging before testing.

Plant mixed, laboratory compacted (PMLC) specimens were fabricated from loose mix that was sampled at the plant and stored in sealed metal 5-gallon buckets for reheating in the laboratory at a later time. To prepare specimens in the laboratory, the loose mix was reheated to 10° C below the discharge temperature, divided into the appropriate weights, and then heated to compaction temperature. Mixtures were not reheated for more than four hours and were not cooled and reheated. Specimens 150 mm in diameter and approximately 180 mm tall were compacted to a target air void content of 7 ± 0.5% using a Superpave gyratory compactor.

Specimens for four mixtures (Virgin PG 58-28, 25% RAP PG 58-28, 25% RAP PG 52-34, 40% RAP PG 52-34) were fabricated using raw materials (aggregate, RAP, and binder) to produce the laboratory mixed, laboratory compacted (LMLC) specimens. The materials were batched using the mixture design proportions, mixed at the recommended temperatures, and short-term oven-aged at 135° C for 4 hours before being compacted using a Superpave gyratory compactor. Specimens 150 mm in diameter and approximately 170 mm tall were compacted to a target air void content of 7 ± 0.5%.

It should be noted that the PMPC, PMLC, and LMLC specimens were fabricated and tested by other UNH researchers. Dynamic modulus and cyclic fatigue tests were performed on the mixtures involved in this study. LMLC specimens were only tested for four mixtures for dynamic modulus and zero mixtures for S-VECD fatigue, but all other fabrication types represent the results from all six mixtures. Following fabrication of the gyratory samples, specimen preparation involved the same process detailed in Section 2.1.4 Mixture Specimen Preparation. The process included coring and cutting the test specimens (100 mm diameter by 150 mm tall for dynamic

modulus and 130 mm tall for S-VECD fatigue) and then attaching studs for LVDT placement. Fatigue test preparation also included gluing end platens to the specimen, as previously detailed. Air void content for the LMLC, PMPC, and PMLC test specimens was 6 ± 0.5%.

2.2.3 Specimen Preparation for Field Cores

Field cores extracted from the test locations measured between 140 to 150 mm in diameter and 30 to 85 mm in thickness. These dimensions are clearly too small for fabrication of standard-size test specimens (100 mm diameter, 150 mm tall). Therefore, a small scale approach was used to evaluate specimens obtained from field cores. The small geometry specimen methodology has been explored in recent research by Li and Gibson (2013) and Diefenderfer et al. (2015), and the results were promising when comparing to full-size specimens. As discussed in Section 1.3.3 Small Specimen Geometry, Diefenderfer et al. concluded that the following small specimen geometries were suitable alternatives to standard size specimens for 9.5 and 12.5 mm NMAS mixtures: 38 x 110 mm, 38 x 135 mm, 50 x 110 mm, and 50 x 135 mm. Furthermore, it was concluded that the 50 x 110 mm and 50 x 135 mm geometries were suitable alternatives for mixtures with 19.0 and 25.0 mm NMAS. Li and Gibson also used 38 x 110 mm specimens with success for mixtures with NMAS less than 19.0 mm. Given the 12.5 mm NMAS of the mixtures in the specimen fabrication methods study, dimensions of 38 mm diameter by 110 mm tall were used to evaluate the small geometry specimens obtained from field cores.

Equipment was manufactured to accommodate fabrication of the small specimens at the University of New Hampshire laboratory. Coring was performed diametrically (i.e. horizontal to traffic loading) with a 38 mm inside-diameter core boring drill, and the field core was slightly offset from the center so that two 38 mm cores could be extracted from each field core. Due to the direction of coring, the loading orientation for testing was perpendicular to the direction of traffic

loading. However, it has been shown by Underwood et al. (2005) that the anisotropy caused by aggregate orientation is not significant for linear viscoelastic testing. Therefore, the horizontal coring method was appropriate for obtaining samples from the field cores.

To prepare the samples for coring, one of the faces was trimmed so that both ends had an even surface (one face was already flat from coring). Then, two parallel cuts were made approximately 5 mm from each side of the core. The field core was then installed into the coring jig, ensuring that the core was aligned beneath the boring drill and slightly offset from the center of the core. The parallel flat ends of the sample were flush with the coring jig walls to ensure that the core was secured when the drill began coring through the sample. Following successful coring of the first small specimen, the field core was then flipped and secured in the jig for the second small specimen to be extracted. Figure 11 shows the coring equipment used to prepare the small geometry specimens. In the images, the wet core drill setup, alignment of the field core in the jig, and process of coring two specimens is shown.

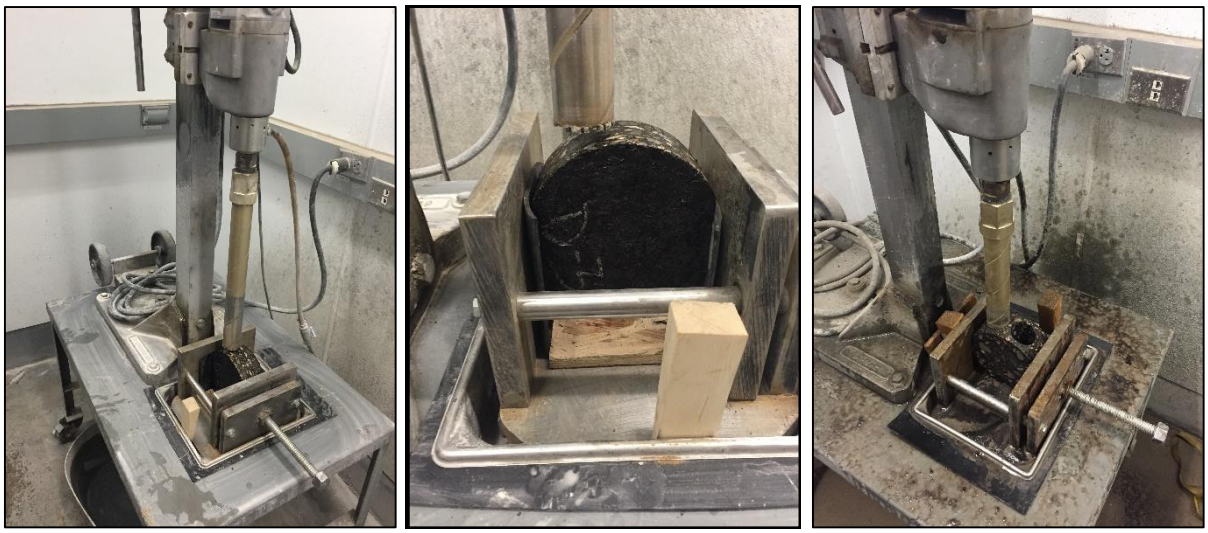

Figure 11: Coring Jig for Preparation of Small Specimens

The two ends of the specimen were then cut with a wet saw so that the final dimensions were 38 mm diameter by 110 ± 2 mm tall for both dynamic modulus and S-VECD fatigue testing.

Figure 12 shows the final specimen dimensions and the field core from which they were extracted. Also shown is a comparison to a standard-size dynamic modulus specimen with dimensions of 100 mm diameter by 150 mm tall.

Figure 12: Two Small Specimens Produced from Field Core (Left) and Comparison with Standard Size Geometry (Right)

Properties of each dynamic modulus and S-VECD fatigue replicate specimen were obtained in accordance with AASTHO T166, including G_{mb} using Equation 1 and air void content using Equation 2. The air void content of field cores and test specimens, height of the test specimens, G_{mb}, and G_{mm} are summarized in Table 8 and Table 9 for dynamic modulus and S-VECD fatigue specimens, respectively. In these tables, the following identifiers are used: A = Virgin PG 58-28; B = 15% RAP PG 58-28; C = 25% RAP PG 58-28; D = 25% RAP PG 52-34; E = 30% RAP PG 52-34; and F = 40% RAP PG 52-34. Air void content could not be controlled in the laboratory for these specimens because they were obtained from actual test sections. Variations in air void content could be caused by differences in production or compaction, differences in construction of the test sections, or heterogeneity within the test strip. Individual weight measurements for calculating G_{mb} and air voids are tabulated in the Appendix.

Table 8: Properties of Dynamic Modulus Specimens for Small Specimen Mixtures

Replicate	Field Core ID	Field Core		Test Specimen			
		Air Voids	Gmm	Gmb	Height (mm)	Air Voids	Average AV
A1	A6	5.8%	2.472	2.351	111.2	4.9%	5.4%
A2	A6	5.8%	2.472	2.333	108.9	5.6%	
A3	A3	6.8%	2.472	2.334	108.6	5.6%	
B1	B10	5.5%	2.471	2.341	110.6	5.3%	5.3%
B2	B10	5.5%	2.471	2.344	109.4	5.1%	
B3	B6	6.3%	2.471	2.333	110.0	5.6%	
C1	C6	5.9%	2.463	2.328	111.1	5.5%	5.9%
C2	C6	5.9%	2.463	2.325	110.5	5.6%	
C3	C10	7.1%	2.463	2.298	110.2	6.7%	
D1	D4	5.8%	2.454	2.312	111.9	5.8%	5.3%
D2	D4	5.8%	2.454	2.351	108.5	4.2%	
D3	D3	5.9%	2.454	2.309	108.6	5.9%	
E1	E6	6.9%	2.466	2.308	110.5	6.4%	6.2%
E2	E9	7.2%	2.466	2.321	110.7	5.9%	
E3	E6	6.9%	2.466	2.314	110.7	6.2%	
F1	F5	4.6%	2.447	2.345	111.3	4.2%	4.5%
F2	F5	4.6%	2.447	2.330	111.4	4.8%	
F3	F2	4.2%	2.447	2.335	109.4	4.6%	

Table 9: Properties of S-VECD Fatigue Specimens for Small Specimen Mixtures

Replicate	Field Core ID	Field Core		Test Specimen			
		Air Voids	Gmm	Gmb	Height (mm)	Air Voids	Average AV
A1	A1	4.8%	2.472	2.382	110.2	3.7%	4.0%
A2	A1	4.8%	2.472	2.368	110.6	4.2%	
A3	A5	5.3%	2.472	2.347	111.9	5.1%	
A4	A5	5.3%	2.472	2.394	110.6	3.2%	
B1	B4	5.0%	2.471	2.410	110.9	2.5%	4.3%
B2	B5	4.5%	2.471	2.384	110.4	3.5%	
B4	B9	6.6%	2.471	2.340	111.2	5.3%	
B5	B9	6.6%	2.471	2.330	109.3	5.7%	
C1	C1	3.6%	2.463	2.386	110.5	3.1%	4.2%
C2	C1	3.6%	2.463	2.374	111.0	3.6%	
C3	C8	5.9%	2.463	2.332	110.6	5.3%	
C4	C8	5.9%	2.463	2.350	111.0	4.6%	
D1	D6	5.0%	2.454	2.355	110.5	4.0%	5.3%
D2	D1	6.4%	2.454	2.286	112.0	6.8%	
D3	D6	5.0%	2.454	2.355	110.5	4.1%	
D4	D2	6.7%	2.454	2.296	110.9	6.4%	
E1	E2	7.7%	2.466	2.275	111.0	7.8%	6.6%
E2	E2	7.7%	2.466	2.310	112.2	6.3%	
E3	E6	6.9%	2.466	2.308	110.5	6.4%	
E4	E9	7.2%	2.466	2.321	110.7	5.9%	
F1	F1	5.4%	2.447	2.326	110.1	5.0%	4.5%
F2	F1	5.4%	2.447	2.319	109.2	5.2%	
F3	F4	4.2%	2.447	2.355	111.2	3.8%	
F4	F4	4.2%	2.447	2.353	111.1	3.9%	

Studs were then attached to the specimen with steel epoxy, as previously detailed. Extension arms were connected to the gluing jig apparatus to accommodate the smaller diameter samples, and a raised plate was used to ensure centering of the studs (with 70 mm gauge length) for the smaller height. The modified gluing apparatus for small specimens is shown in Figure 13. Platens for fatigue testing were also designed and manufactured for the small specimen setup. The setup includes steel platens (shown in middle left of Figure 14) that magnetize to the gluing jig

and have cutouts to lessen the load placed on the small specimen. Approximately 8 g total of Devcon® 10110 epoxy was used to attach the specimen to the smaller "standoff" pieces (shown in top left of Figure 14), made of aluminum, which are screwed into the end platens. The epoxy was allowed four hours to cure before the specimen was removed from the jig. End platens were then removed and specimens were placed in an environmental chamber until the appropriate test temperature was achieved. Either spring-loaded or loose core LVDTs were instrumented to measure deformations on the specimen during testing. Three replicate specimens for dynamic modulus and three or four specimens for fatigue were tested for each mixture. The standoff pieces were attached to the aluminum fixture shown in the bottom left of Figure 14 for fatigue testing in the AMPT.

Figure 13: Gluing Jig Apparatus for Applying Studs to Small Specimens

Figure 14: Machined Parts and Gluing Jig for Small Specimen S-VECD Fatigue Testing

CHAPTER 3: TEST DESCRIPTIONS

3.1 BINDER TESTING AND ANALYSIS

Binder testing and analysis was performed on the virgin and RAP mixture involved in the silo storage study. It should be noted that all binder extraction/recovery and testing was performed by Rutgers University. Binder testing for the specimen fabrication methods study was not within the scope of this thesis.

Following extraction and recovery of the asphalt binders, testing was performed using Dynamic Shear Rheometer (DSR) and Bending Beam Rheometer (BBR) testing devices. The DSR is a device that applies a shear stress to an asphalt binder sample at various temperatures and frequencies to determine the rheological properties. An asphalt binder sample is placed between a base plate and an oscillating top plate, which applies the shear stress. DSR testing follows the specifications of AASHTO T315: *Determining the Rheological Properties of Asphalt Binder Using a Dynamic Shear Rheometer (DSR)*. In this study, the 4 mm geometry configuration, shown in Figure 15, was used to measure the shear modulus (G*) and phase angle (δ) of the extracted/recovered asphalt binders. The advantage of using the 4 mm geometry is that a much smaller amount of material is required for testing over the range of required temperatures. Typically, data from the BBR is necessary to provide the low temperature mechanical information needed to construct the master curve; however, the 4 mm geometry eliminates this need.

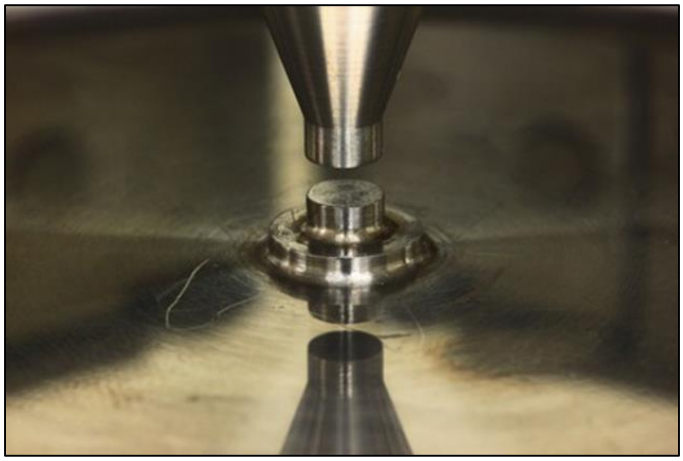

Figure 15: 4 mm Geometry for DSR

The BBR device is used to assess flexural creep stiffness and low temperature performance in terms of the binder's stiffness and relaxation capabilities. The test involves a simply supported beam of asphalt binder that is loaded in the center. BBR testing follows the specifications of AASHTO T313: *Determining the Flexural Creep Stiffness of Asphalt Binder Using the Bending Beam Rheometer (BBR)*.

In addition to the testing on extracted and recovered binders, virgin tank binder was conditioned in a Rolling Thin Film Oven (RTFO) and then subjected to DSR and BBR testing. The RTFO is a device that simulates the short-term aging of asphalt binders that occurs during plant production. Asphalt binder samples are placed in glass jars inside a rotating carriage and subjected to elevated temperatures. Current laboratory conditioning methods that simulate short-term aging specify that the asphalt material is heated for 85 minutes at 325° F, according to AASHTO T240: *Effect of Heat and Air on a Moving Film of Asphalt (Rolling Thin-Film Oven Test)*. The virgin PG 64-22 tank binder was conditioned in the RTFO at conditioning times of 45, 85, 135, 170, and 300 minutes at 325° F to assess how well the RTFO conditioning simulated the plant production short-term aging associated with the virgin mixture in this study.

3.1.1 Performance Grading

The Superpave performance-based asphalt specification system uses the concept of performance grading to classify asphalt binders based on the conditions in which they will be servicing. The performance grade (PG) uses a high and low temperature designation to characterize the asphalt binder. The high temperature is the average seven-day maximum pavement temperature (° C) at 50% statistical reliability and the low temperature is the minimum pavement temperature (° C) at 50% statistical reliability. For example, a common PG grade for New Hampshire is PG 64-22. The performance grading system classifies both the high and low grades in 6° increments. PG grading involves testing on unaged, RTFO-aged, and PAV-aged (Pressure Aging Vessel) binders with the DSR at high and intermediate temperatures and with the BBR at low temperatures. The relevant specification for PG grading is AASHTO M320.

The recovered binders used in this study were each tested for the high temperature PG grade, and were treated as RTFO-aged binders. RTFO-conditioned virgin tank binder was also evaluated. The high temperature PG grade is determined by the values of $G^*/\sin\delta$ from DSR testing, where lower values correspond to higher PG grades. Continuous grading is used to find the temperature, regardless of the 6° increments, in which the $G^*/\sin\delta$ value is equal to the minimum value of 2.20 kPa. Shear modulus, G^*, indicates the binder's stiffness or ability to resist shear stress. Phase angle, δ, represents the time lag between the shear stress and binder response. A larger phase angle indicates a more viscous (as opposed to elastic) response in the asphalt binder. Higher PG grades indicate aging of the binder due to the increase in stiffness that occurs from oxidative aging or other age hardening processes. This is evident by a higher shear modulus, which indicates an increase in stiffness capabilities, and/or a lower phase angle, which indicates more elastic behavior of the binder.

Intermediate and low temperature PG grades were also evaluated for the binders in this study. The intermediate temperature continuous grade corresponds to the temperature at which the value of G* sin δ from DSR testing is equal to the maximum of 5000 kPa. Higher intermediate PG grades are correlated to more elastic behavior in the binder, indicating short-term aging. The low temperature PG grade is obtained from BBR testing, and corresponds to the controlling critical low temperature at which the log of creep stiffness (S) has a maximum of 300 MPa or the m-value has a minimum of 0.300. Warmer low temperature grades are indicative of short-term aging.

3.1.2 Stiffness, m-Value, and ΔT_{cr}

As previously described, the BBR device is a flexural creep stiffness test that applies a load on a simply supported beam of asphalt binder. Typical test results from BBR testing are shown in Figure 16. The two important values from this test are log creep stiffness, S, and slope, m-value. Stiffness represents the binder's ability to resist stress. Greater stiffness indicates short-term aging due to the oxidative process of age-hardening that occurs in asphalt binders. The slope of the curve, or m-value, represents the binder's relaxation capabilities. A steeper slope (higher m-value) shows that the binder has a lower ability to resist cracking at low temperatures. The temperature at which S is equal to 300 MPa at a loading time of 60 seconds is the critical low temperature grade from BBR stiffness, $T_{cr\ (Stiffness)}$. The temperature at which the slope, or m-value, of the creep stiffness curve is equal to 0.300 at a loading time of 60 seconds is the critical low temperature grade from BBR m-value, $T_{cr\ (m\text{-}value)}$.

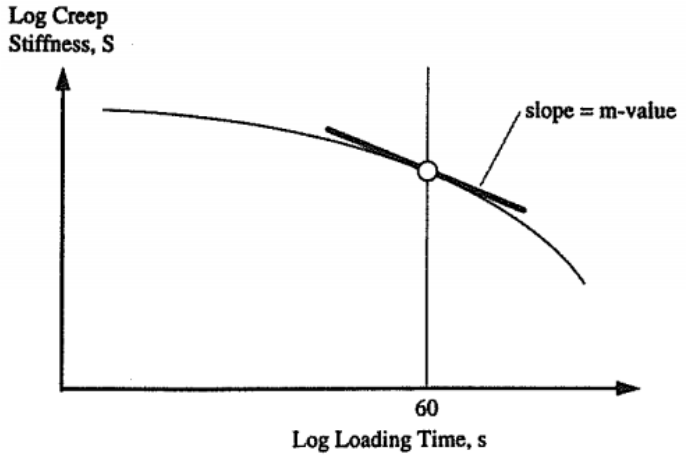

Figure 16: Definition of BBR Stiffness and m-Value
Source: Brown et al. (2009)

The critical low temperature grade can either be controlled by S or m-value, determined by the parameter that corresponds to the warmest low temperature. S-controlled binders are controlled by stiffness and have "extra" relaxation capability, while m-controlled binders have less ability to relax. Presently, most unaged binders are m-controlled in the asphalt industry. As binders age, they become more m-controlled and lose relaxation capabilities.

Anderson et al. (2011) showed that the difference between the critical low temperature grades from stiffness (S) and m-value is a good indicator of non-load related cracking potential of asphalt binders. This parameter is defined as ΔT_{cr} and is shown in Equation 3. As ΔT_{cr} becomes more m-controlled (i.e. a greater difference between S and m-value critical temperatures), the asphalt binder loses relaxation capabilities and becomes more susceptible to cracking. Anderson et al. initially proposed a value of -2.5° C as an identifiable risk of cracking where preventative action should be considered. Rowe (2011) recommended a value of -5° C as a cracking limit where immediate remediation should be considered.

Equation 3: BBR ΔT_{cr}

$$\Delta T_{cr} = T_{cr\,(Stiffness)} - T_{cr\,(m-value)}$$

Where:

- ΔT_{cr} = Difference in critical low temperature PG grade
- $T_{cr\ (Stiffness)}$ = Critical low temperature grade predicted using BBR S (stiffness)
- $T_{cr\ (m\text{-}value)}$ = Critical low temperature grade predicted using BBR m-value (slope)

3.1.3 Binder Master Curves and Rheological Indices

DSR testing was performed at temperatures of 95, 80, 70, 60, 45, 35, 25, 15, 5, -5, and -15° C and loading frequencies within a strain range of 0.005 to 0.02. Complex shear modulus (G*) master curves for the recovered binders were generated using the DSR results. The asphalt binder master curves were constructed by collecting the complex modulus (G*) and phase angle (δ) over a wide range of temperatures and loading frequencies. The master curve was then generated using the time-temperature superposition principle. The software package RHEA™ by Abatech, Inc. was used to construct the master curves, using Equation 4 to fit the master curve. Master curve construction is performed at a certain reference temperature, often 25° C, and all of the test data is shifted with respect to this temperature. The form or shape of the G* master curve provides an indication of the "aging" characteristics of the asphalt binder. As aging increases, the shape of the master curves become flatter and the shear modulus becomes stiffer.

Equation 4: Binder Complex Shear Modulus Master Curve

$$\log|G^*| = a + \frac{b}{[1 + e * \exp(c + d * \log(\omega_r))]^{\frac{1}{e}}}$$

Where:

- *a, b, c, d, e* = regression coefficients
- ω_r = angular frequency

The rheological parameters ω_o and R from the Christensen-Anderson-Marasteanu (CAM) rheological model master curve are also of interest. Figure 17 shows how these rheological parameters are defined from the CAM complex shear modulus master curve. Crossover frequency,

ω_o, is the frequency at which phase angle is equal to 45°. A decrease in crossover frequency indicates higher degrees of aging in binders. The rheological index parameter, R-value, is measured as the difference between the log of the glassy modulus, G_g, and log of the complex shear modulus measured at the crossover frequency. A higher R-value results in a flatter master curve, which indicates a more gradual transition from elastic behavior to steady-state flow. An increase in R-value is also indicative of age hardening in the asphalt binder. By plotting crossover frequency versus R-value, the relative change in aging or rejuvenation (opposite of aging) can be explored. Age hardening would be expected for data in the lower right of the plot as crossover frequency decreases and R-value increases.

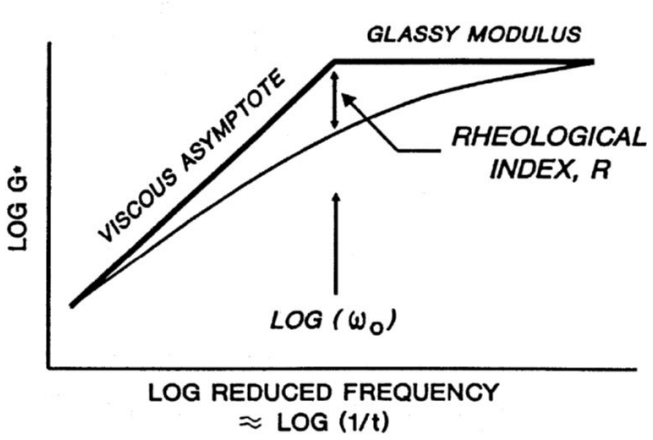

Figure 17: Definition of CAM Rheological Indices ω_o and R-Value
Source: Christensen and Anderson (1992)

3.1.4 Glover-Rowe Parameter

Along with a general trend of aging, the master curve analysis can also be utilized to evaluate the non-load associated cracking potential based on the work by Glover et al. (2005), Anderson et al. (2011), and Rowe et al. (2014). The rheological Glover parameter, G'/(η'/G'), was initially proposed by Glover et al. (2005) to relate storage shear modulus, G', and dynamic viscosity, η', to binder ductility. Anderson et al. (2011) related this binder ductility parameter to non-load associated cracking in airfield pavements, and Rowe (2011) re-defined this parameter in

terms of |G*| and δ based on analysis of Black Space diagrams. The Glover-Rowe parameter, shown in Equation 5, can be measured by construction of a master curve from DSR testing. The parameter specifically uses shear modulus and phase angle at 15° C and a frequency of 0.005 rad/sec.

Equation 5: Glover-Rowe Parameter

$$\frac{|G^*|(\cos\delta)^2}{\sin\delta}$$

Where:

- G^* = Shear modulus at 15° C, 0.005 rad/sec
- δ = Phase angle at 15° C, 0.005 rad/sec

When expressed in this manner, the limiting value of 9E-04 MPa at 0.005 rad/sec proposed by Glover et al. (2005) becomes $G^*(\cos\delta)^2/(\sin\delta) < 180$ kPa. The master curve information can then be expressed within Black Space (G* vs phase angle). Rowe's Black Space provides a means of assessing an asphalt binder and pre-screening it to determine if it is susceptible to cracking, using the same principles initially proposed by Glover et al. A value exceeding 180 kPa corresponds to damage onset and a value exceeding 450 kPa corresponds to significant cracking. Binder aging can be assessed by a migration closer to the Glover-Rowe parameter cracking limits in Black Space.

3.2 MIXTURE TESTING AND ANALYSIS

Dynamic modulus and S-VECD cyclic fatigue testing was performed on the silo storage mixtures, as well as the specimen fabrication methods mixtures. In addition, the LVECD pavement life evaluation software was used to analyze the silo storage mixtures. The Asphalt Mixture Performance Tester (AMPT), shown in Figure 18, was used for both dynamic modulus testing and fatigue testing. The software used on the AMPT was UTS 019 for dynamic modulus and UTS 032

for fatigue testing. The test setup with additional fixtures for small specimen testing is shown in Figure 19 for dynamic modulus and fatigue testing.

Figure 18: Asphalt Mixture Performance Tester (AMPT)

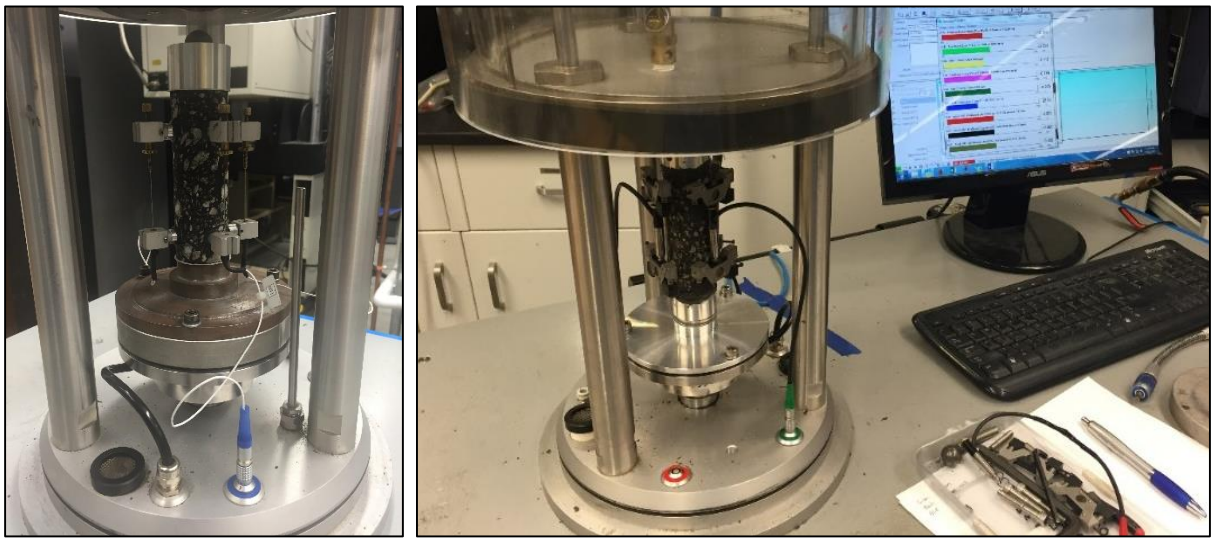

Figure 19: Dynamic Modulus and S-VECD Fatigue Setup for Small Specimens

3.2.1 Dynamic Modulus

The AMPT was used to perform dynamic modulus testing in unconfined uniaxial compression following the protocol given in AASHTO TP79: *Standard Method of Test for*

Determining the Dynamic Modulus and Flow Number for Asphalt Mixtures Using the Asphalt Mixture Performance Tester (AMPT). Three replicate specimens were tested for each condition (i.e. each storage time or fabrication method type). These specimens were tested at target temperatures of 4.4° C, 21.1° C, and 37.8° C and frequencies of 25, 10, 5, 1, 0.5, and 0.1 Hz. Dynamic modulus testing consists of sinusoidal loading of 20 cycles for each frequency (10 cycles for 0.1 Hz). The complex modulus values were obtained from the final six cycles of each loading series (i.e. when the material reached steady state conditions). Loose core or spring-loaded LVDTs were used for instrumentation. These LVDTs attached to the glued studs and measured deformations within the 70 mm gauge length. Load levels were determined so that the resulting strain amplitudes were between 35 and 75 microstrain.

Following testing of specimens in the AMPT, the output provided was raw data only: time, force applied by the actuator, temperature, and deformations for each of the LVDTs. Using the UTS 019 software, the raw data output included data collected at every 0.001 seconds, resulting in approximately 180,000 total data points for each test. The desired properties from this test are dynamic modulus and phase angle at each frequency, which are measures of the material's stiffness and viscoelastic capabilities. These values are calculated through the raw data provided, but several data analysis steps were needed to arrive at the two calculated parameters. Previously, a hand-fitting Excel process was used to calculate dynamic modulus results at UNH. As part of this graduate work, a MATLAB code was developed in order to make the process simpler, more efficient, and much quicker. The code sorts the raw data from the AMPT, fits a five-parameter curve corresponding to the data, and calculates dynamic modulus and phase angle properties depending on the curve parameters.

Figure 20 shows typical data obtained from dynamic modulus testing. An important observation in this figure is the time lag (shown in red) between the peak of the applied stress and peak compression of the strain response. Phase angle (δ) is calculated as a function of time lag. For purely elastic materials, δ = 0° (no time lag, completely "in-phase") and for purely viscous materials, δ = 90° (completely "out-of-phase"). The figure also shows generally how the various parameters from Equation 6 influence the overall sinusoidal curve. The parameters can be defined or approximated as follows:

- *D1*: Approximates the starting ordinate of the curve, but also is affected by the exponential *n* value.
- *n*: Exponential term that gives slope to the overall sine curve. Stress is controlled and generally has a very small *n*; however, the asphalt specimen accumulates creep over the test duration, so *n* may become larger for the microstrain values as the test progresses.
- *A*: Amplitude; a measure of the height of the curve.
- ω_t: Determines the frequency of the sine wave; can be predicted by 2π*(test frequency).
- α: Shifts the curve left to right; can be restricted to $0 \leq \alpha \leq 2\pi$ because of the period of a sine curve.

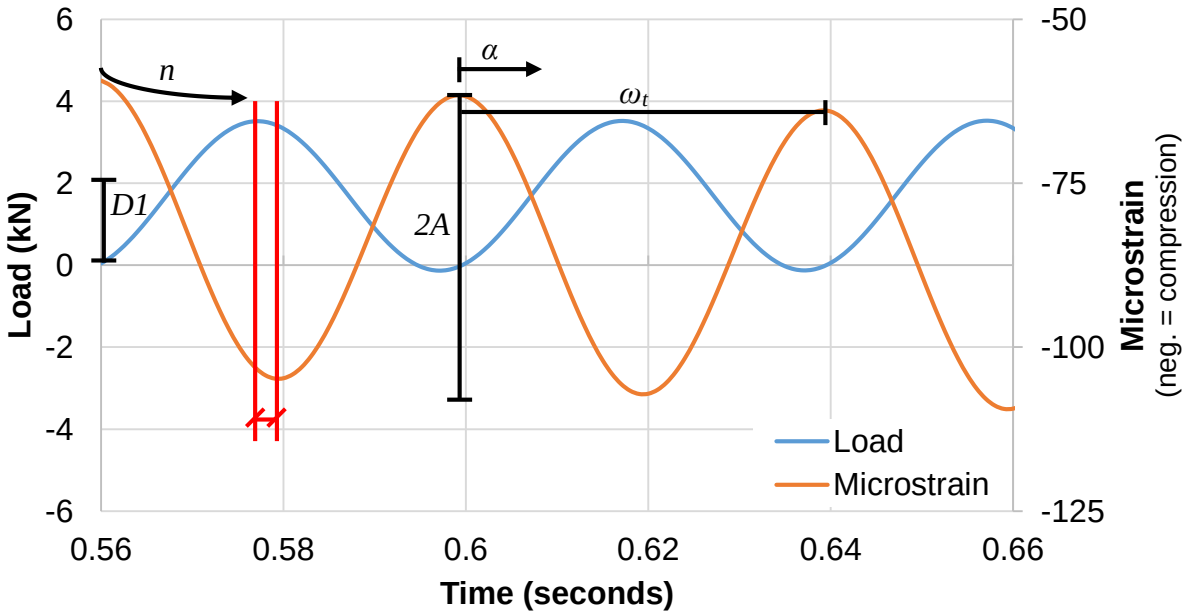

Figure 20: Example Dynamic Modulus Data and Definition of Sinusoidal Fit Parameters

Dynamic modulus and phase angle are functions that can be evaluated using the five parameters of the sinusoidal curve. Therefore, the data was fit to the curve defined in Equation 6 to determine the coefficients that accurately represent the raw data. An example of the data after fitting in MATLAB is shown in Figure 21. In this figure, the blue curves represent the raw data while the red curves represent the fitted curve of the last six cycles (once steady state conditions are reached). The error between the two curves at each data point was minimized so that the fitted data overlapped the raw data. After the curve is fit, further data analysis processes are performed to calculate dynamic modulus and phase angle. Essentially, dynamic modulus can be estimated by the ratio of the stress amplitude to the strain amplitudes, and phase angle can be estimated as a function of the time lag between stress and strains.

Equation 6: Dynamic Modulus Raw Data Curve Fitting

$$Load/Strain = D1 * {Z_{time}}^{n} + (A * \sin((\omega_t * Z_{time}) - \alpha))$$

Where:

- $D1$, n, A, ω_t, α = fitting coefficients that can be estimated using the definitions in Figure 20
- Z_{time} = zeroed time

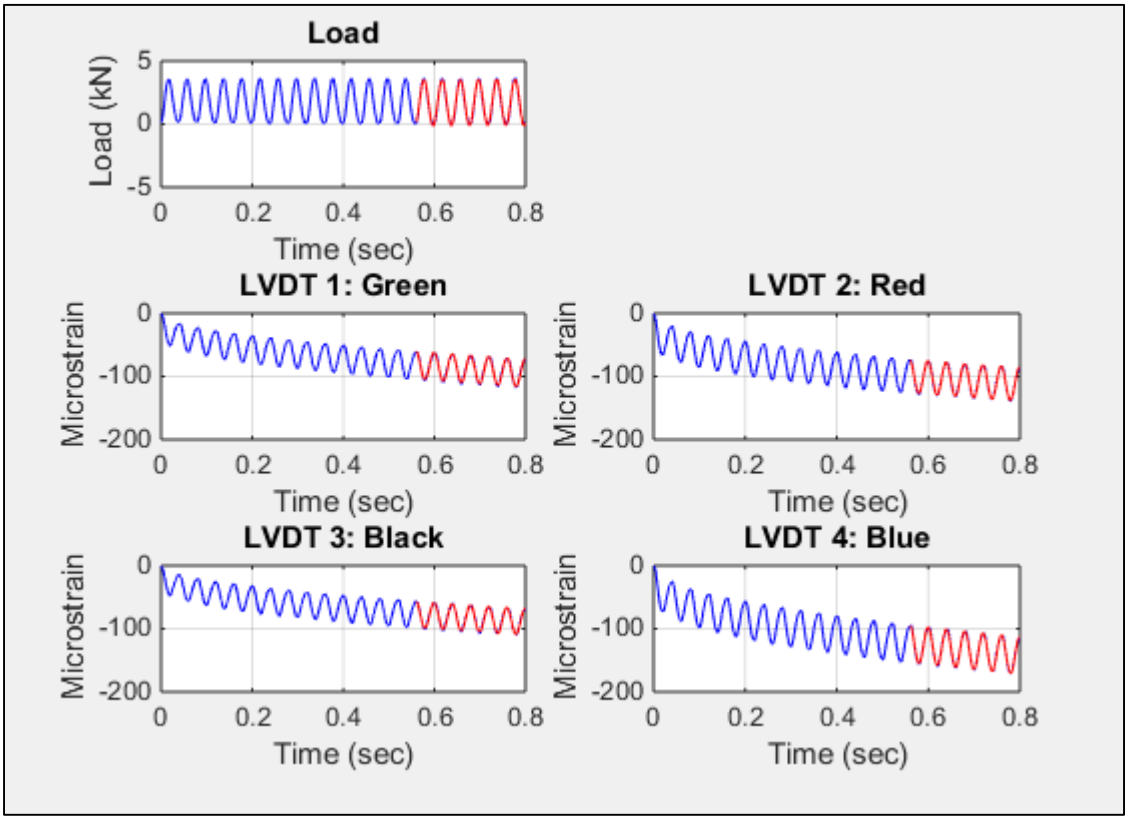

Figure 21: Curve-Fitting of Dynamic Modulus Results in MATLAB

After obtaining the dynamic modulus and phase angles at each frequency and temperature for the individual replicates, the data can be represented by one curve that shows the average behavior of the mix over a range of frequencies/temperatures. Asphalt is a thermorheologically simple material, meaning that the time-temperature superposition can be applied so that measurements at various temperatures or frequencies can be shifted to form one master curve. This allows researchers to evaluate mixtures over a wide range of frequencies without testing an excessive amount or at extreme temperatures. The average dynamic modulus isotherms (data from a certain temperature) were shifted to a generalized logistic function (Equation 7) to construct the master curve at a reference temperature of 21.1° C. The time-temperature shift factors were

allowed to free-shift, meaning no underlying shape of the shift factor versus temperature curve was assumed.

Equation 7: Sigmoidal Fit for Dynamic Modulus Master Curve

$$\log|E^*| = D + A[1 + Te^{-B(\log\omega - M)}]^{-1/T}$$

Where:

- $|E^*|$ = Dynamic Modulus
- ω = reduced frequency
- *A, B, D, M, T* = fitting parameters

Master curve construction was done primarily in the software package RHEA™ by Abatech. However, the small specimens were fit manually in Excel due to problems arising with the software likely due to the phase angle values. Testing on the small-scale specimens from the field cores was conducted at lower temperatures (2.9° C, 18.0° C, and 30.0° C) than standard due to high creep levels observed at the standard temperatures. Load levels at the 30.0° C temperature reached the minimum that the AMPT would allow; therefore a higher temperature could not be used because creep limits determined by the specifications would be exceeded.

Other analyses performed within RHEA™ included calculation of inflection point frequency and the Kaelble C_2 parameter. The fitting parameters determined from the dynamic modulus master curve in Equation 7 are used to determine the frequency at which the inflection point of the master curve occurs. The inflection point frequency corresponds to the peak of the phase angle master curve and indicates where the material behavior transitions from being dominated by the binder to the aggregate skeleton, essentially transitioning from the more viscous regime to a more elastic regime. This is similar in concept to the crossover frequency in binders where the phase angle is equal to 45° and the material behavior transitions from viscous to elastic. The inflection point frequency is defined as follows:

Equation 8: Inflection Point Frequency

$$inflection\ point\ frequency = 10^{-\left(\beta/\gamma\right)}$$

The shift factor curves determined from the dynamic modulus master curve construction are fit using the Kaelble modified Williams Landel Ferry (WLF) form described by Rowe et al. (2014):

Equation 9: Kaelble-Modified WLF Shift Factor

$$\log a_T = -C_1\left\{\frac{T - T_k}{C_2 + |T - T_k|} - \frac{T_r - T_k}{C_2 + |T_r - T_k|}\right\}$$

Where:

- a_T = shift factor
- T = temperature
- T_r = reference temperature
- T_k = Kaelble defining temperature
- C_1, C_2 = fitting parameters

The T_k value represents an inflection point in the shift factor curve and was set to 4.4° C in this study. The C_2 coefficient describes the slope of the log a_T versus temperature curve and therefore is an indication of the temperature susceptibility of the mixture. A higher C_2 value occurs when the slope of the shift factor curve is shallower, indicating a reduced temperature susceptibility of the asphalt mixture.

In addition to evaluating master curves, the results of the complex modulus testing were also plotted in Black Space (modulus versus phase angle). The combination of stiffness and phase angle, as evaluated in Black Space, can indicate a material's resistance to cracking. Higher phase angles are indicative of the ability to relax under loading instead of fracturing. A material's position

further down and to the right in Black Space (lower stiffness, higher phase angle) is an indicator of better cracking performance.

3.2.2 S-VECD Fatigue Cracking

Simplified VECD (S-VECD) model is a mode-of-loading independent, mechanistic model that allows the prediction of fatigue cracking performance under various stress/strain amplitudes at different temperatures from only a few tests. The S-VECD model is composed of two material properties: the damage characteristic curve that defines how fatigue damage evolves in a mixture and the energy-based failure criterion.

Fatigue testing was performed in uniaxial tension on the AMPT. Specimens were cut to dimensions of 100 mm in diameter by 130 mm tall (38 mm by 110 mm for small specimens) and glued to end platens that were fixed in the AMPT. Testing was performed at 20.0° C and 10 Hz. The mixtures were tested with three or four replicate specimens at varying microstrain levels ranging from 300 to 450 microstrain to cover a range of numbers of cycles to failure. Fatigue testing was not performed on the 25% RAP mixtures in the silo storage study due to a lack of available specimens. Details of the test method can be found in AASHTO TP 107: *Determining the Damage Characteristic Curve of Asphalt Concrete from Direct Tension Cyclic Fatigue Tests*. Since the S-VECD test ends with the complete failure of the specimen, properties measured from this test reflect the fatigue cracking resistance of the asphalt mixture in both crack initiation and propagation stages.

Cyclic testing was conducted in crosshead-controlled mode, in which the machine actuator's displacement was programmed to reach a constant peak level at each loading cycle. The actual on-specimen strain levels were significantly lower than the programmed ones due to machine compliance. Fingerprint dynamic modulus tests were conducted by determining the

dynamic modulus ratio (DMR) to check the variability of the test specimens before running the direct tension cyclic tests. A DMR in the range of 0.9 to 1.1 guarantees that the linear viscoelastic properties obtained from the dynamic modulus tests can be used properly in the S-VECD analysis.

All cyclic tests were performed at a minimum of three different amplitudes to cover a range of numbers of cycles to failure (N_f). Once the fatigue tests are conducted, the damage characteristic curves are developed by calculating the secant pseudo-stiffness (C) and the damage parameter (S) at each cycle of loading. These values are cross-plotted to form the damage characteristic curve. For all the mixtures, the exponential form shown in Equation 10 was used to fit the C versus S characteristic curves.

Equation 10: S-VECD Fatigue Damage Characteristic Curve

$$C = e^{aS^b}$$

Where:

- a, b = fitting coefficients
- C = secant pseudo-stiffness
- S = damage parameter

The S-VECD fatigue failure criterion, called the G^R method, involves the released pseudo strain energy. This released pseudo strain energy concept focuses on the dissipated energy that is related to energy release due to damage evolution only. The G^R characterizes the overall rate of damage accumulation during fatigue testing. A characteristic relationship, which is found to exist in both RAP and non-RAP mixtures, can be derived between the rate of change of the averaged released pseudo strain energy during fatigue testing (G^R) and the final fatigue life (N_f). Using this relationship, an index parameter, N_f at G^R = 100, has been recently developed to quickly and simply interpret results in the G^R-N_f space. This parameter represents the number of cycles to failure equivalent to a G^R value of 100. Although the parameter does not capture the slope of the

power equation that is fit to the replicates in the G^R-N_f space, it is a simple way to compare mixtures. Another measure used in this study to characterize fatigue performance was endurance limit, which represents the strain level below which there will be no damage accumulation.

The analysis of S-VECD fatigue is conducted using the alpha-Fatigue software by Instrotek. Using the G^R relationship and the S-VECD model, the fatigue life of asphalt concrete under different modes of loading and at different temperatures and strain amplitudes can be predicted from dynamic modulus tests and cyclic direct tension tests at three to four strain amplitudes.

3.2.3 LVECD Pavement Fatigue Life Evaluation

The layered viscoelastic critical distresses (LVECD) program was performed by North Carolina State University to predict the long-term fatigue performance of pavements under traffic loading in the silo storage study. Eslaminia et al. (2012) developed the layered viscoelastic structural program with the material level continuum damage model to calculate the required stresses and strains for the fatigue behavior prediction using three-dimensional viscoelastic calculations under moving loads. The LVECD simulations were performed for both thin and thick pavement structures using the required parameters including design time, structural layout, traffic, and climate. The thin pavement structure had an asphalt layer of 100 mm and aggregate base of 200 mm; the thick pavement had an asphalt layer of 300 mm with the same base. The aggregate base and the subgrade were modeled using the linear elastic properties with the modulus values of 350 MPa and 100 MPa, respectively. Two climates were evaluated: Boston, Massachusetts and Raleigh, North Carolina using pavement temperatures obtained from the Enhanced Integrated Climate Model (EICM). Also, a single tire with the standard loading of 80 kN at the center of

pavement was utilized. The average annual daily truck traffic (AADTT) was assumed to be 2,000. The pavement cross-sections for LVECD simulations can be seen in Figure 22.

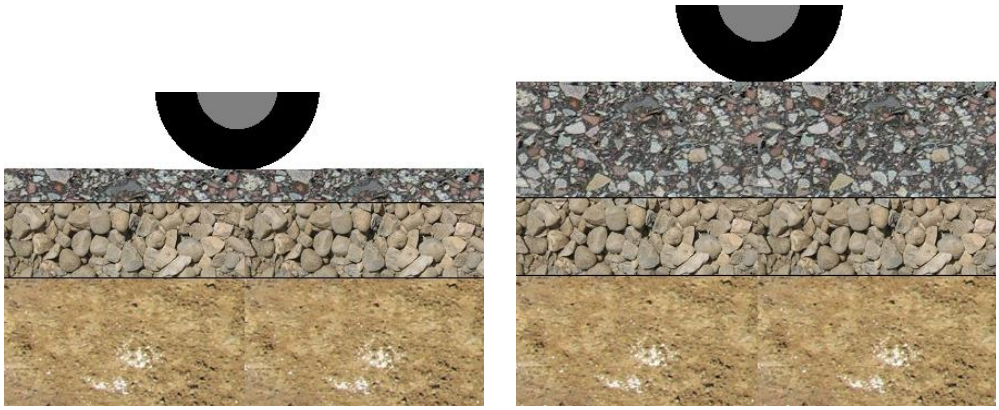

Figure 22: LVECD Thin and Thick Pavement Cross-Sections

For fatigue cracking resistance evaluation, LVECD calculates the damage growth and the damage factor based on Miner's law (Equation 11). If the damage factor is equal to zero, the element does not experience any damage, while a damage factor of one indicates total failure of the element. Cracking damage in this model is evaluated by the number of elements that experienced more than 20% damage ($N/N_f > 0.20$).

Equation 11: Miner's Law for LVECD Damage

$$\sum_{i=1}^{T} D_i = \frac{N_i}{N_{fi}}$$

Where:

- D = damage
- T = total number of periods
- N_i = traffic for period i
- N_{fi} = allowable failure repetitions under the conditions that prevail in period i

CHAPTER 4: RESULTS AND DISCUSSION

The main objectives of the silo storage study were to 1) determine if silo storage time has a significant impact on the properties of virgin and RAP mixtures and 2) determine whether these potential changes are due to short-term aging within the silo and/or an interaction between virgin and RAP binders. Binder and mixture tests were performed in order to meet these objectives, and the results from binder testing are included in Section 4.1 while the results from mixture testing are included in Section 4.2. Extraction and recovery of asphalt binders were performed on the virgin and RAP mixtures, and tank binder was prepared for RTFO conditioning on the virgin binder. Binder testing and analysis included performance grading and ΔT_{cr} analysis, complex shear modulus master curve construction, Glover-Rowe parameter analysis, and rheological indices analysis. Mixture testing included dynamic modulus stiffness testing, S-VECD cyclic fatigue testing, and LVECD simulations. Dynamic modulus tests were performed on the virgin and 25% RAP mixtures, while fatigue and LVECD analyses were only available for the virgin mixture.

4.1 BINDER TESTING FOR SILO STORAGE STUDY

4.1.1 Performance Grading and ΔT_{cr}

The results from performance grading of the extracted and recovered binders are shown in Figure 23 to Figure 25. The results represent one replicate for each storage time. The general trend in PG grade results shows an increase in high temperature PG grade of 0.39° C per hour of silo storage time and 0.53° C/hr for the binder extracted and recovered from the virgin and RAP mixes, respectively. An increase in intermediate temperature PG grade of 0.20° C/hr was observed for the virgin mix while the RAP mix had no measurable trend. The low temperature PG grade increased

0.14° C/hr and 0.21° C/hr for virgin and RAP mixtures, respectively, with the low temperature grade being m-slope dependent for both. Warmer temperatures for high, intermediate, and low PG grades indicate stiffening of the binders. As binder becomes stiffer, it is capable of resisting higher shear stress and can meet the specifications of warmer PG grades. Stiffening of the binder is indicative of age hardening (e.g. oxidation, volatilization) as a result of longer silo storage durations. Interestingly, the RAP experienced greater increases, which shows that an interaction between the RAP and virgin binder could be occurring within the silo.

Figure 26 shows the critical low temperatures for both S and m-value obtained from BBR testing at each silo storage time. All storage times for both virgin and 25% RAP mixtures were m-controlled. As previously explained, the difference between the S and m-value critical temperatures is represented as ΔT_{cr} (Equation 3), and this parameter has been used to identify cracking susceptibility in asphalt binders. Figure 27 shows a general trend of the BBR ΔT_{cr} remaining relatively constant and then negatively increasing (i.e. greater difference between S and m-value critical low temperature) towards the cracking limits after 5 hours of storage time. The recovered binder from the virgin mixture consistently has a smaller ΔT_{cr} than the 25% RAP mixture, indicating that the virgin asphalt binder has undergone less aging.

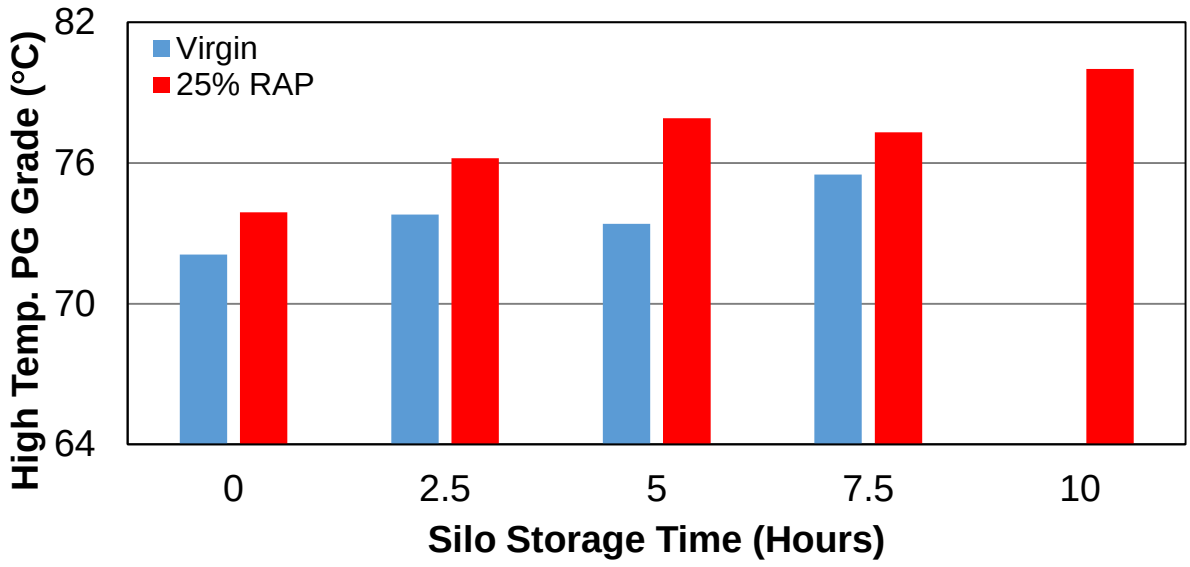

Figure 23: Binder High Temperature PG Grades for Silo Storage Mixtures

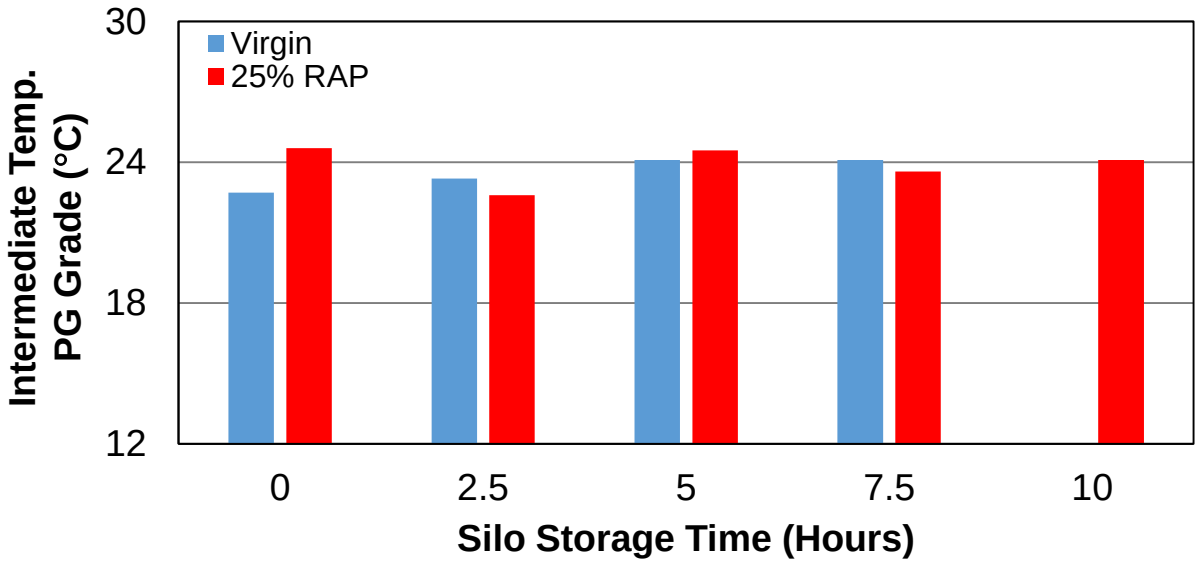

Figure 24: Binder Intermediate Temperature PG Grades for Silo Storage Mixtures

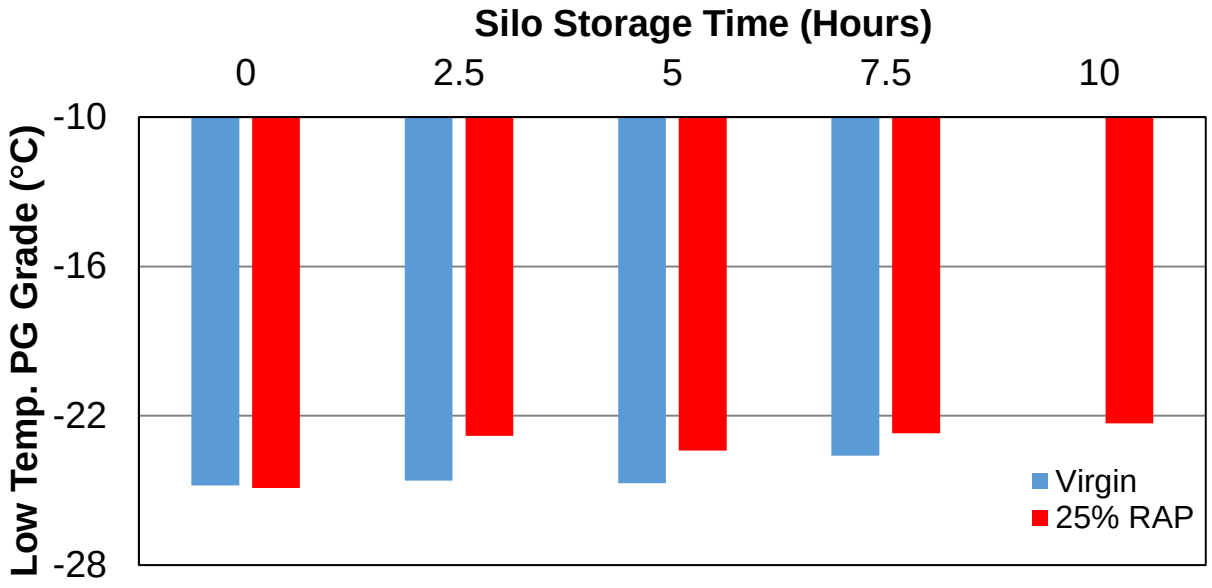

Figure 25: Binder Low Temperature PG Grades for Silo Storage Mixtures

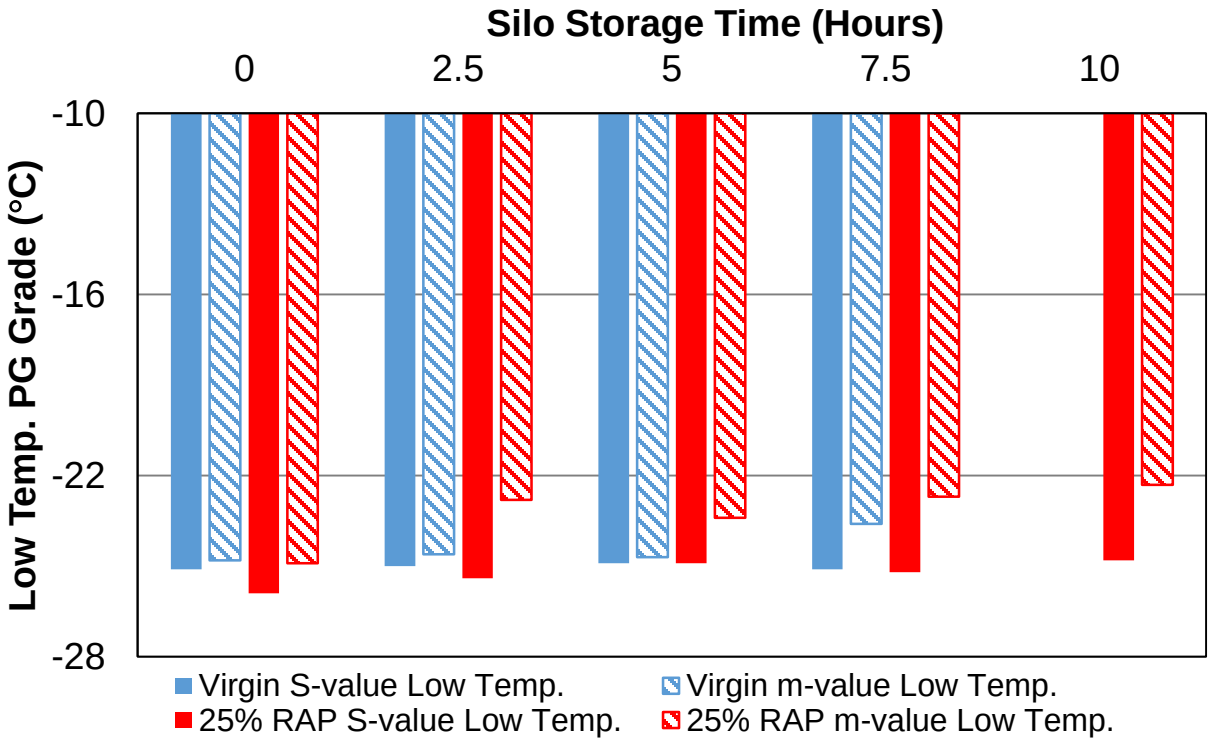

Figure 26: Binder Critical S and m-value Temperatures for Silo Storage Mixtures

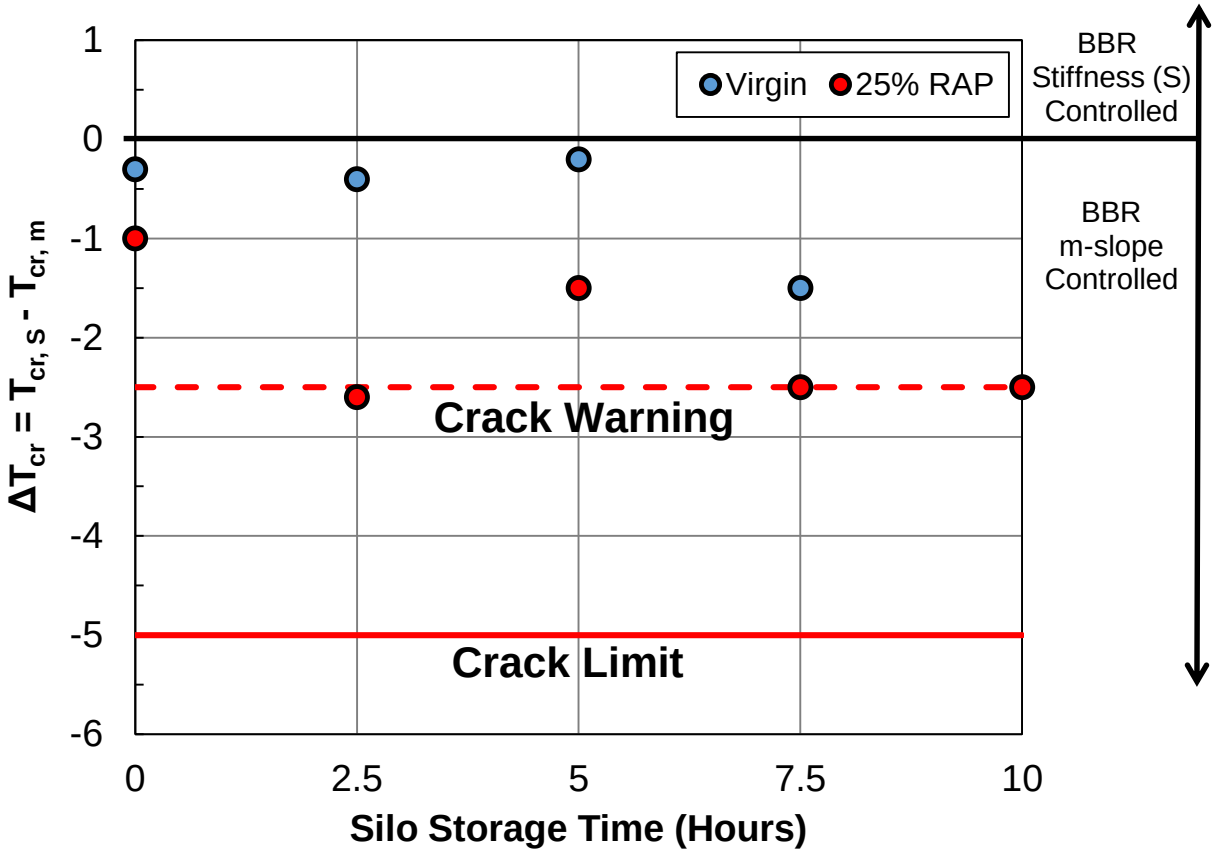

Figure 27: Binder ΔT_{cr} Results for Silo Storage Mixture

4.1.2 Complex Shear Modulus Master Curves

The impact of silo storage length on the complex shear modulus master curves is shown in Figure 28 and Figure 29. One replicate binder sample was tested for each storage time. The stiffness of the extracted and recovered binders appears to increase with longer storage times, and these increases are more evident at the intermediate and low frequencies (high temperatures). While the differences may not be significant at each storage time, the 7.5 hours storage time is stiffest and the 0 hours storage time is softest for the virgin mixture. For the 25% RAP mixture, the 10 hours storage time is stiffest and the 0 hours storage time is softest. The intermediate storage times do not appear much stiffer than one another.

Black Space plots for these recovered binders are shown in Figure 30 and Figure 31. These plots show similar results to the master curves, as there does not seem to be much distinction among the intermediate times but the higher storage times appear stiffer than the 0 hours mixture. At similar complex modulus values, the phase angles seem to decrease slightly, indicating more elastic behavior for the binder. The elastic behavior provides insight into the aging characteristics because as aging occurs within the binder, it becomes stiffer and may lose its viscous characteristics.

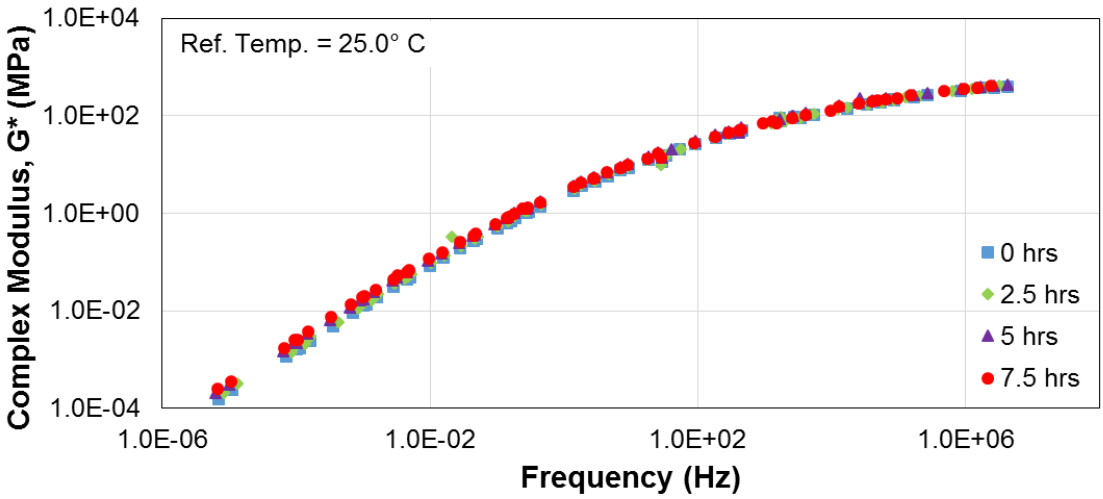

Figure 28: Binder Shear Modulus Master Curve for Virgin Silo Storage Mixtures

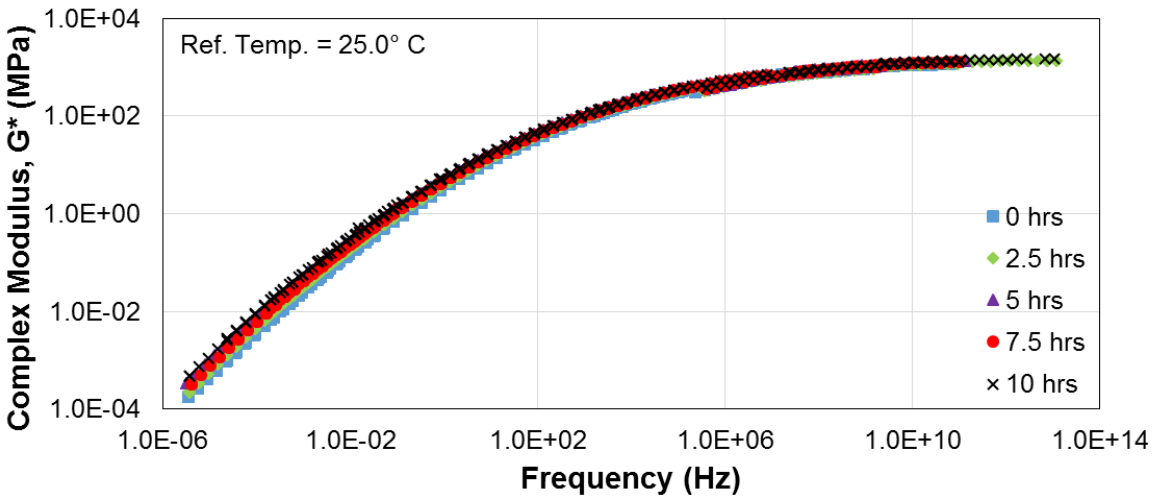

Figure 29: Binder Shear Modulus Master Curve for 25% RAP Silo Storage Mixtures

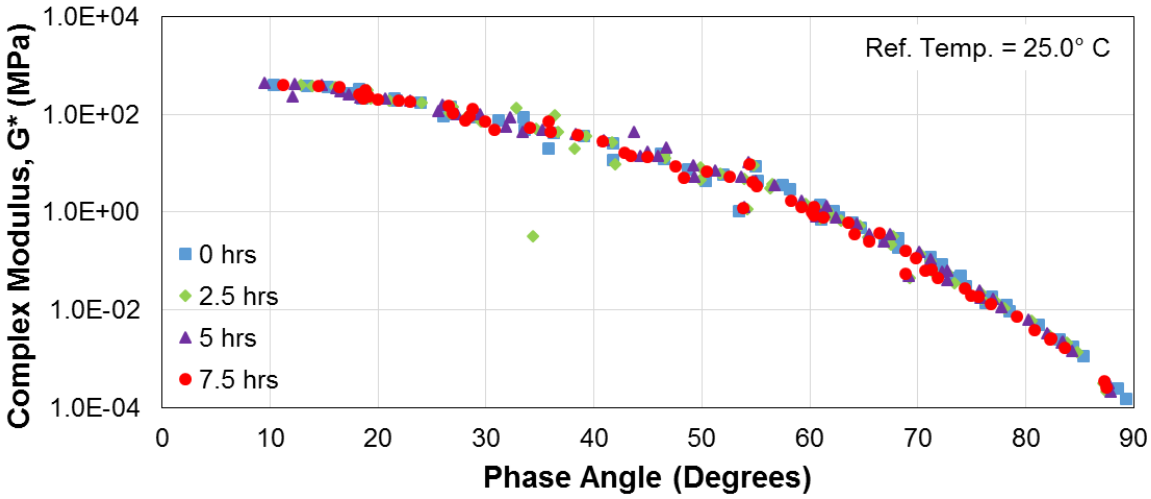

Figure 30: Binder Black Space Plot for Virgin Silo Storage Mixtures

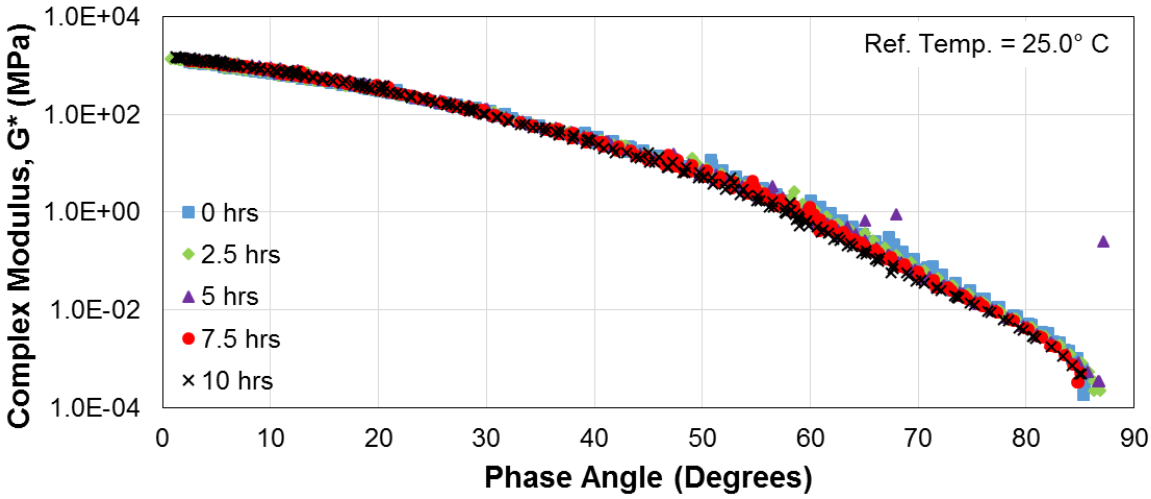

Figure 31: Binder Black Space Plot for 25% RAP Silo Storage Mixtures

4.1.3 Glover-Rowe Parameter and Rheological Indices

Figure 32 shows a Black Space plot for the silo storage binders. The Glover-Rowe parameter values corresponding to cracking limits are shown as bands graphed across this plot. The figure shows that as silo storage time increases, the extracted asphalt binder becomes more aged and migrates to areas where potential, non-load associated cracking is a concern. The results

also show that the 25% RAP mixture initiates and moves closer to the threshold values. Calculated values for the Glover-Rowe parameter among the binders can be found in the Appendix.

The measured crossover frequency and R-value is shown in Figure 33. A lower crossover frequency is achieved by the binder reaching a phase angle of 45° at a lower frequency, which indicates more elastic behavior of the binder. A higher R-value results in a flatter master curve, another indication of aging. The figure clearly shows that a change in the CAM rheological indices occurs due to longer silo storage times, indicating that aging is occurring over time. The binder extracted from the RAP mixture begins closer to the bottom right and shows larger changes than the extracted virgin binder.

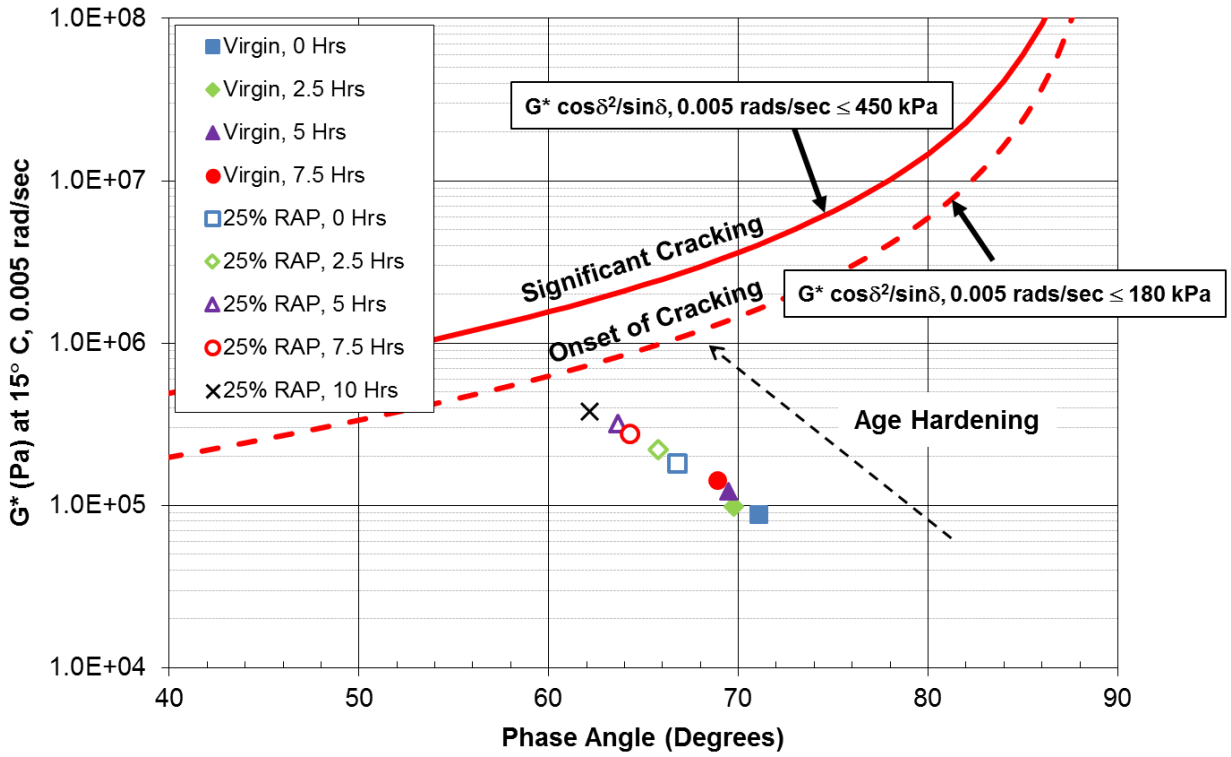

Figure 32: Glover-Rowe Parameter Analysis in Black Space for Silo Storage Binders

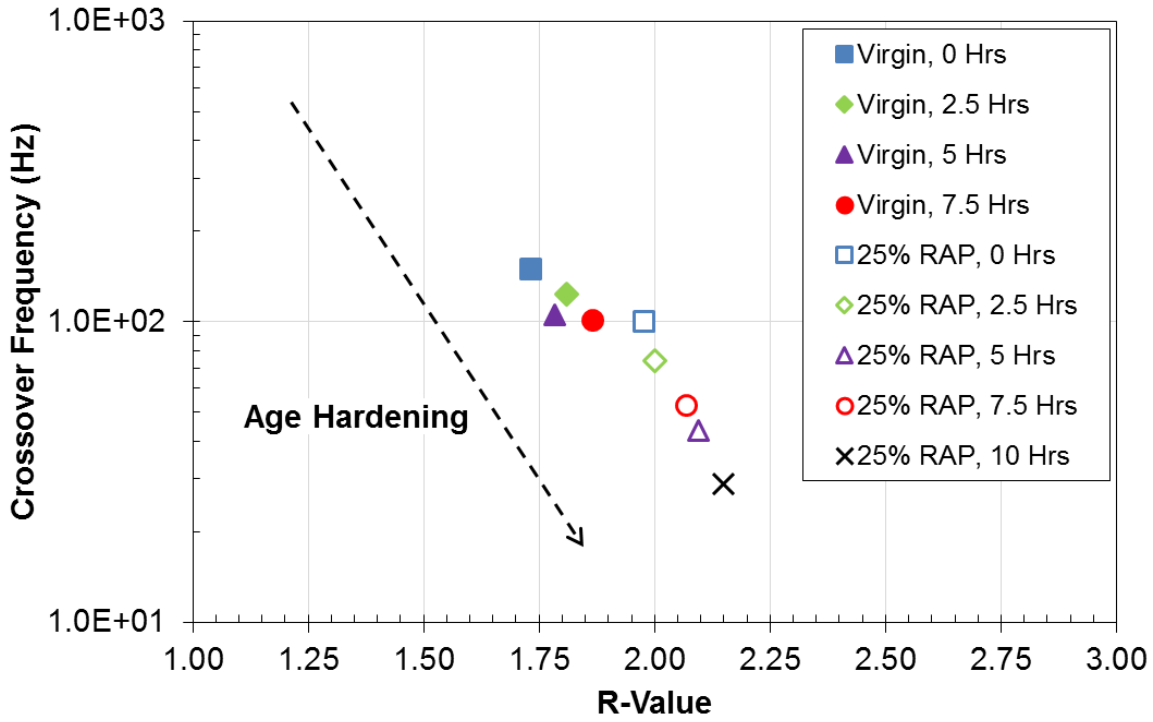

Figure 33: Rheological Indices Analysis for Silo Storage Binders

4.1.4 RTFO Conditioning

Tank binder obtained for the virgin mixture was conditioned in the RTFO for varying times (45, 85, 130, 175, and 300 minutes) to evaluate the reliability of laboratory simulations for short-term aging, which specify 85 minutes in the RTFO. The results of the RTFO conditioning at various times are shown for the Glover-Rowe parameter and rheological indices in Figure 34 and Figure 35, respectively. These results indicate that using the specified time of 85 minutes in the RTFO does not simulate the aging that occurred during plant production and silo storage for the virgin mixtures. In fact, it can be seen that RTFO conditioning does not show similar stiffness (G* and δ) and CAM rheological indices to 0 hours of silo storage time until approximately 170 minutes, which is twice the amount specified in AASHTO T240. This clearly indicates that current laboratory conditioning methods do not necessarily simulate asphalt plant production.

The large differences in this case are likely a result of the relatively high (~350° F) production temperatures that would have aged the asphalt binder, especially under extended silo storage times. However, it must be noted that these variations during plant production do occur in reality, and current laboratory conditioning methods do not necessarily capture those effects. Several factors that occur during actual plant production may not be considered during the RTFO conditioning process. In this scenario, the asphalt mixture that would be placed in the field could be much more susceptible to cracking than indicated by laboratory simulation techniques. The implications in this regard are significant because the pavement life would be shortened, affecting the performance and cost-effectiveness of the pavement.

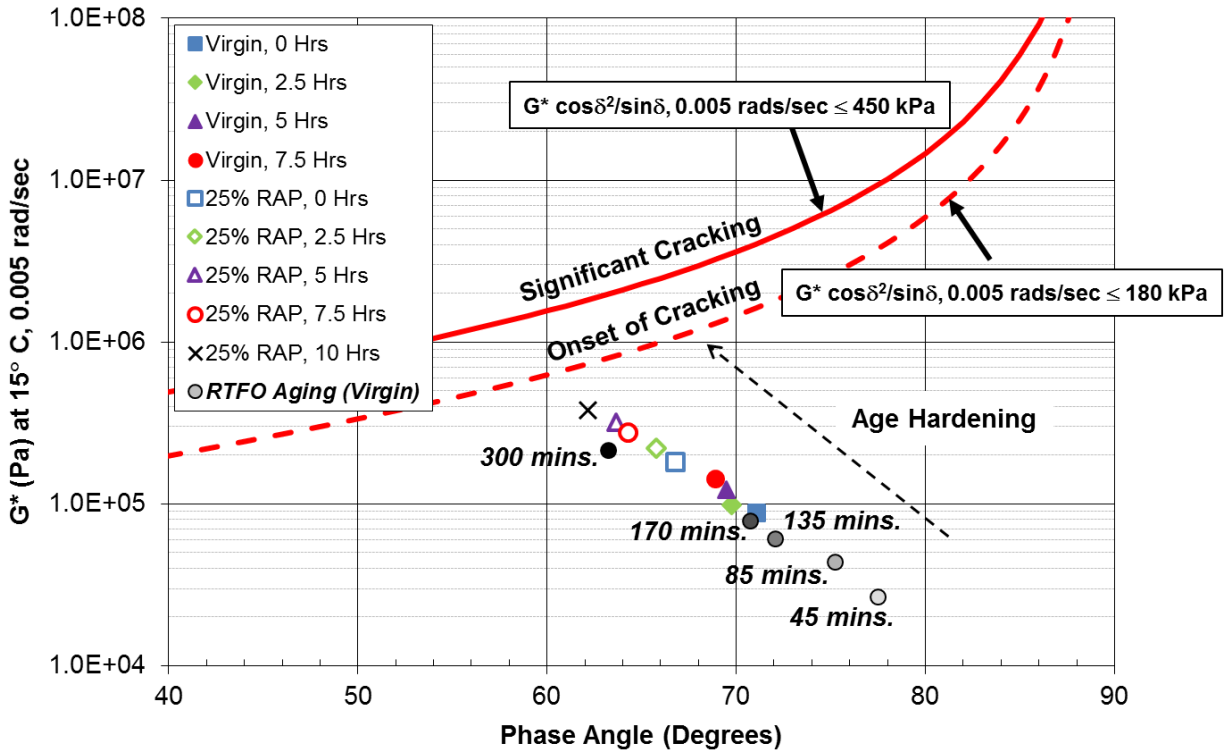

Figure 34: RTFO Conditioning: Glover-Rowe Parameter Analysis in Black Space for Silo Storage Binders

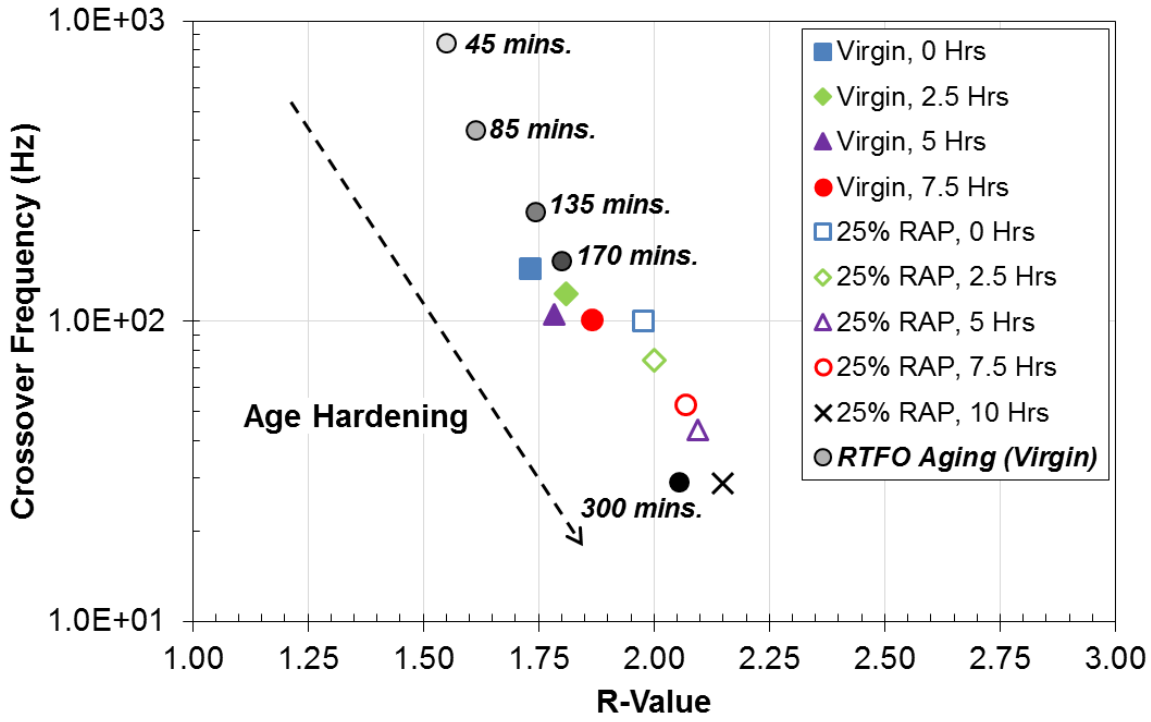

Figure 35: RTFO Conditioning: Rheological Indices Analysis for Silo Storage Binders

4.2 MIXTURE TESTING FOR SILO STORAGE STUDY

4.2.1 Dynamic Modulus

Dynamic modulus master curves were constructed for varying silo storage times, as shown in Figure 36 to Figure 39. Two common methods of plotting dynamic modulus include log-log and semi-log (x-axis) plots; both methods are shown in the figures. Each master curve represents the fitted sigmoidal function from the average of three replicate specimens. The coefficient of variation (ratio of standard deviation to mean) was calculated for the dynamic modulus raw data at each temperature-frequency combination, and those results can be seen in Figure 108 and Figure 109 in the Appendix. In summary, the average % COV was generally in the 3-10% range, while the 0 hours 25% RAP mixture had very high variability.

Both the virgin and RAP mixtures show an increase in dynamic modulus (i.e. stiffness) as the mixtures remain in the silo for longer periods. The RAP mixture shows greater increases with storage time than the virgin mixtures, but air void contents of the RAP mixture could be contributing to the stiffness increases. It is known that stiffness increases as air void content decreases in asphalt mixtures. A combination of silo storage effects and air void content could be impacting the greater increases observed with the RAP mixture.

A statistical analysis was also conducted on the dynamic modulus raw data using independent sample t-tests with a confidence interval of 95%. A p-value less than 0.05 indicates statistical significance between the two groups. T-test results are shown in Table 10 and Table 11. In the tables, statistical significance is highlighted in green while values close to the p-value (0.045-0.050) are in yellow. Statistically, the 0, 2.5, and 5 hours mixtures are all similar for the virgin material. The 7.5 hours virgin mixture is statistically different from the 0 and 2.5 hours storage times. The RAP mixture at 7.5 and 10 hours shows significant differences from 0 hours.

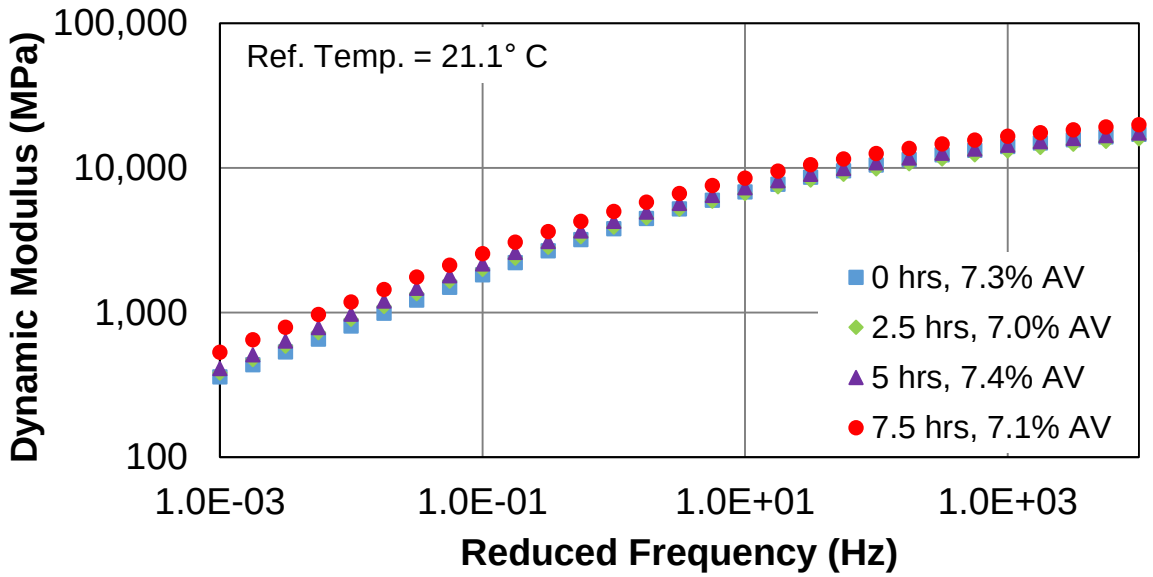

Figure 36: Dynamic Modulus Master Curve (log-log) for Virgin Silo Storage Mixtures

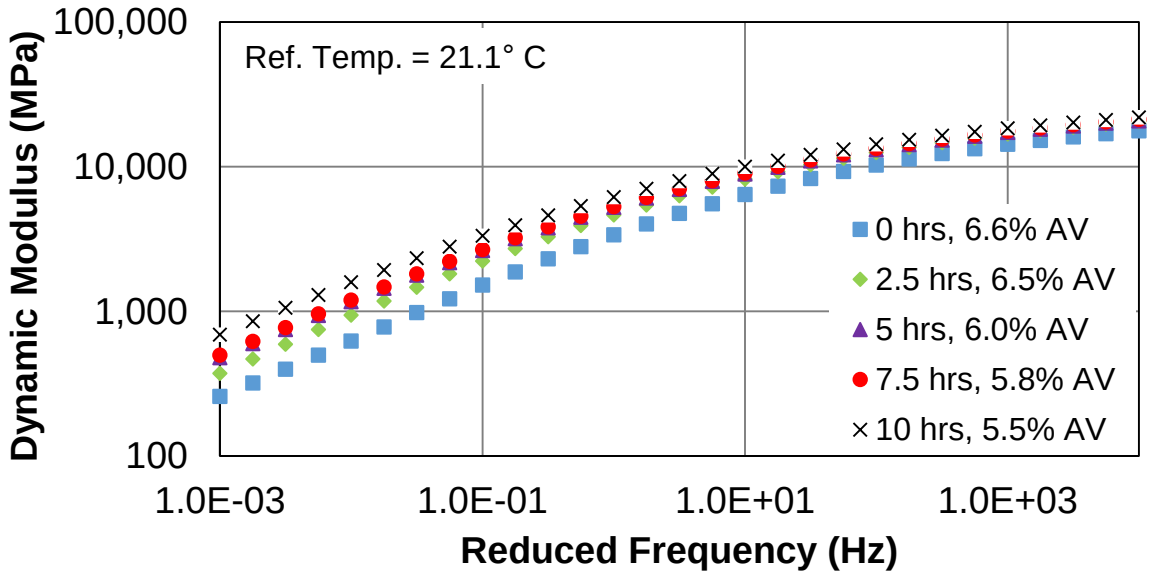

Figure 37: Dynamic Modulus Master Curve (log-log) for 25% RAP Silo Storage Mixtures

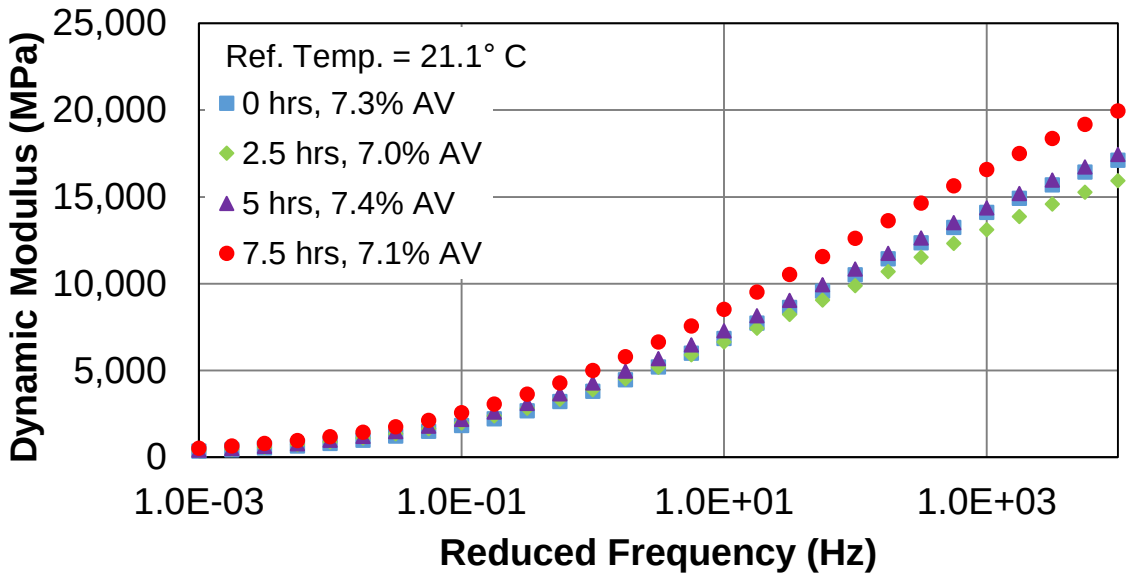

Figure 38: Dynamic Modulus Master Curve (semi-log) for Virgin Silo Storage Mixtures

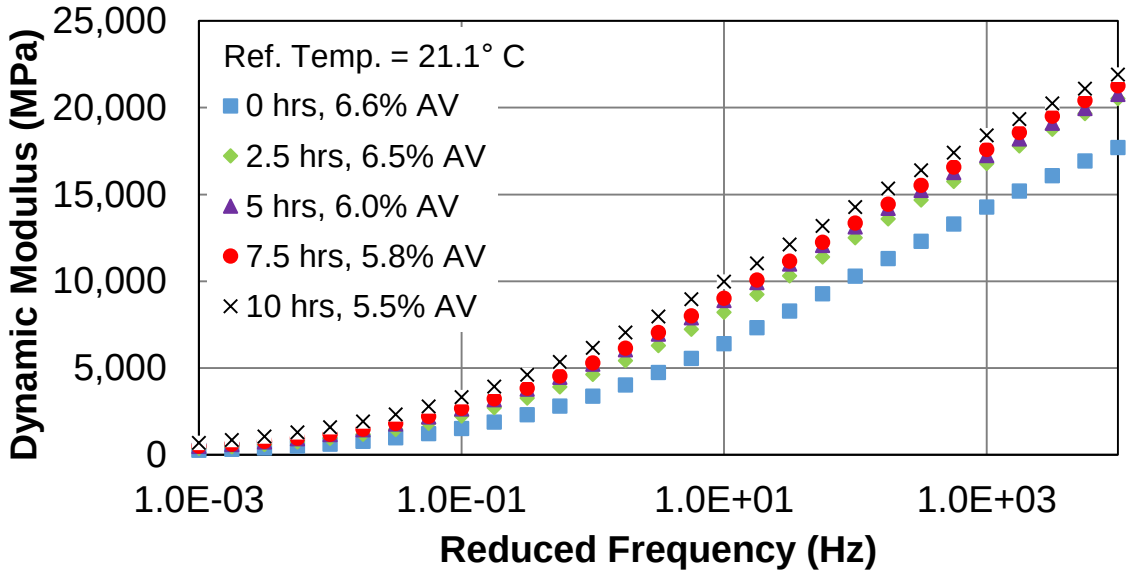

Figure 39: Dynamic Modulus Master Curve (semi-log) for 25% RAP Silo Storage Mixtures

Table 10: Statistical T-Test p-Values for Dynamic Modulus of Virgin Silo Storage Mixtures

		0 hrs vs. 2.5 hrs	0 hrs vs. 5 hrs	0 hrs vs. 7.5 hrs
4.4° C	25 Hz	0.850	0.213	0.044
	10 Hz	0.474	0.265	0.063
	5 Hz	0.272	0.336	0.091
	1 Hz	0.190	0.390	0.103
	0.5 Hz	0.166	0.413	0.098
	0.1 Hz	0.405	0.422	0.092
21.1° C	25 Hz	0.145	0.046	0.001
	10 Hz	0.159	0.049	0.001
	5 Hz	0.155	0.052	0.000
	1 Hz	0.168	0.069	0.001
	0.5 Hz	0.148	0.064	0.001
	0.1 Hz	0.168	0.083	0.000
37.8° C	25 Hz	0.106	0.056	0.003
	10 Hz	0.098	0.044	0.002
	5 Hz	0.116	0.041	0.002
	1 Hz	0.147	0.050	0.001
	0.5 Hz	0.152	0.044	0.001
	0.1 Hz	0.225	0.091	0.002

Table 11: Statistical T-Test p-Values for Dynamic Modulus of 25% RAP Silo Storage Mixtures

		0 hrs vs. 2.5 hrs	0 hrs vs. 5 hrs	0 hrs vs. 7.5 hrs	0 hrs vs. 10 hrs
4.4° C	25 Hz	0.154	0.093	0.052	0.038
	10 Hz	0.130	0.070	0.044	0.025
	5 Hz	0.131	0.063	0.041	0.057
	1 Hz	0.153	0.061	0.044	0.057
	0.5 Hz	0.173	0.124	0.104	0.063
	0.1 Hz	0.152	0.098	0.087	0.052
21.1° C	25 Hz	0.149	0.093	0.079	0.043
	10 Hz	0.164	0.096	0.086	0.046
	5 Hz	0.173	0.093	0.087	0.047
	1 Hz	0.170	0.038	0.078	0.039
	0.5 Hz	0.164	0.037	0.074	0.008
	0.1 Hz	0.097	0.035	0.024	0.007
37.8° C	25 Hz	0.143	0.061	0.076	0.066
	10 Hz	0.134	0.059	0.070	0.055
	5 Hz	0.079	0.058	0.064	0.046
	1 Hz	0.080	0.058	0.018	0.010
	0.5 Hz	0.084	0.060	0.017	0.008
	0.1 Hz	0.101	0.066	0.015	0.008

Using the sigmoidal fit master curves, dynamic modulus ratios were calculated comparing each mixture to its respective 0 hours value. Figure 40 shows the ratio of dynamic modulus values with respect to the 0 hours master curve across all frequencies for the fitted master curves obtained from RHEA™. The averages of all these values are then summarized in Figure 41. Dynamic modulus ratios are also calculated using raw data (not fitted) in Figure 42 and Figure 43.

The figures show that the virgin mixtures exhibit a slightly higher ratio in the lower frequencies, and the ratio increases with storage time. On average, the 7.5 hours virgin mixture is approximately 1.3 times stiffer than the 0 hours mixture. Increases in dynamic modulus ratios are much greater among the lower frequencies and higher temperatures. Stiffening of the virgin

mixtures implies that there is short-term aging or additional binder absorption occurring within the silo, particularly at longer storage times such as 7.5 hours.

The RAP mixtures show higher ratios and larger differences across the frequency range than the virgin mixtures. The RAP mixture at 2.5 hours has a similar ratio to the virgin mixture at 7.5 hours. It is clear that the RAP mixture experiences greater stiffness changes than the virgin mixture as silo storage time increases. This could imply that there is blending or diffusion between RAP and virgin binders in the silo, in addition to short-term aging that is experienced with the virgin mixture. The differences in air void contents could also be contributing to some of the stiffening observed.

The dynamic modulus results also demonstrate the behavior of asphalt mixtures in regards to aggregate/ binder dominance. At the high frequencies (low temperatures) area of the master curve, binder is more dominant; at low frequencies (high temperatures), the aggregate skeleton is more dominant due to the soft binder. The aggregate skeleton dominance is apparent in the semi-log master curves. Any aging from silo storage time is less impactful on the areas where aggregate skeleton is more dominant because aggregates do not age like binders. The greater separation observed in the log-log master curves and ratio figures are a function of the lower dynamic modulus values among the low frequencies/high temperatures.

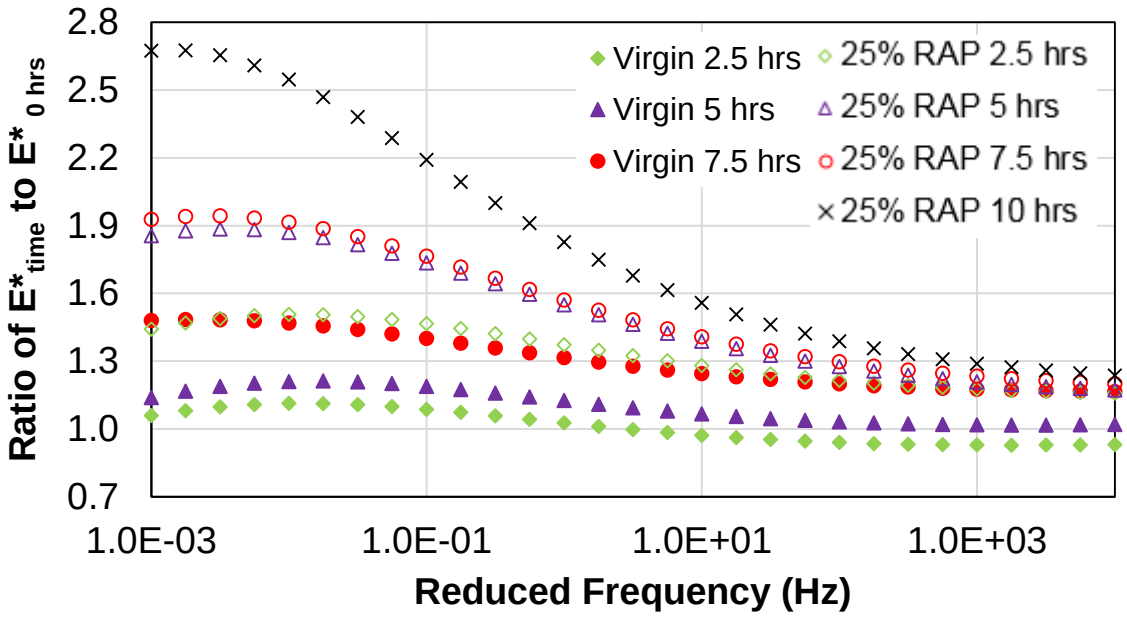

Figure 40: Dynamic Modulus Ratios of Fitted Data for Silo Storage Mixtures

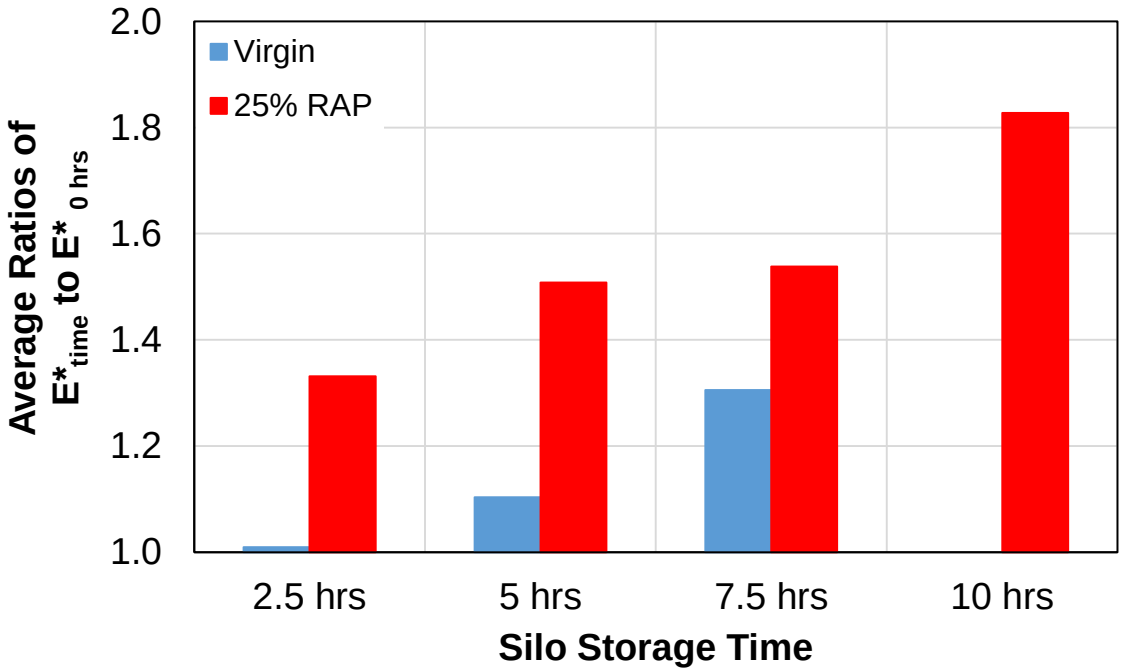

Figure 41: Dynamic Modulus Average Ratios for Silo Storage Mixtures

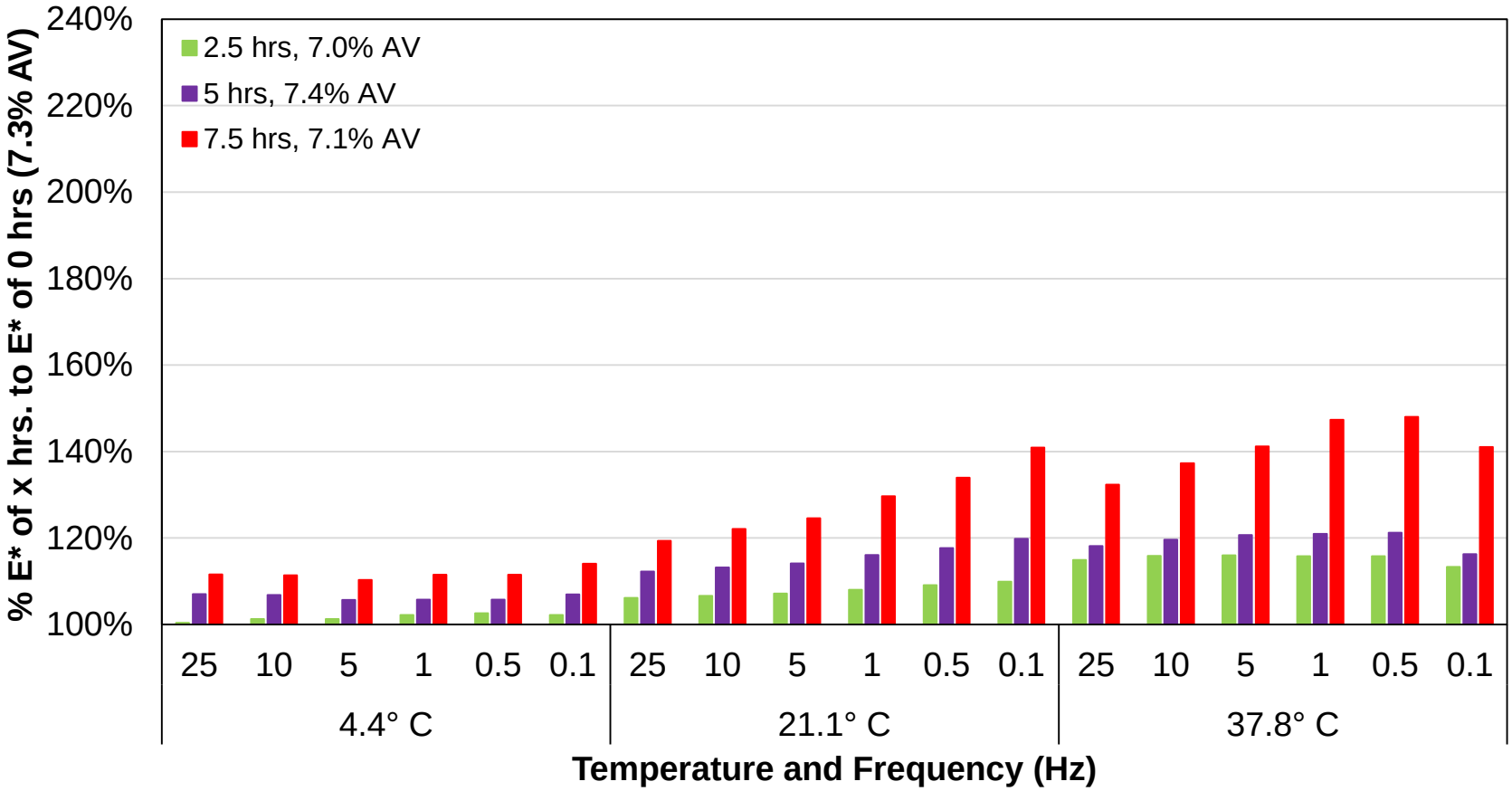

Figure 42: Dynamic Modulus Ratios of Raw Data for Virgin Silo Storage Mixtures

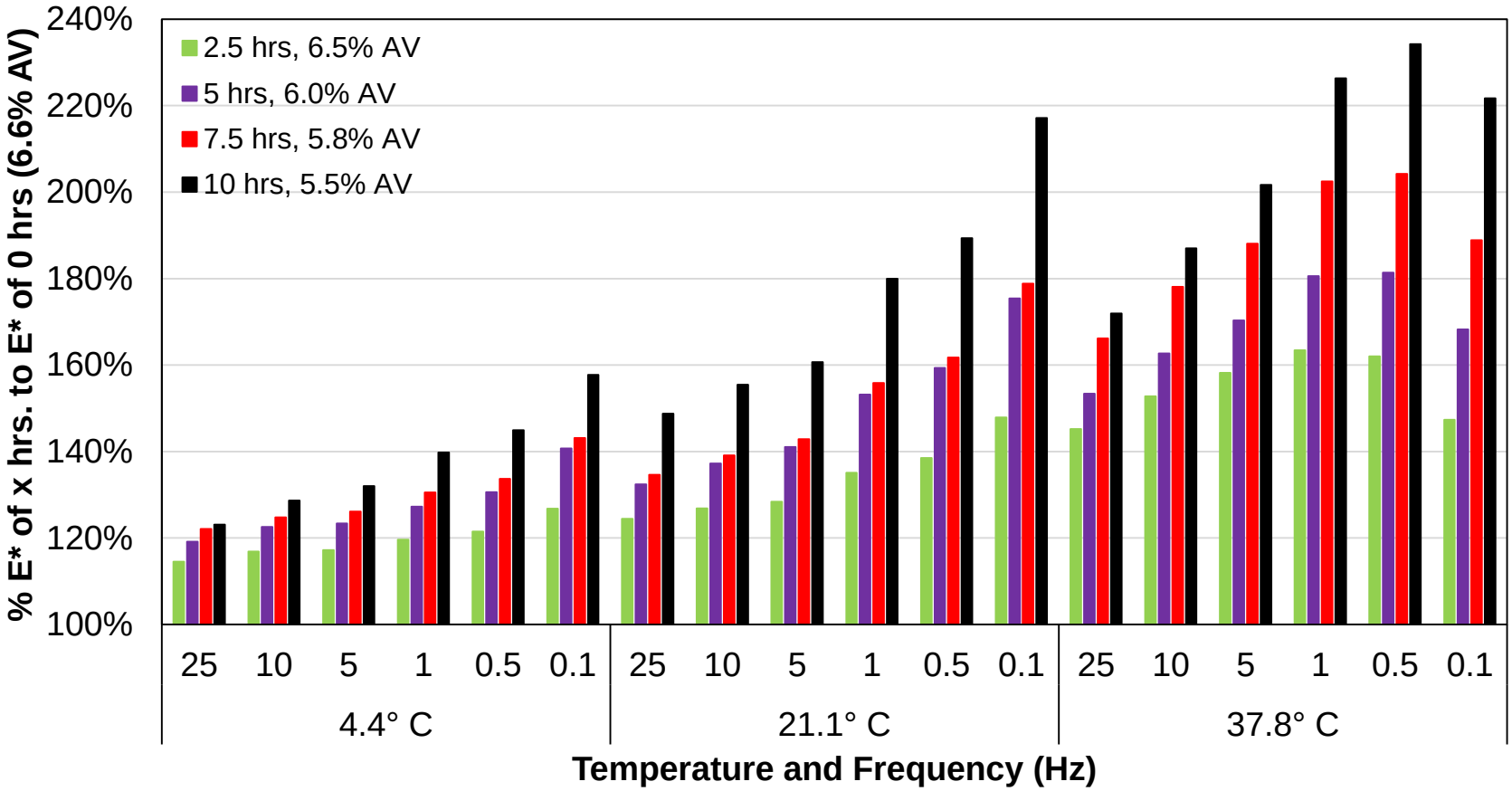

Figure 43: Dynamic Modulus Ratios of Raw Data for 25% RAP Mixtures

Figure 44 and Figure 45 show Black Space plots for the virgin and RAP mixtures. In Black Space, lower phase angles at similar modulus values indicate that the mixture may be more prone to cracking. The red bands are shown in the figures to aid in evaluating mixtures in Black Space. As the data points migrate from the solid band to the dashed band, the mixture exhibits more elastic behavior, indicative of age hardening. At higher stiffness values, the silo storage time has little effect on the phase angle for both mixtures. At lower stiffness values and near the inflection point, there is a decrease in phase angle with longer storage times. The virgin mixture shows larger differences near the inflection point and the RAP mixture shows larger differences at the low stiffness values.

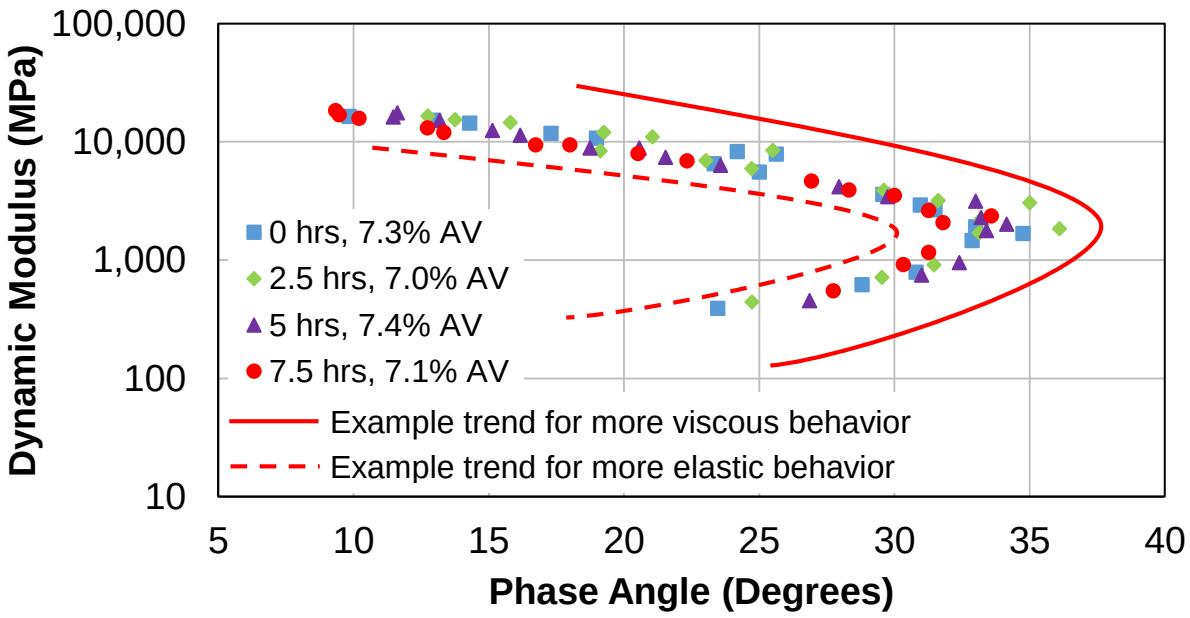

Figure 44: Black Space Plots for Virgin Silo Storage Mixtures

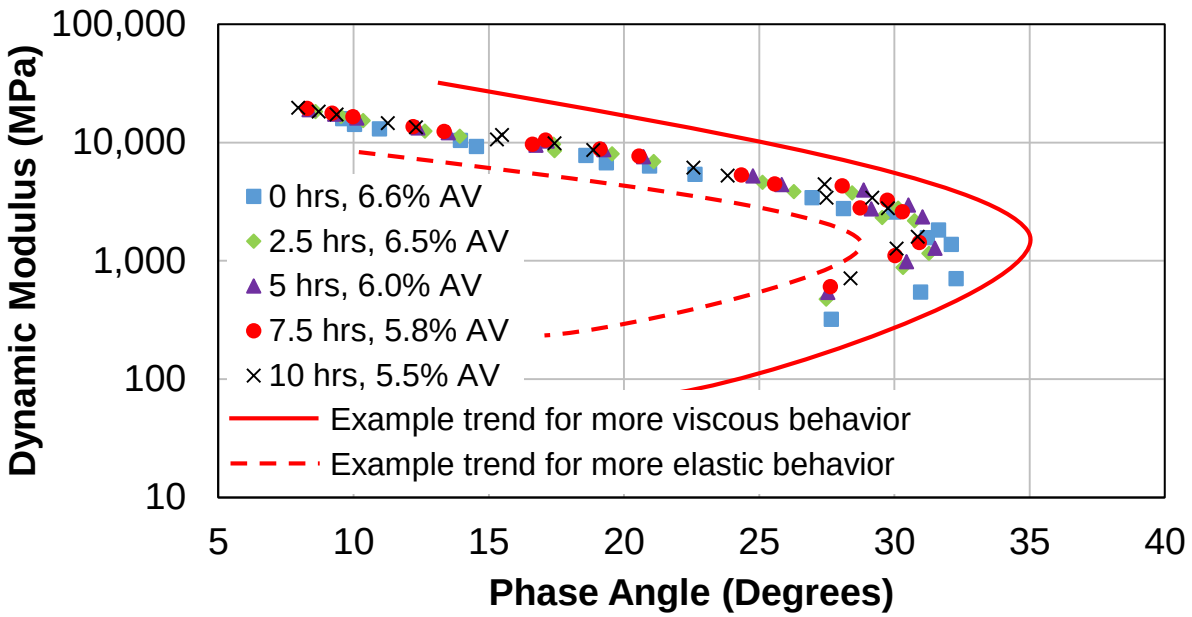

Figure 45: Black Space Plots for 25% RAP Silo Storage Mixtures

Phase angle master curves were constructed similar to the dynamic modulus master curve construction, as the isotherms were shifted in RHEA™ to form one curve. The phase angle master curves are shown in Figure 46 and Figure 47 for the virgin and 25% RAP mixture, respectively. In general, the phase angles were lower among the higher storage times, indicating more elastic behavior and potential age hardening of the mixtures. Statistical analyses (Table 12 and Table 13) of the phase angle raw data generally show little statistical significance, but the RAP mixture does show significance at 7.5 and 10 hours. It should be noted that phase angle results are often more variable than dynamic modulus results, particularly at lower frequencies (higher temperatures).

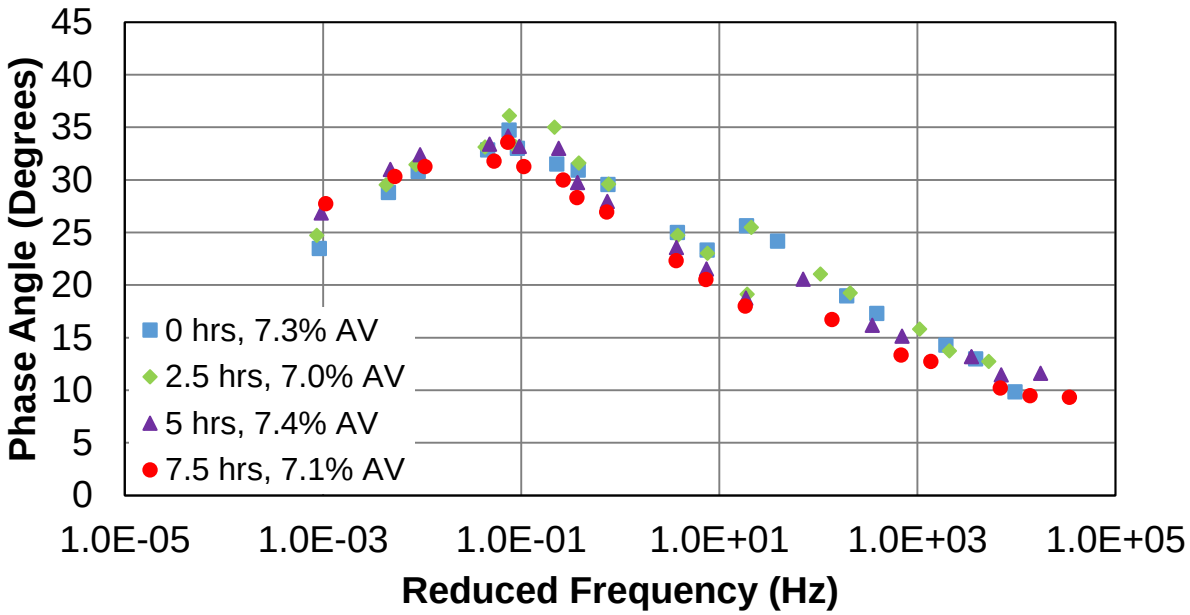

Figure 46: Phase Angle Master Curves for Virgin Silo Storage Mixtures

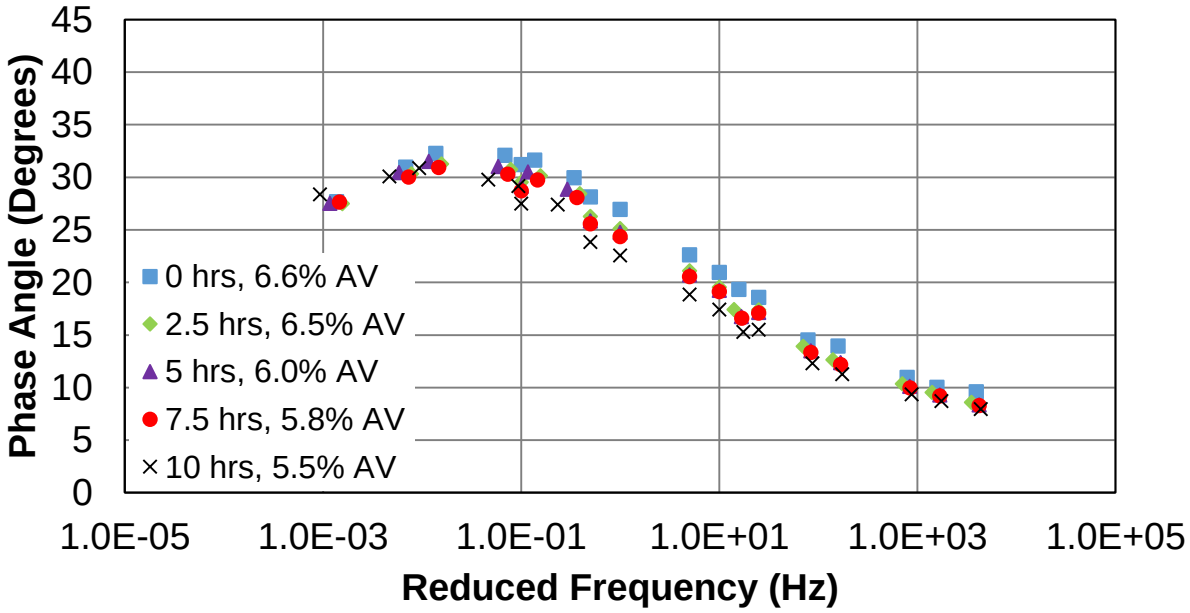

Figure 47: Phase Angle Master Curves for 25% RAP Silo Storage Mixtures

Table 12: Statistical T-Test p-Values for Phase Angles of Virgin Silo Storage Mixtures

		0 hrs vs. 2.5 hrs	0 hrs vs. 5 hrs	0 hrs vs. 7.5 hrs
4.4° C	25 Hz	0.227	0.545	0.810
	10 Hz	0.784	0.657	0.248
	5 Hz	0.649	0.772	0.213
	1 Hz	0.590	0.600	0.213
	0.5 Hz	0.596	0.540	0.162
	0.1 Hz	0.751	0.461	0.099
21.1° C	25 Hz	0.004	0.004	0.001
	10 Hz	0.714	0.111	0.182
	5 Hz	0.745	0.181	0.239
	1 Hz	0.968	0.174	0.254
	0.5 Hz	0.501	0.295	0.261
	0.1 Hz	0.296	0.665	0.662
37.8° C	25 Hz	0.256	0.725	0.656
	10 Hz	0.696	0.824	0.034
	5 Hz	0.602	0.374	0.116
	1 Hz	0.420	0.135	0.622
	0.5 Hz	0.394	0.012	0.033
	0.1 Hz	0.360	0.035	0.010

Table 13: Statistical T-Test p-Values for Phase Angles of 25% RAP Silo Storage Mixtures

		0 hrs vs. 2.5 hrs	0 hrs vs. 5 hrs	0 hrs vs. 7.5 hrs	0 hrs vs. 10 hrs
4.4° C	25 Hz	0.051	0.008	0.008	0.003
	10 Hz	0.595	0.389	0.346	0.160
	5 Hz	0.456	0.296	0.228	0.084
	1 Hz	0.118	0.044	0.052	0.005
	0.5 Hz	0.602	0.378	0.268	0.079
	0.1 Hz	0.145	0.060	0.074	0.011
21.1° C	25 Hz	0.179	0.051	0.010	0.001
	10 Hz	0.199	0.057	0.004	0.001
	5 Hz	0.191	0.049	0.002	0.001
	1 Hz	0.131	0.056	0.002	0.002
	0.5 Hz	0.139	0.047	0.003	0.002
	0.1 Hz	0.202	0.046	0.000	0.003
37.8° C	25 Hz	0.180	0.254	0.015	0.005
	10 Hz	0.152	0.205	0.011	0.004
	5 Hz	0.145	0.155	0.006	0.002
	1 Hz	0.105	0.077	0.039	0.037
	0.5 Hz	0.189	0.277	0.155	0.175
	0.1 Hz	0.857	0.895	0.974	0.535

The dynamic modulus sigmoidal fit functions were used to determine the inflection point frequency (Figure 48) and the Kaelble modified WLF C_2 (Figure 49) parameter. The virgin and RAP mixtures decrease in inflection point frequency from 0 hours to 5 hours, then the virgin mixture slightly increases while the RAP mixture stays constant and then decreases at 10 hours. A decrease in inflection point frequency indicates that the mixture transitions from a viscous state to an elastic state sooner. The modified WLF Kaelble C_2 parameter from the shift factor curve shows similar values at the shorter storage times then an increase at the later storage time for both the virgin and RAP mixtures. This indicates that the mixtures have reduced temperature susceptibility at longer storage times, particularly 7.5-10 hours.

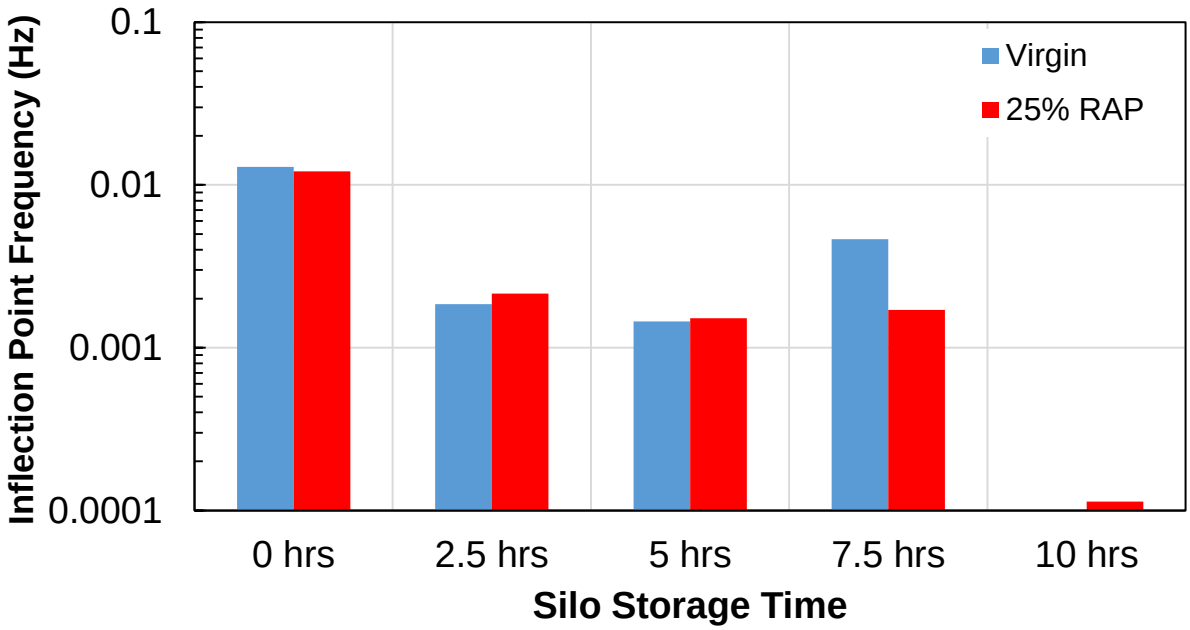

Figure 48: Inflection Point Frequency Values for Silo Storage Mixtures

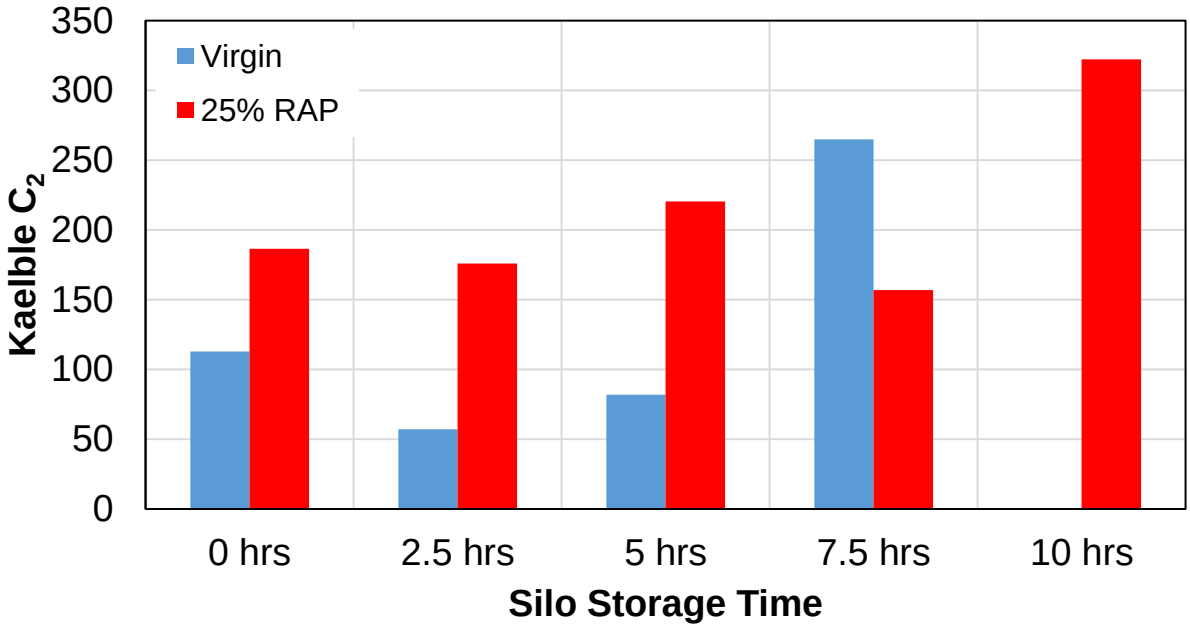

Figure 49: Kaelble C_2 Values for Silo Storage Mixtures

The comparison of plant compacted specimens and reheated lab compacted specimens were also of interest in this study. Dynamic modulus testing was performed on the 25% RAP

reheated loose mix compacted in the laboratory (PMLC) for comparison to the results presented above; Figure 50 summarizes these results. The lab-compaction method certainly causes stiffening of the mixtures, potentially up to 230%. The increases are greater among lower frequencies and higher temperatures. A comparison of fabrication methods such as reheating is also explored in Section 4.3 Mixture Testing for Specimen Fabrication Methods Study.

It is also interesting to note that the higher storage times (7.5 and 10 hours) experienced almost no difference between laboratory compacted and plant compacted methods. This reinforces the concept of RAP-virgin blending within the silo. The laboratory reheating method causes the RAP and virgin binders to blend because full blending is not achieved after typical production phases (i.e. 0 hours of storage time). When materials are stored for longer times in the silo, the blending caused by laboratory reheating is mitigated because much of the blending and stiffening already occurred as a result of being kept in the silo. It was observed that laboratory reheating of the 0 hours mixture caused similar effects to longer storage times, as both events stiffened the mixtures significantly (230%).

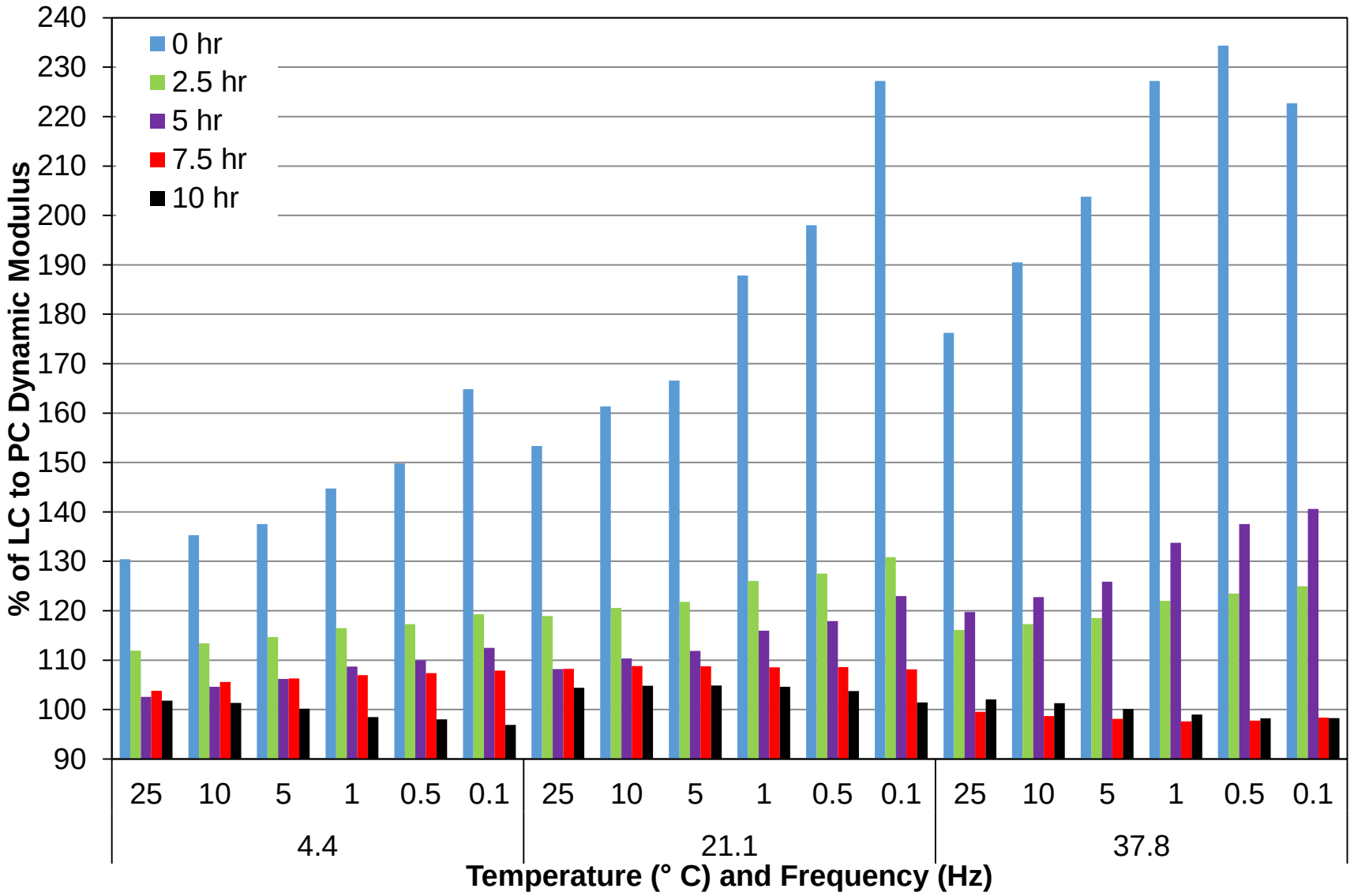

Figure 50: Dynamic Modulus Ratios of Lab Compacted to Plant Compacted 25% RAP Silo Storage Mixtures

4.2.2 S-VECD Fatigue Cracking

The results from the S-VECD testing and analysis on the virgin mixtures are shown in Figure 51 to Figure 55. Fatigue data for the 25% RAP mixtures was not available due to lack of materials. The damage characteristic curves for each of the individual replicate specimens are shown in the Appendix, while Figure 51 represents the average behavior of the replicate specimens. In the damage characteristic curves, C represents normalized pseudo-stiffness while S represents damage as the test progresses. The plots show a clear increase in pseudo-stiffness with an increase in silo storage time. This typically indicates better fatigue resistance, but the fatigue performance cannot be fully characterized until the entire pavement structure is considered.

Figure 52 shows the relationship between the failure criterion G^R, a parameter that characterizes damage accumulation, and number of cycles to failure, N_f. Typically, mixtures that are closer to the upper right corner of the G^R-N_f space indicate better fatigue resistance. There appears to be little distinction between the mixtures, but it is important to keep in mind that fatigue performance in the field also depends on the location within the pavement structure and loading conditions.

One method of simplifying the G^R-N_f space into one value that has been introduced recently is the index parameter, N_f at $G^R = 100$. This value was obtained using the power-law equation that forms the lines in Figure 52 and identifying the value at which $G^R = 100$. The index parameter values are shown in Figure 53. Greater N_f values indicate better fatigue resistance, but again, there seems to be little distinction between these mixes. Other S-VECD fatigue analyses included strain vs. N_f (Figure 54) and endurance limit predictions (Figure 55). It was observed that silo storage time did not have a significant effect on the number of cycles to failure for various strain levels. Although the 5 hours mixture has a higher number of cycles to failure at similar strain

levels, there is not a consistent trend among the mixtures. A similar observation was made for the endurance limit, which represents the strain level below which there will be no damage accumulation. Again, the silo storage time of 5 hours indicated a greater endurance limit, but there was not a consistent trend observed with the other storage times.

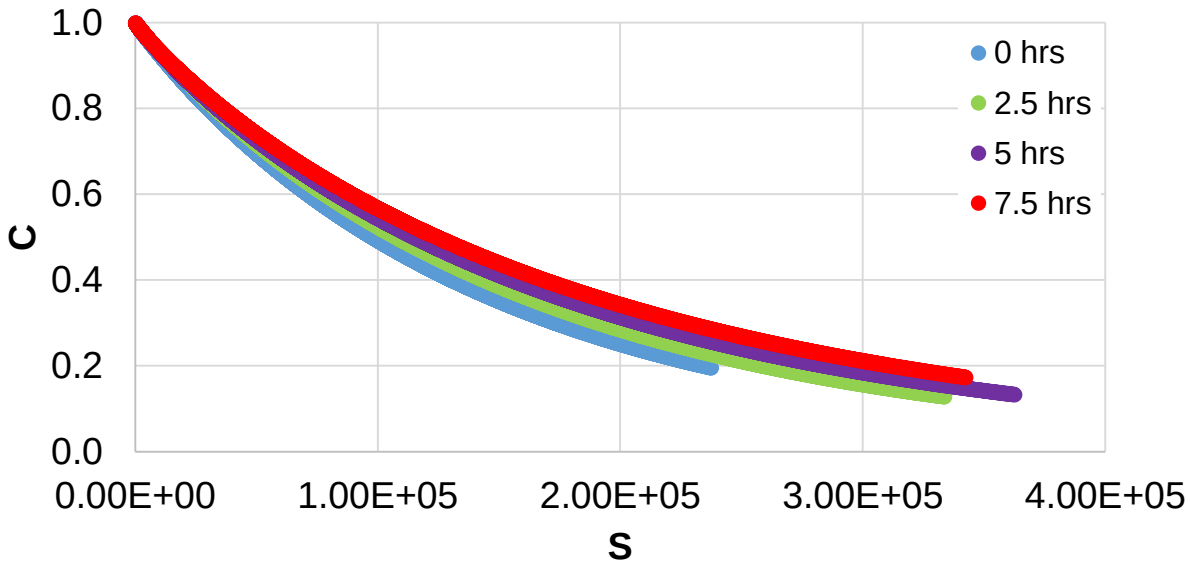

Figure 51: S-VECD Fatigue Damage Characteristic Curves for Virgin Silo Storage Mixtures

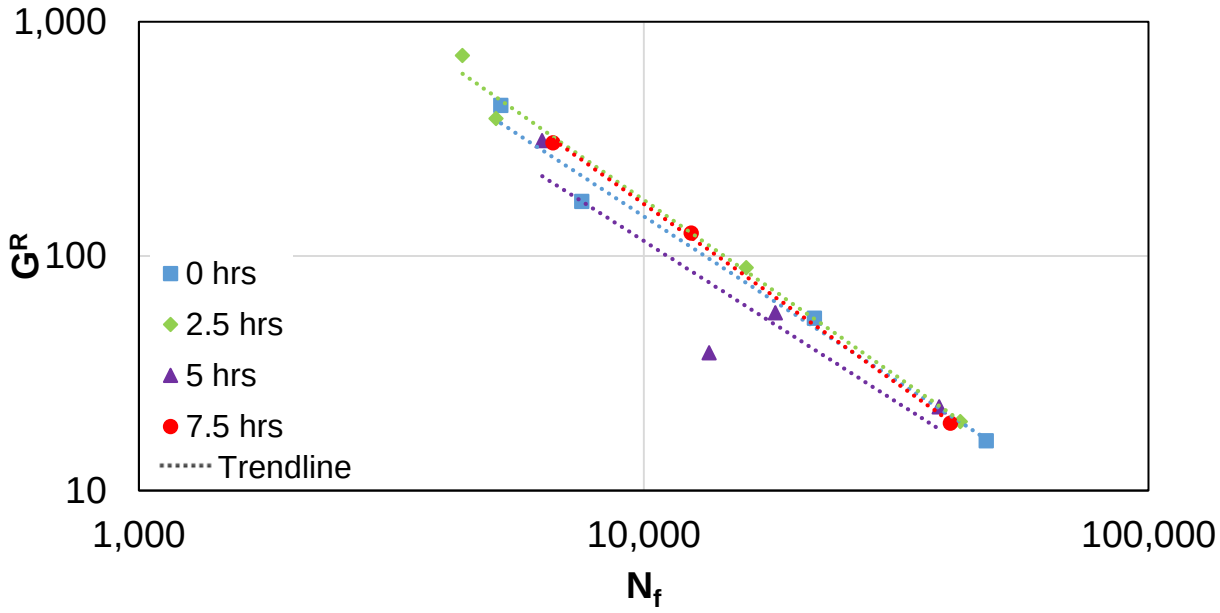

Figure 52: S-VECD Fatigue Failure Criterion Results for Virgin Silo Storage Mixtures

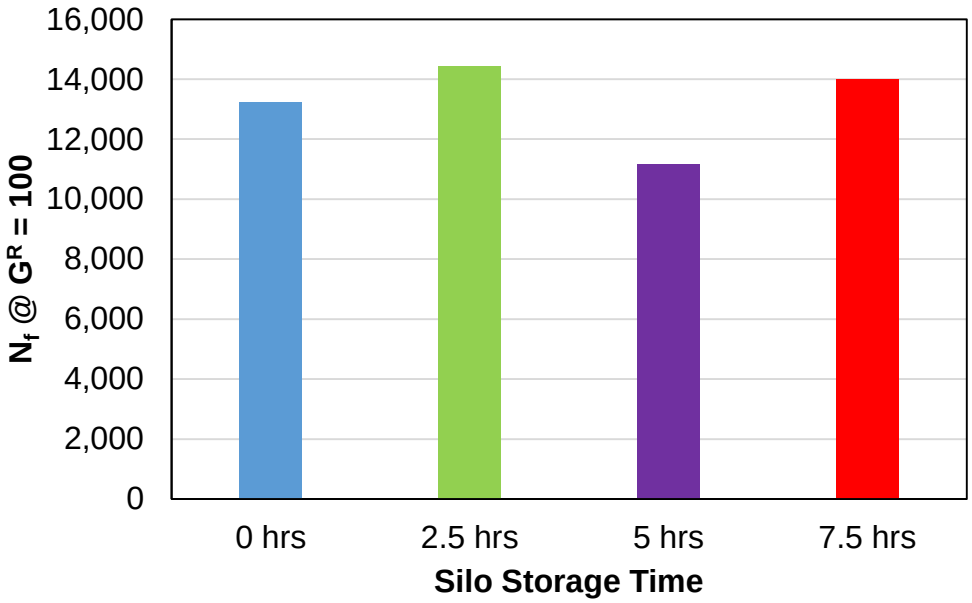

Figure 53: S-VECD Fatigue Index Parameter Results for Virgin Silo Storage Mixtures

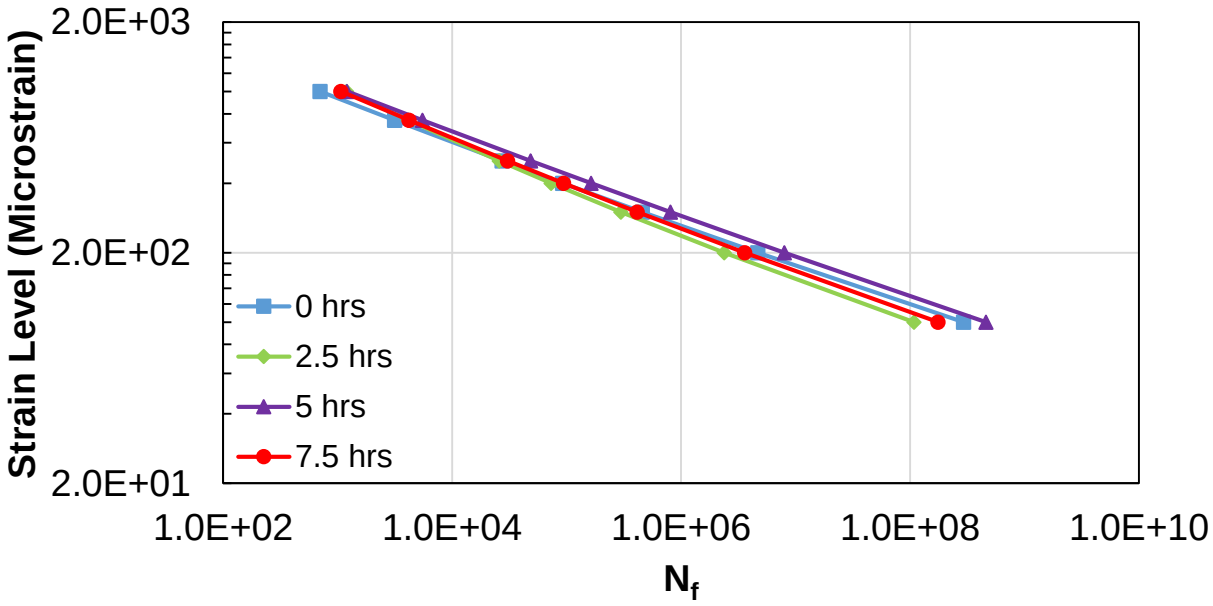

Figure 54: S-VECD Fatigue Strain Level versus Number of Cycles to Failure for Virgin Silo Storage Mixtures

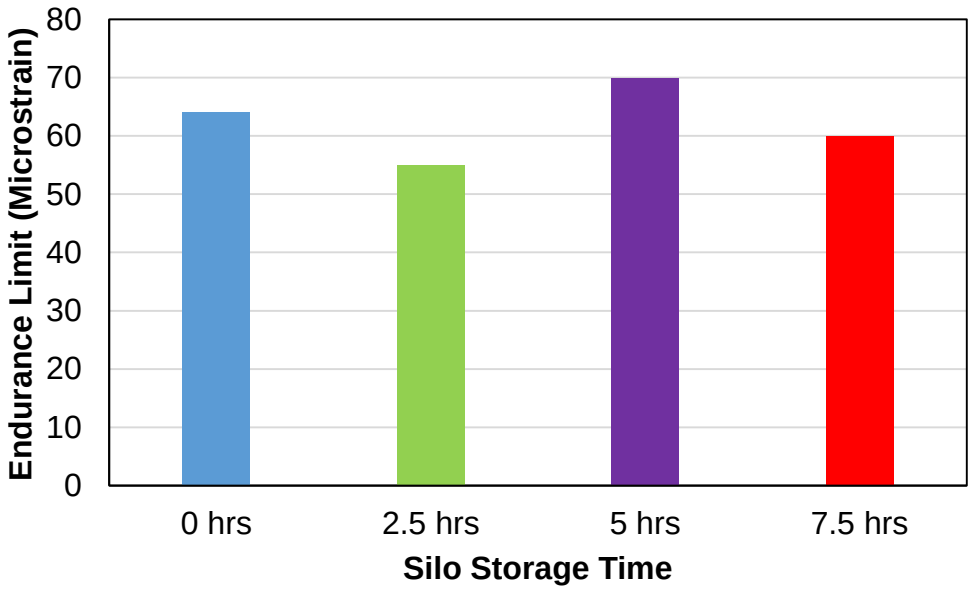

Figure 55: S-VECD Fatigue Endurance Limit Results at 20.0° C for Virgin Silo Storage Mixtures

4.2.3 LVECD Pavement Fatigue Life Evaluation

The layered viscoelastic critical distresses (LVECD) pavement fatigue life evaluation software was also performed on the virgin mixtures by members of the research team at NCSU. LVECD uses results from the dynamic modulus and S-VECD fatigue data. Therefore, the RAP mixture was not available for this analysis because of the absence of fatigue data. Figure 56 and Figure 57 present the results from LVECD analysis for thin and thick pavements in climates of Boston, MA and Raleigh, NC, respectively. Although LVECD was verified by several researchers (Park and Kim, 2013, Norouzi and Kim, 2015) for various conditions, this software has not been fully calibrated, and the transfer function to convert the predicted damage obtained from LVECD to cracking area in the field is still under development. Therefore, quantitative numbers such as amount of cracking cannot be accurately predicted, but a ranking of the mixtures and relative damage is appropriate. The results show that an increase in silo storage time causes increases in fatigue damage for both types of pavements and climates. In both climates and pavement

structures, the 7.5 hours storage time experienced much more damage than the 0 hours condition, while the intermediate times were similar in magnitude. Increases of approximately 40% from 0 to 7.5 hours storage times for the thin pavements and tripling of the damage for thick pavements were observed, although the magnitude of damage in thick pavements is much lower.

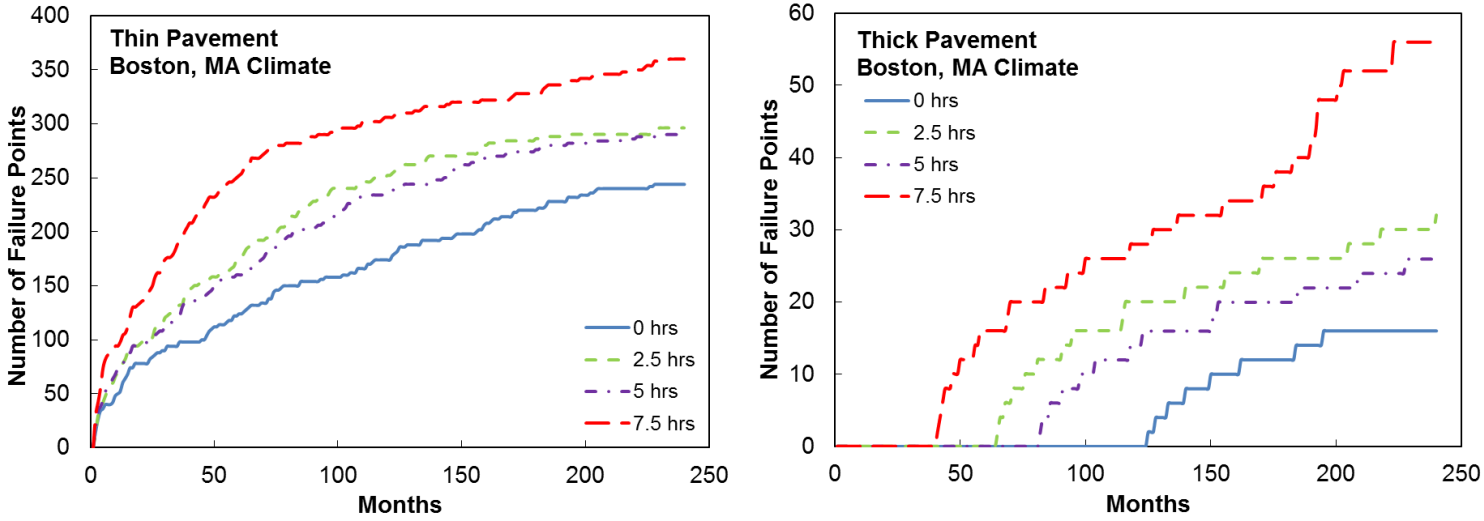

Figure 56: LVECD Analysis Results for Virgin Silo Storage Mixtures in Boston, MA Climate

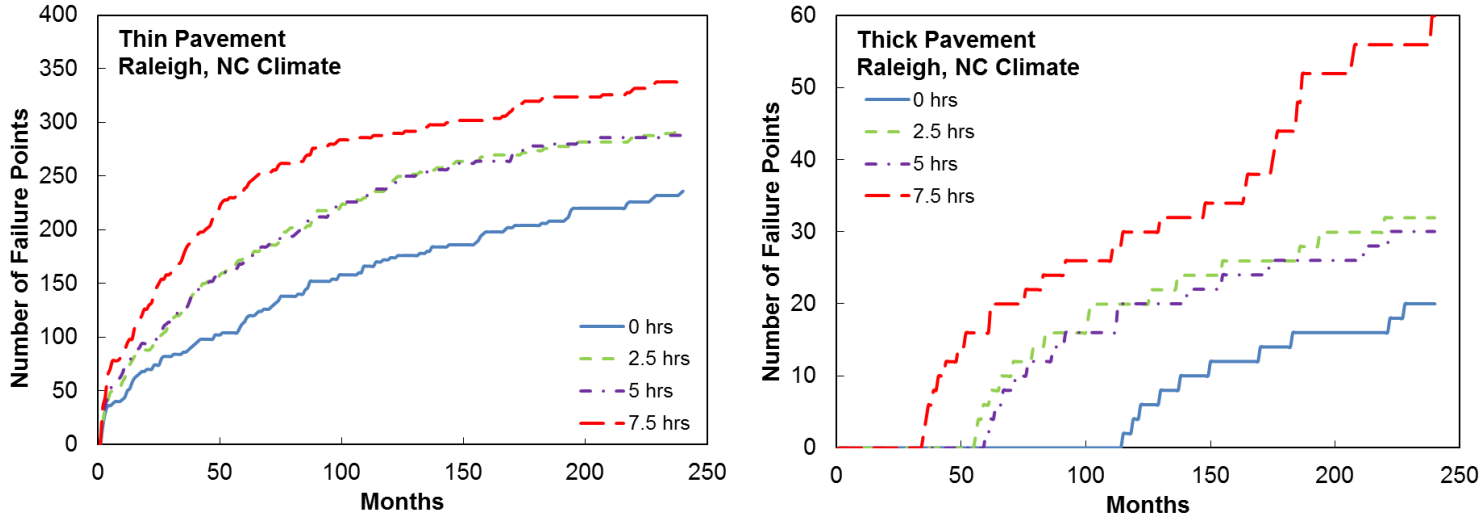

Figure 57: LVECD Analysis Results for Virgin Silo Storage Mixtures in Raleigh, NC Climate

4.3 MIXTURE TESTING FOR SPECIMEN FABRICATION METHODS STUDY

The main objective of this study was to compare four different fabrication types: plant mixed, plant compacted (PMPC), plant mixed, lab compacted (PMLC), lab mixed, lab compacted (LMLC), and small geometry specimens obtained from field cores. For each fabrication type, six mixtures were evaluated: Virgin, PG 58-28; 15% RAP, PG 58-28; 25% RAP, PG 58-28; 25% RAP, PG 52-34; 30% RAP, PG 52-34; and 40% RAP, PG 52-34. A small specimen methodology (38 mm x 110 mm) was explored for use with the field cores obtained from test sections. The effect of RAP content and binder grade among the field core mixtures is presented in this section, along with a comparison of the four fabrication methods. Mixture testing performed on the small specimens included dynamic modulus stiffness tests and S-VECD cyclic fatigue tests. A comparison of fabrication types was explored through those same test methods.

An evaluation of RAP content and binder grades among the PMPC, PMLC, and LMLC mixtures can be found in Appendix A: PMPC, PMLC, and LMLC Results. Dynamic modulus and S-VECD fatigue testing were performed by other UNH researchers on these materials. Key conclusions from those results are as follows:

- **PMPC Mixtures:** The PG 58-28 base binder mixtures experienced a slight stiffening effect and lower phase angles with increasing RAP content, as expected. However, the PG 52-34 mixtures showed the opposite trend in Black Space, as increasing RAP content caused an increase in phase angle, which was not expected. The PG 52-34 base binder mixtures also showed softer response than the virgin PG 58-28 mixture and slight increases in stiffness with increasing RAP content. In summary, the base binder grade showed a larger impact on the dynamic modulus than the RAP content.

- **PMLC Mixtures:** The stiffness of both the PG 58-28 and PG 52-34 base binder mixtures showed a decrease in stiffness with increasing RAP content and the 25% RAP, PG 52-34 mixture had a higher stiffness than the 25% RAP, PG 58-28 mixture. These results do not follow expected trends with RAP content and binder grade.
- **LMLC Mixtures:** The phase angles for the PG 52-34 mixtures did not follow expected trends with RAP content or in relation to the PG 58-28 mixtures. Also, the base binder PG grade showed a larger impact on the dynamic modulus and phase angle than RAP percentage.

4.3.1 Field Core Specimens: Dynamic Modulus Results

Cores were taken from each of the test sections in the field and then two small geometry specimens were fabricated from each field core. There were challenges testing the small geometry specimens at high temperatures; the small cross sectional area and soft binder grades required small loads that were close to the minimum capacity for AMPT control and resulted in a significant amount of creep in the specimens. For that reason, there is a large degree of variability in the results, particularly phase angle values, at the low frequency/high temperature range. The average dynamic modulus master curves created from three replicate specimens are shown in Figure 58 (log-log) and Figure 59 (semi-log) below. Air void contents were not controlled for these specimens as they were obtained from existing pavement sections; the average air void contents for the mixtures are shown in the legend.

At the intermediate and high frequency range, both the PG 58-28 and PG 52-34 base binder mixtures show an increase in stiffness with RAP content, and a decrease in stiffness for the mixtures with the softer base binder. The only exception is the 25% RAP 58-28 mixture, for which higher air void content may be contributing to the response. Differences in air void contents may

also contribute to the magnitude of difference between the 30% and 40% RAP mixtures. Statistical significance was determined using 95% confidence interval t-tests, and tabulated results from this analysis are shown in the Appendix. The PG 58-28 base binders are statistically similar to one another, except at the high frequencies where the 15% RAP 58-28 mixture is significantly different. The PG 52-34 base binder mixtures are all statistically similar.

The average Black Space curves and phase angle master curves for the field cores are shown in Figure 60 and Figure 61, respectively. Data from the high test temperature (30° C) are not included in these figures because of the uncertainty among the shift factors that were deemed misrepresentative of the mixture. The shifted phase angle isotherms for all test temperatures are included in the Appendix to provide a basis for removing the high temperature. It can be observed in these figures that the high temperature isotherms do not align with the master curve constructed from the other isotherms.

While most results are very similar to one another, there appears to be a slight decrease in phase angle (closer to the dashed band) among the higher RAP contents for the PG 58-28 base binder mixtures. The PG 52-34 base binder mixtures show an increase in phase angle with higher RAP content. The trends with the PG 52-34 base binders are not expected for a softer binder, but do follow the observations from the other specimen types that are summarized above and detailed in Appendix A: PMPC, PMLC, and LMLC Results. One possible explanation for the unexpected trend observed with the softer binder may be the method by which the PG 52-34 binder was produced. The presence of re-refined engine oil bottoms (REOB) could cause the observed behavior due to the manner in which these materials age. However, testing was not done for detection of REOB and its presence in the mixtures is purely speculative.

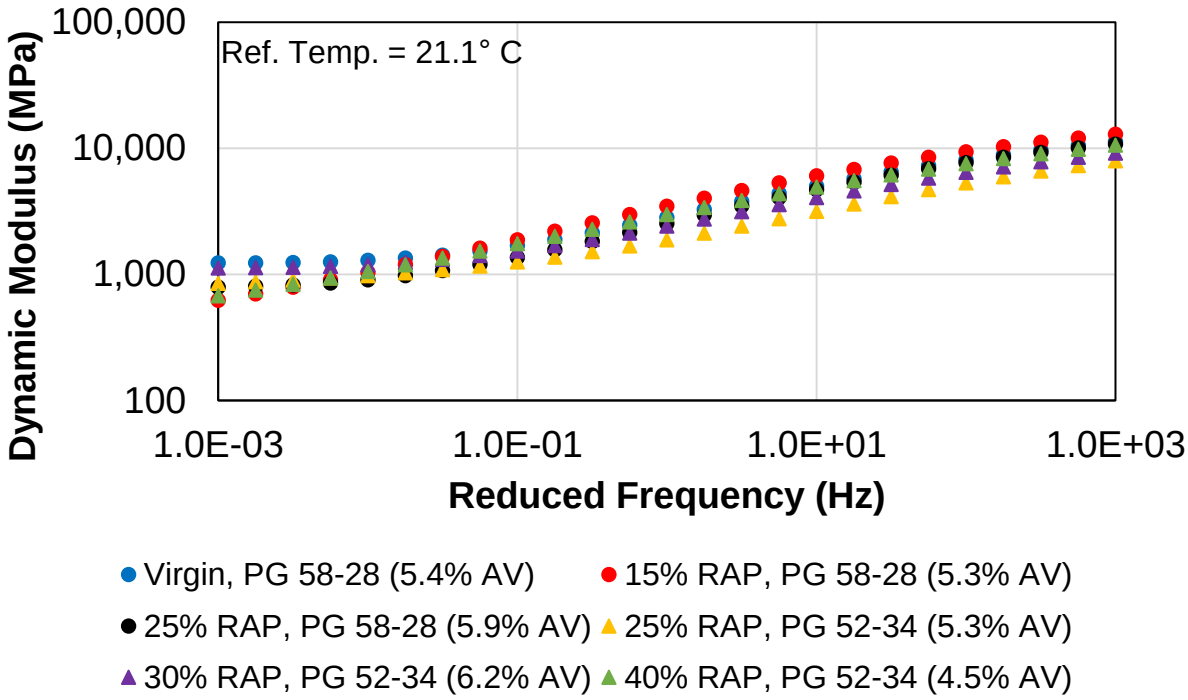

Figure 58: Dynamic Modulus Master Curve (log-log) for Field Core Mixtures

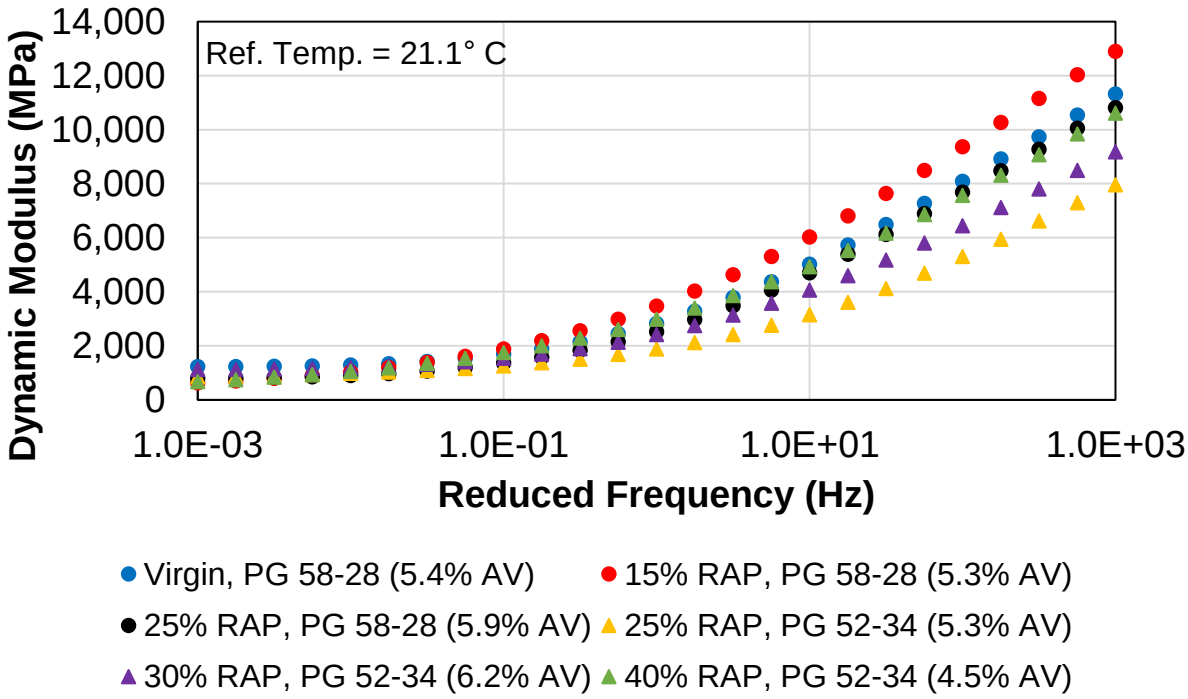

Figure 59: Dynamic Modulus Master Curve (semi-log) for Field Core Mixtures

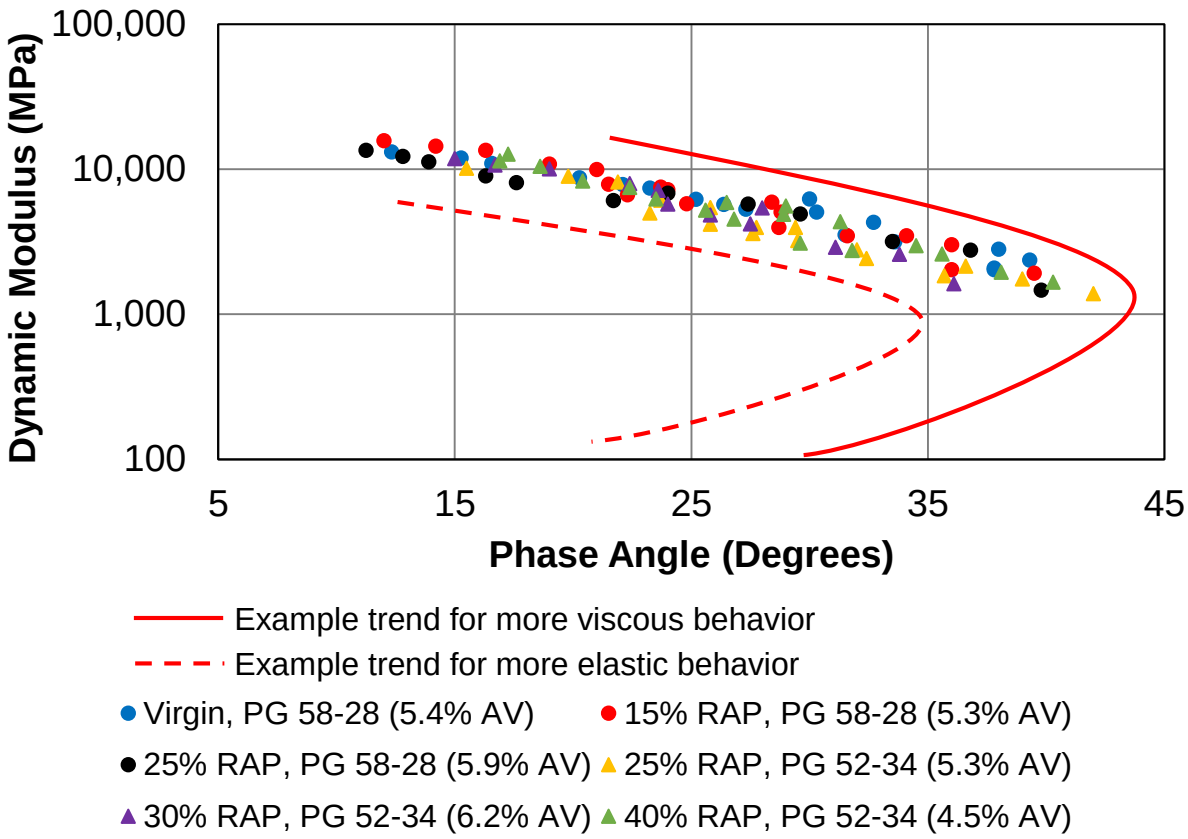

Figure 60: Black Space Plots for Field Core Mixtures

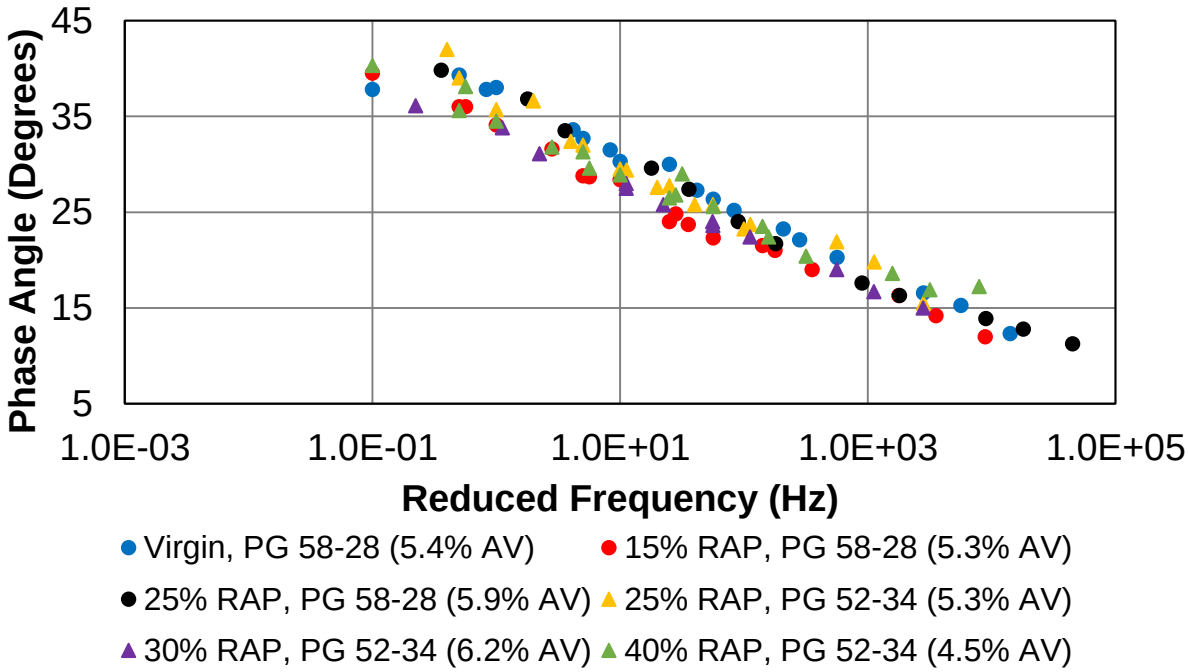

Figure 61: Phase Angle Master Curves for Field Core Mixtures

4.3.2 Field Core Specimens: S-VECD Fatigue Results

Testing on the small geometry specimens went smoothly with the modified setup, and there seemed to be no problems with using small specimens as an alternative to standard size specimens. The high creep levels observed at the high test temperatures can be overcome by installing a smaller load cell in the AMPT. Fatigue analysis on the small specimens obtained from field cores included damage characteristic curves (Figure 62), fatigue failure criterion (Figure 63), index parameter calculation (Figure 64), strain limit versus number of cycles to failure (Figure 65), and endurance limit (Figure 66). The damage characteristic curves are similar in terms of RAP contents (except the PG 52-34 25% RAP mixture), but the PG 52-34 binders exhibit lower pseudo-stiffness values. The fatigue failure criterion and index parameter results show that the PG 52-34 mixtures generally have better fatigue resistance, which is consistent with the other fabrication types. The PG 52-34 mixtures show better fatigue resistance (higher N_f at $G^R = 100$) with an increase in RAP content, which is opposite of the trend seen in PMLC mixtures. Figure 65 shows that higher RAP contents experience greater strain levels for similar number of cycles to failure, which indicates better fatigue resistance.

The endurance limit results interestingly show different effects of RAP content with the PG 58-28 base binder than with the PG 52-34 base binder. There is an increase in endurance limit (i.e. longer fatigue life) among the PG 58-28 binders as RAP content is increased, which aligns with the results seen in the other fatigue results (Figure 62 to Figure 65). However, the endurance limit for the PG 52-34 binder decreased as RAP content was increased, which is opposite the effect seen in the other figures. It should also be noted that analysis using the software alpha-Fatigue was not successful for two of the mixtures for predicting strain limit and endurance limit.

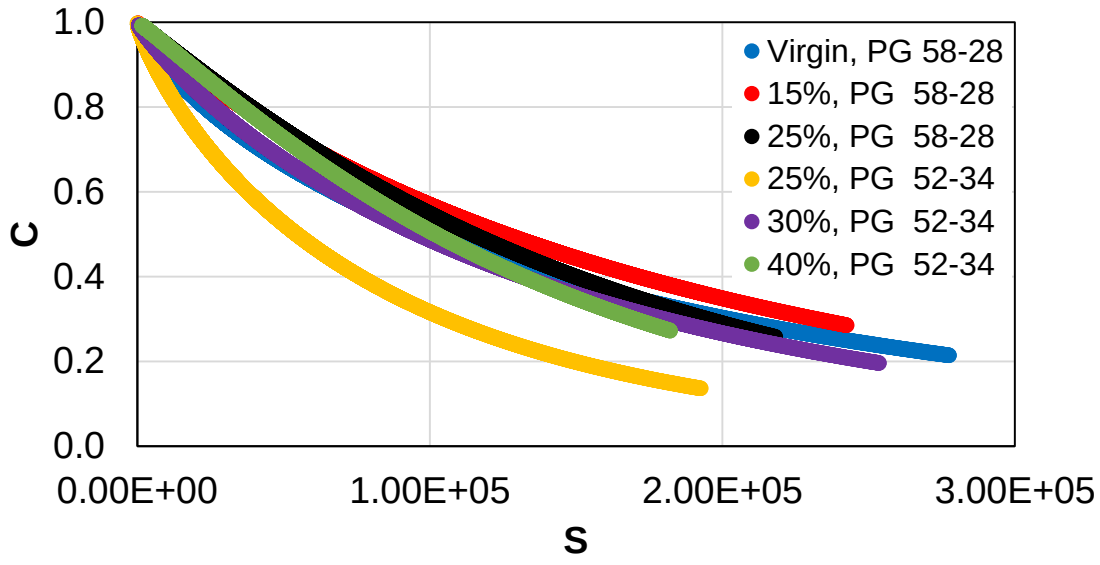

Figure 62: S-VECD Fatigue Damage Characteristic Curves for Field Core Mixtures

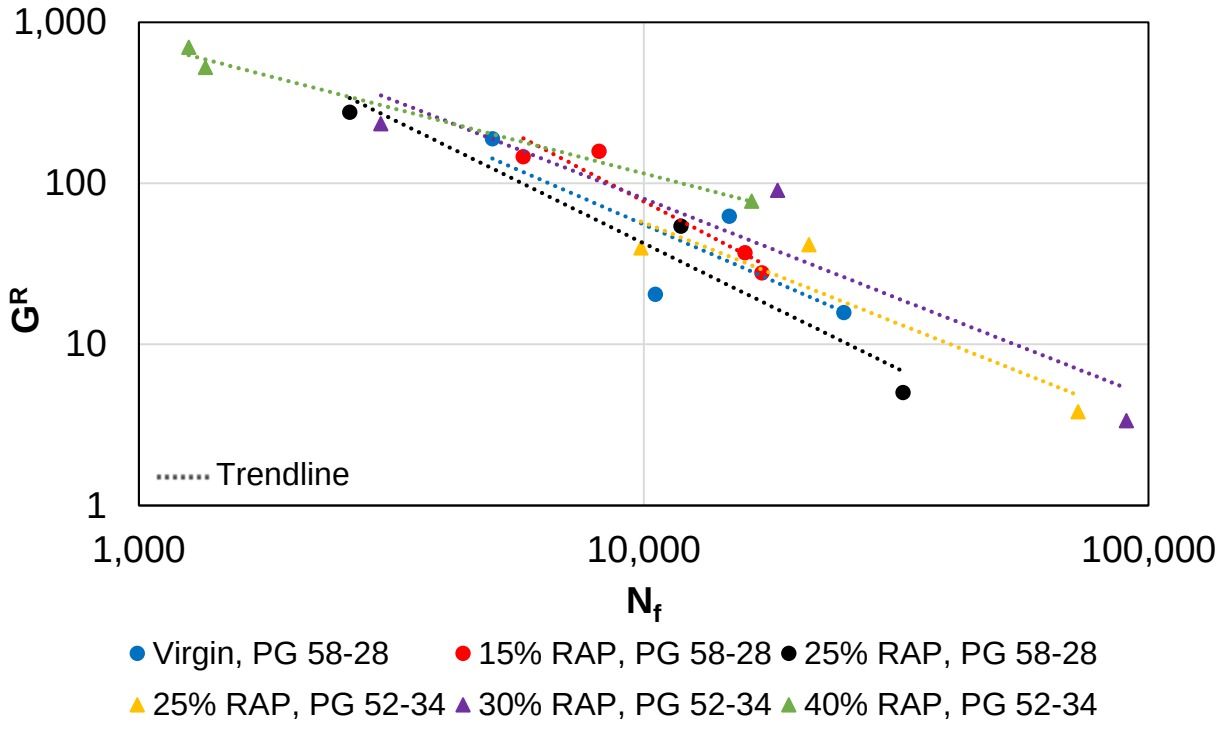

Figure 63: S-VECD Fatigue Failure Criterion Results for Field Core Mixtures

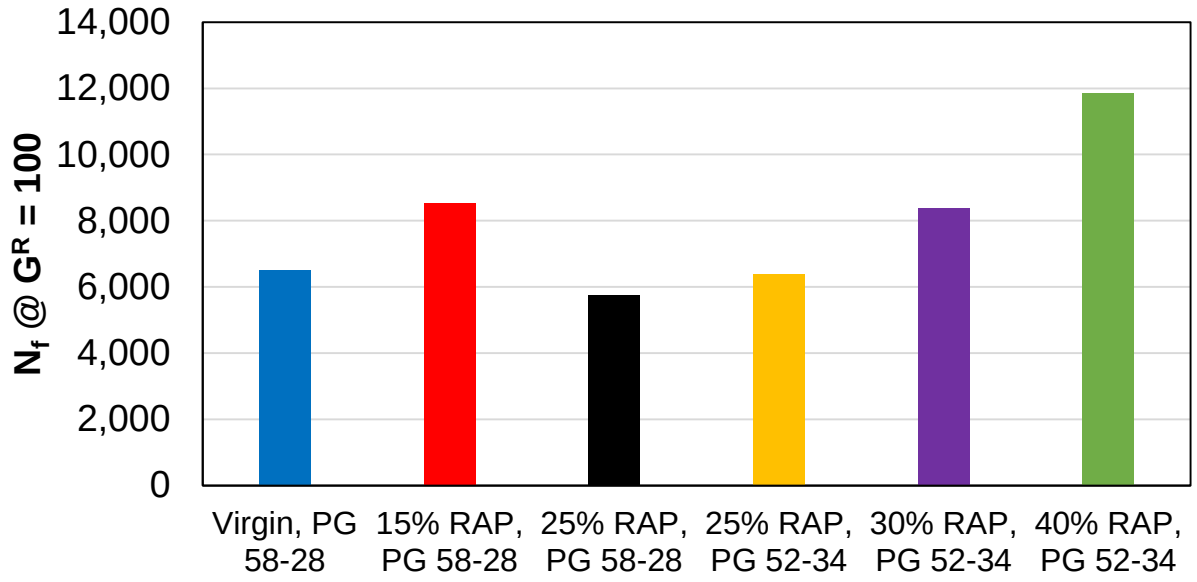

Figure 64: S-VECD Fatigue Index Parameter Results for Field Core Mixtures

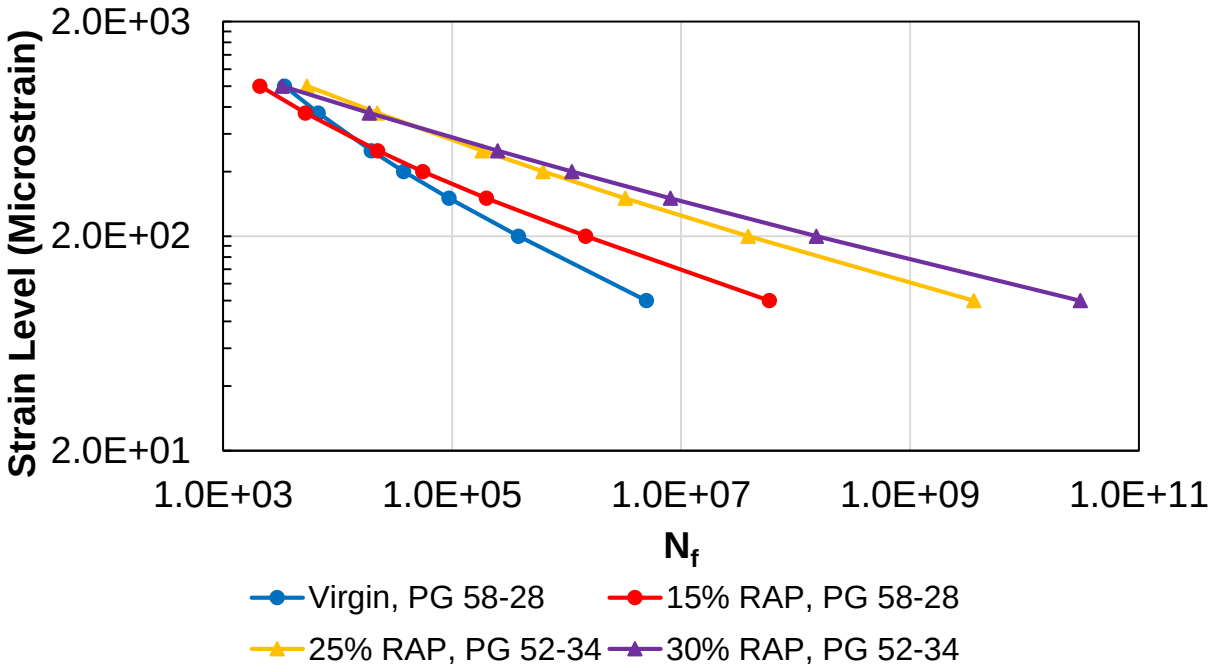

Figure 65: S-VECD Fatigue Strain Level versus Number of Cycles to Failure for Field Core Mixtures

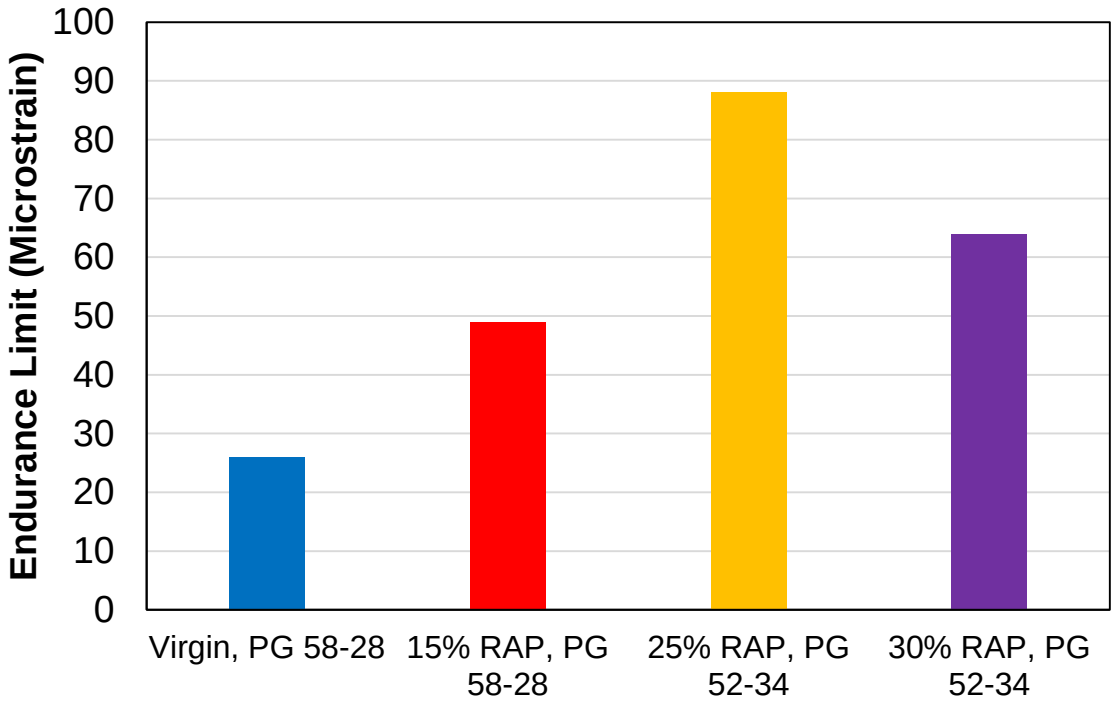

Figure 66: S-VECD Fatigue Endurance Limit Results at 20.0° C for Field Core Mixtures

4.3.3 Comparison of Fabrication Methods: Dynamic Modulus Results

The various specimen fabrication methods involved in the high RAP pooled fund study are compared with dynamic modulus results in Figure 67 to Figure 72 for each of the six mixtures. The PMPC, PMLC, and LMLC specimens all have air void contents that were controlled in the laboratory and are in the 6.5% to 7.5% range. Specimens fabricated from field cores have lower air void contents, as noted on each graph. Variability in the dynamic modulus raw data for these mixtures is shown in Figure 110 to Figure 112 in the Appendix. A simple ranking of the fabrication types in terms of dynamic modulus over a majority of the frequency range (intermediate to high frequencies) is summarized in Table 14. In general, the field core and PMLC mixtures were stiffest, followed by LMLC then PMPC fabrication methods. Figure 73 to Figure 78 compares all six mixtures in Black Space, and statistical analyses can be found in the Appendix. The field cores

were tested at different temperatures than the other specimen types; therefore, statistical comparisons were not possible for field cores versus other methods.

The impact of reheating the loose mixture for compaction in the laboratory is shown by comparing the PMLC and PMPC specimens. The lab compacted specimens (PMLC) have higher stiffness and the difference between the lab compacted and plant compacted stiffness decreases with higher RAP contents; for the 25% RAP 58-28 mixture, there is little difference between the PMPC and PMLC master curves. The differences are larger for the mixtures with the softer PG 52-34 binder. It is apparent that reheating the mixture causes an age hardening effect that is not replicated by plant compaction (PMPC). Similar results were observed with the silo storage mixtures, as the laboratory reheating caused significant stiffening. Among the higher RAP contents (and longer storage times), the effect of reheating is lower perhaps because there is sufficient amounts of already-aged material in the mixtures. RAP materials that have already been aged a significant amount possess a lower rate of aging, which is reflected by the reheating procedure for higher RAP contents. The curves in Black Space show little difference as a result of reheating the mixture.

The difference between measurements that would be made during the mix design process and those made on the material actually fabricated during plant production can be evaluated by comparing the LMLC and PMPC specimens. This comparison was only done for the virgin 58-28, 25% RAP 58-28, 25% RAP 52-34, and 40% RAP 52-34 mixtures. All of the LMLC master curves are stiffer than the PMPC master curves and are statistically different. The PG 58-28 mixtures show larger differences than the PG 52-34 mixtures between the LMLC and PMPC master curves. The mixtures with lower RAP contents also show larger differences between the LMLC and PMPC master curves. One likely reason for the differences in LMLC and PMPC master curves is the

differences in aging; the LMLC mixtures were subject to short-term oven aging while the PMPC mixtures were subject to aging through plant production. The higher asphalt content and finer gradations during production likely also contribute to the differences observed. A comparison of plant and laboratory mixing can also be compared between PMLC and LMLC specimens. Dynamic modulus results show that PMLC specimens are consistently stiffer than the LMLC specimens, indicating that the mixing process in the laboratory does not age the material as much as the plant does during production.

It is recognized that the Black Space curves for the LMLC specimens show much different curves than all the other fabrication types, and the inflection point occurs at lower phase angles (more elastic behavior). The LMLC curves display odd behavior for viscoelastic response in typical HMA mixtures. Testing and analysis of the LMLC mixtures was done by the FHWA mobile lab, and it was not clear as to the cause for the odd behavior of the Black Space curves. The shape of the dynamic modulus master curves for LMLC mixtures appears reasonable, but the phase angle values are suspect (apparent in the Black Space plots).

The impact of compaction method can be evaluated by comparing the PMPC specimens and the field cores. The dynamic modulus master curves for the field cores are consistently stiffer than those measured from the PMPC specimens, however the average air void contents of the field cores are lower, which will contribute to the differences observed. The 25% RAP 58-28 and 30% RAP 52-34 have air void contents close to the laboratory compacted specimens, and slightly higher dynamic modulus values from field cores are observed for these mixtures. The Black Space curves are similar for the field cores and PMPC specimens. It should also be noted that the field core results show different shapes at the lower frequencies, as the lower asymptote of the S-shaped curve is reached at higher frequencies than expected. This is a result of the uncertainty in the high

temperature testing, because shifting of the high temperature isotherms are equivalent to low frequencies on the master cure.

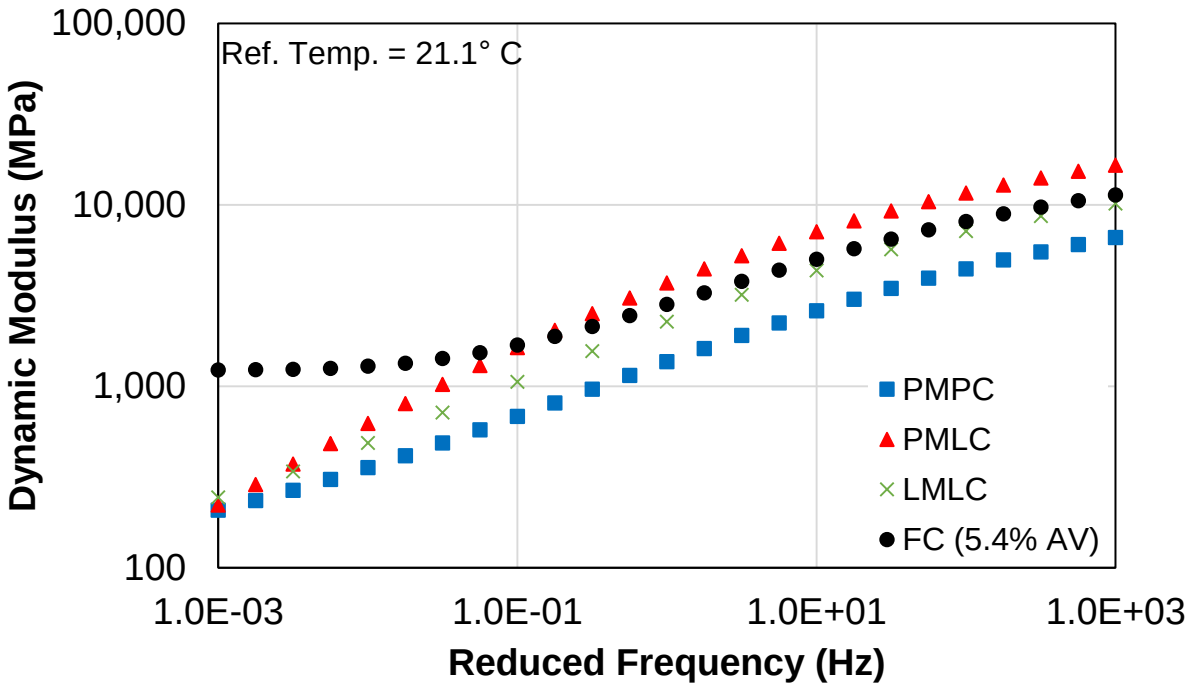

Figure 67: Dynamic Modulus Master Curve for PMPC, PMLC, LMLC, and FC Virgin, PG 58-28 Mixtures

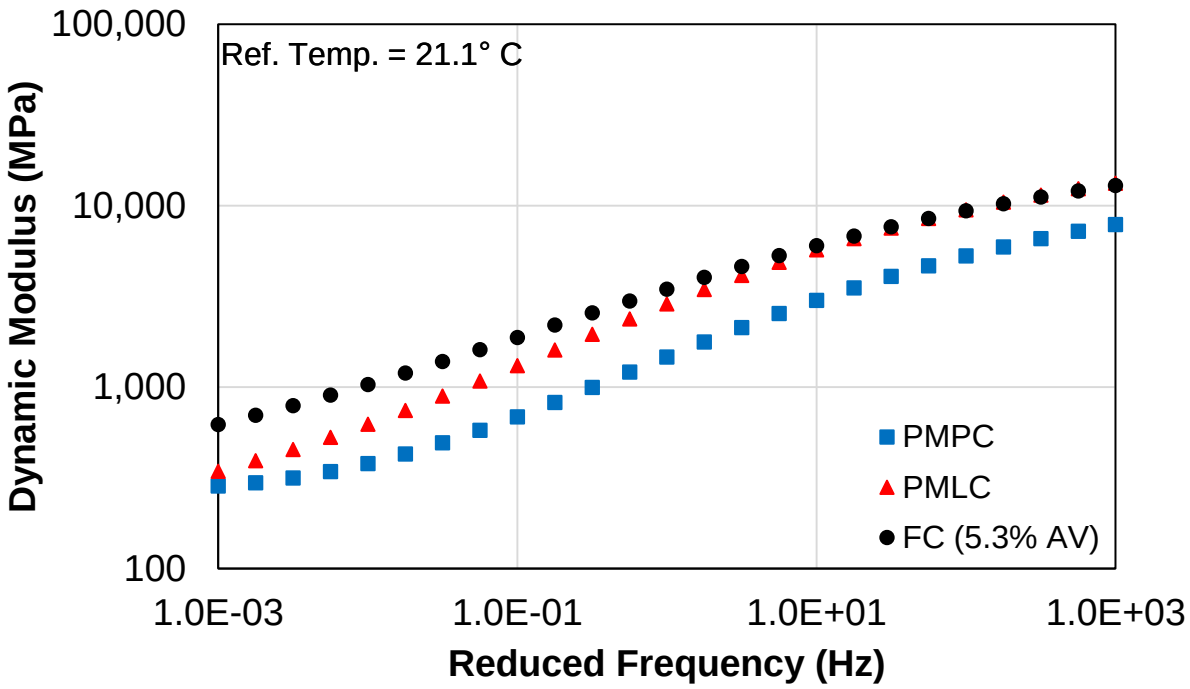

Figure 68: Dynamic Modulus Master Curve for PMPC, PMLC, and FC 15% RAP, PG 58-28 Mixtures

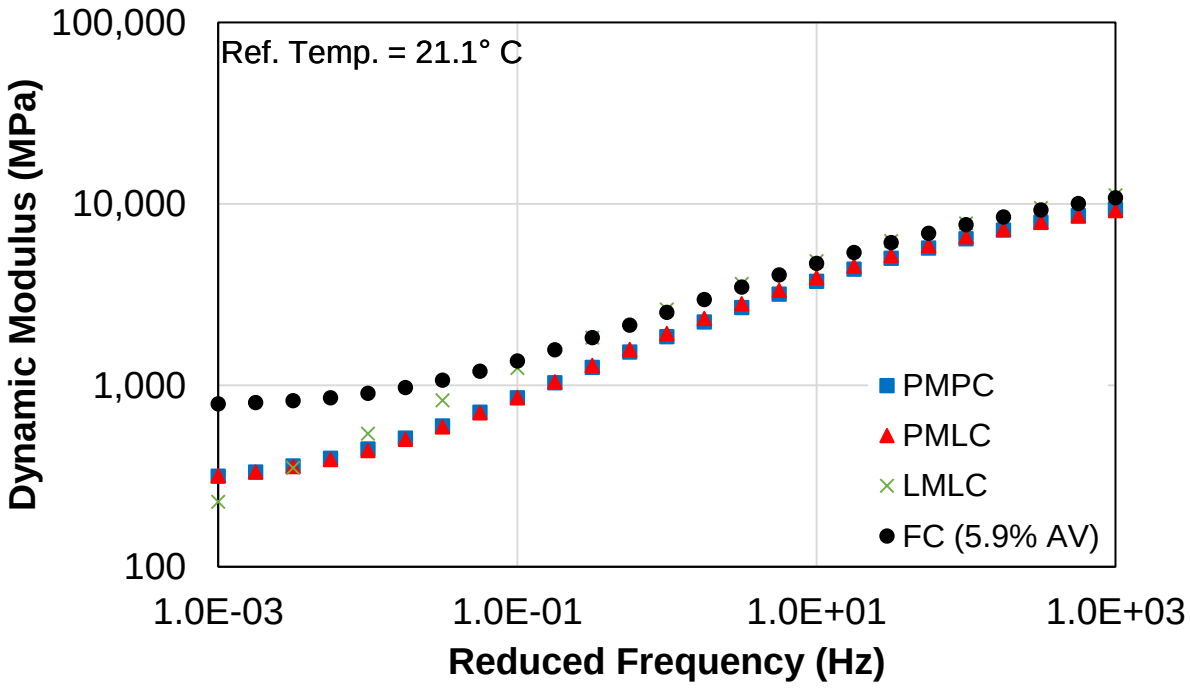

Figure 69: Dynamic Modulus Master Curve for PMPC, PMLC, LMLC, and FC 25% RAP, PG 58-28 Mixtures

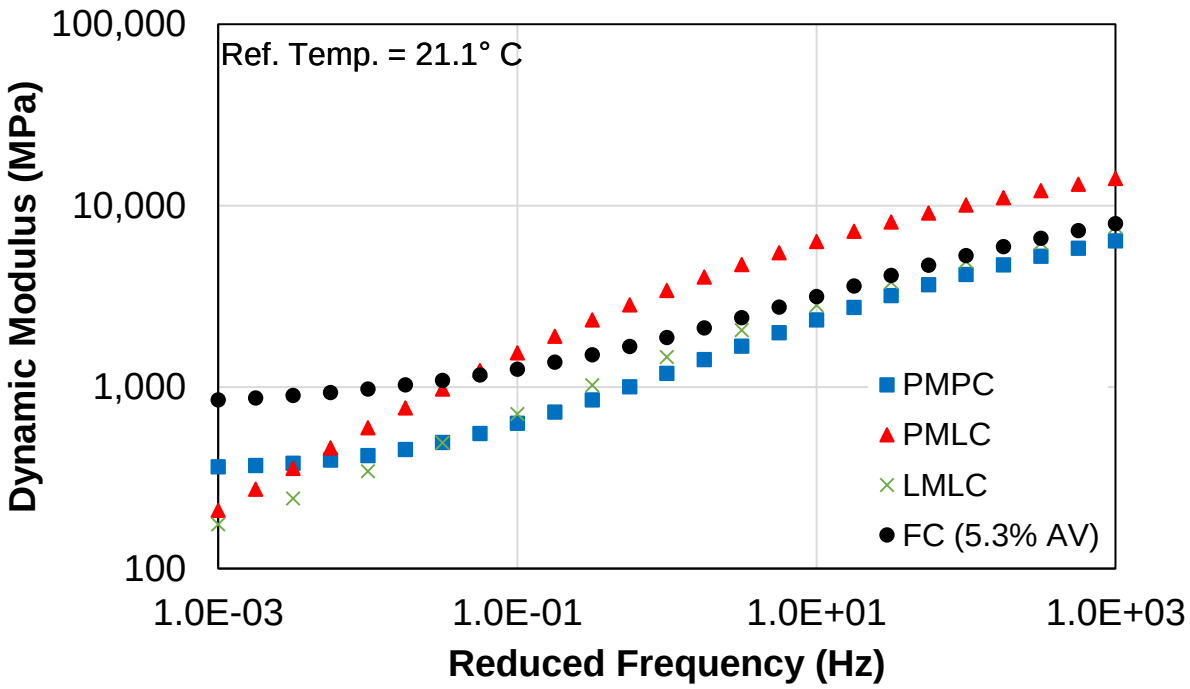

Figure 70: Dynamic Modulus Master Curve for PMPC, PMLC, LMLC, and FC 25% RAP, PG 52-34 Mixtures

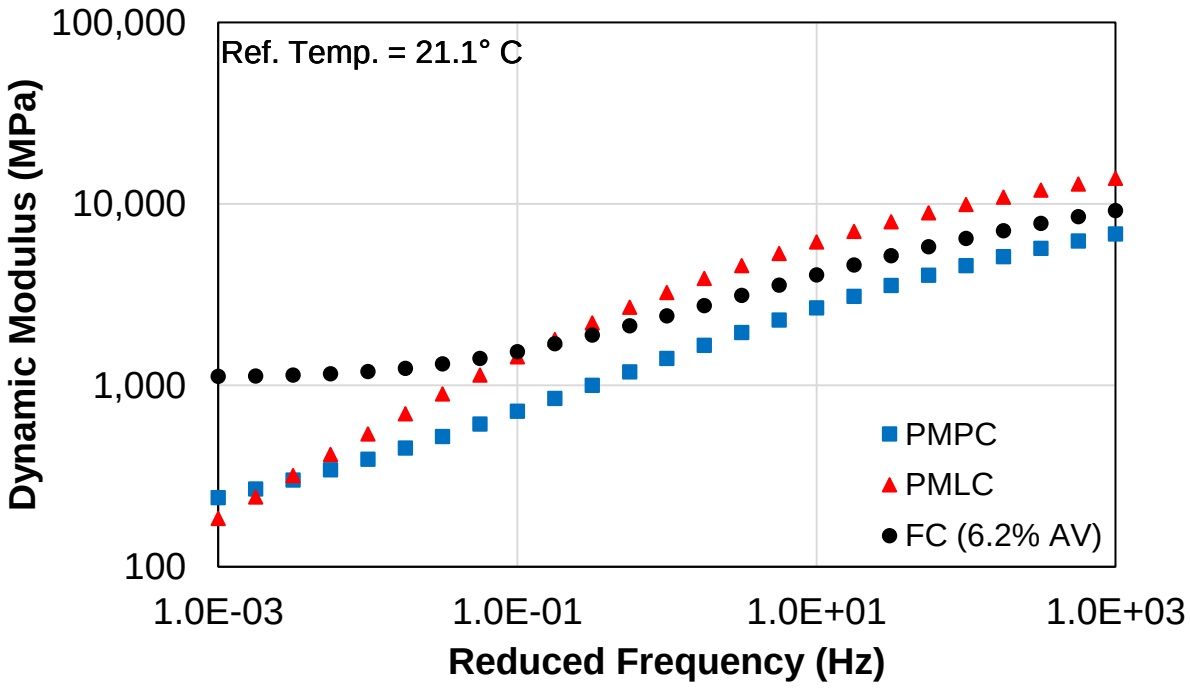

Figure 71: Dynamic Modulus Master Curve for PMPC, PMLC, and FC 30% RAP, PG 52-34 Mixtures

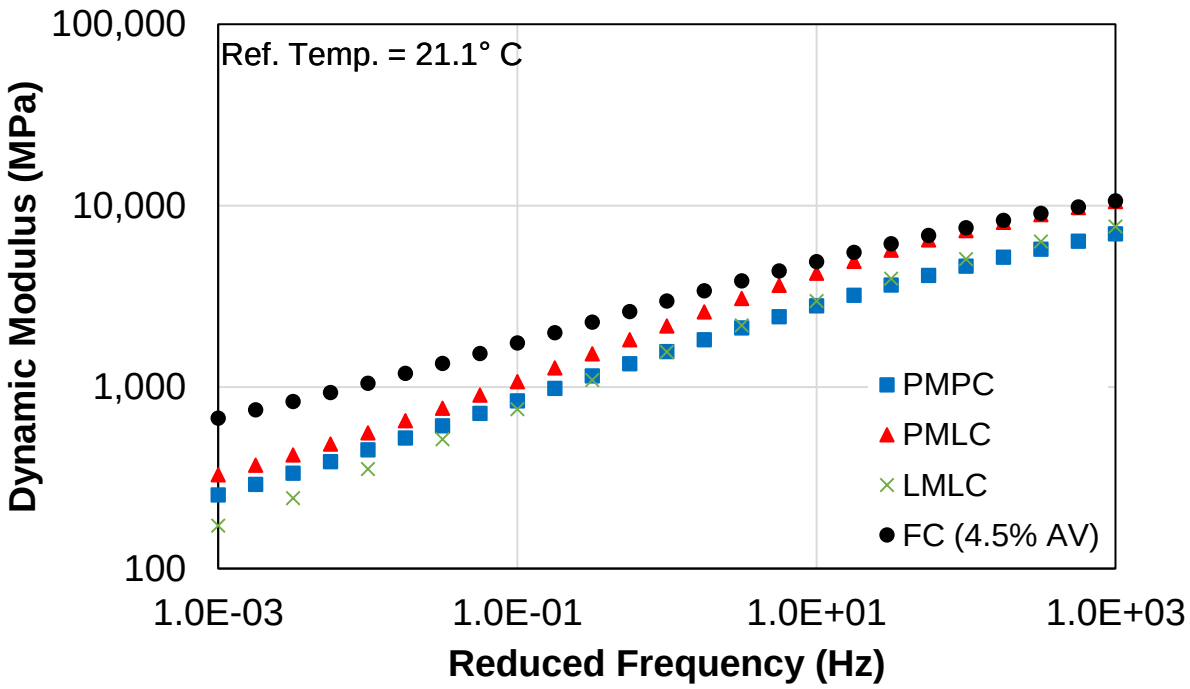

Figure 72: Dynamic Modulus Master Curve for PMPC, PMLC, LMLC, and FC 40% RAP, PG 52-34 Mixtures

Table 14: Approximate Dynamic Modulus Rankings of Specimen Fabrication Types

	PMPC	PMLC	LMLC	FC
Virgin, PG 58-28	4	1	3	2
15% RAP, PG 58-28	3	2	-	1
25% RAP, PG 58-28	2	2	1	1
25% RAP, PG 52-34	4	1	3	2
30% RAP, PG 52-34	3	1	-	2
40% RAP, PG 52-34	3	2	3	1
Average Ranking	**3.2**	**1.5**	**2.5**	**1.5**

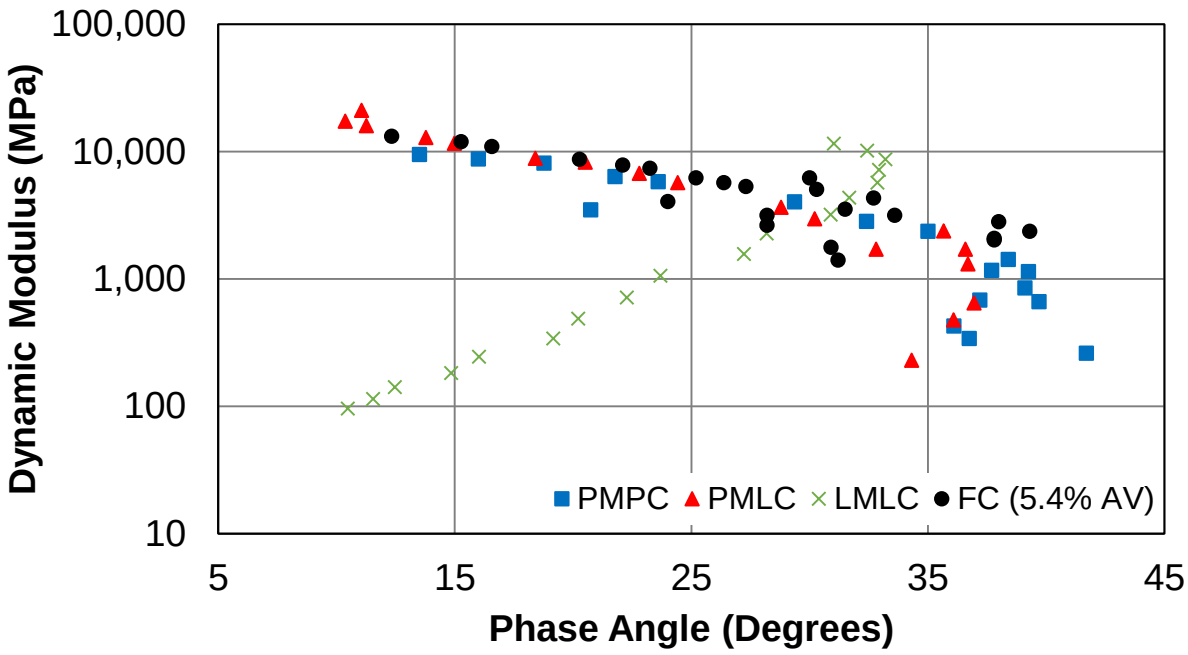

Figure 73: Black Space Plots for PMPC, PMLC, LMLC, and FC Virgin, PG 58-28 Mixtures

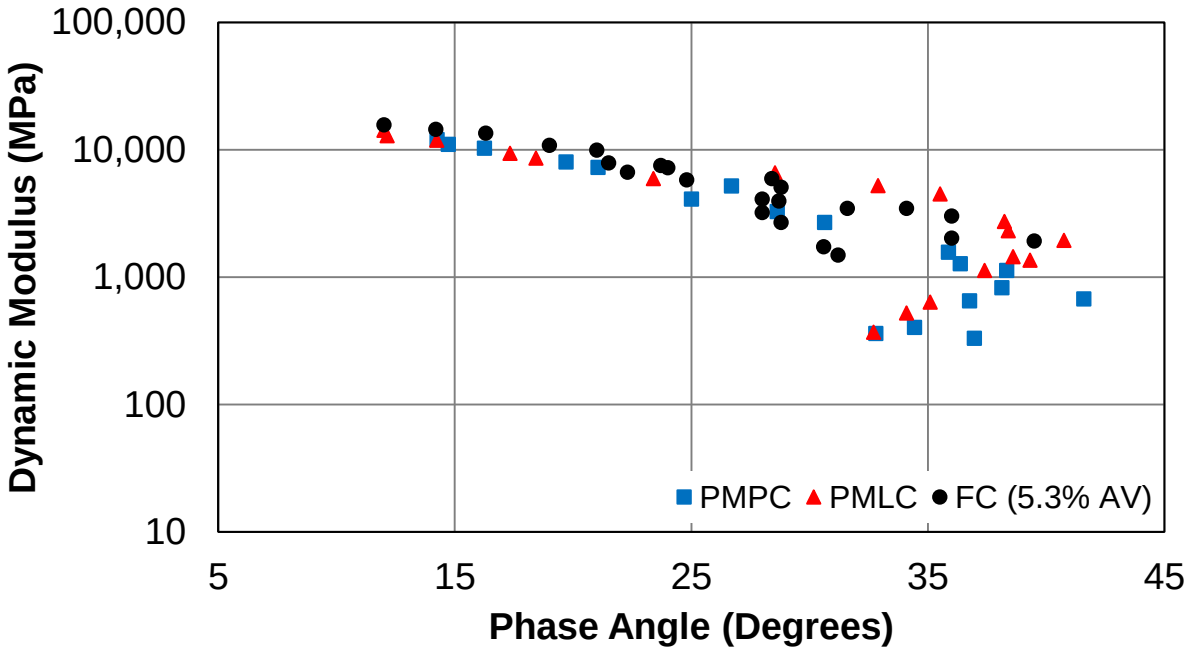

Figure 74: Black Space Plots for PMPC, PMLC, and FC 25% RAP, PG 58-28 Mixtures

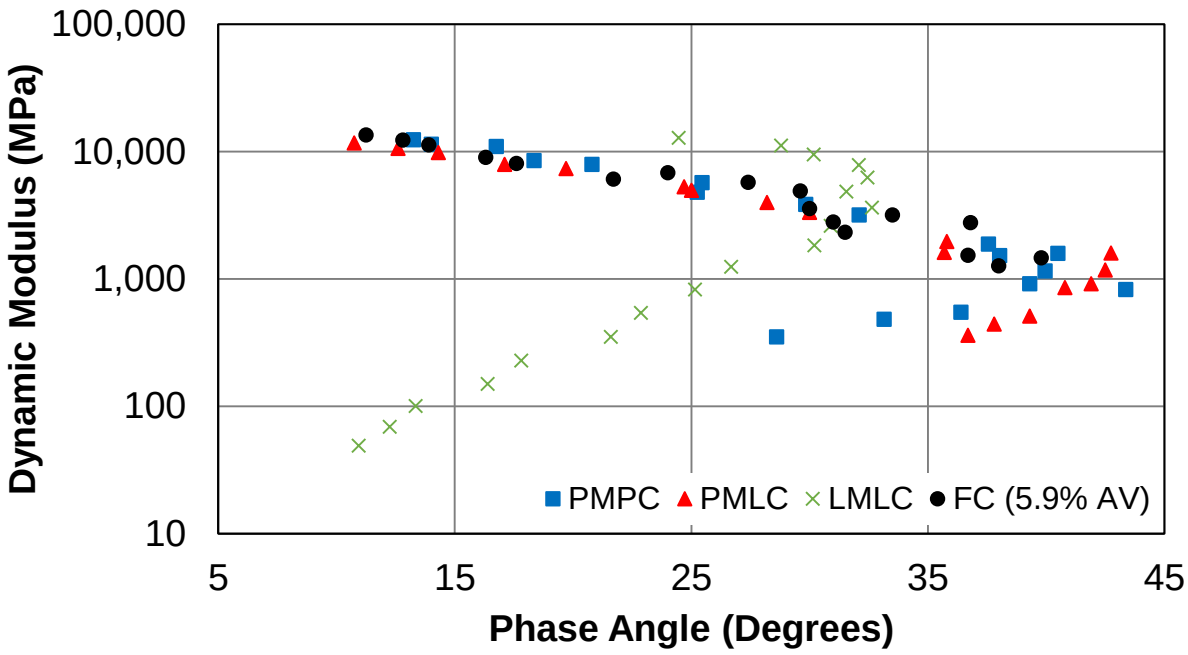

Figure 75: Black Space Plots for PMPC, PMLC, LMLC, and FC 25% RAP, PG 58-28 Mixtures

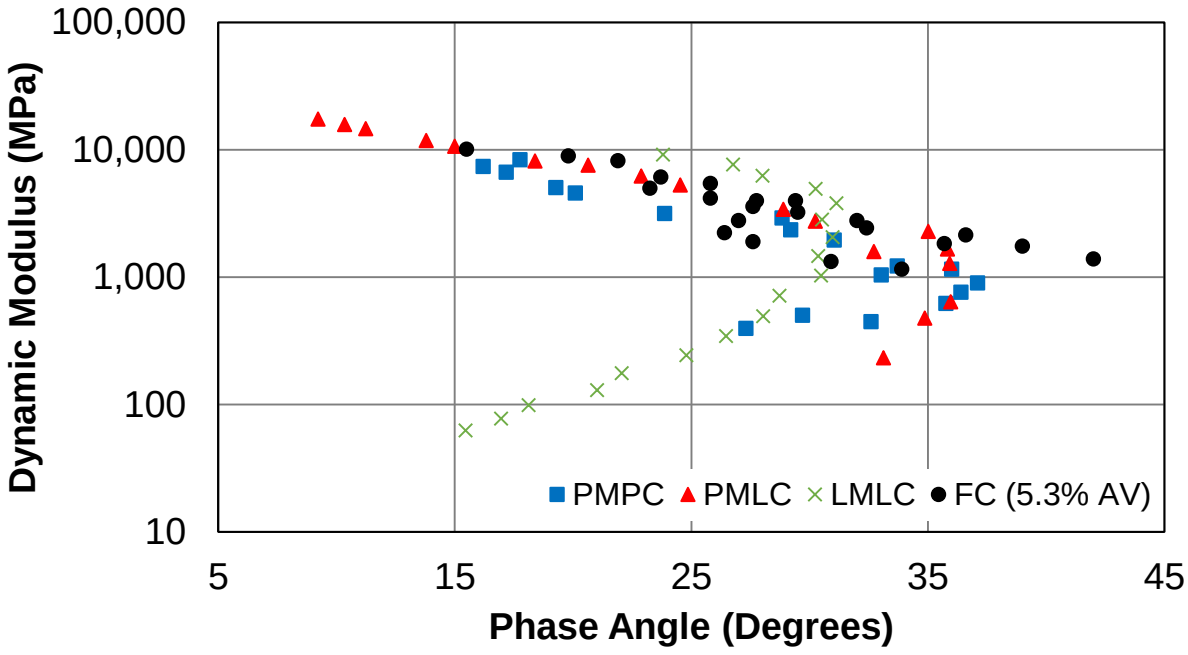

Figure 76: Black Space Plots for PMPC, PMLC, LMLC, and FC 25% RAP, PG 52-34 Mixtures

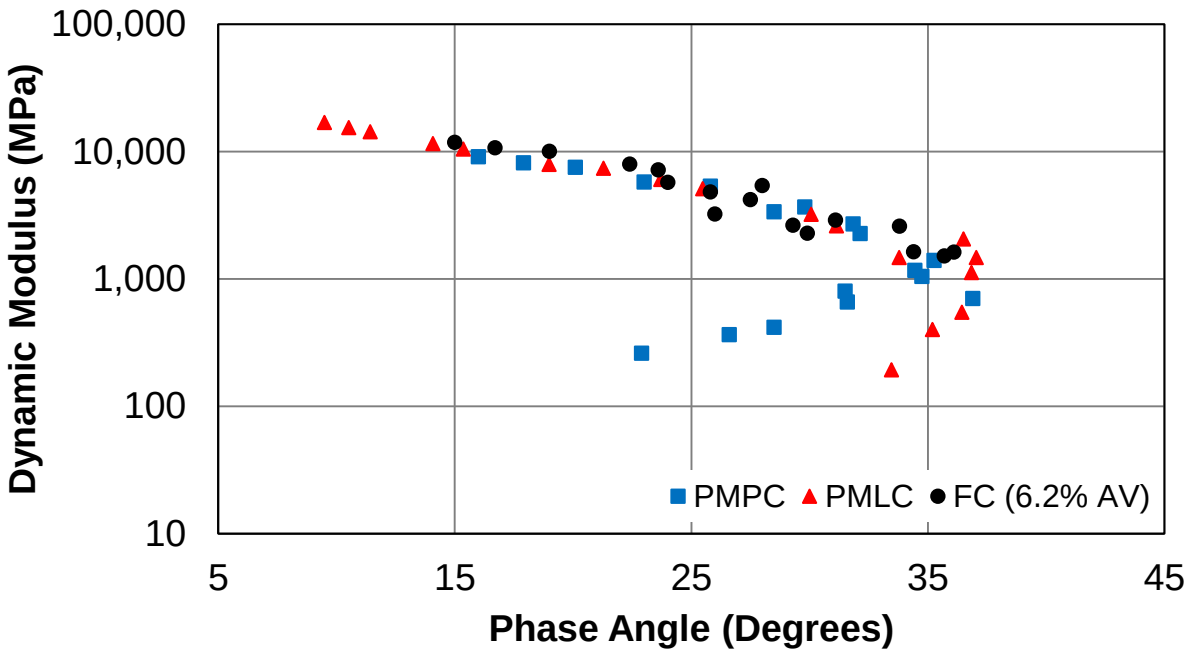

Figure 77: Black Space Plots for PMPC, PMLC, and FC 30% RAP, PG 52-34 Mixtures

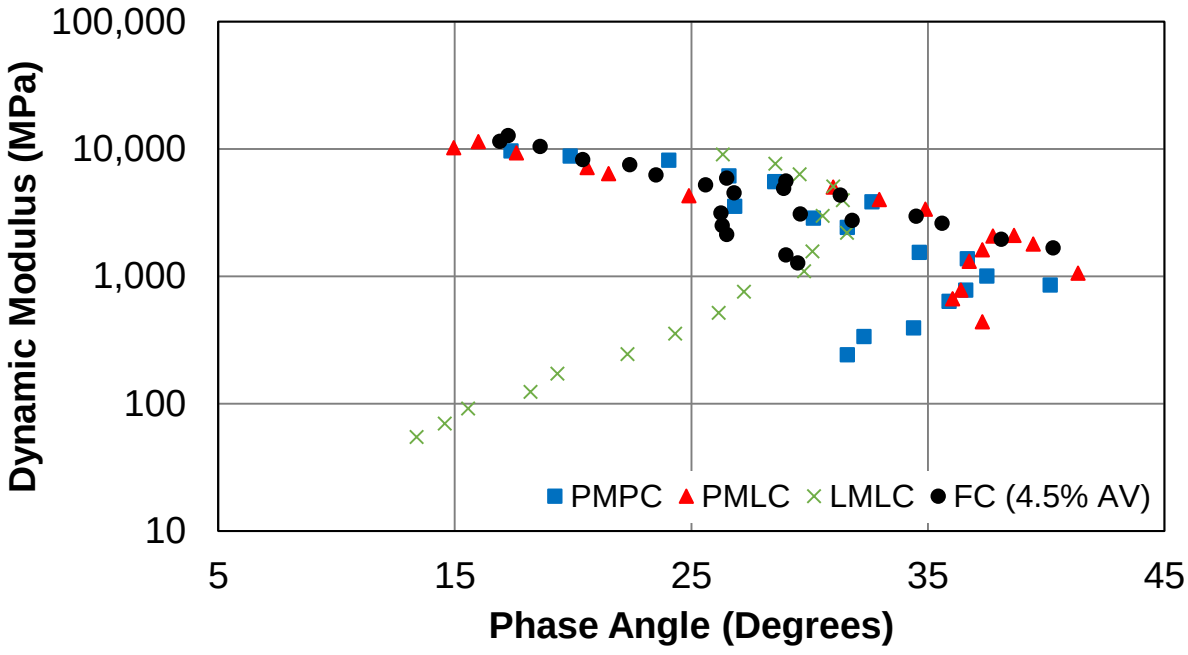

Figure 78: Black Space Plots for PMPC, PMLC, LMLC, and FC 40% RAP, PG 52-34 Mixtures

4.3.4 Comparison of Fabrication Methods: S-VECD Fatigue Results

The PMPC, PMLC, and field core specimen fabrication methods are compared for each of the six mixtures using damage characteristic curves (Figure 79 to Figure 84) and fatigue failure criterion results (Figure 85 to Figure 90). The field core specimens consistently show greater pseudo-stiffness responses than PMPC and PMLC specimens in the damage characteristic curves. However, the fatigue failure criterion results show that the small specimens from field cores exhibit fatigue resistance in between that of PMPC and PMLC mixtures. A consistent trend is not realized when comparing PMPC and PMLC specimens, but, in general, the PMLC specimens seem closer to the upper-right for the damage characteristic curves. The G^R-N_f results show better fatigue resistance for PMLC mixtures with the PG 58-28 binders, but the PG 52-34 mixtures are very similar in terms of fabrication method.

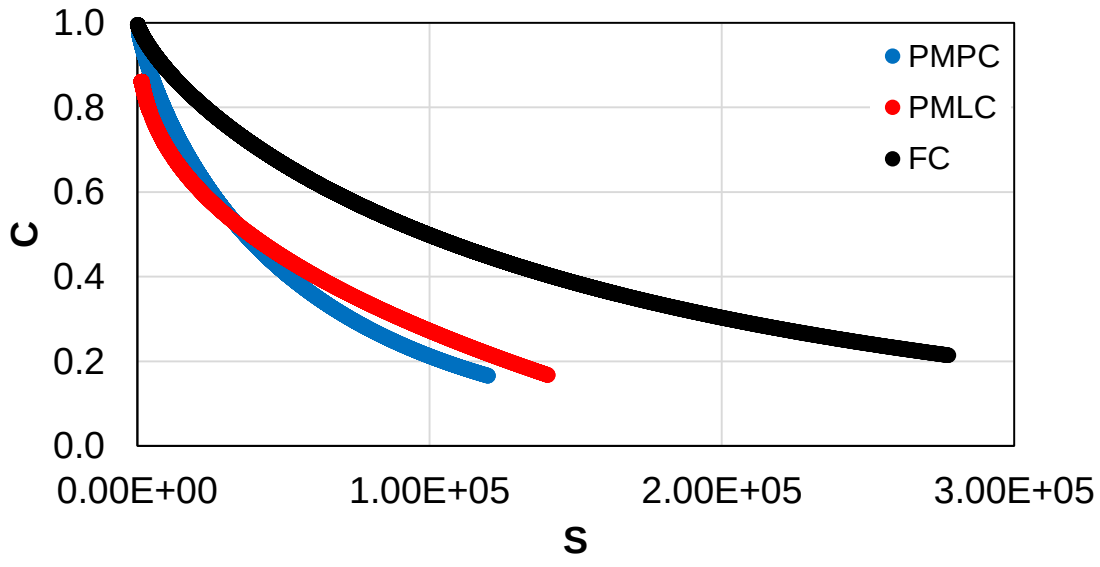

Figure 79: S-VECD Fatigue Damage Characteristic Curves for PMPC, PMLC, and FC Virgin, PG 58-28 Mixtures

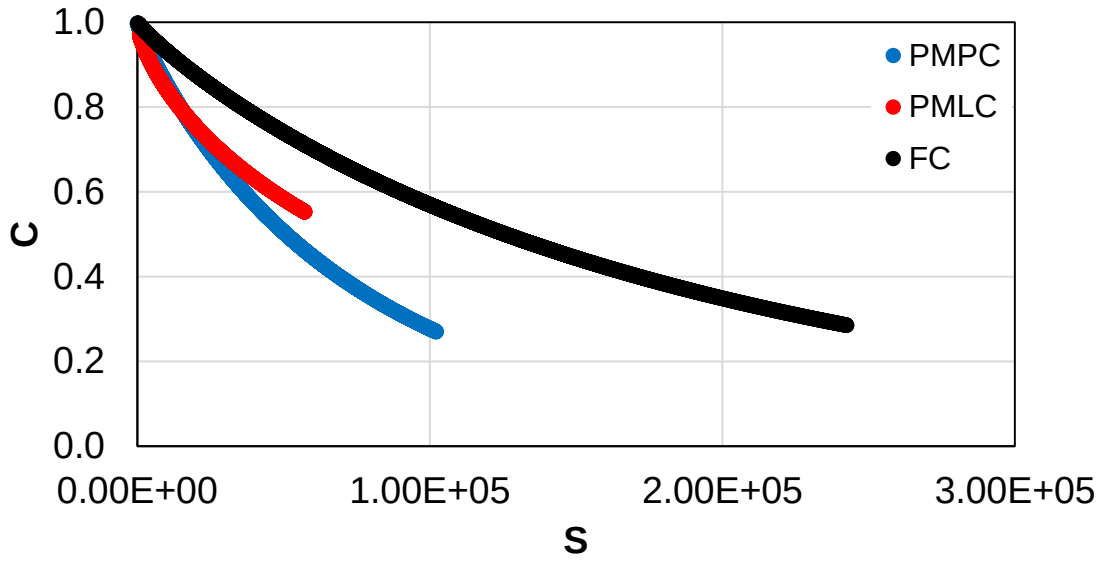

Figure 80: S-VECD Fatigue Damage Characteristic Curves for PMPC, PMLC, and FC 15% RAP, PG 58-28 Mixtures

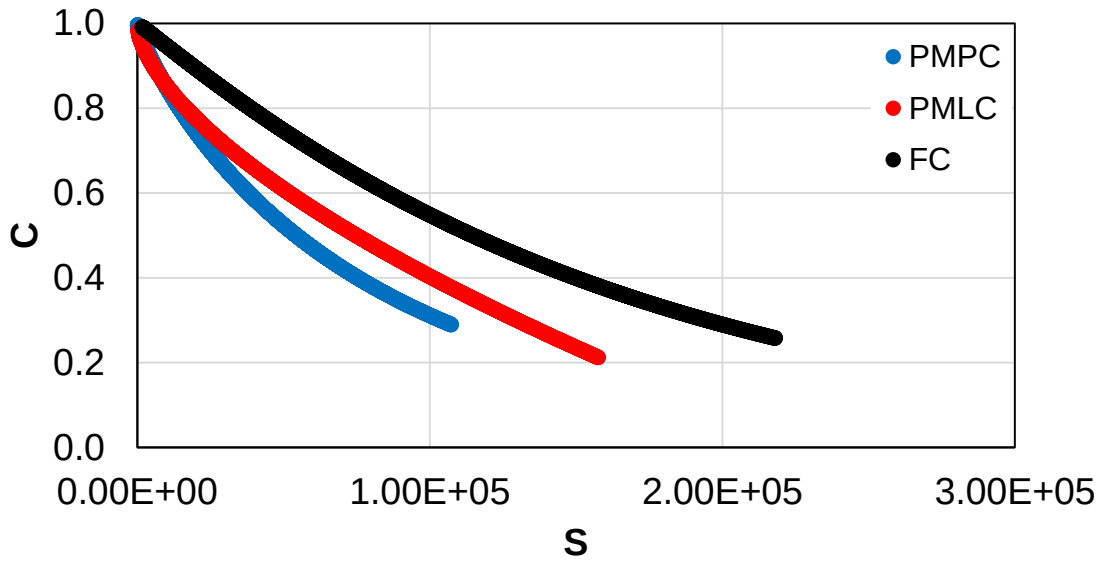

Figure 81: S-VECD Fatigue Damage Characteristic Curves for PMPC, PMLC, and FC 25% RAP, PG 58-28 Mixtures

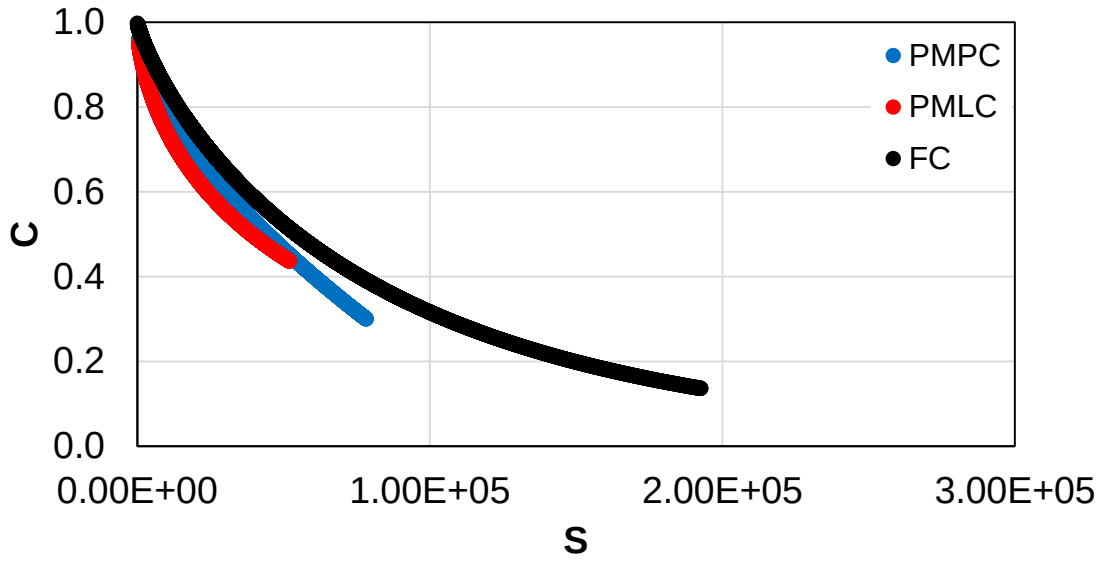

Figure 82: S-VECD Fatigue Damage Characteristic Curves for PMPC, PMLC, and FC 25% RAP, PG 52-34 Mixtures

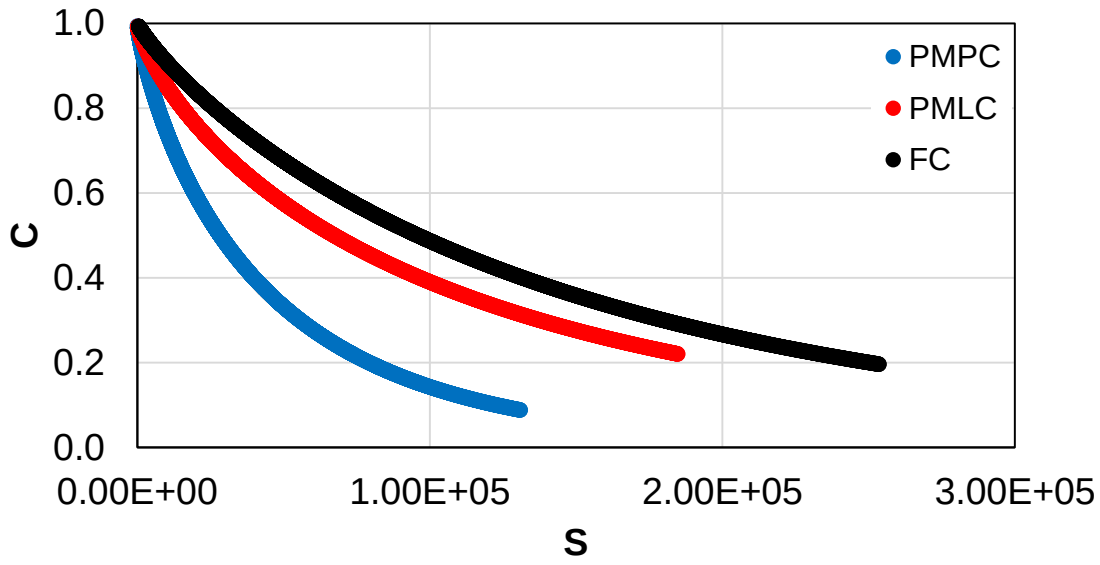

Figure 83: S-VECD Fatigue Damage Characteristic Curves for PMPC, PMLC, and FC 30% RAP, PG 52-34 Mixtures

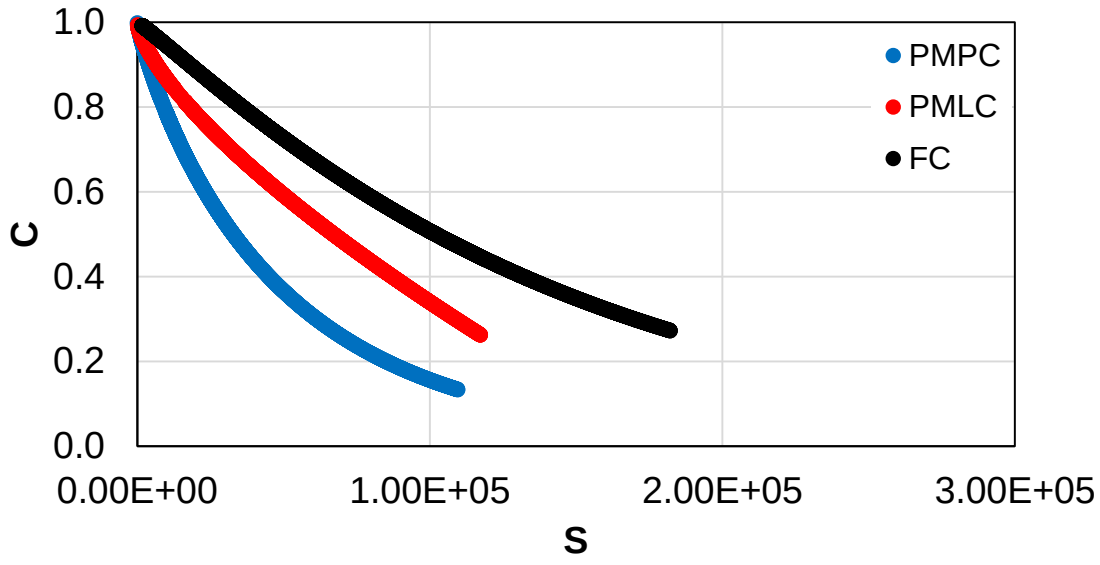

Figure 84: S-VECD Fatigue Damage Characteristic Curves for PMPC, PMLC, and FC 40% RAP, PG 52-34 Mixtures

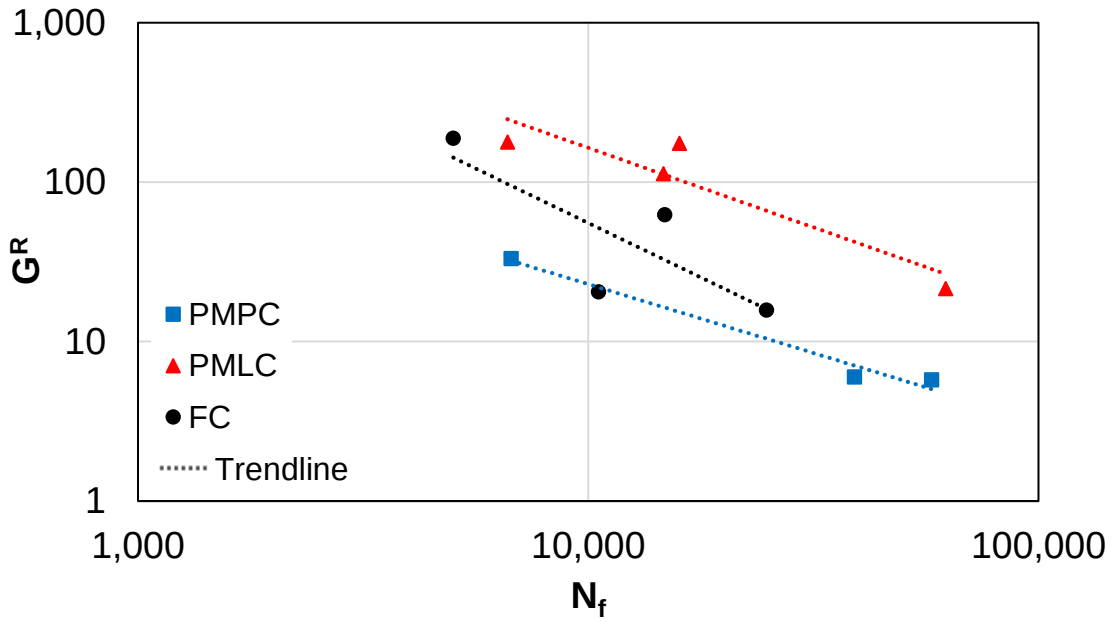

Figure 85: S-VECD Fatigue Failure Criterion Results for PMPC, PMLC, and FC Virgin, PG 58-28 Mixtures

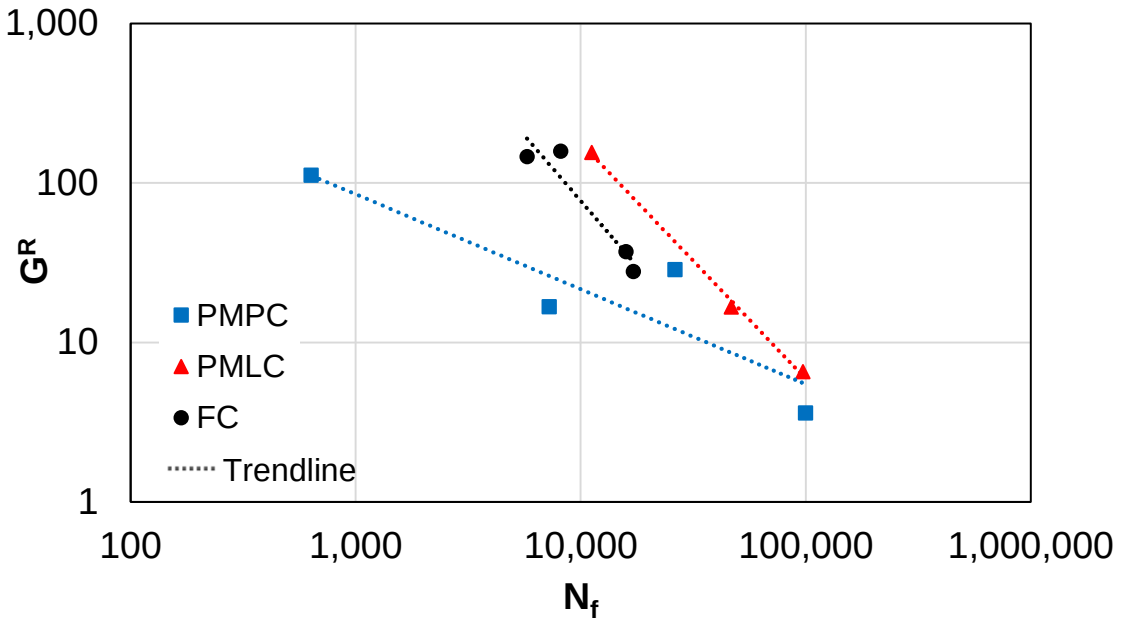

Figure 86: S-VECD Fatigue Failure Criterion Results for PMPC, PMLC, and FC 15% RAP, PG 58-28 Mixtures

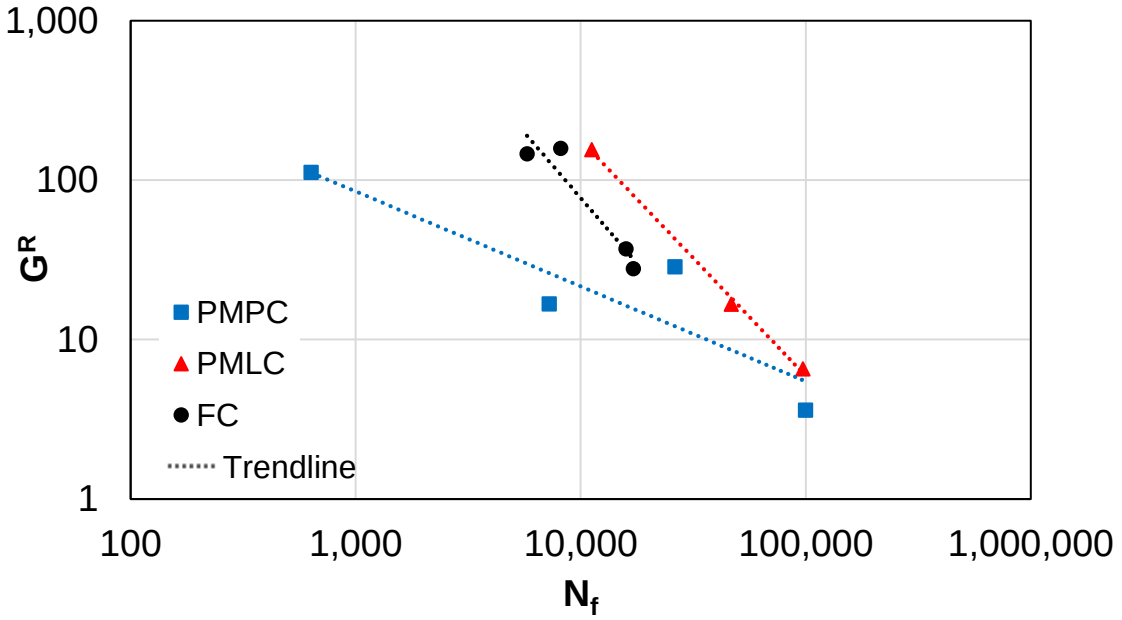

Figure 87: S-VECD Fatigue Failure Criterion Results for PMPC, PMLC, and FC 25% RAP, PG 58-28 Mixtures

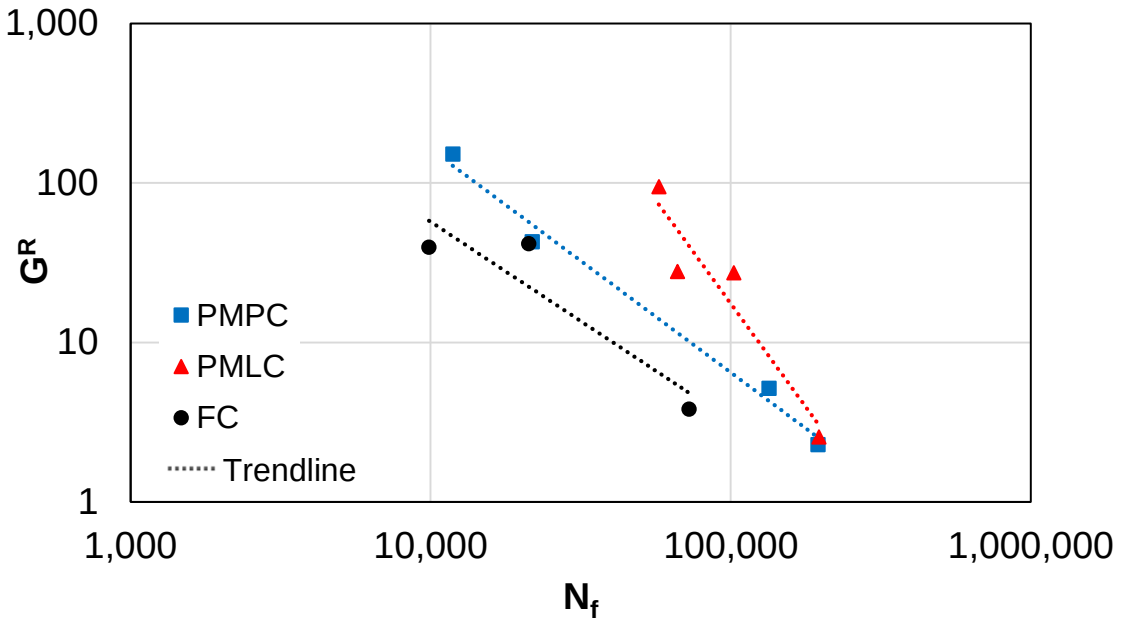

Figure 88: S-VECD Fatigue Failure Criterion Results for PMPC, PMLC, and FC 25% RAP, PG 52-34 Mixtures

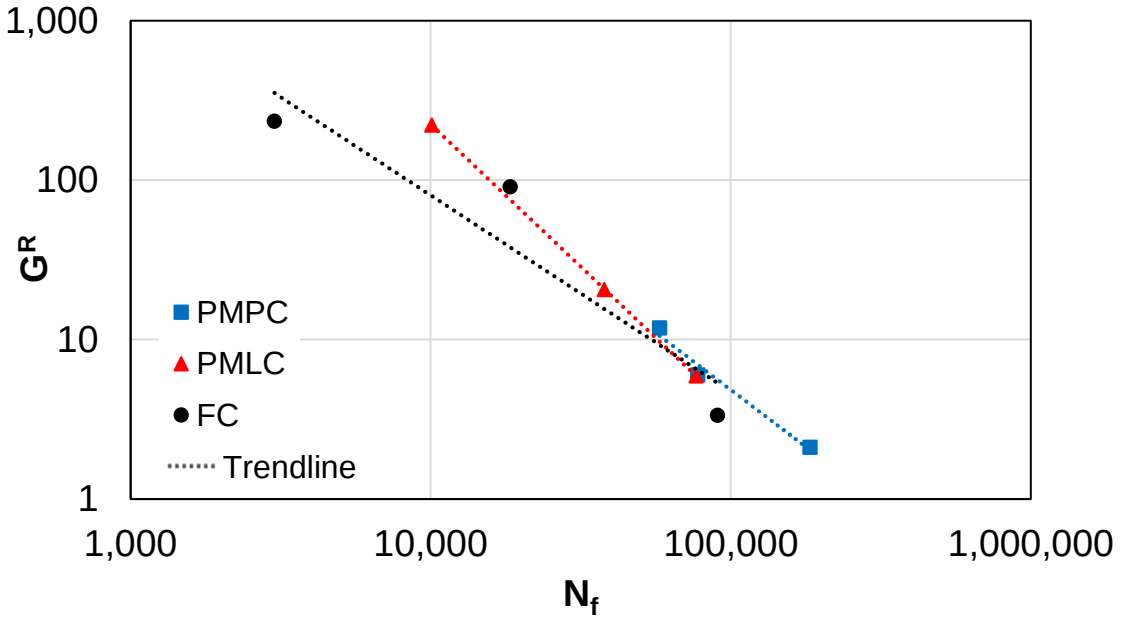

Figure 89: S-VECD Fatigue Failure Criterion Results for PMPC, PMLC, and FC 30% RAP, PG 52-34 Mixtures

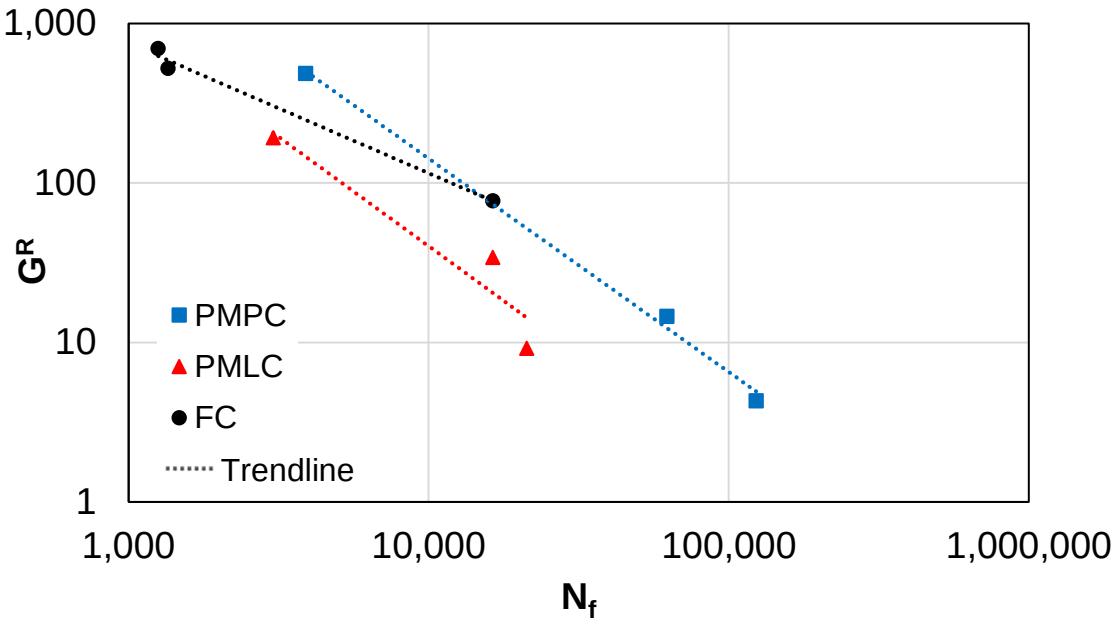

Figure 90: S-VECD Fatigue Failure Criterion Results for PMPC, PMLC, and FC 40% RAP, PG 52-34 Mixtures

CHAPTER 5: SUMMARY AND CONCLUSIONS

5.1 RESEARCH SUMMARY

The main objective of the research included in this thesis is to gain a better understanding of the true properties of asphalt mixtures that are placed in the field. It is important for researchers and practitioners to accurately and efficiently characterize the material that is placed in service so that satisfactory performance is maintained and rehabilitation is not needed earlier than expected. The two studies included in this research explored areas that can help better characterize the material properties of asphalt mixtures placed in the field. The silo storage study, part of *Transportation Pooled Fund 5(230): Evaluation of Plant Produced RAP Mixtures in the Northeast*, investigated the effects of storage time in silos at production plants on virgin and RAP mixtures. As mixtures are exposed to elevated temperatures in the silo for longer periods of time, there is a potential for age hardening to occur which may have a detrimental effect on the long-term performance of the pavement. The second study, as part of *Performance of High RAP Pavement Sections in New Hampshire*, compared various specimen fabrication methods (PMPC, PMLC, LMLC, and field cores) that attempt to accurately characterize mixture properties. The feasibility of using small geometry specimens has been investigated in recent research, and this method was used to evaluate the properties of small specimens obtained from field cores of test sections. The effect of base binder grade and higher amounts of RAP was also evaluated as part of the specimen fabrication methods study. Variations in the methods in which specimens are prepared for laboratory testing or inconsistency in silo storage time can lead to inaccurate determinations of asphalt properties.

A number of different laboratory tests were performed to evaluate the mixtures in these projects. Binder testing was performed by Rutgers University on the extracted and recovered binders from the silo storage mixtures, and analysis of the binders included performance grading, BBR ΔT_{cr}, complex shear modulus master curves and Black Space, Glover-Rowe parameter, and rheological indices. Virgin tank binder was also conditioned in the Rolling Thin Film Oven to compare current short-term aging laboratory simulation protocols to actual plant production effects. Mixture testing was performed on the silo storage and specimen fabrication methods study mixtures. Dynamic modulus and S-VECD fatigue testing was conducted to evaluate properties of the various mixtures. A pavement life evaluation software, LVECD, was also performed on the silo storage mixtures to predict performance within a pavement structure.

5.2 CONCLUSIONS

In the silo storage study, the effect of silo storage time on virgin and RAP mixtures was evaluated. Results from extensive testing on the binders and mixtures clearly indicate that the mixtures undergo stiffening, likely due to aging, as silo storage time increases. Both virgin and RAP mixtures experienced changes as a result of being stored in the silo, but the RAP mixture may have experienced larger changes. This indicates that there may be a combination of short-term aging within the silo and a blending or diffusion process occurring with the RAP mixture. The larger changes among the RAP mixture may also have been affected by the decreasing air void content.

Interestingly, the RAP mixture experienced a higher degree of aging even though RAP contains already-aged materials and possesses lower aging rates. The chemical interactions that occur between RAP and virgin binders are not fully understood and there are currently many research projects aimed at characterizing this interaction. A literature review showed that there is

a potential for a diffusion or blending interaction to occur between RAP and virgin binders at elevated temperatures. Following typical plant production stages, the RAP and virgin binders are not fully blended and some of the already-aged RAP binder, which possesses stiffer properties, is not "accessible" to the mixture, i.e., does not contribute to the properties that control the overall mixture. As the mixture is exposed to high temperatures in a silo for extended periods of time, it is hypothesized that more of the stiffened RAP binder becomes accessible due to the blending of the binders. Therefore, the binders are aged through oxidation or volatilization in the silo and the RAP-virgin binder interaction causes more aging due to the RAP binder becoming a more prominent component of the mixture.

The primary objective of the silo storage study was to gain a better understanding of the relation between production parameters, particularly silo storage time, and mixture performance. This study indicated that silo storage time can have a significant impact on field performance. RTFO aging also showed that current laboratory conditioning methods do not necessarily simulate plant production. It was not until 170 minutes (twice the specified conditioning time of 85 minutes) that the virgin tank binder correlated with the properties observed through normal plant production of these mixtures. Similar to other production parameters, the length of silo storage time is not typically controlled and depends on several factors. There are many situations whereby plants will need to vary production parameters, such as temperature and silo storage times. It is important to recognize that control of these parameters is currently not practical, but it is also important to understand the impacts of plant production variations on the properties of the asphalt mixture.

The effect of specimen fabrication method, RAP content, and binder grade was also explored in this thesis. Six test sections were constructed in 2011 along I-93 southbound in New Hampshire, and field cores were obtained from each test section. The four different specimen

fabrication methods included the following: plant mixed, plant compacted specimens; plant mixed, laboratory compacted specimens; laboratory mixed, laboratory compacted specimens; and small geometry specimens obtained from field cores. The six mixture types included the following: virgin, PG 58-28; 15% RAP, PG 58-28; 25% RAP, PG 58-28; 25% RAP, PG 52-34; 30% RAP, PG 52-34; and 40% RAP, PG 52-34.

Mixture testing showed that mixtures with the PG 58-28 base binder are stiffer than those with the PG 52-34 base binder, and mixtures experienced an increase in stiffness with increasing RAP content. The impact of the change in binder grade on stiffness was greater than the impact of the change in RAP content. This trend was observed for the LMLC, PMPC, and field core specimens. The trends observed with the PMLC specimens were different, likely due to the impact of reheating the material in the laboratory; the lower RAP content mixtures and PG 52-34 base binder mixtures were affected by the reheating to a greater extent. Mixtures containing a larger proportion of virgin binder and mixtures with softer binders will undergo a greater change in stiffness due to reheating than mixtures containing already-aged RAP materials. Black Space results showed that the PG 58-28 base binder mixtures experienced a decrease in phase angle with increasing RAP content, whereas the mixtures with the PG 52-34 base binder had lower phase angles and showed an increase in phase angle with increasing RAP content. This trend is not expected behavior for a softer binder and may be due to the method by which the PG 52-34 binder was produced. The use of a paraffinic oil, such as recycled engine oil bottoms (REOB), to produce the PG 52-34 could possibly cause the observed behavior; however, testing for the presence of REOB in the binder was not done.

A comparison of fabrication methods showed that the small specimens obtained from field cores and PMLC mixtures were stiffest, followed by LMLC mixtures then PMPC mixtures. A

comparison of PMPC and PMLC mixtures showed that the laboratory reheating process caused a stiffening of the mixtures that may not be the same as the short-term aging of plant compaction. Comparing PMLC and LMLC mixtures showed that laboratory mixing of the raw materials did not age the materials as much as the age hardening that occurs during plant production. Testing on field cores showed that field compaction may be stiffer than current laboratory fabrication methods, which would result in shorter service life due to increased cracking susceptibility. The small specimen geometry approach was a successful alternative for testing field core samples which are too small for standard size specimens to be fabricated. However, problems arose when testing at high temperatures and low frequencies due to the small cross-sectional area and soft binders used.

It is clear that there is a need for asphalt manufacturers and researchers to gain a better understanding of how production aspects affect performance. The silo storage study showed that a key process in the production of asphalt mixtures may be a cause for performance issues over the long-term. Silo storage time is not typically controlled at production plants and the time that materials are kept in the silo has a significant effect on mixture performance. Future testing is needed to fully characterize the effects of silo storage time, but this thesis showed that the storage aspect of production should be investigated further. It was also discovered in this research that the manner in which specimens are fabricated for laboratory testing plays a significant role in the properties assumed for the mixture. Both projects emphasized the need for researchers and practitioners to better understand the properties of asphalt mixtures placed in the field. This thesis presented results that can help in that endeavor, but future work is needed to pursue that objective further.

5.3 RECOMMENDATIONS FOR FUTURE WORK

Future work is needed to gain a more complete understanding of production variations and, in particular, silo storage time. Different PG grades and RAP contents, binder absorption, and other material properties should be explored in future testing. The relation to haul time must also be considered as both processes expose the mixtures to elevated temperatures for relatively long durations. Additional work would be beneficial to further explore the effects of production parameters on mixture properties.

Another consideration for future work with the silo storage study is the practicality of limiting storage time. It is clear that limiting storage time to 10 hours, for example, is not practical at asphalt production plants. It would be interesting to research the effects of even longer storage times (e.g. 20, 30 hours) because these results would be of interest to practitioners. A number of events may occur during production management, including weather delays, holidays, or project adjustments, that may result in material that must be kept in silos for longer durations. Practitioners would benefit from knowing how these longer durations affect the mixture performance, and may be better equipped to determine whether the mixture can be placed in the field or not.

Future work relating to the specimen fabrications study would also be beneficial to asphalt researchers and practitioners. The trends observed with the PG 52-34 mixtures did not follow expectations and the presence of REOB is suspected. Future testing could include detection of REOB in these mixtures to investigate the trends observed. It is also recommended that future research projects attempt to quantify the difference between specimen fabrication methods so that normalization or adjustments can be made depending on the method used. This study showed that there are significant differences between methods, and these variations could lead to characterizing the mixture properties incorrectly. Finally, the small geometry specimens approach seems

promising for evaluation of in-place mixtures. Forensic analysis or existing pavement conditions can be successfully evaluated using this method. However, more research needs to be done to confirm that results are consistent and representative using this approach. Standards need to be developed for wide-spread testing using the small-scale methodology, and there are ongoing projects that are currently investigating development of AASHTO standards with this method.

REFERENCES

Anderson, M., G. King, D. Hanson, and P. Blankenship. "Evaluation of the Relationship Between Asphalt Binder Properties and Non-Load Related Cracking." *Journal of the Association of Asphalt Paving Technologists*, Vol. 80, 2011, pp. 615-661.

Brown, E.R., P. Kandhal, F. Roberts, Y.R. Kim, D.Y. Lee, and T. Kennedy. "Hot Mix Asphalt Materials, Mixture Design and Construction." 3rd Edition, National Center for Asphalt Technology at Auburn University, National Asphalt Pavement Association, Latham, MD, 2009.

Christensen, D. W., and D. A. Anderson. "Interpretation of Dynamic Mechanical Test Data for Paving Grade Asphalt Cements." *Journal of the Association of Asphalt Paving Technologists,* Vol. 61, 1992, pp. 67-116.

Daniel, J.S., N. Gibson, S. Tarbox, A. Copeland, and A. Andriescu. "Effect of Long-Term Aging on RAP Mixtures: Laboratory Evaluation of Plant Produced Mixtures." *Journal of the Association of Asphalt Paving Technologists,* Vol. 82, 2013, pp. 327-365.

Diefenderfer, B., B. Bowers, and S. Diefenderfer. "Asphalt Mixture Performance Characterization Using Small-Scale Cylindrical Specimens." Publication VCTIR 15-R26, Virginia Center for Transportation Innovation and Research, Virginia Department of Transportation, 2015.

Diefenderfer, S., and H. Nair. "Evaluation of Production, Construction, and Properties of High Reclaimed Asphalt Pavement Mixtures." *Transportation Research Record: Journal of the Transportation Research Board*, *No. 2445*, Transportation Research Board of the National Academics, Washington, D.C., 2014, pp. 75-82.

Eslaminia, M., S. Thirunavukkarasu, M. N. Guddati, and Y. R. Kim. "Accelerated Pavement Performance Modeling Using Layered Viscoelastic Analysis." *Proceedings of the 7th International RILEM Conference on Cracking in Pavements*, Delft, Netherlands, 2012, pp. 20-22.

Glover, C., R. Davison, C. Domke, Y. Ruan, P. Juristyarini, D. Knorr, and S. Jung. "Development of a New Method for Assessing Asphalt Binder Durability with Field Evaluation." Publication FHWA-TX-05-1872-2. National Research Council, Washington, D.C, 2005.

Huang, B., G. Li, D. Vukosavljevic, X. Shu, and B. Egan. "Laboratory Investigation of Mixing Hot-Mix Asphalt with Reclaimed Asphalt Pavement." *Transportation Research Record: Journal of the Transportation Research Board*, *No. 1929*, Transportation Research Board of the National Academics, Washington, D.C., 2005, pp. 37-45.

Islam, M.R., and R.A. Tarefder. "A Study of Asphalt Aging Through Beam Fatigue Test." *Transportation Research Record: Journal of the Transportation Research Board*, Transportation Research Board of the National Academics, Washington, D.C., 2015, in press.

Johnson, E., G. Johnson, S. Dai, D. Linell, G. McGraw, and M. Watson. "Incorporation of Recycled Asphalt Shingles in Hot Mixed Asphalt Pavement Mixtures." Minnesota Department of Transportation, 2010.

Kim, Y.R., Y. Seo, M. King, and M. Momen. "Dynamic Modulus Testing of Asphalt Concrete in Indirect Tension Mode." *Transportation Research Record: Journal of the Transportation Research Board*, *No. 1891*, Transportation Research Board of the National Academics, Washington, D.C., 2004, pp. 163-173.

Kriz, P., D. Grant, B. Veloza, M. Gale, A. Blahey, J. Brownie, R. Shirts, and S. Maccarrone. "Blending and Diffusion of Reclaimed Asphalt Pavement and Virgin Asphalt Binders." *Journal of the Association of Asphalt Paving Technologists*, Vol. 83, 2014, pp. 225-270.

Li, X., and N. Gibson. "Using Small Scale Specimens for AMPT Dynamic Modulus and Fatigue Tests." *Journal of the Association of Asphalt Paving Technologists*, Vol. 82, 2013, pp. 579-615.

McDaniel, R., A. Shah, G. Huber, and A. Copeland. "Effects of Reclaimed Asphalt Pavement Content and Virgin Binder Grade on Properties of Plant Produced Mixtures." *Journal of the Association of Asphalt Paving Technologists*, Vol. 81, 2012, pp. 369-401.

Mensching, D., J.S. Daniel, T. Bennert, M. Mederios Jr., M. Elwardany, W. Mogawer, E. Hajj, and M. Alavi. "Low Temperature Properties of Plant-Produced RAP Mixtures in the Northeast." *Journal of the Association of Asphalt Paving Technologists*, Vol. 83, 2014, pp. 37-79.

Mogawer, M., T. Bennert, J.S. Daniel, R. Bonaquist, A. Austerman, and A. Booshehrian. "Performance Characteristics of Plant-Produced High RAP Mixtures." *Journal of the Association of Asphalt Paving Technologists*, Vol. 81, 2012, pp. 403-439.

Norouzi, A., and Y. R. Kim. "Mechanistic Evaluation of the Fatigue Cracking in Asphalt Pavements." *International Journal of Pavement Engineering*, 2015, in press.

Park, H.J., and Y.R. Kim. "Investigation into Top-Down Cracking of Asphalt Pavements in North Carolina." *Transportation Research Record: Journal of the Transportation Research Board*, *No. 2368*, Transportation Research Board of the National Academics, Washington, D.C., 2013, pp. 45-55.

Rowe, G.M. Prepared Discussion for the AAPT paper by Anderson et al.: Evaluation of the Relationship between Asphalt Binder Properties and Non-Load Related Cracking. *Journal of the Association of Asphalt Paving Technologists*, Vol. 80, 2011, pp. 649-662.

Rowe, G.M., G. King, and M. Anderson. "The Influence of Binder Rheology on the Cracking of Asphalt Mixes on Airport and Highway Projects." *ASTM Journal of Testing and Evaluation*, 42(5), 2014.

Sabouri, M., T. Bennert, J.S. Daniel, and Y.R. Kim. "Evaluating Laboratory-Produced Asphalt Mixtures with RAP in Terms of Rutting, Fatigue, Predictive Capabilities, and High RAP

Content Potential." *Transportation Research Record: Journal of the Transportation Research Board*, Transportation Research Board of the National Academics, Washington, D.C., 2015, in press.

Tarbox, S., and J.S. Daniel. "Effects of Long-Term Oven Aging on Reclaimed Asphalt Pavement Mixtures." *Transportation Research Record: Journal of the Transportation Research Board*, *No. 2294*, Transportation Research Board of the National Academics, Washington, D.C., 2012, pp. 1-15.

Underwood, B.S., A. Heidari, M. Guddati, and Y.R. Kim. "Experimental Investigation of Anisotropy in Asphalt Concrete" *Transportation Research Record: Journal of the Transportation Research Board*, *No. 1929*, Transportation Research Board of the National Academics, Washington, D.C., 2005, pp. 238-247.

Underwood, B.S., and Y.R. Kim. "Improved Calculation Method of Damage Parameter in Viscoelastic Continuum Damage Model." *International Journal of Pavement Engineering*, Vol. 11, 2010, pp. 459-476.

Xiao, F., B. Putnam, and S. Amirkhanian. "Plant and Laboratory Compaction Effects on Performance Properties of Plant-Foamed Asphalt Mixtures Containing RAP." *Journal of Materials in Civil Engineering*, American Society of Civil Engineers, 2014.

Zhao, S., B. Huang, X. Shu, and M. Woods. "Quantitative Characterization of Binder Blending: How Much RAP/RAS Binder is Mobilized During Mixing." *Transportation Research Record: Journal of the Transportation Research Board*, Transportation Research Board of the National Academics, Washington, D.C., 2015, in press.

APPENDICES

APPENDIX A: PMPC, PMLC, AND LMLC RESULTS

A.1 Plant Mixed, Plant Compacted Specimens: Dynamic Modulus Results

Four replicate specimens were produced and tested for each mixture during each day of production. The average dynamic modulus curves for the six mixtures over all three production days are shown in Figure 91 (log-log) and Figure 92 (semi-log). Each curve represents the average of twelve specimens. The PG 58-28 base binder mixtures experience a slight stiffening effect with increasing RAP content. The PG 52-34 base binder mixtures all show softer response than the virgin PG 58-28 mixture and show slight increases in stiffness with increasing RAP content. The PG 58-28 and PG 52-34 base binder mixtures do not have statistically significant differences in dynamic modulus from one another over most of the master curve range. In summary, the base binder grade shows a larger impact on the dynamic modulus than the RAP content.

The average Black Space curves for the six mixtures are shown in Figure 93. The three mixtures with the PG 58-28 binder are very similar in Black Space, with a slight decrease in the phase angle with RAP. The mixtures with PG 52-34 binder have lower phase angles than the PG 58-28 mixtures and also show an increase in phase angle with increasing RAP content. This is similar to the trends observed with the LMLC specimens and is not expected behavior for a softer binder. It is shown in the phase angle master curves (Figure 94) that the PG 58-28 base binder mixtures experience lower phase angles (more elastic behavior) with increasing RAP content, as expected. However, the PG 52-34 base binder shows the opposite trend and is similar to the Black Space curves, as increasing RAP content caused an increase in phase angle.

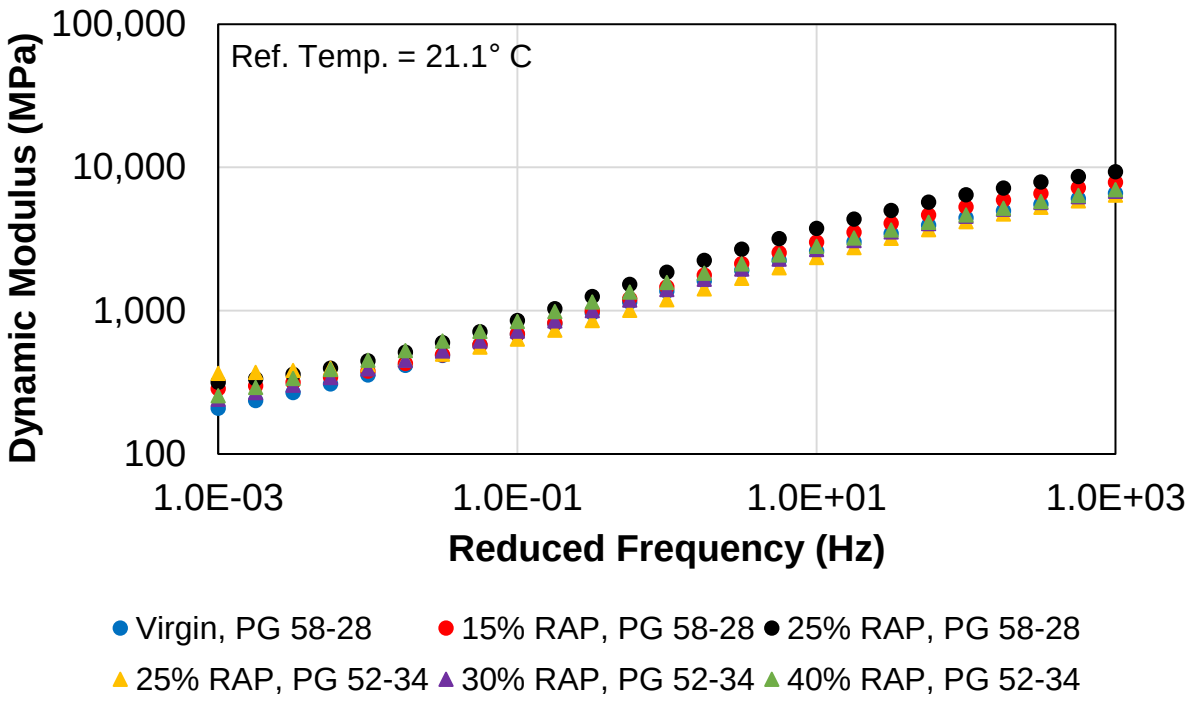

Figure 91: Dynamic Modulus Master Curve (log-log) for PMPC Mixtures

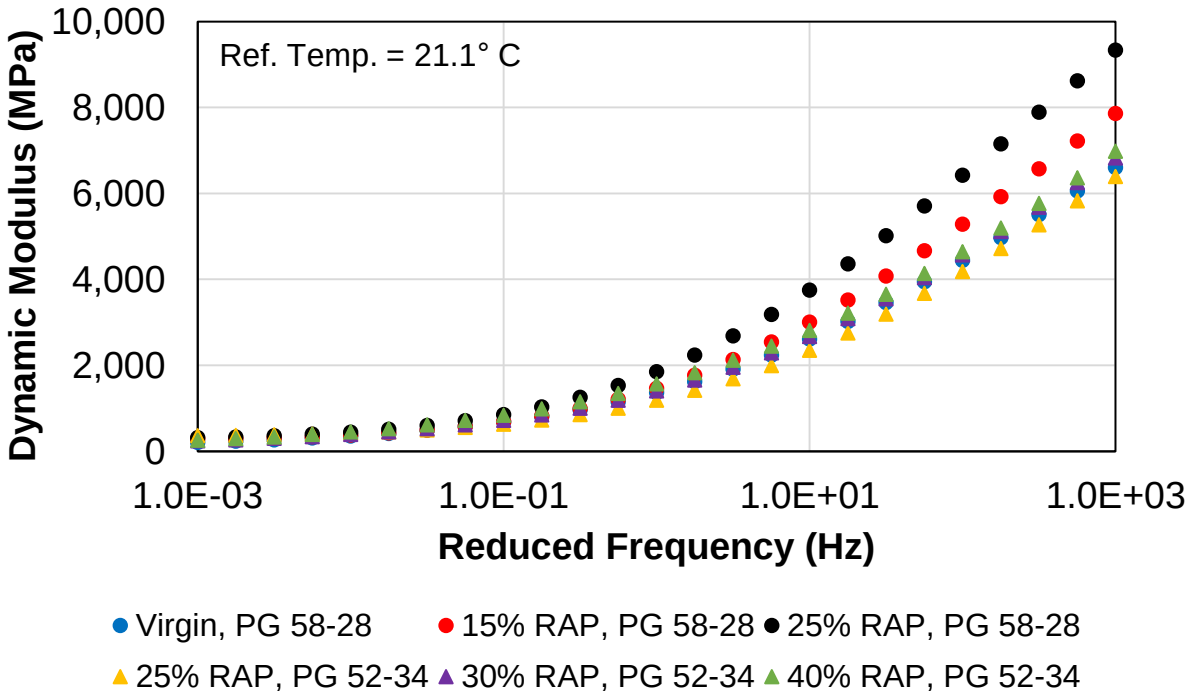

Figure 92: Dynamic Modulus Master Curve (semi-log) for PMPC Mixtures

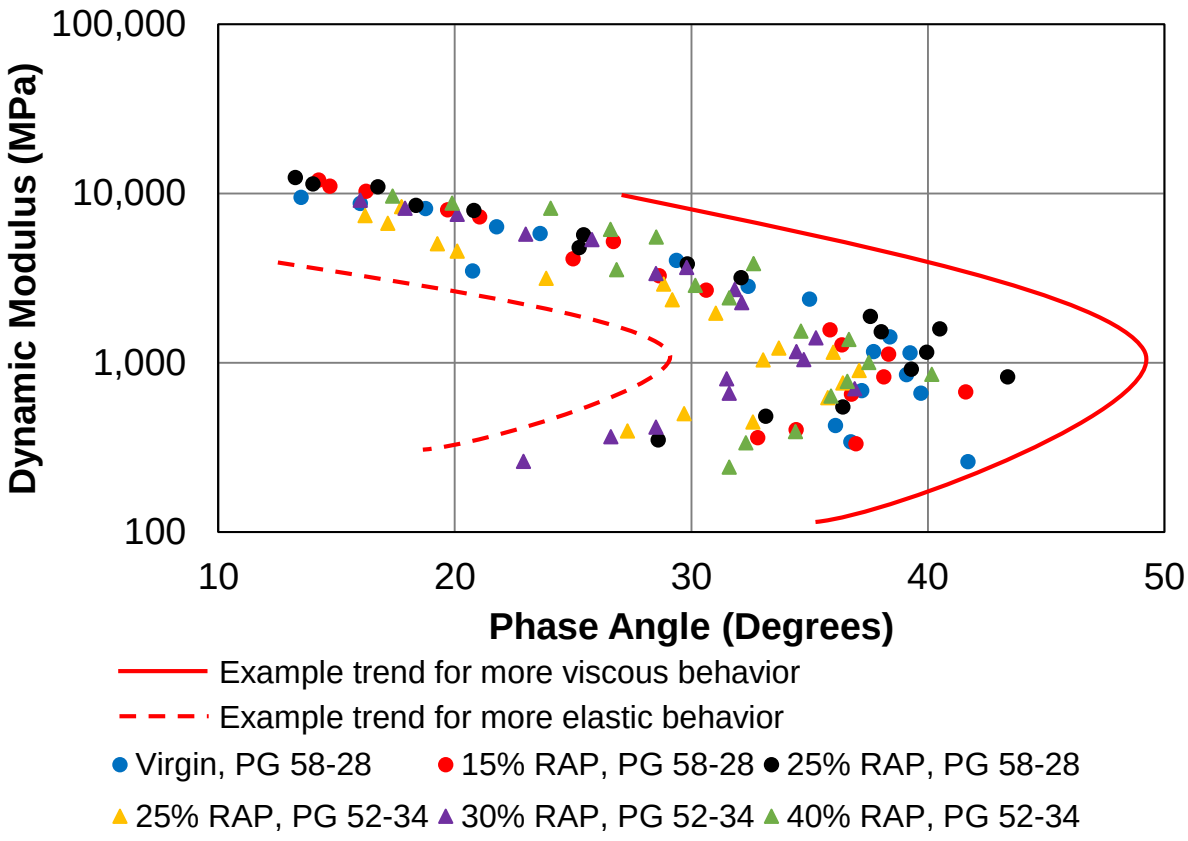

Figure 93: Black Space Plots for PMPC Mixtures

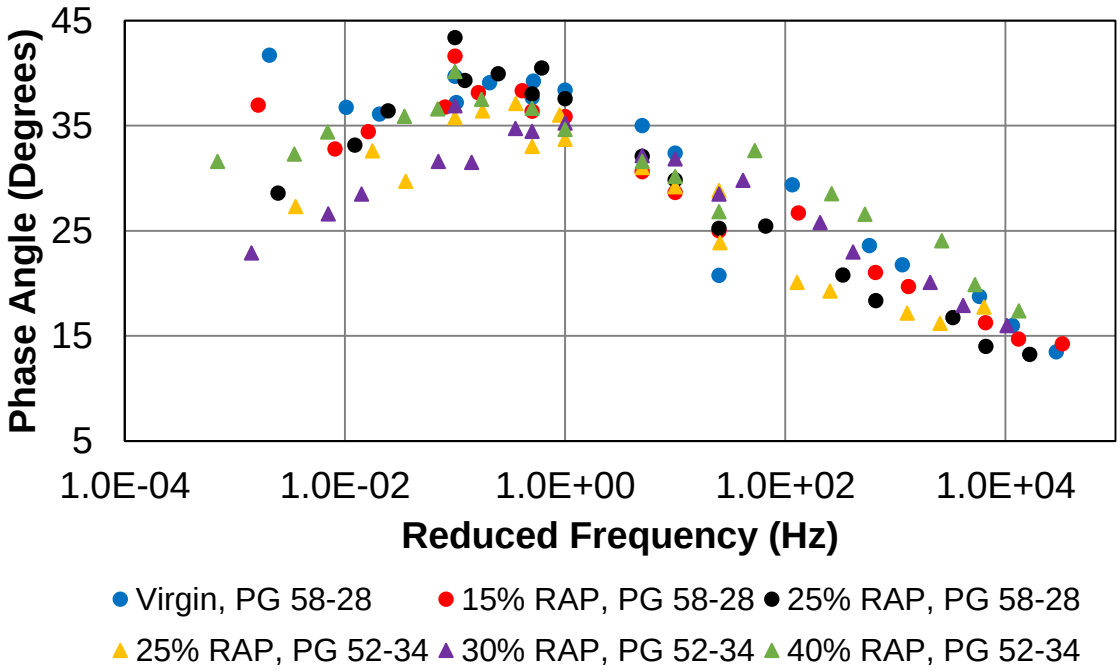

Figure 94: Phase Angle Master Curves for PMPC Mixtures

A.2 Plant Mixed, Plant Compacted Specimens: S-VECD Fatigue Results

S-VECD fatigue testing was conducted in uniaxial tension mode using the AMPT. Analysis of the results included the average damage characteristic curves for each mixture (Figure 95), fatigue failure criterion of replicate specimens (Figure 96), and calculation of the index parameter, N_f at G^R = 100 (Figure 97). The damage characteristic curves for the PMPC specimens show that better fatigue resistance is expected (closer to upper right of plot) for higher RAP contents among the PG 58-28 base binder mixtures. The PG 52-34 mixtures show different results, as the 25% RAP mixture is closest to the upper-right. Also, the PG 52-34 base binder mixtures generally have lower pseudo-stiffness values (C) than PG 58-28 mixtures. The trends observed with the fatigue failure criterion are inconsistent among RAP content, but the PG 52-34 seems to show better fatigue resistance than the PG 58-28 mixtures.

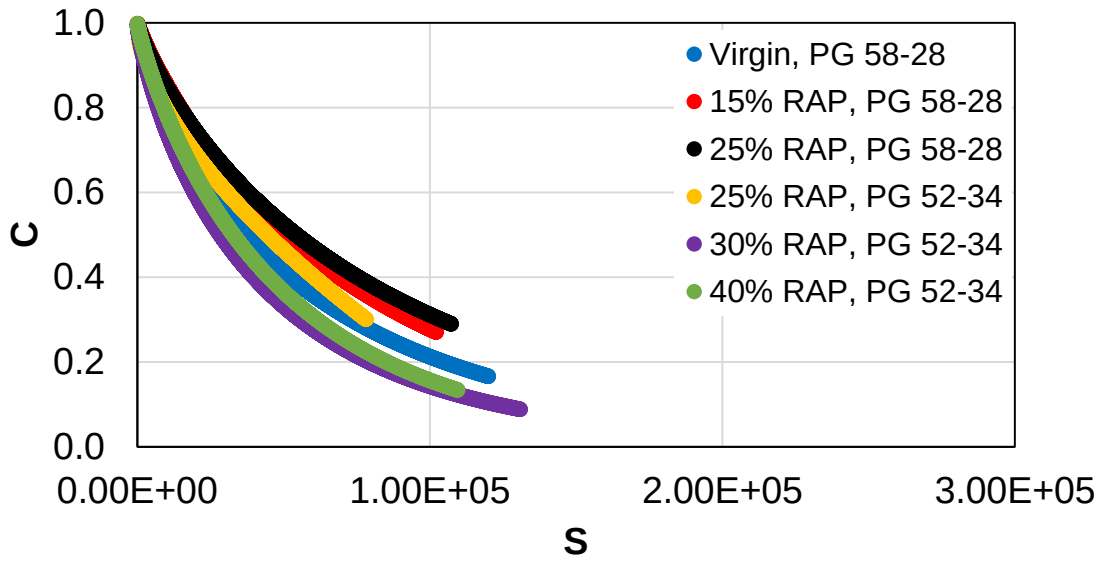

Figure 95: S-VECD Fatigue Damage Characteristic Curves for PMPC Mixtures

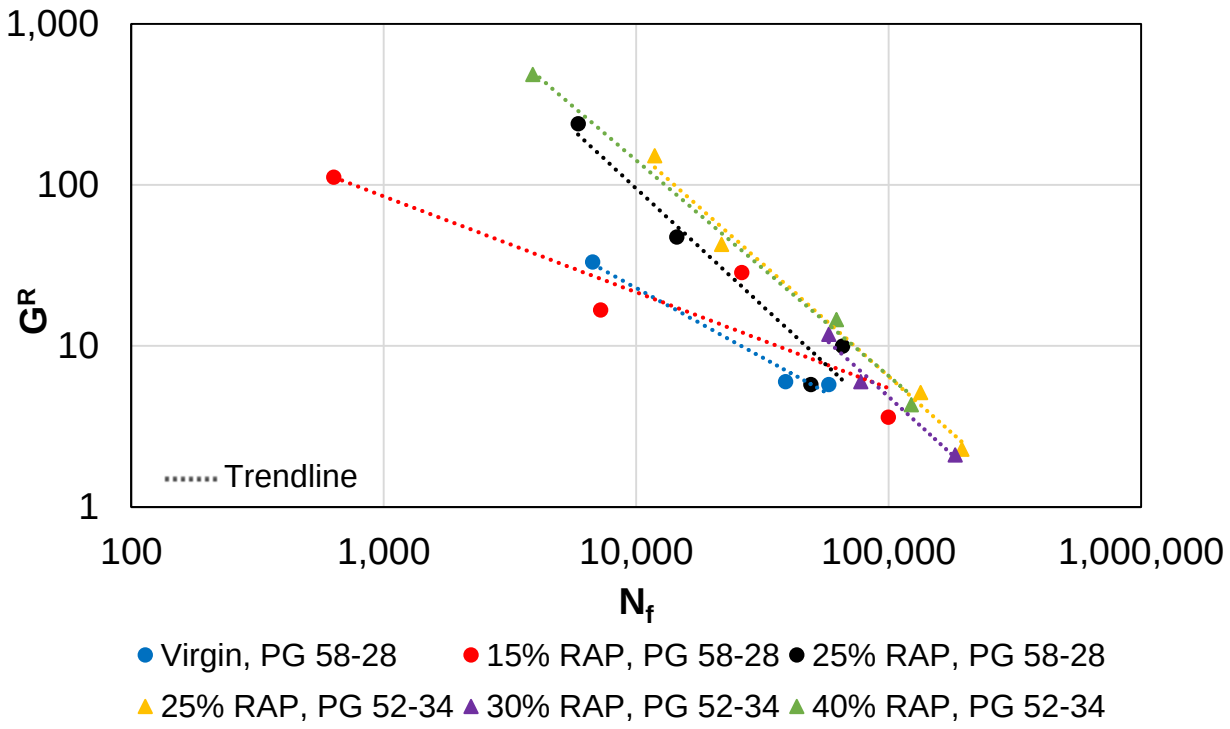

Figure 96: S-VECD Fatigue Failure Criterion Results for PMPC Mixtures

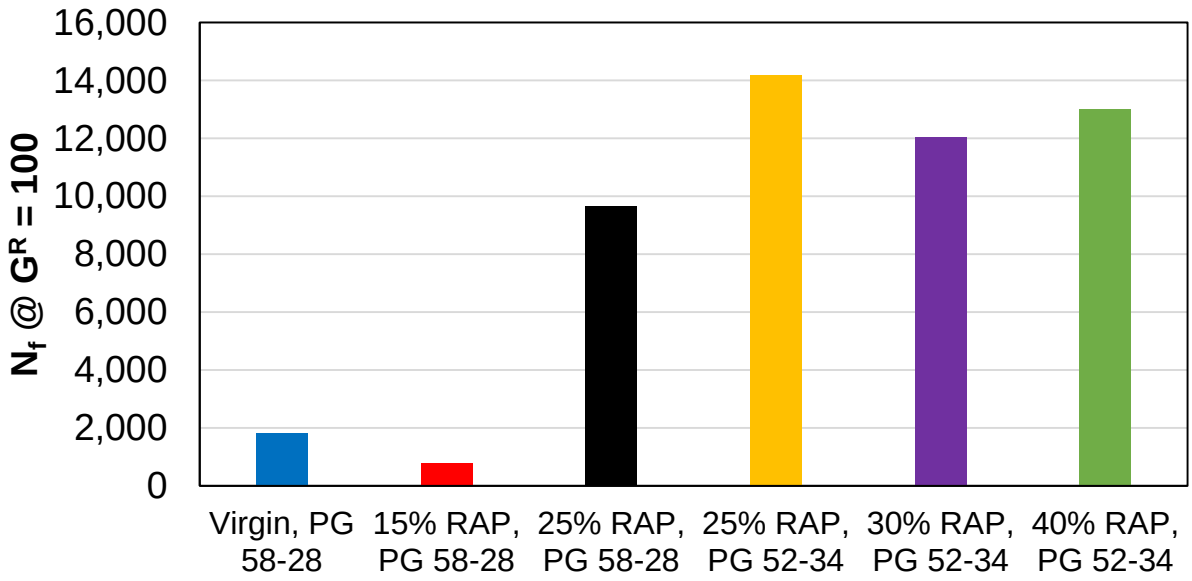

Figure 97: S-VECD Fatigue Index Parameter Results for PMPC Mixtures

A.3 Plant Mixed, Lab Compacted Specimens: Dynamic Modulus Results

The loose mixture sampled at the plant during production was brought back to the lab and reheated to produce three replicate specimens for each mixture. The average dynamic modulus curves for the six mixtures are shown in Figure 98 and Figure 99. The stiffness of both the PG 58-28 and PG 52-34 base binder mixtures show a decrease in average stiffness as the RAP content increases. The 25% RAP 52-34 mixture has a higher stiffness than the 25% RAP 58-28 mixture. These results do not follow expected trends with RAP content and binder grade; the differences are likely a result of the reheating process that was required to fabricate specimens from loose mix. The Black Space and phase angle master curves for the six mixtures are shown in Figure 100 and Figure 101. There are no discernable trends with respect to RAP content or base binder grade with these results.

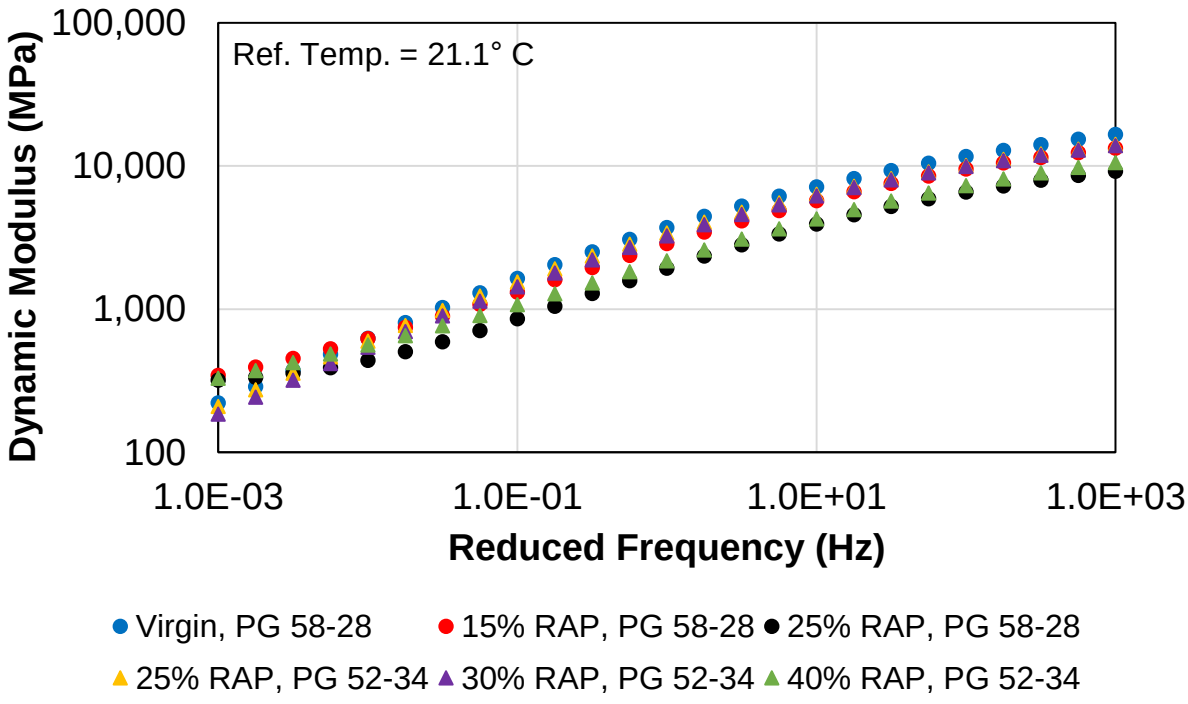

Figure 98: Dynamic Modulus Master Curve (log-log) for PMLC Mixtures

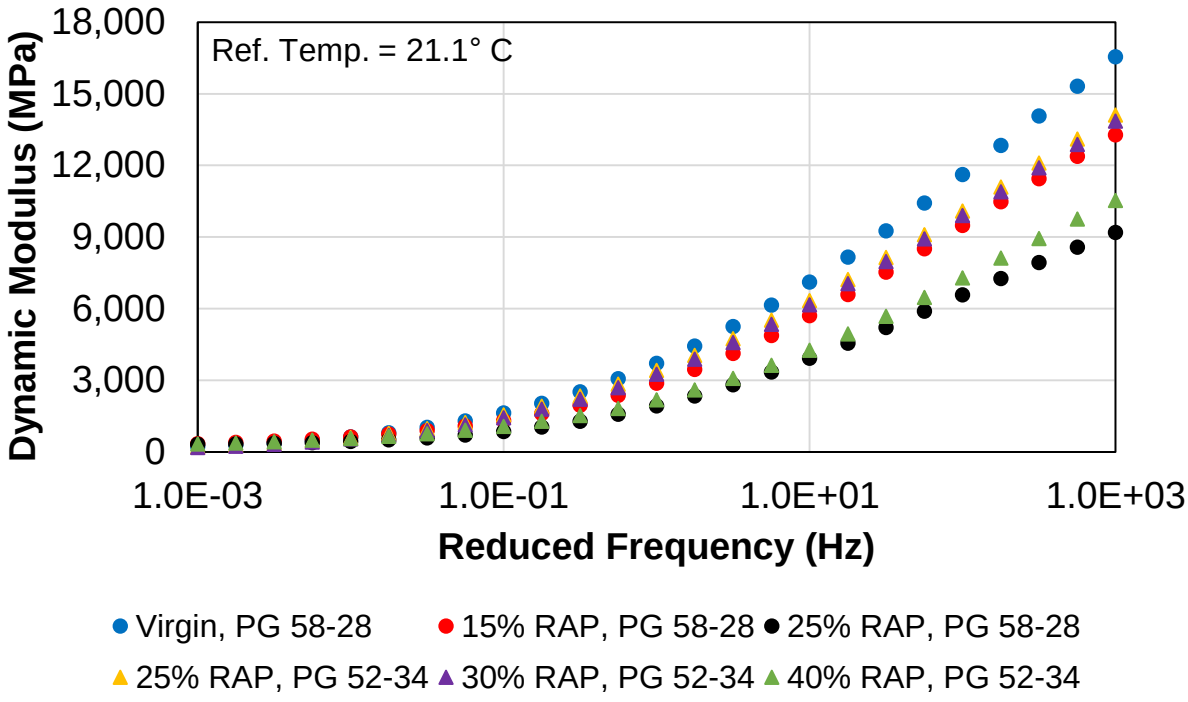

Figure 99: Dynamic Modulus Master Curve (semi-log) for PMLC Mixtures

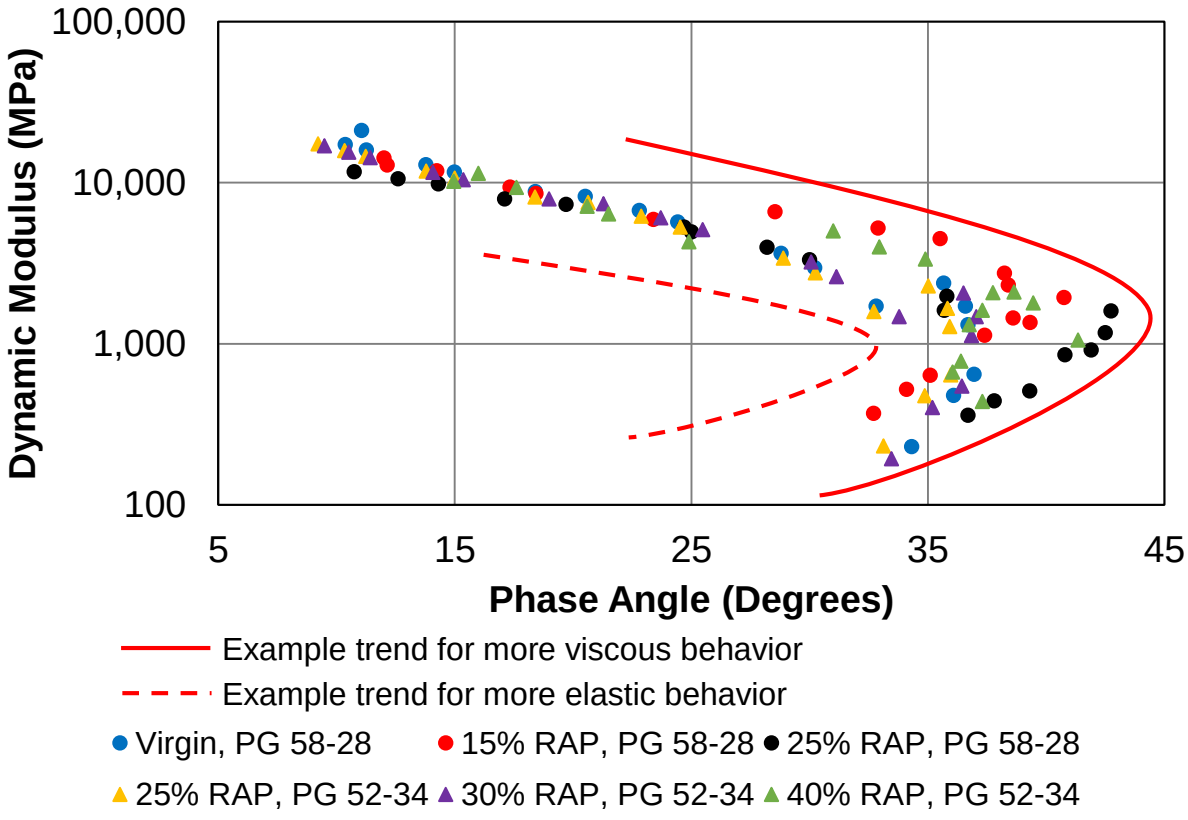

Figure 100: Black Space Plots for PMLC Mixtures

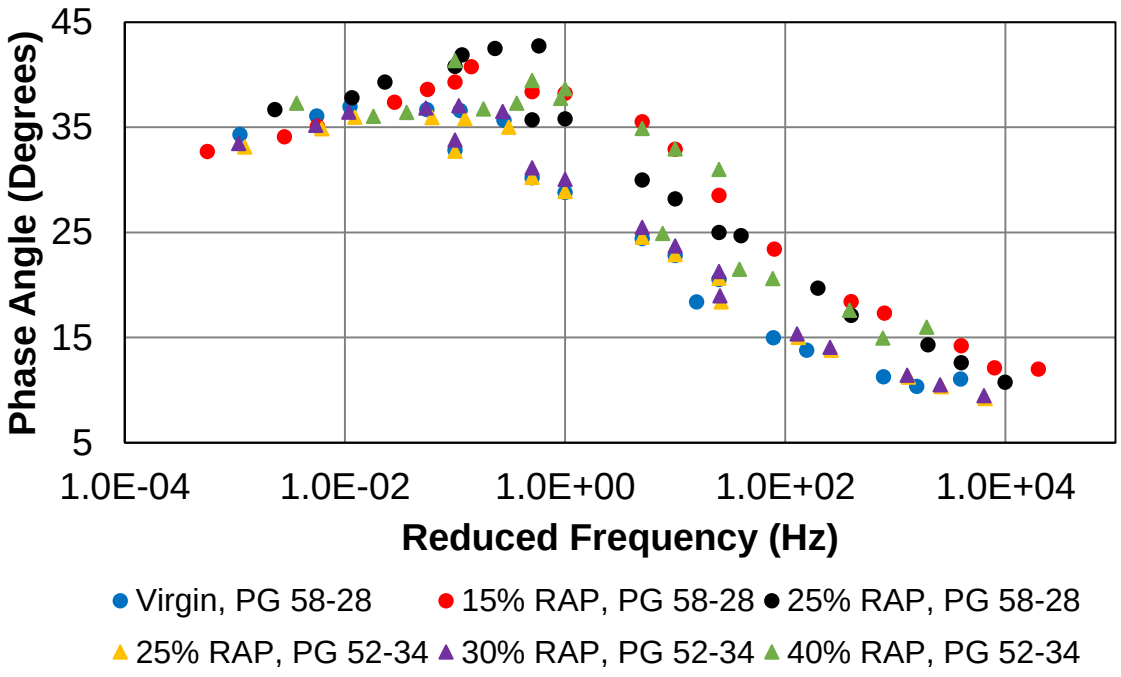

Figure 101: Phase Angle Master Curves for PMLC Mixtures

A.4 Plant Mixed, Lab Compacted Specimens: S-VECD Fatigue Results

Fatigue results for PMLC specimens are shown in Figure 102 to Figure 104. The damage characteristic curves show little difference between the mixtures, but identify the lowest RAP content (virgin for PG 58-28 and 25% for PG 52-34) as the worst performer. However, the full pavement structure must be considered when analyzing these results, as explained previously. The results of the fatigue failure criterion and index parameter align more with expectations, as better fatigue resistance (higher N_f) is observed among lower RAP contents. Also, the PG 52-34 mixtures generally have better fatigue resistance than the PG 58-28 mixture perhaps because of the relaxation capabilities of a softer binder.

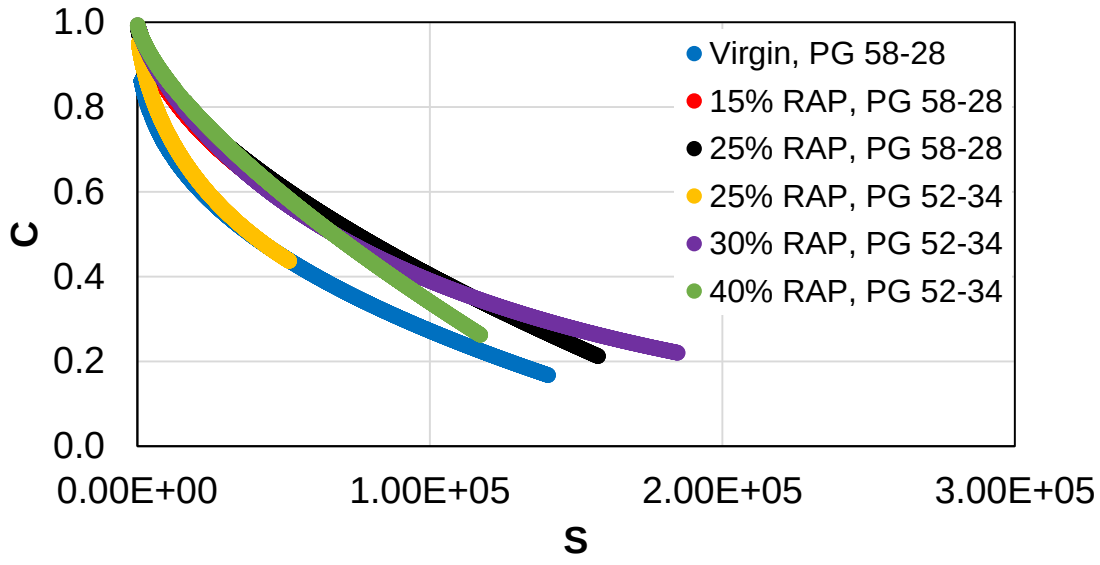

Figure 102: S-VECD Fatigue Damage Characteristic Curves for PMLC Mixtures

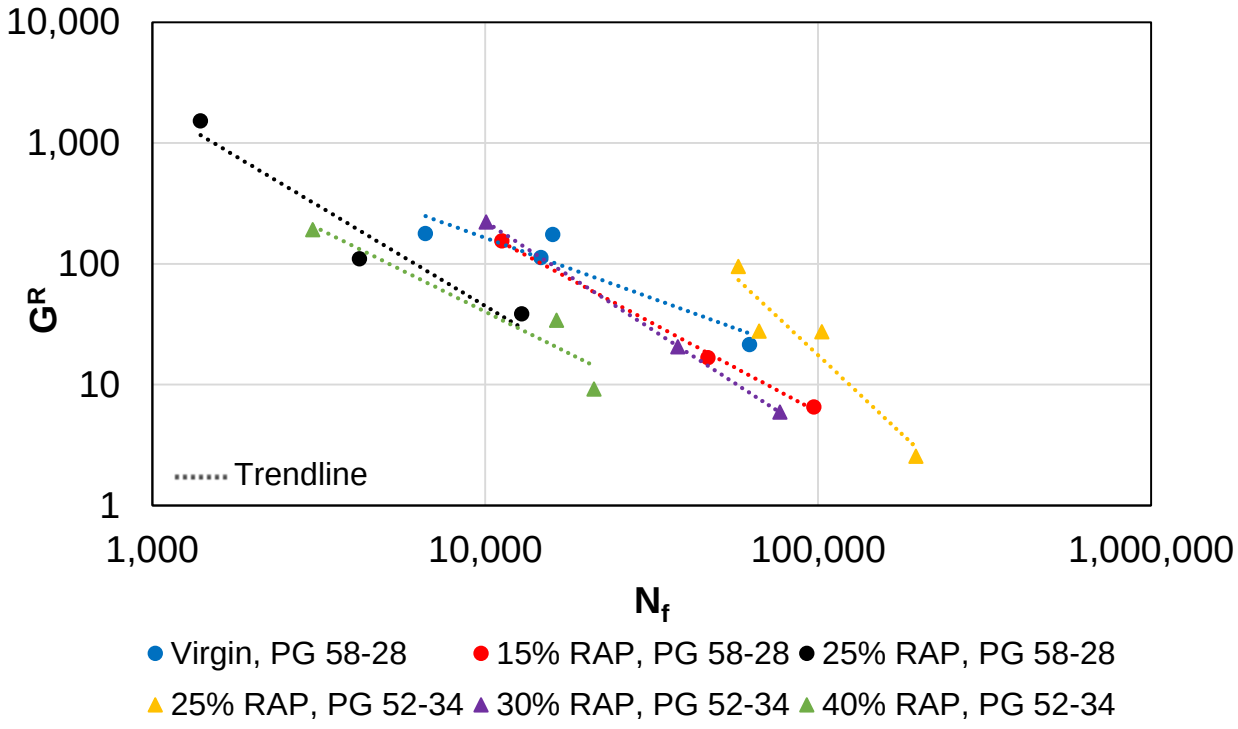

Figure 103: S-VECD Fatigue Failure Criterion Results for PMLC Mixtures

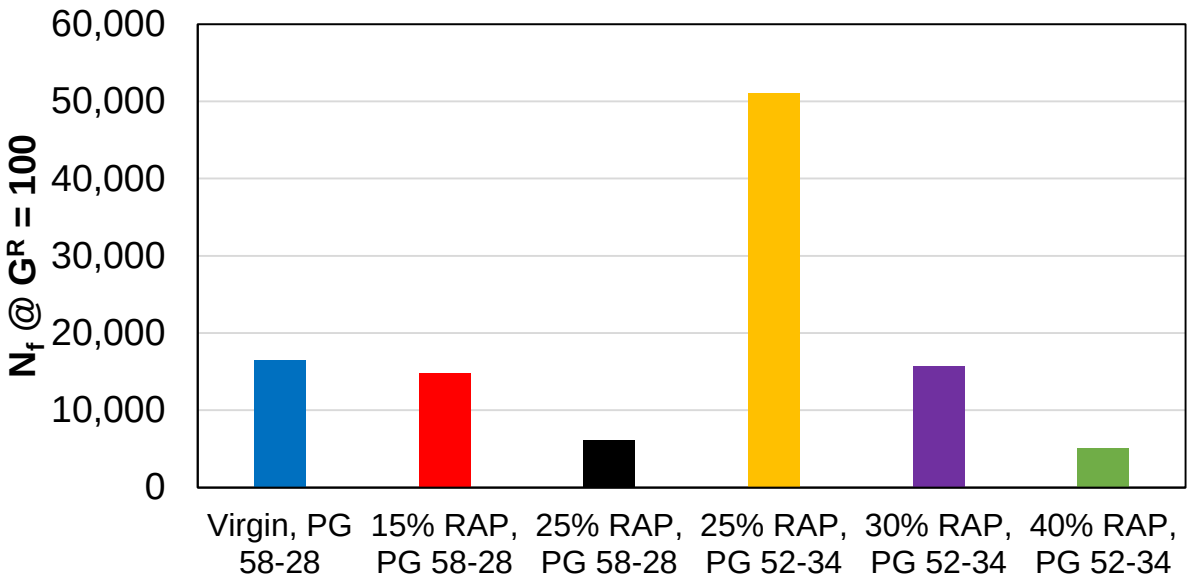

Figure 104: S-VECD Fatigue Index Parameter Results for PMLC Mixtures

A.5 Lab Mixed, Lab Compacted Specimens: Dynamic Modulus Results

The dynamic modulus of LMLC specimens was measured on four of the six mixtures, and four replicate specimens were fabricated and tested for each mixture. The average dynamic modulus master curves for the four mixtures are shown in Figure 105 and Figure 106. The virgin and the 25% RAP PG 58-28 mixture have similar curves, with the 25% RAP mixture showing slightly stiffer response over the mid to high frequency range. The two mixtures with the PG 52-34 base binder show softer response than the PG 58-28 base binder mixtures, but there is very little difference between the PG 52-34 RAP contents.

Figure 107 shows the average Black Space curves for the LMLC specimens. The phase angles for the virgin and the 25% RAP PG 58-28 curves follow the expected trend that the addition of RAP decreases the maximum phase angle. However, the relationship is reversed at the lower stiffness values. The 25% RAP PG 52-34 mixture has a smaller phase angle than the 25% RAP PG 58-28 mixture, which is not expected with the softer binder. Also, the PG 52-34 base binders show an increase in phase angle with the increase in RAP near the inflection point. In summary,

the PG grade of the base binder shows a larger impact on the dynamic modulus and phase angle than the RAP percentage for the specimens that were mixed and produced in the lab. The phase angles for the PG 52-34 mixtures do not follow expected trends with RAP content or in relation to the PG 58-28 mixtures.

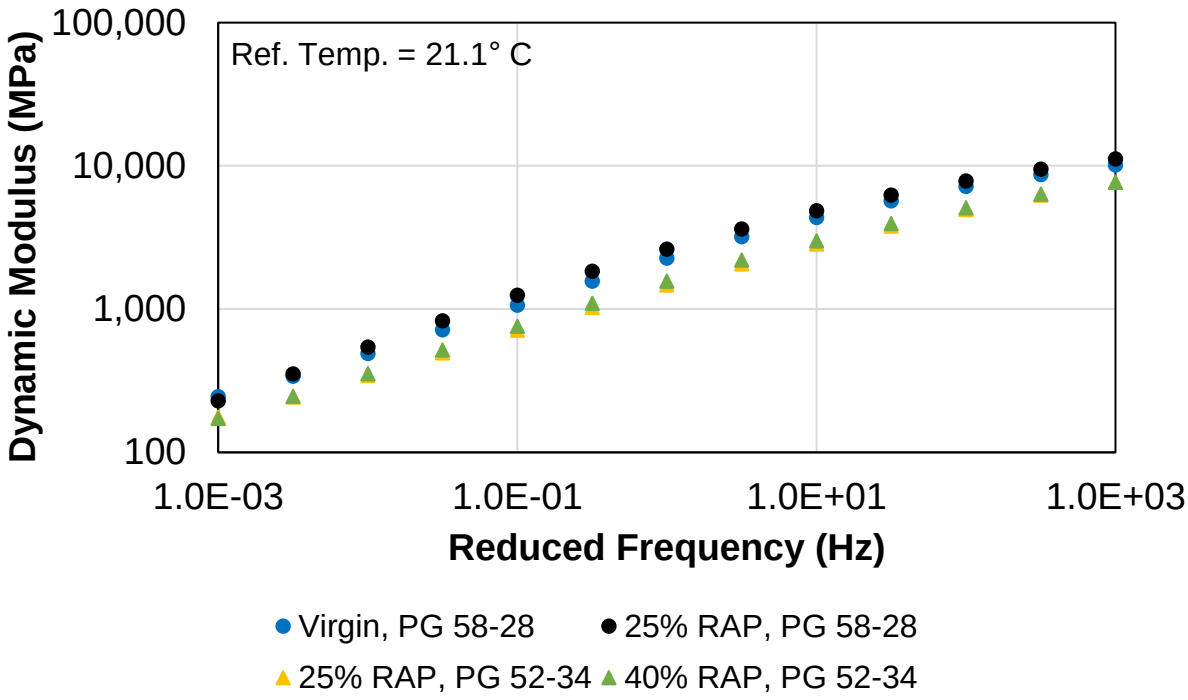

Figure 105: Dynamic Modulus Master Curve (log-log) for LMLC Mixtures

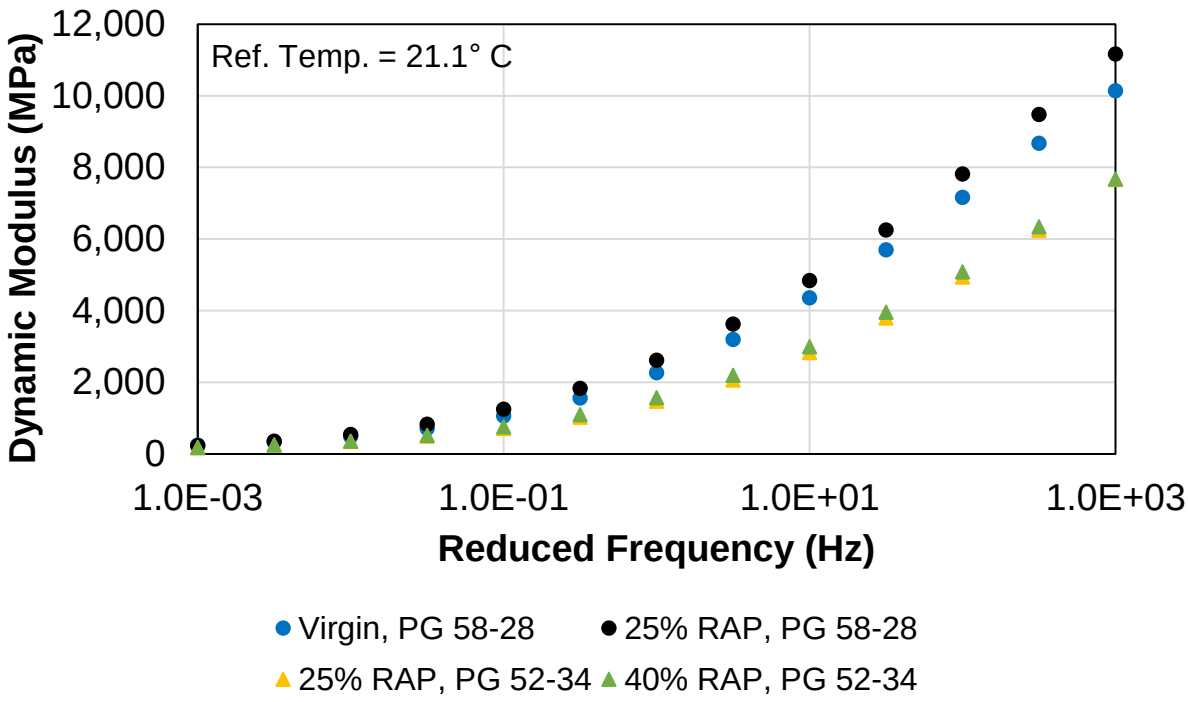

Figure 106: Dynamic Modulus Master Curve (semi-log) for LMLC Mixtures

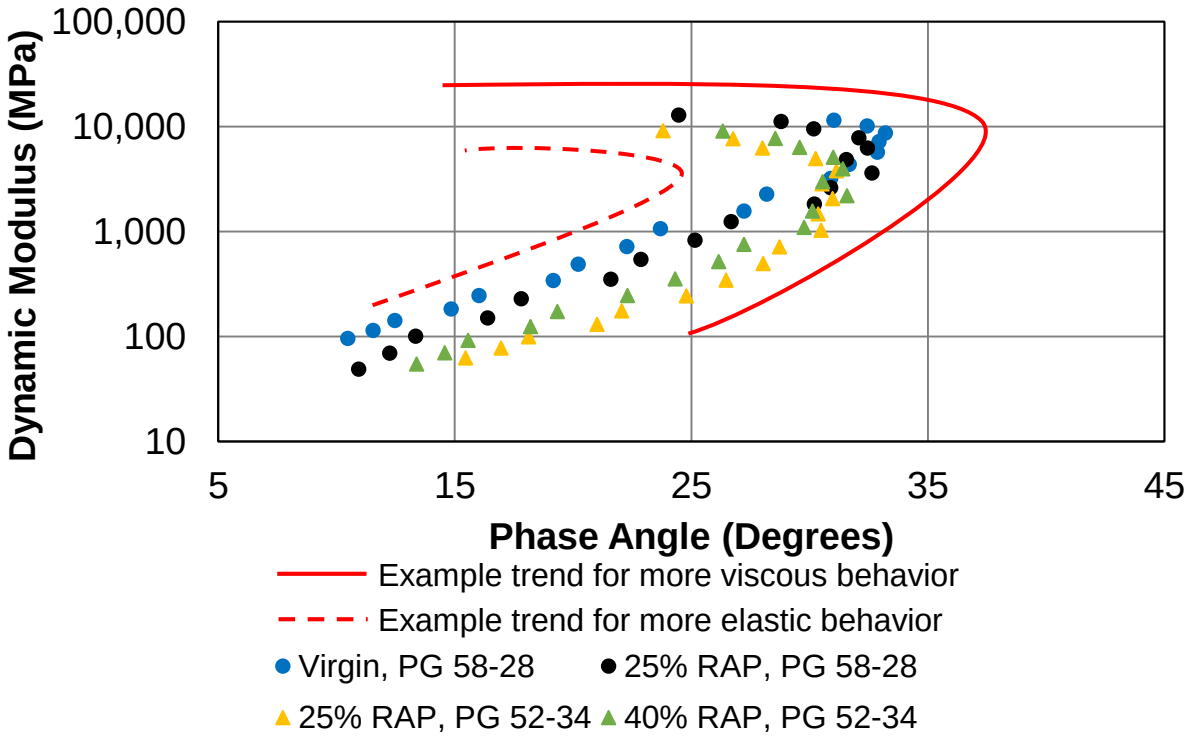

Figure 107: Black Space Plots for LMLC Mixtures

APPENDIX B: MEASUREMENTS AND DATA

B.1 Test Specimen Measurements

Table 15: Individual Weight Measurements (AASHTO T166) of Dynamic Modulus Specimens for Virgin Silo Storage Mixtures

Silo Time	Specimen #	Final Cut Specimen			Gyratory Specimen		
		Wet (g)	SSD (g)	Dry (g)	Wet (g)	SSD (g)	Dry (g)
0 hrs	1	1583.7	2760.4	2757.0	3928.8	6894.4	6858.8
0 hrs	2	1594.1	2768.4	2765.3	3934.3	6886.7	6844.2
0 hrs	3	1563.9	2736.5	2732.6	3911.4	6879.3	6840.9
2.5 hrs	1	1579.6	2745.1	2742.0	3960.0	6931.1	6892.2
2.5 hrs	2	1602.8	2775.1	2772.3	3964.8	6922.2	6887.5
2.5 hrs	3	1593.8	2770.2	2767.0	3940.2	6912.3	6875.6
5 hrs	1	1596.8	2774.2	2771.7	3954.2	6929.3	6891.2
5 hrs	2	1568.1	2726.4	2722.4	3951.3	6920.5	6887.6
5 hrs	3	1597.1	2776.0	2772.8	3960.6	6913.0	6881.7
7.5 hrs	1	1608.4	2787.5	2783.0	3962.5	6911.9	6875.0
7.5 hrs	2	1588.8	2756.8	2753.3	3956.3	6904.9	6863.6
7.5 hrs	3	1600.4	2773.0	2768.6	3956.0	6899.4	6855.3

Table 16: Individual Weight Measurements (AASHTO T166) of S-VECD Fatigue Specimens for Virgin Silo Storage Mixtures

Silo Time	Specimen #	Final Cut Specimen			Gyratory Specimen		
		Wet (g)	SSD (g)	Dry (g)	Wet (g)	SSD (g)	Dry (g)
0 hrs	1	1361.9	2366.0	2361.0	3923.7	6879.0	6843.4
0 hrs	2	1387.8	2391.8	2388.6	3955.0	6899.0	6863.7
0 hrs	3	1346.2	2349.4	2344.4	3925.0	6908.9	6860.1
0 hrs	4	1367.3	2374.0	2371.0	3937.0	6893.6	6861.4
2.5 hrs	1	1366.6	2369.2	2366.6	3947.2	6905.0	6868.6
2.5 hrs	2	1359.0	2355.3	2351.9	3944.3	6907.9	6874.7
2.5 hrs	3	1352.6	2350.5	2346.8	3948.5	6916.2	6884.7
2.5 hrs	4	1367.6	2364.3	2361.2	3953.1	6913.2	6875.7
5 hrs	1	1360.6	2369.2	2366.2	3948.5	6914.7	6874.8
5 hrs	2	1350.5	2354.8	2350.6	3929.3	6910.0	6862.9
5 hrs	3	1368.9	2369.0	2365.5	3968.4	6927.3	6896.9
5 hrs	4	1355.0	2355.3	2351.8	3944.1	6924.9	6880.8
7.5 hrs	1	1383.6	2380.9	2377.7	3976.0	6914.6	6867.3
7.5 hrs	2	1388.9	2397.0	2392.7	3963.7	6913.9	6874.5
7.5 hrs	3	1383.5	2387.5	2383.5	3967.8	6918.4	6884.7
7.5 hrs	4	1376.7	2372.6	2361.2	3970.0	6916.3	6864.7

Table 17: Field Core Measurements (AASHTO T166): Virgin, PG 58-28 Specimens

Field Core ID	Dry (g)	Wet (g)	SSD (g)	Gmb	% Air	Estimated Thickness (mm)
A1	2858.4	1648.4	2862.5	2.354	4.8%	71.8
A2	2828.9	1635.9	2831.8	2.365	4.3%	71.1
A3	2400.8	1367.2	2409.1	2.304	6.8%	60.3
A4	2601.4	1504.7	2603.6	2.367	4.2%	65.4
A5	2806.8	1612.0	2811.4	2.340	5.3%	70.5
A6	2991.5	1717.3	3001.6	2.329	5.8%	75.2
A7	3186.7	1818.9	3203.4	2.302	6.9%	80.1
A8	3284.3	1905.4	3295.8	2.362	4.4%	82.5
A10	3105.6	1795.4	3110.0	2.362	4.4%	78.0

Table 18: Field Core Measurements (AASHTO T166): 15% RAP, PG 58-28 Specimens

Field Core ID	Dry (g)	Wet (g)	SSD (g)	Gmb	% Air	Estimated Thickness (mm)
B1	2411.6	1385.0	2415.0	2.341	5.2%	60.6
B2	2421.2	1400.9	2424.5	2.365	4.3%	60.8
B3	1503.6	874.9	1510.0	2.368	4.2%	37.8
B4	2921.0	1681.9	2925.6	2.349	5.0%	73.4
B5	2820.4	1628.9	2823.6	2.361	4.5%	70.9
B6	2322.3	1326.0	2329.3	2.315	6.3%	58.4
B7	2158.2	1236.9	2162.3	2.332	5.6%	54.2
B8	2263.2	1286.8	2272.7	2.296	7.1%	56.9
B9	2959.2	1692.8	2975.3	2.307	6.6%	74.4
B10	2385.5	1368.5	2390.5	2.334	5.5%	59.9

Table 19: Field Core Measurements (AASHTO T166): 25% RAP, PG 58-28 Specimens

Field Core ID	Dry (g)	Wet (g)	SSD (g)	Gmb	% Air	Estimated Thickness (mm)
C1	3234.4	1875.7	3238.6	2.373	3.6%	81.3
C2	3081.3	1770.2	3089.9	2.335	5.2%	77.4
C3	3204.6	1861.7	3206.0	2.384	3.2%	80.5
C4	2647.8	1534.3	2650.0	2.373	3.6%	66.5
C5	2666.8	1525.2	2684.8	2.300	6.6%	67.0
C6	3037.5	1737.4	3048.2	2.317	5.9%	76.3
C7	2602.7	1469.8	2622.9	2.257	8.4%	65.4
C8	2936.1	1677.8	2944.7	2.318	5.9%	73.8
C9	2773.8	1590.0	2785.8	2.320	5.8%	69.7
C10	2793.8	1587.1	2808.4	2.288	7.1%	70.2

Table 20: Field Core Measurements (AASHTO T166): 25% RAP, PG 52-34 Specimens

Field Core ID	Dry (g)	Wet (g)	SSD (g)	Gmb	% Air	Estimated Thickness (mm)
D1	2612.0	1480.8	2618.5	2.296	6.4%	65.6
D2	2875.0	1629.8	2885.1	2.290	6.7%	72.2
D3	3139.8	1790.7	3150.8	2.309	5.9%	78.9
D4	2617.6	1493.4	2626.0	2.311	5.8%	65.8
D5	2410.7	1387.9	2413.1	2.351	4.2%	60.6
D6	3223.2	1851.7	3234.6	2.331	5.0%	81.0
D8	2596.0	1482.0	2606.3	2.309	5.9%	65.2
D9	2444.6	1396.7	2457.6	2.304	6.1%	61.4
D10	2349.4	1330.0	2361.1	2.279	7.2%	59.0

Table 21: Field Core Measurements (AASHTO T166): 30% RAP, PG 52-34 Specimens

Field Core ID	Dry (g)	Wet (g)	SSD (g)	Gmb	% Air	Estimated Thickness (mm)
E2	2825.6	1598.8	2839.9	2.277	7.7%	71.0
E3	1472.7	830.5	1481.5	2.262	8.3%	37.0
E4	1296.0	728.6	1310.1	2.229	9.6%	32.6
E5	2614.4	1480.8	2628.3	2.278	7.6%	65.7
E6	2784.7	1581.8	2795.2	2.295	6.9%	70.0
E7	1483.9	846.1	1487.5	2.314	6.2%	37.3
E8	2645.1	1510.4	2651.1	2.319	6.0%	66.5
E9	2549.9	1442.0	2555.8	2.289	7.2%	64.1
E10	1687.6	959.2	1691.0	2.306	6.5%	42.4

Table 22: Field Core Measurements (AASHTO T166): 40% RAP, PG 52-34 Specimens

Field Core ID	Dry (g)	Wet (g)	SSD (g)	Gmb	% Air	Estimated Thickness (mm)
F1	3105.5	1773.3	3114.9	2.315	5.4%	78.0
F2	2453.8	1410.9	2457.6	2.344	4.2%	61.7
F3	2695.9	1537.7	2704.7	2.310	5.6%	67.7
F4	3320.0	1912.3	3328.3	2.345	4.2%	83.4
F5	2919.9	1675.3	2926.2	2.334	4.6%	73.4
F6	2102.5	1194.4	2104.9	2.309	5.6%	52.8
F8	2111.6	1192.6	2117.5	2.283	6.7%	53.1
F10	2023.3	1144.0	2026.0	2.294	6.3%	50.8

Table 23: Individual Weight Measurements (AASHTO T166) of Dynamic Modulus Specimens for Small Specimen Mixtures

Replicate	Field Core ID	Wet (g)	SSD (g)	Dry (g)
A1	A6	169.7	295.1	294.8
A2	A6	162.1	283.5	283.2
A3	A3	162.2	283.1	282.2
B1	B10	166.4	290.0	289.3
B2	B10	164.9	287.2	286.7
B3	B6	165.5	288.9	287.9
C1	C6	163.9	286.6	285.6
C2	C6	165.1	288.9	287.8
C3	C10	160.6	283.3	282.0
D1	D4	164.6	289.8	289.4
D2	D4	163.6	284.4	284.0
D3	D3	161.1	283.7	283.1
E1	E6	163.0	287.1	286.4
E2	E9	165.2	289.7	289.0
E3	E6	164.3	288.9	288.3
F1	F5	168.2	293.0	292.6
F2	F5	165.8	290.2	289.9
F3	F2	166.4	290.5	289.8

Table 24: Individual Weight Measurements (AASHTO T166) of S-VECD Fatigue Specimens for Small Specimen Mixtures

Replicate	Field Core ID	Wet (g)	SSD (g)	Dry (g)
A1	A1	163.9	282.3	282.0
A2	A1	162.8	281.4	280.9
A3	A5	164.3	285.9	285.4
A4	A5	164.9	282.7	282.0
B1	B4	168.6	288.0	287.7
B2	B5	166.9	287.1	286.6
B4	B9	162.0	282.0	280.8
B5	B9	157.3	274.6	273.3
C1	C1	182.3	313.7	313.5
C2	C1	178.7	308.4	307.9
C3	C8	159.2	278.0	277.1
C4	C8	161.4	280.3	279.4
D1	D6	161.9	280.9	280.2
D2	D1	157.3	279.0	278.2
D3	D6	162.5	282.1	281.6
D4	D2	164.0	289.9	289.1
E1	E2	153.3	272.7	271.6
E2	E2	159.7	280.9	280.0
E3	E6	163.0	287.1	286.4
E4	E9	165.2	289.7	289.0
F1	F1	167.1	292.4	291.4
F2	F1	165.1	289.4	288.2
F3	F4	163.5	284.0	283.8
F4	F4	163.7	284.5	284.2

B.2 Binder Test Data

Table 25: Summarized Results of Silo Storage Binder Testing

Virgin Mix										
Silo Storage Time	**Performance Grade (° C)**					**Rheological Indices**				
	High Temp (RTFO)	**Intermediate Temp**	**Low Temperature**			**R-value**	**Crossover Frequency**	**Glover-Rowe Analysis (15° C, 0.005 rad/s)**		
			Stiffness (S)	**m-slope**	**BBR ΔT_{crit}**			**G* (Pa)**	**δ (degrees)**	**G-R (kPa)**
0 hrs	72.1	22.7	-25.1	-24.8	-0.3	1.732	149.1	8.78E+04	71.1	9.8
2.5 hrs	73.8	23.3	-25.0	-24.6	-0.4	1.808	123.4	9.84E+04	69.8	12.5
5 hrs	73.4	24.1	-24.9	-24.7	-0.2	1.784	105.5	1.22E+05	69.5	16.0
7.5 hrs	75.5	24.1	-25.1	-23.6	-1.5	1.866	101.2	1.43E+05	68.9	19.8
25% RAP Mix										
Silo Storage Time	**Performance Grade (° C)**					**Rheological Indices**				
	High Temp (RTFO)	**Intermediate Temp**	**Low Temperature**			**R-value**	**Crossover Frequency**	**Glover-Rowe Analysis (15° C, 0.005 rad/s)**		
			Stiffness (S)	**m-slope**	**BBR ΔT_{crit}**			**G* (Pa)**	**δ (degrees)**	**G-R (kPa)**
0 hrs	73.9	24.6	-25.9	-24.9	-1.0	1.977	100.2	1.83E+05	66.8	31.0
2.5 hrs	76.2	22.6	-25.4	-22.8	-2.6	2.002	74.2	2.20E+05	65.8	40.7
5 hrs	77.9	24.5	-24.9	-23.4	-1.5	2.094	43.5	3.19E+05	63.6	70.2
7.5 hrs	77.3	23.6	-25.2	-22.7	-2.5	2.070	52.6	2.77E+05	64.3	58.0
10 hrs	80.0	24.1	-24.8	-22.3	-2.5	2.150	29.0	3.78E+05	62.2	93.1

B.3 Dynamic Modulus Data

Table 26: Dynamic Modulus Test Data for Virgin Silo Storage Mixtures

Silo Storage Time	Replicate #	~4.4° C						~21.1° C						~37.8° C					
		25 Hz	10 Hz	5 Hz	1 Hz	0.5 Hz	0.1 Hz	25 Hz	10 Hz	5 Hz	1 Hz	0.5 Hz	0.1 Hz	25 Hz	10 Hz	5 Hz	1 Hz	0.5 Hz	0.1 Hz
		Dynamic Modulus (MPa)																	
0 hours	1	16889.5	15410.8	14357.4	11801.2	10699.2	8286.8	8046.1	6718.3	5717.9	3736.6	3037.1	1755.2	2885.1	2085.0	1606.1	866.3	677.6	426.7
	2	16517.8	15420.4	14583.1	12038.3	11046.9	8587.0	7858.4	6436.2	5453.5	3497.1	2843.3	1616.8	2652.3	1908.5	1449.6	782.6	613.1	391.0
	3	15810.3	14731.2	14095.7	11496.2	10498.2	7932.3	7742.5	6417.9	5480.7	3535.7	2859.4	1649.3	2427.4	1755.6	1340.8	716.5	561.4	352.8
2.5 hrs	1	16340.8	15307.2	14468.5	11958.2	10944.8	8400.5	7892.4	6504.3	5533.0	3569.2	2909.2	1662.4	2781.1	2012.1	1525.4	805.2	627.4	384.3
	2	16673.4	15525.6	14571.3	12146.3	11058.8	8569.1	8453.1	7103.3	6092.4	4038.3	3317.9	1949.0	3221.4	2347.4	1806.6	975.6	760.3	462.8
	3	16404.5	15298.4	14546.4	12018.0	11081.2	8389.0	8757.9	7255.0	6213.3	4024.4	3306.8	1908.7	3149.8	2301.4	1767.1	958.7	757.3	479.0
5 hrs	1	17663.3	16409.1	15356.7	12465.8	11487.9	8988.9	9363.0	7806.6	6733.9	4498.0	3702.5	2205.2	3175.2	2316.4	1783.8	945.8	738.3	436.1
	2	16275.0	14813.5	13804.1	11264.3	10170.3	7715.4	8246.6	6824.6	5809.7	3748.2	3057.6	1740.9	2904.9	2129.5	1646.6	887.4	701.7	433.0
	3	18732.2	17438.1	16323.1	13630.0	12449.1	9819.6	8938.5	7527.1	6457.6	4252.2	3522.2	2071.7	3327.8	2432.5	1876.0	1028.0	805.5	492.0
7.5 hrs	1	17320.9	15897.7	14792.7	12127.0	11094.6	8637.4	9244.8	7773.7	6724.8	4506.5	3771.9	2285.1	3464.3	2592.3	2043.9	1146.9	905.7	543.1
	2	18301.0	16757.6	15645.7	12997.6	11871.0	9324.5	9329.1	7998.1	6993.2	4738.4	4037.6	2450.2	3587.5	2693.7	2113.8	1199.2	935.6	568.3
	3	19306.1	18076.8	17032.3	14281.4	12999.3	10335.5	9643.9	8124.9	7021.4	4718.3	3895.2	2340.8	3490.2	2607.8	2050.3	1139.4	900.1	539.5

Table 27: Phase Angle Test Data for Virgin Silo Storage Mixtures

Silo Storage Time	Replicate #	~4.4° C						~21.1° C						~37.8° C					
		25 Hz	10 Hz	5 Hz	1 Hz	0.5 Hz	0.1 Hz	25 Hz	10 Hz	5 Hz	1 Hz	0.5 Hz	0.1 Hz	25 Hz	10 Hz	5 Hz	1 Hz	0.5 Hz	0.1 Hz
		Phase Angle (Degrees)																	
0 hours	1	7.0	9.2	10.2	13.2	14.2	19.0	24.0	21.9	23.6	28.5	29.5	32.7	36.0	32.2	32.0	30.2	28.6	23.4
	2	9.0	11.9	13.2	15.5	17.5	23.0	25.9	23.4	24.8	29.2	30.7	35.0	27.0	33.0	33.2	30.2	28.4	22.4
	3	13.5	17.8	19.5	23.3	25.2	30.6	27.0	24.7	26.7	31.0	32.6	36.6	31.5	33.8	33.4	32.0	29.4	24.6
2.5 hrs	1	13.5	14.1	16.5	19.8	21.6	27.5	18.0	22.5	24.1	29.2	31.1	36.3	34.5	33.0	33.2	31.8	29.8	25.0
	2	11.3	11.9	13.2	17.1	18.0	21.6	20.3	23.3	25.2	29.9	32.1	36.2	34.5	33.4	33.4	32.0	30.6	26.4
	3	13.5	15.3	17.7	20.8	23.6	27.5	19.1	23.2	24.8	29.7	31.7	35.9	36.0	33.2	32.8	30.6	28.2	22.8
5 hrs	1	15.4	15.0	17.6	19.8	21.3	26.1	20.2	22.2	23.7	28.9	30.3	34.2	36.0	34.0	33.8	33.6	31.8	28.6
	2	10.5	10.6	11.8	13.6	14.6	19.2	18.0	21.4	23.6	28.2	30.0	35.4	27.0	33.8	33.6	32.0	30.6	25.8
	3	9.0	8.8	10.2	12.0	12.6	16.4	18.0	21.0	23.4	26.7	28.9	32.8	36.0	31.8	32.8	31.6	30.6	26.2
7.5 hrs	1	10.0	10.4	10.8	13.8	14.2	18.0	18.0	19.2	20.6	25.0	26.4	31.4	33.0	31.2	31.4	31.8	30.6	28.2
	2	9.0	8.6	9.4	12.4	13.0	16.8	18.0	23.6	25.8	30.6	31.9	38.0	27.0	30.8	31.6	30.0	29.6	26.4
	3	9.0	9.4	10.4	12.0	12.8	15.4	18.0	18.8	20.6	25.2	26.6	31.4	30.0	31.8	32.4	32.0	30.8	28.6

Table 28: Dynamic Modulus Test Data for 25% RAP Silo Storage Mixtures

Silo Storage Time	Replicate #	~4.4° C						~21.1° C						~37.8° C					
		25 Hz	10 Hz	5 Hz	1 Hz	0.5 Hz	0.1 Hz	25 Hz	10 Hz	5 Hz	1 Hz	0.5 Hz	0.1 Hz	25 Hz	10 Hz	5 Hz	1 Hz	0.5 Hz	0.1 Hz
		Dynamic Modulus (MPa)																	
0 hours	1	18094.0	16408.0	15208.0	12504.0	11490.0	8581.0	9393.0	7885.0	6829.0	4530.0	3755.0	2236.0	3588.0	2618.0	2035.0	1069.0	815.6	453.2
	2	14352.0	12873.0	11741.0	9024.0	7920.0	5575.0	6671.0	5288.0	4404.0	2655.0	2111.0	1135.0	1954.0	1324.0	976.7	489.8	380.9	245.0
	3	15376.0	13260.0	12213.0	9743.0	8388.0	6042.0	7226.0	5835.0	4908.0	3031.0	2436.0	1333.0	2219.0	1519.0	1123.0	562.9	431.3	264.8
2.5 hrs	1	17662.0	16294.0	15248.0	12615.0	11520.0	8928.0	9583.0	8114.0	7074.0	4769.0	4007.0	2434.0	3848.0	2854.0	2233.0	1176.0	892.2	483.8
	2	19665.0	17669.0	16157.0	13203.0	11865.0	8977.0	9709.0	8011.0	6827.0	4472.0	3681.0	2177.0	3579.0	2606.0	2015.0	1041.0	783.4	421.7
	3	17449.0	15754.0	14499.0	11585.0	10395.0	7707.0	9688.0	7984.0	6820.0	4558.0	3811.0	2346.0	3843.0	2882.0	2293.0	1250.0	961.3	513.3
5 hrs	1	20595.0	18644.0	17036.0	13782.0	12447.0	9552.0	10279.0	8584.0	7398.0	4952.0	4116.0	2461.0	3678.0	2667.0	2062.0	1064.0	800.5	436.1
	2	18564.0	17077.0	15968.0	13183.0	11956.0	9305.0	10386.0	8716.0	7564.0	5198.0	4401.0	2766.0	3943.0	2965.0	2369.0	1302.0	1009.0	554.2
	3	17814.0	16407.0	15319.0	12825.0	11896.0	9568.0	10168.0	8779.0	7804.0	5496.0	4710.0	3026.0	4281.0	3251.0	2612.0	1465.0	1143.0	629.6
7.5 hrs	1	18174.0	16756.0	15709.0	13028.0	11962.0	9385.0	10584.0	8887.0	7727.0	5282.0	4385.0	2682.0	4289.0	3212.0	2539.0	1375.0	1053.0	577.1
	2	20060.0	18106.0	16818.0	13893.0	12605.0	9734.0	10158.0	8594.0	7516.0	5201.0	4421.0	2784.0	4230.0	3179.0	2545.0	1401.0	1083.0	592.0
	3	20158.0	18232.0	16853.0	13903.0	12592.0	9794.0	10616.0	8964.0	7812.0	5437.0	4622.0	2947.0	4380.0	3333.0	2693.0	1520.0	1188.0	649.8
10 hrs	1	18696.0	17670.0	16938.0	14544.0	13520.0	10714.0	11719.0	9970.0	8738.0	6267.0	5396.0	3577.0	4538.0	3534.0	2927.0	1724.0	1393.0	796.3
	2	20149.0	18677.0	17610.0	14828.0	13632.0	10694.0	11561.0	9830.0	8576.0	5972.0	5062.0	3220.0	4381.0	3314.0	2678.0	1521.0	1194.0	668.0
	3	20032.0	18390.0	17161.0	14344.0	13141.0	10444.0	11363.0	9753.0	8617.0	6144.0	5264.0	3417.0	4422.0	3366.0	2733.0	1557.0	1226.0	670.8

Table 29: Phase Angle Test Data for 25% RAP Silo Storage Mixtures

Silo Storage Time	Replicate #	~4.4° C						~21.1° C						~37.8° C					
		25 Hz	10 Hz	5 Hz	1 Hz	0.5 Hz	0.1 Hz	25 Hz	10 Hz	5 Hz	1 Hz	0.5 Hz	0.1 Hz	25 Hz	10 Hz	5 Hz	1 Hz	0.5 Hz	0.1 Hz
		Phase Angle (Degrees)																	
0 hours	1	9.5	10.4	11.2	13.6	12.9	18.6	18.7	21.0	22.7	27.0	28.2	31.1	30.2	31.7	32.0	31.7	30.3	26.5
	2	9.3	8.6	9.7	13.4	14.6	18.4	18.8	21.2	22.9	27.4	28.6	31.6	30.5	32.2	32.6	32.6	31.2	27.5
	3	10.1	11.1	12.1	14.8	16.1	21.0	18.3	20.6	22.3	26.5	27.6	31.0	29.2	31.0	31.7	32.5	31.5	29.0
2.5 hrs	1	8.6	9.6	10.4	12.6	14.0	17.5	17.9	20.2	21.9	26.1	27.3	30.6	29.4	31.1	31.6	31.7	30.5	26.6
	2	8.1	9.0	9.8	11.9	13.0	16.3	16.2	18.1	19.5	23.2	24.4	27.7	26.8	28.6	29.4	30.5	29.9	28.2
	3	9.1	10.1	10.9	13.5	14.8	18.5	18.1	20.4	21.9	26.0	27.2	30.3	29.2	30.7	31.3	31.6	30.6	27.7
5 hrs	1	8.4	9.5	10.4	12.9	14.2	17.7	18.1	20.4	22.0	26.2	27.3	30.5	30.2	31.7	32.0	31.7	30.4	26.4
	2	8.5	9.4	10.2	12.4	13.6	16.7	17.0	19.0	20.4	24.6	25.5	28.8	28.7	30.4	31.0	31.6	30.5	27.7
	3	8.2	9.0	9.8	11.8	12.8	15.8	16.4	18.3	19.8	23.5	24.8	28.1	27.7	29.5	30.1	31.2	30.5	28.5
7.5 hrs	1	8.4	9.4	10.1	12.4	13.6	17.0	17.6	19.5	20.9	24.6	25.9	28.8	28.2	29.6	30.1	30.2	29.2	26.4
	2	8.0	9.1	9.9	12.1	13.2	16.5	17.1	19.2	20.7	24.6	25.8	28.9	28.4	30.2	30.7	31.3	30.4	27.9
	3	8.4	9.2	10.0	12.1	13.2	16.3	16.6	18.6	20.1	23.9	25.0	28.4	27.6	29.4	30.1	31.2	30.5	28.6
10 hrs	1	7.8	8.5	9.1	10.9	11.9	14.9	15.0	16.9	18.3	21.7	23.0	26.6	26.9	28.8	29.5	31.0	30.4	29.2
	2	8.1	8.9	9.6	11.6	12.7	15.9	16.1	18.2	19.7	23.6	24.9	28.5	27.7	29.3	29.7	30.2	29.2	26.9
	3	8.0	8.8	9.4	11.3	12.3	15.2	15.4	17.2	18.7	22.4	23.7	27.4	27.6	29.5	30.2	31.4	30.6	29.0

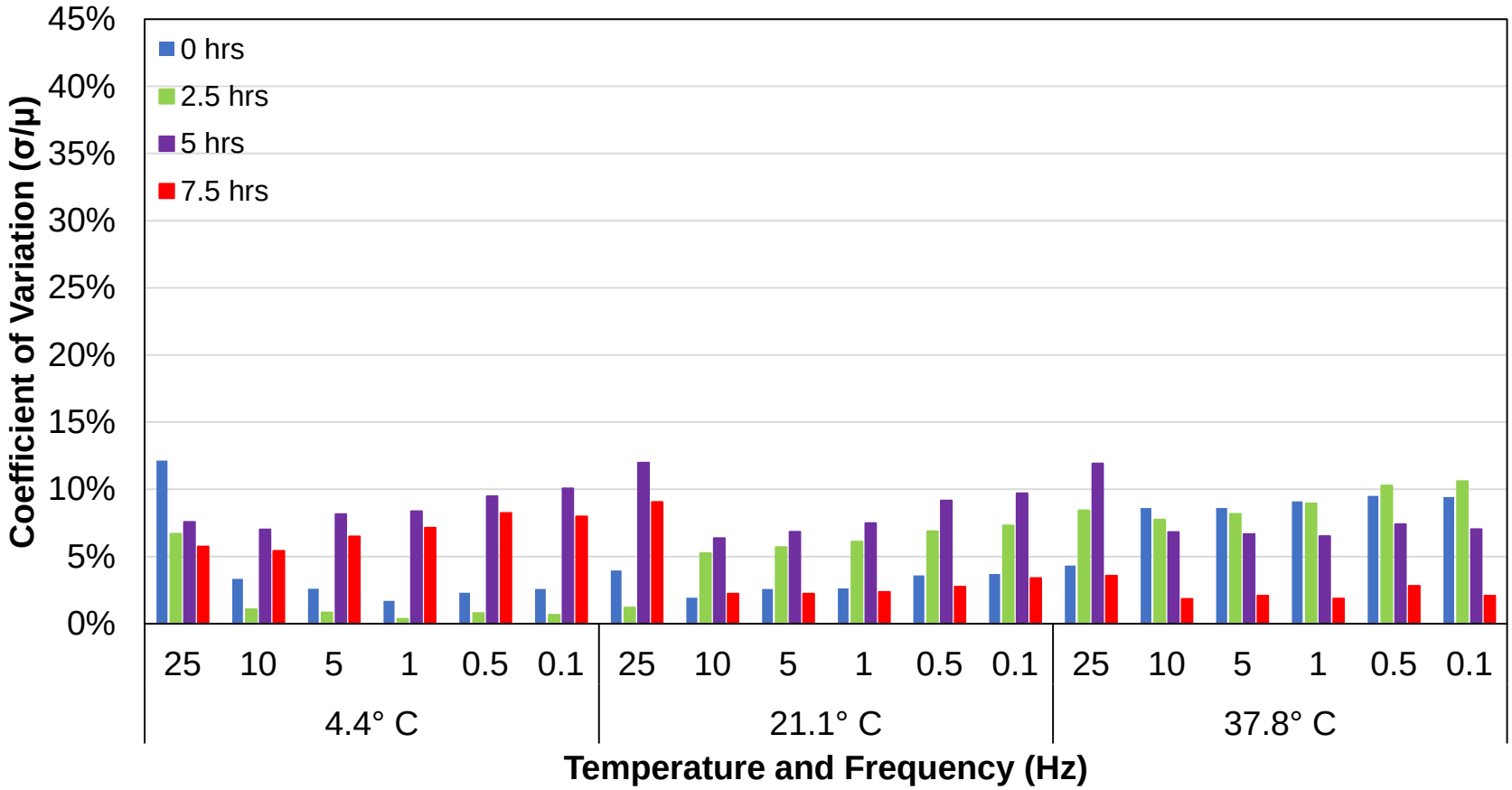

Figure 108: Coefficient of Variation for Dynamic Modulus Raw Data Virgin Silo Storage Mixtures

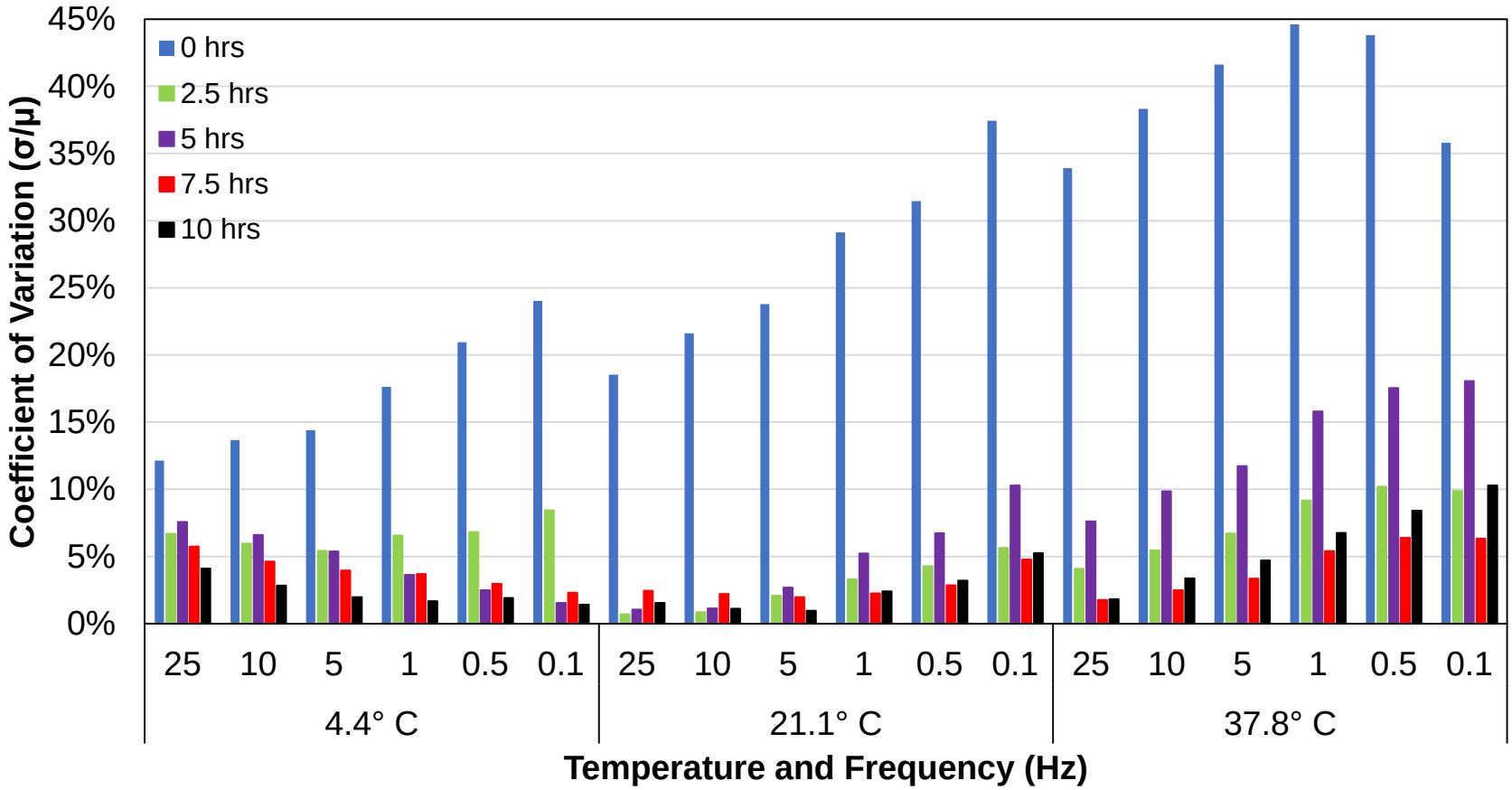

Figure 109: Coefficient of Variation for Dynamic Modulus Raw Data 25% RAP Silo Storage Mixtures

Table 30: Dynamic Modulus Test Data for Field Core Mixtures

Mix	Replicate #	2.9° C						18.0° C						21.1° C						30.0° C				
		25 Hz	10 Hz	5 Hz	1 Hz	0.5 Hz	0.1 Hz	25 Hz	10 Hz	5 Hz	1 Hz	0.5 Hz	0.1 Hz	25 Hz	10 Hz	5 Hz	1 Hz	0.5 Hz	0.1 Hz	25 Hz	10 Hz	5 Hz	1 Hz	0.5 Hz
		Dynamic Modulus (MPa)																						
Virgin, PG 58-28	1	13930.25	12500.87	11344.34	9011.05	8026.87	5650.86	-	-	-	-	-	-	6025.85	4846.11	4047.02	2497.69	2014.75	-	-	-	-	-	-
	2	13298.29	12084.99	11256.35	8937.48	8054.74	6033.34	-	-	-	-	-	-	5680.55	4533.38	3849.65	2545.46	2129.26	-	-	-	-	-	-
	3	12308.56	11182.75	10364.11	8197.03	7438.62	5435.30	7407.29	6208.18	5308.33	3523.28	3164.85	2024.41	6976.68	5778.89	5043.41	3383.99	2957.93	2086.14	4043.87	3160.21	2640.84	1772.59	1402.71
15% RAP, PG 58-28	1	16593.47	15194.95	14034.53	11267.24	10224.52	7594.10	7402.00	6165.78	5387.55	3741.93	3272.10	2322.62	7584.78	6213.9	5313.23	3922.06	3521.40	2138.35	3686.32	2912.76	2431.26	1589.58	1365.43
	2	15527.87	14234.60	13271.97	10733.08	9778.05	7482.24	8017.16	6856.56	5929.74	4098.42	3566.09	2188.86	6924.56	5708.59	4928.83	3193.86	2693.05	1738.02	4217.43	3309.08	2784.65	1777.81	1532.54
	3	14944.48	13838.23	13126.98	10570.26	9800.98	7445.98	8162.59	6944.78	6044.18	4044.30	3568.06	1571.26	7133.44	5862.26	4955.98	3296.51	2840.23	1889.79	4357.24	3395.80	2837.01	1821.85	1556.59
25% RAP, PG 58-28	1	13281.73	12100.81	11150.93	9004.89	8123.02	6252.40	6404.53	5358.84	4537.08	2998.76	2573.96	1424.32	-	-	-	-	-	-	3448.50	2710.93	2246.84	1454.92	1243.13
	2	12725.79	11576.53	10622.25	8498.75	7636.57	5733.01	6398.90	5323.13	4577.14	3054.28	2646.80	1425.24	-	-	-	-	-	-	3614.90	2794.66	2319.10	1446.58	1221.04
	3	14449.37	13147.64	12026.05	9430.13	8457.60	6273.48	7695.13	6538.35	5598.69	3486.63	3073.43	1540.74	-	-	-	-	-	-	3657.25	2895.76	2424.72	1703.57	1333.70
25% RAP, PG 52-34	1	9185.31	8036.51	7320.54	5353.43	4728.88	3419.96	-	-	-	-	-	-	3434.72	2751.12	2350.63	1529.84	1311.32	-	-	-	-	-	-
	2	10206.79	9017.06	8228.31	6075.68	5395.93	3870.87	-	-	-	-	-	-	3442.30	2749.2	2343.73	1510.55	-	-	-	-	-	-	-
	3	11004.16	9799.47	8997.59	6886.39	6155.84	4628.54	4980.09	4172.23	3595.45	2430.08	2145.28	1386.05	5044.41	4187.95	3646.47	2474.41	2183.51	1539.37	2776.39	2237.06	1899.97	1325.35	1152.11
30% RAP, PG 52-34	1	11249.40	9973.45	9093.36	6988.90	6304.85	4580.86	5012.58	4179.50	3538.67	2464.76	2136.29	1342.16	-	-	-	-	-	-	3156.36	2616.49	2272.68	1721.13	1567.82
	2	11628.75	10438.86	9589.34	7554.31	6754.22	4975.72	6768.93	5798.67	5248.45	3604.32	3332.65	2099.86	-	-	-	-	-	-	3506.33	2830.42	2381.81	1618.97	1383.95
	3	12542.64	11645.40	11533.98	9349.31	8431.36	6637.91	5465.57	4519.69	3831.71	2622.06	2316.15	1431.06	-	-	-	-	-	-	3063.36	2454.90	2188.32	1556.41	1597.02
40% RAP, PG 52-34	1	14336.24	13039.19	12072.04	9756.11	9001.30	7150.53	6189.66	5184.65	4487.52	3169.64	2831.67	2004.75	6013.01	4991.12	4310.07	2906.47	2517.19	1673.20	3346.75	2670.34	2267.78	1555.47	1329.41
	2	11242.31	10099.25	9206.45	7188.68	6562.19	4841.78	5833.98	4876.03	4232.50	2853.33	2497.03	1798.57	6369.31	5368.28	5041.33	3561.48	3172.13	2002.17	2926.55	2348.80	1987.46	1354.68	1167.83
	3	12596.88	11194.85	10174.36	7859.20	6951.49	4778.65	6711.38	5629.10	4877.00	3252.42	2930.32	2054.06	5338.64	4335.08	3691.04	2434.89	2137.35	1330.02	3122.65	2511.42	2144.33	1511.10	1326.53

Table 31: Phase Angle Test Data for Field Core Mixtures

Mix	Replicate #	2.9° C						18.0° C						21.1° C						30.0° C				
		25 Hz	10 Hz	5 Hz	1 Hz	0.5 Hz	0.1 Hz	25 Hz	10 Hz	5 Hz	1 Hz	0.5 Hz	0.1 Hz	25 Hz	10 Hz	5 Hz	1 Hz	0.5 Hz	0.1 Hz	25 Hz	10 Hz	5 Hz	1 Hz	0.5 Hz
		Phase Angle (Degrees)																						
Virgin, PG 58-28	1	9.00	13.20	15.60	20.40	22.20	27.00	-	-	-	-	-	-	32.25	33.90	35.10	41.10	42.30	-	-	-	-	-	-
	2	15.00	18.00	18.90	22.20	23.10	27.90	-	-	-	-	-	-	29.25	31.80	35.10	42.00	43.80	-	-	-	-	-	-
	3	13.00	14.60	15.20	18.20	21.00	24.20	23.25	25.20	27.30	31.50	33.60	37.80	28.50	25.2	27.90	30.90	31.80	37.80	24.00	28.20	28.20	30.90	31.20
15% RAP, PG 58-28	1	9.00	14.40	15.00	18.00	20.10	21.90	21.00	19.20	21.30	23.70	24.90	32.10	31.50	35.1	36.00	45.00	50.10	55.50	27.00	25.20	25.80	27.90	28.80
	2	9.00	12.00	14.40	16.20	17.40	20.40	18.00	20.40	21.60	25.80	26.40	34.20	22.50	26.7	26.10	28.50	29.70	33.30	27.00	28.80	29.40	30.90	31.20
	3	18.00	16.20	19.50	22.80	25.50	28.80	25.50	27.30	31.50	36.60	43.50	41.70	18.00	23.4	24.30	28.80	28.20	29.70	30.00	30.00	31.20	33.00	33.60
25% RAP, PG 58-28	1	9.00	12.30	14.70	16.20	17.70	22.20	24.75	26.10	28.50	31.80	35.10	45.00	-	-	-	-	-	-	29.25	32.40	31.20	34.80	37.80
	2	9.75	12.60	13.20	16.20	16.50	21.30	21.75	25.80	27.30	33.60	37.20	33.60	-	-	-	-	-	-	27.00	27.30	29.40	35.70	33.90
	3	15.00	13.50	13.80	16.50	18.60	21.60	25.50	30.30	33.00	35.10	38.10	40.80	-	-	-	-	-	-	33.75	33.30	33.90	39.60	42.30
25% RAP, PG 52-34	1	18.00	21.60	24.90	28.80	31.20	35.70	-	-	-	-	-	-	26.25	27	28.80	30.60	31.80	-	-	-	-	-	-
	2	15.00	19.80	23.10	23.10	25.20	28.80	-	-	-	-	-	-	28.50	30.6	30.60	33.90	-	-	-	-	-	-	-
	3	13.50	18.00	17.70	19.20	21.00	23.70	23.25	25.80	27.60	32.40	36.60	42.00	28.50	30.9	36.60	42.60	46.20	47.10	27.00	26.40	27.60	30.90	33.90
30% RAP, PG 52-34	1	18.00	14.10	16.80	19.20	19.80	24.90	21.75	23.40	24.90	28.80	30.00	32.10	-	-	-	-	-	-	24.75	29.40	31.50	36.60	37.20
	2	9.00	13.50	14.40	17.10	18.90	21.60	27.00	30.60	32.40	36.00	40.20	43.80	-	-	-	-	-	-	24.00	27.30	27.00	31.50	32.70
	3	18.00	22.50	25.80	30.90	32.10	37.50	23.25	23.40	25.20	28.50	31.20	32.40	-	-	-	-	-	-	29.25	31.20	31.20	35.10	37.20
40% RAP, PG 52-34	1	20.25	19.50	23.70	25.80	27.90	36.60	21.75	20.40	21.00	24.90	28.50	31.50	21.00	23.4	24.90	27.30	27.30	31.50	23.25	25.20	25.80	29.10	30.00
	2	18.00	16.80	18.00	21.00	22.50	27.90	21.00	24.00	25.50	28.50	30.00	39.90	28.50	32.7	37.80	42.60	45.90	49.80	27.00	27.30	26.10	28.20	27.30
	3	13.50	14.40	14.10	14.40	16.80	22.50	27.75	32.40	33.90	35.40	36.90	42.90	30.00	30.6	31.20	33.60	33.60	39.60	28.50	26.40	27.60	29.70	31.20

Table 32: Dynamic Modulus Test Data for PMPC Mixtures

Mix	Replicate #	4.4° C						21.1° C						37.8° C					
		25 Hz	10 Hz	5 Hz	1 Hz	0.5 Hz	0.1 Hz	25 Hz	10 Hz	5 Hz	1 Hz	0.5 Hz	0.1 Hz	25 Hz	10 Hz	5 Hz	1 Hz	0.5 Hz	0.1 Hz
		Dynamic Modulus (MPa)																	
Virgin, PG 58-28	1	7833.5	7047.4	6475.1	5118.9	4774.4	3338.3	3847.8	3143.4	2678.6	1647.0	1354.7	764.6	1194.4	897.4	721.2	430.5	365.4	276.2
	2	6738.5	6156.2	5697.1	4494.7	4183.4	2913.4	3396.6	2724.9	2257.9	1351.4	1110.5	620.0	1050.9	792.5	632.7	392.8	353.1	273.1
	3	12397.0	11550.0	10899.0	8415.2	7510.0	5162.5	3233.4	2608.8	2181.0	1272.7	1030.8	600.9	1367.2	1001.3	805.3	523.3	531.7	1494.2
15% RAP, PG 58-28	1	11370.3	10572.7	9991.5	7701.7	6975.9	4747.2	3858.1	3060.0	2527.1	1456.2	1177.7	614.1	1270.6	937.1	744.4	459.9	414.1	406.6
	2	10736.5	9741.2	9044.6	7132.9	6660.9	4520.1	4565.0	3622.3	3005.9	1773.6	1443.7	779.3	1118.0	823.1	662.9	425.5	389.3	380.6
	3	11979.3	10969.7	10173.9	7925.7	7035.1	5502.9	3898.5	3109.5	2533.9	1469.2	1199.2	624.0	1167.8	845.9	654.6	389.0	336.2	261.6
25% RAP, PG 58-28	1	12842.7	12021.3	11752.0	9050.4	8512.6	6274.4	4318.3	3494.7	2966.7	1804.0	1505.1	810.3	1609.2	1132.8	893.0	499.4	424.4	277.4
	2	14020.3	12747.1	12145.9	9492.3	8885.9	6231.3	5315.7	4174.0	3407.4	2000.0	1624.4	890.2	1815.7	1375.2	1113.4	720.2	660.5	506.5
	3	8328.0	7606.4	7162.4	5548.4	5137.3	3652.7	4739.7	3856.7	3173.0	1834.4	1436.3	773.3	1578.9	1142.7	889.6	515.2	440.4	325.0
25% RAP, PG 52-34	1	9251.2	8256.7	7470.3	5753.8	5179.5	3597.3	3172.8	2542.5	2112.9	1301.8	1110.4	649.2	1210.5	930.7	764.0	492.6	428.1	340.0
	2	6049.2	5324.8	4796.2	3654.1	3342.2	2260.4	2751.2	2253.0	1887.6	1170.7	994.7	600.1	1284.2	1032.4	902.3	611.5	556.2	546.2
	3	8391.3	7383.2	6609.7	4938.9	4434.2	3105.5	2831.1	2260.6	1878.6	1188.4	1014.4	614.7	1146.6	883.4	733.3	479.5	430.0	362.5
30% RAP, PG 52-34	1	9052.2	8173.5	7554.2	5851.3	5497.0	3782.7	3388.3	2735.2	2292.9	1427.3	1195.5	722.4	1142.0	880.8	718.1	448.1	370.9	267.9
	2	8984.9	7967.0	7219.7	5510.9	4996.4	3543.0	3333.7	2716.4	2296.6	1448.6	1202.5	737.6	1096.1	836.2	681.4	428.7	376.6	257.1
	3	7819.6	7067.1	6578.8	4967.7	4673.8	3068.5	3386.4	2671.7	2218.3	1326.9	1099.4	643.1	1061.3	824.8	686.1	441.3	409.5	300.4
40% RAP, PG 52-34	1	9100.4	8388.2	7880.3	5941.3	5439.6	3975.0	3137.8	2561.9	2158.2	1370.1	1207.4	730.4	969.5	750.8	607.7	364.7	309.0	205.2
	2	9114.1	8320.7	7760.7	5659.2	4997.5	3412.1	3068.9	2503.1	2102.9	1340.4	1143.5	680.9	1068.7	840.9	705.6	446.2	396.2	290.2
	3	9128.7	8188.7	7553.9	5827.5	5246.8	3536.2	4413.5	3541.4	2991.7	1903.3	1768.7	1149.4	1132.7	867.1	696.3	429.8	359.8	269.4

Table 33: Phase Angle Test Data for PMPC Mixtures

Mix	Replicate #	4.4° C						21.1° C						37.8° C					
		25 Hz	10 Hz	5 Hz	1 Hz	0.5 Hz	0.1 Hz	25 Hz	10 Hz	5 Hz	1 Hz	0.5 Hz	0.1 Hz	25 Hz	10 Hz	5 Hz	1 Hz	0.5 Hz	0.1 Hz
		Dynamic Modulus (MPa)																	
Virgin, PG 58-28	1	13.5	14.4	17.4	20.1	21.6	26.7	24.8	28.8	32.4	36.3	36.3	39.9	36.0	39.9	38.1	37.5	36.3	38.1
	2	9.0	14.4	17.1	19.8	22.2	27.6	6.0	30.6	33.3	38.4	37.2	41.4	42.0	38.4	38.1	37.2	37.2	45.3
	3	18.0	19.2	21.8	25.4	27.0	33.8	31.5	37.8	39.3	40.5	39.6	37.8	39.8	39.0	35.4	33.6	33.9	47.7
15% RAP, PG 58-28	1	18.0	15.7	17.0	21.0	22.6	28.5	27.0	30.4	32.8	38.0	38.0	44.1	41.5	38.8	37.4	35.2	33.0	35.6
	2	15.8	16.2	19.2	21.9	23.7	28.2	24.0	26.7	28.2	33.6	34.2	39.0	37.5	36.0	35.7	33.9	33.6	43.2
	3	9.0	12.2	12.6	16.2	16.8	23.4	24.0	28.8	30.9	36.0	36.9	41.7	36.0	39.6	37.2	34.2	31.8	32.1
25% RAP, PG 58-28	1	11.3	15.3	17.3	17.8	20.4	25.7	21.0	27.6	29.1	34.8	35.4	40.5	36.0	37.2	37.2	34.8	31.8	36.0
	2	10.5	12.6	16.8	19.2	21.6	25.2	30.0	28.6	31.8	37.4	37.6	42.8	45.0	42.8	43.2	40.8	35.9	21.3
	3	18.0	14.1	16.2	18.0	20.4	25.5	24.8	33.3	35.4	40.5	41.1	46.8	40.5	39.9	37.5	33.6	31.8	28.5
25% RAP, PG 52-34	1	18.0	15.0	15.2	17.6	18.6	21.8	27.0	28.2	29.4	32.4	31.6	34.8	33.8	32.4	30.6	28.2	27.0	26.1
	2	18.0	18.0	17.7	19.8	20.7	24.6	32.5	34.2	35.8	38.4	38.4	40.4	39.0	42.3	44.1	27.9	38.4	20.1
	3	17.3	15.6	18.6	20.4	21.0	25.2	27.0	25.2	27.9	30.3	29.1	32.1	35.3	36.6	34.5	33.0	32.4	35.7
30% RAP, PG 52-34	1	18.0	18.0	19.5	22.2	25.2	29.1	27.8	29.7	30.9	33.6	33.2	34.5	36.0	30.6	30.6	27.3	25.8	20.7
	2	10.5	13.8	16.5	19.2	21.0	23.7	30.0	33.4	34.0	37.4	37.2	40.2	32.3	33.3.	32.1	29.7	27.6	25.8
	3	19.5	21.9	24.3	27.6	31.2	36.6	27.8	32.4	31.5	34.8	33.0	36.0	36.0	32.4	32.1	28.5	26.4	22.2
40% RAP, PG 52-34	1	18.0	21.4	26.4	28.0	30.2	34.6	26.5	27.8	31.2	34.6	37.4	42.2	36.0	36.0	35.1	33.3	30.3	30.3
	2	16.1	21.6	26.7	30.2	31.8	37.7	27.0	28.5	28.5	30.0	30.0	32.1	40.5	39.6	39.3	39.3	37.8	38.4
	3	18.0	16.6	19.1	21.6	23.6	25.6	27.0	34.2	35.1	39.3	42.6	46.2	36.0	34.2	33.3	30.6	28.8	26.1

Table 34: Dynamic Modulus Test Data for PMLC Mixtures

Mix	Replicate #	4.4° C						21.1° C						37.8° C					
		25 Hz	10 Hz	5 Hz	1 Hz	0.5 Hz	0.1 Hz	25 Hz	10 Hz	5 Hz	1 Hz	0.5 Hz	0.1 Hz	25 Hz	10 Hz	5 Hz	1 Hz	0.5 Hz	0.1 Hz
		Dynamic Modulus (MPa)																	
Virgin, PG 58-28	1	22106.0	16627.0	15289.0	12258.0	10989.0	8272.0	8266.0	6778.0	5759.0	3697.0	3007.0	1724.0	2407.0	1725.0	1310.0	630.4	460.7	216.6
	2	19471.0	16451.0	15202.0	12316.0	11085.0	8415.0	8168.0	6714.0	5681.0	3630.0	2971.0	1717.0	2560.0	1862.0	1441.0	721.3	533.4	259.2
	3	18328.0	15948.0	14799.0	12066.0	10900.0	8358.0	8271.0	6727.0	5679.0	3627.0	2905.0	1695.0	2550.0	1828.0	1402.0	694.2	515.2	251.5
15% RAP, PG 58-28	1	11934.4	10904.3	10106.7	8255.9	7637.8	5487.2	7019.2	5625.8	4921.4	2919.3	2441.3	1443.8	2032.9	1510.5	1174.0	669.1	528.7	360.5
	2	15984.0	14343.5	13087.6	10102.7	9122.4	6099.8	6833.8	5411.7	4520.6	2732.6	2289.9	1281.4	2004.8	1496.6	1192.6	679.0	585.8	444.0
	3	12466.9	11347.4	10518.3	8311.5	7603.9	5234.8	5953.8	4627.6	4044.7	2568.5	2208.3	1344.1	2101.7	1555.0	1197.7	667.1	536.8	363.2
25% RAP, PG 58-28	1	9055.6	8382.7	7889.8	6558.9	6119.5	4694.2	4918.4	3977.5	3347.4	2002.7	1644.0	881.6	1753.0	1299.3	1034.4	582.2	523.3	490.3
	2	12764.4	11553.1	10606.6	8417.6	7736.9	5431.0	4738.6	3721.6	3048.5	1720.9	1368.6	694.8	1421.5	1021.9	784.6	430.5	348.0	235.9
	3	11314.3	10123.2	9338.2	7473.5	6969.8	4898.3	5184.1	4226.8	3572.1	2185.7	1834.3	992.8	1877.7	1387.7	1079.0	600.0	524.9	413.1
25% RAP, PG 52-34	1	15961.0	14465.0	13351.0	10788.0	9685.0	7345.0	7528.0	6183.0	5290.0	3402.0	2688.0	1550.0	2507.0	1830.0	1413.0	707.6	523.0	252.1
	2	16921.0	15406.0	14266.0	11612.0	10499.0	8070.0	7838.0	6426.0	5475.0	3524.0	2897.0	1687.0	2460.0	1795.0	1390.0	704.1	527.5	259.2
	3	16422.0	14936.0	13812.0	11166.0	10105.0	7673.0	7293.0	6012.0	5137.0	3265.0	2668.0	1520.0	2260.0	1621.0	1238.0	612.3	454.1	221.9
30% RAP, PG 52-34	1	16155.0	14699.0	13594.0	10948.0	9868.0	7441.0	7381.0	6040.0	5112.0	3218.0	2617.0	1474.0	2158.0	1529.0	1158.0	558.7	409.5	197.5
	2	16181.0	14726.0	13597.0	10976.0	9877.0	7445.0	7408.0	5967.0	5007.0	3130.0	2531.0	1421.0	2114.0	1512.0	1164.0	562.8	413.2	198.2
	3	15675.0	14367.0	13367.0	10908.0	9899.0	7574.0	7404.0	6121.0	5224.0	3303.0	2695.0	1522.0	2254.0	1617.0	1233.0	604.6	446.3	215.9
40% RAP, PG 52-34	1	10077.5	9073.0	8406.4	6392.3	5707.2	3756.9	4774.0	3815.4	3251.8	2027.0	1768.7	1031.2	2140.4	1686.9	1360.1	810.2	683.9	461.3
	2	11300.6	10152.9	9239.7	7053.8	6307.6	4259.4	4911.1	3841.8	3193.8	1976.9	1668.0	1006.1	1921.2	1479.4	1196.6	696.5	592.6	376.5
	3	11004.3	9738.6	8820.7	6793.3	6167.6	4174.3	5391.3	4335.2	3640.8	2269.9	1937.5	1130.5	2402.5	1862.5	1529.9	919.4	801.5	526.6

Table 35: Phase Angle Test Data for PMLC Mixtures

Mix	Replicate #	4.4° C						21.1° C						37.8° C					
		25 Hz	10 Hz	5 Hz	1 Hz	0.5 Hz	0.1 Hz	25 Hz	10 Hz	5 Hz	1 Hz	0.5 Hz	0.1 Hz	25 Hz	10 Hz	5 Hz	1 Hz	0.5 Hz	0.1 Hz
		Dynamic Modulus (MPa)																	
Virgin, PG 58-28	1	10.3	10.7	11.6	14.2	15.4	18.8	20.6	22.5	24.0	27.9	29.0	31.5	35.9	36.7	36.7	37.0	35.9	34.7
	2	12.7	10.4	11.3	13.8	15.0	18.5	20.6	23.1	24.8	29.3	30.4	33.3	35.6	36.6	36.7	37.0	36.5	34.2
	3	10.2	10.1	10.9	13.4	14.5	17.9	20.4	22.8	24.6	29.2	31.3	33.7	35.6	36.5	36.7	36.9	35.8	34.1
15% RAP, PG 58-28	1	9.0	12.6	12.9	15.6	17.1	20.4	29.0	33.0	36.8	39.4	39.6	41.0	36.8	36.0	35.1	32.7	30.9	28.8
	2	15.0	11.8	14.6	17.8	19.4	25.2	23.6	27.9	29.9	34.2	33.9	34.9	40.5	41.4	40.5	38.4	38.4	38.1
	3	12.0	12.0	15.2	18.6	18.8	24.6	33.0	37.8	39.9	41.1	41.7	42.0	45.0	38.4	36.6	34.2	33.0	31.2
25% RAP, PG 58-28	1	12.0	12.6	15.0	17.1	20.7	26.1	22.5	28.8	29.1	34.8	34.5	39.3	45.0	44.4	43.8	42.3	42.0	44.4
	2	9.0	10.8	12.3	15.6	17.4	22.5	27.0	28.8	32.1	38.1	37.8	43.5	37.5	39.0	37.5	34.5	30.9	25.2
	3	11.3	14.4	15.6	18.6	21.0	25.5	25.5	27.0	28.8	34.5	34.8	39.6	45.8	44.1	44.4	41.1	40.5	40.5
25% RAP, PG 52-34	1	9.3	10.4	11.3	14.0	15.3	18.8	20.5	22.7	24.3	28.8	30.6	32.7	34.6	35.4	35.5	35.6	34.6	33.0
	2	9.1	10.2	11.0	13.5	14.6	18.0	20.5	22.7	24.4	28.7	29.7	32.5	35.0	35.8	36.0	36.2	35.1	33.5
	3	9.3	10.5	11.4	13.9	15.1	18.4	21.0	23.2	24.9	29.3	30.4	33.0	35.5	36.3	36.4	36.1	35.0	32.9
30% RAP, PG 52-34	1	9.7	10.7	11.6	14.3	15.6	19.2	21.3	23.8	25.5	30.1	31.2	33.9	37.0	37.6	37.4	37.1	35.7	33.9
	2	9.6	10.7	11.6	14.2	15.5	19.1	21.4	23.8	25.6	30.2	31.3	33.8	36.5	36.9	36.5	36.0	34.8	33.1
	3	9.1	10.2	11.1	13.7	15.0	18.6	21.1	23.6	25.3	29.9	30.9	33.6	36.0	36.6	36.6	36.2	35.1	33.4
40% RAP, PG 52-34	1	14.3	17.3	21.9	25.1	25.6	28.2	29.2	34.3	36.8	40.1	41.6	43.8	36.0	36.9	36.3	36.0	36.0	37.8
	2	18.0	14.3	16.5	18.9	20.1	23.7	33.7	32.6	33.3	36.9	36.6	37.5	39.0	37.8	36.3	35.4	34.2	34.2
	3	15.7	13.4	14.4	17.8	18.8	22.8	30.0	32.0	34.7	39.0	40.2	42.8	38.2	37.2	37.6	37.8	38.0	39.9

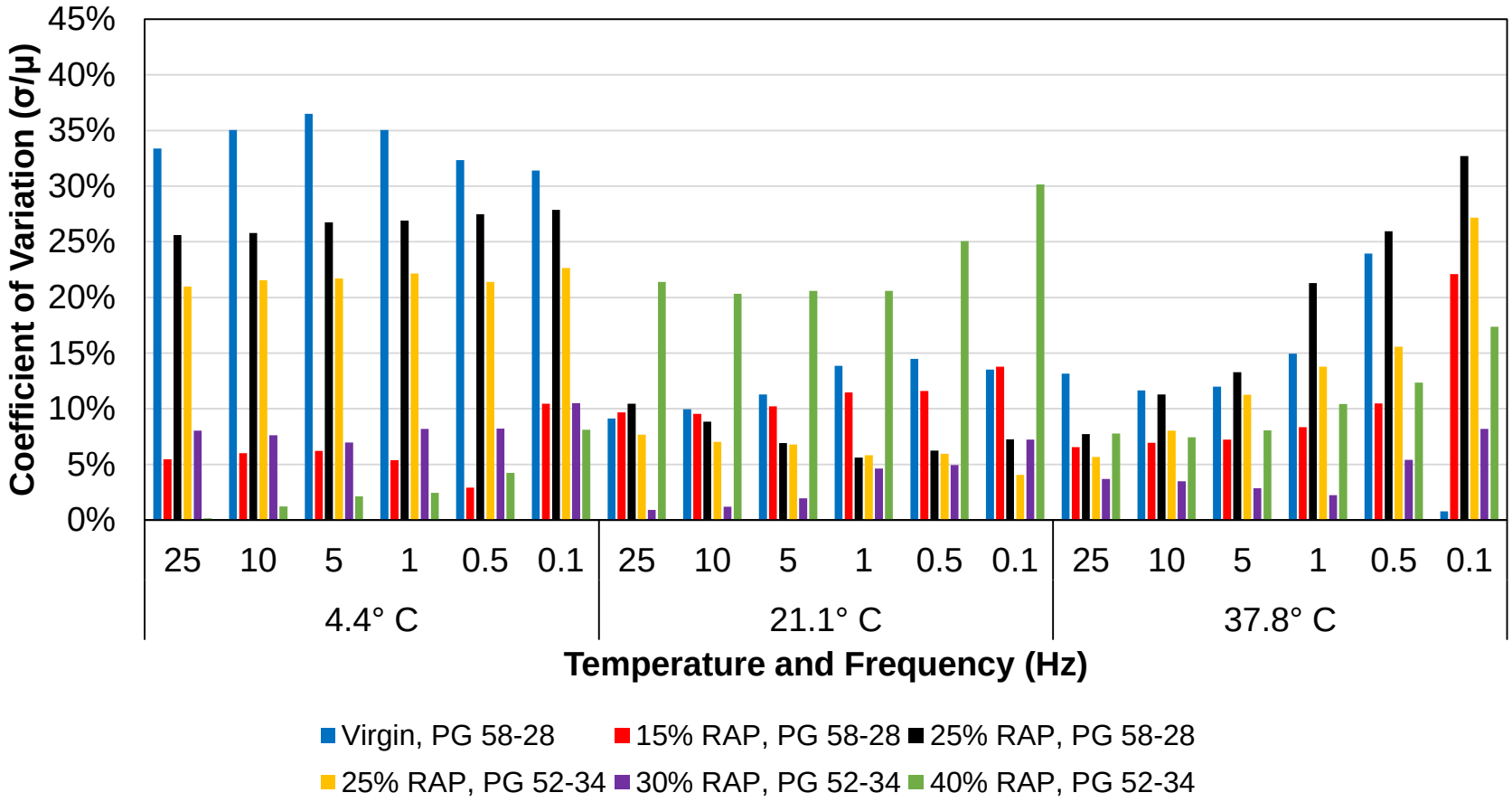

Figure 110: Coefficient of Variation for Dynamic Modulus Raw Data PMPC Mixtures

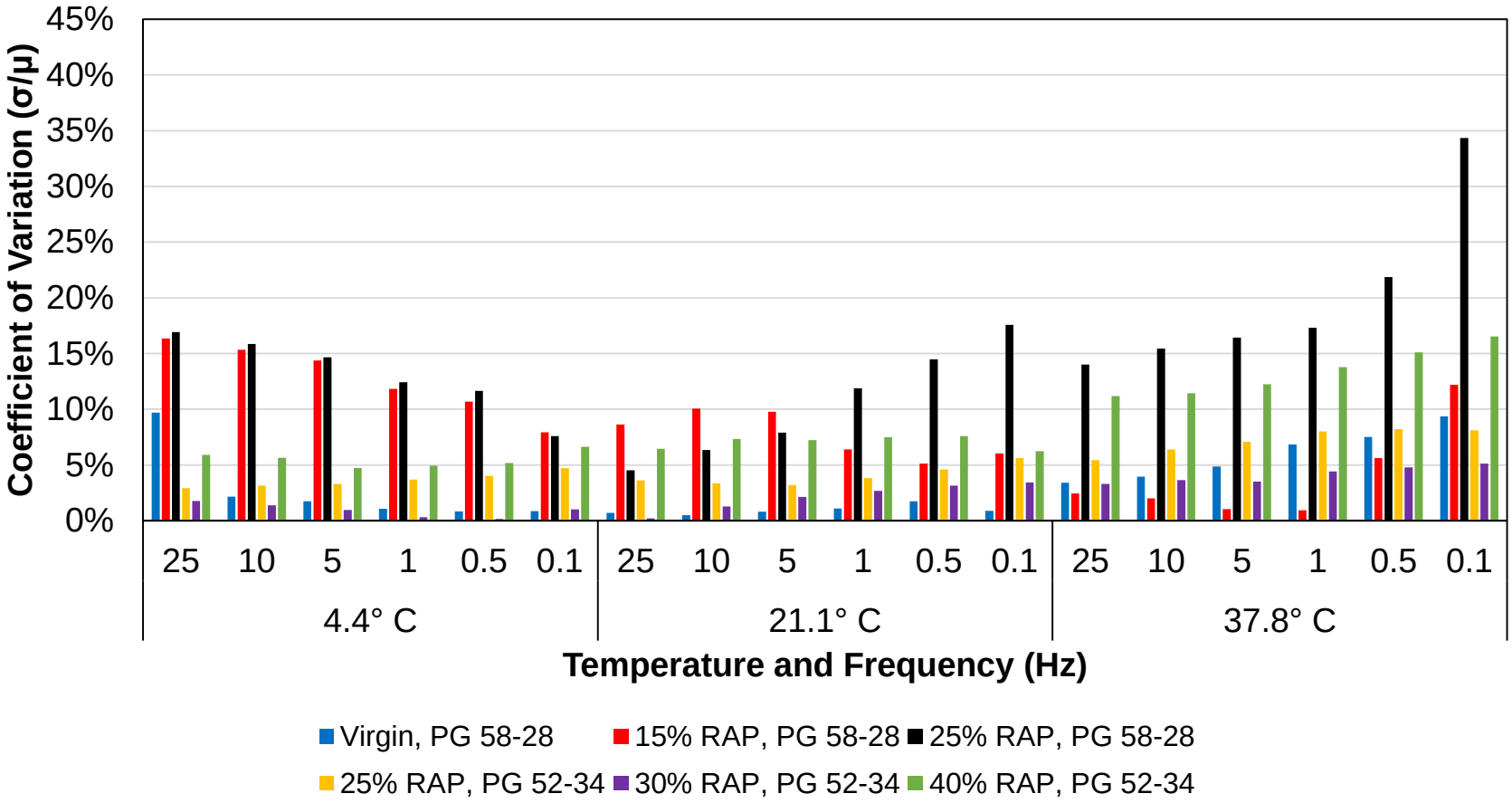

Figure 111: Coefficient of Variation for Dynamic Modulus Raw Data PMLC Mixtures

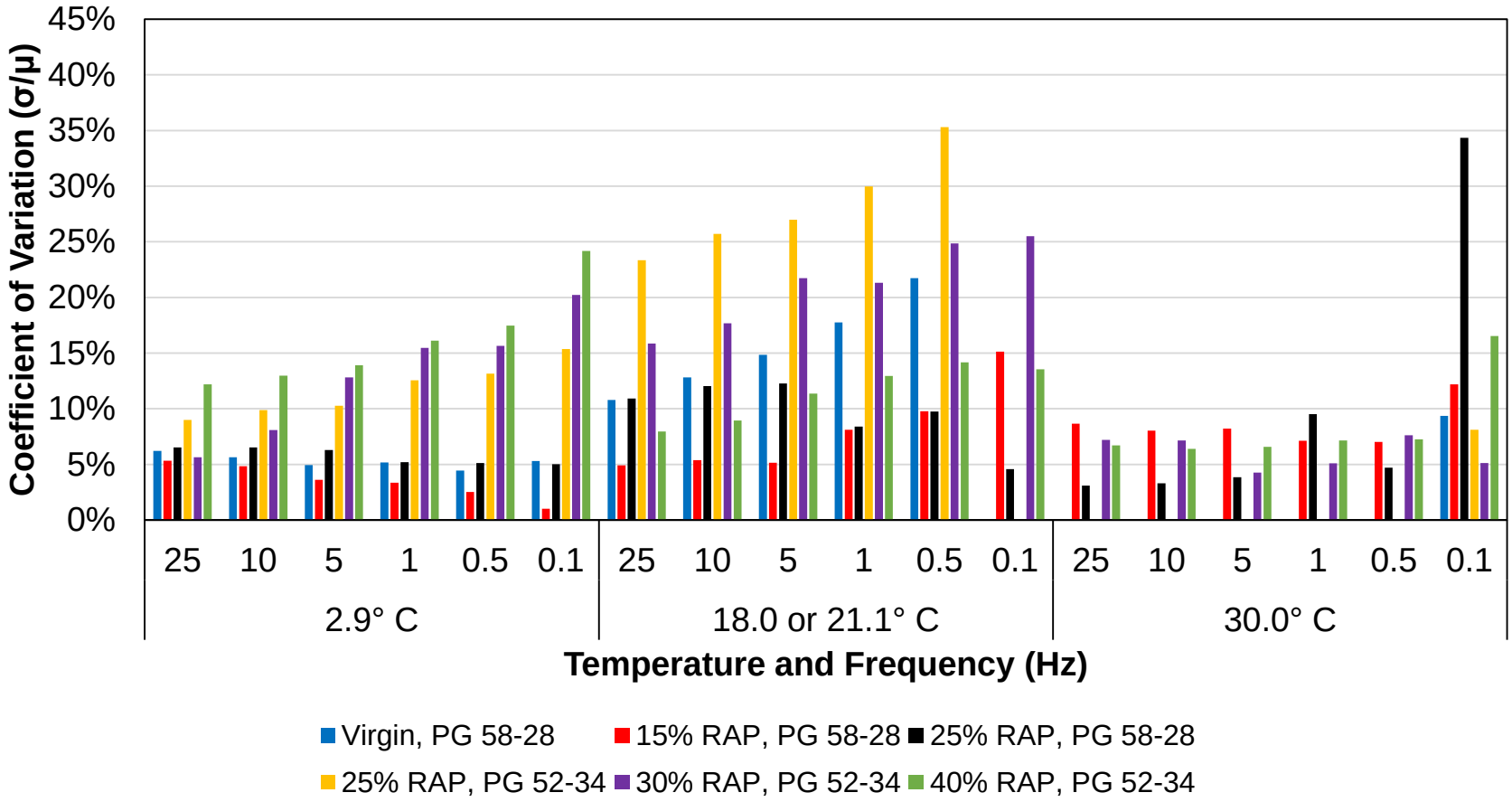

Figure 112: Coefficient of Variation for Dynamic Modulus Raw Data Field Core Mixtures

B.4 Dynamic Modulus Master Curve Data

Table 36: Dynamic Modulus Sigmoid Fit Coefficients for Virgin Silo Storage Mixtures

	0 hrs	2.5 hrs	5 hrs	7.5 hrs
A	2.812125	3.221365	3.404563	2.951433
B	0.502124	0.429833	0.433501	0.467322
D	1.560238	1.151029	1.004491	1.494092
M	-1.888973	-2.733080	-2.839640	-2.333730
T	0.930143	0.758970	0.903598	0.957942

Table 37: Dynamic Modulus Sigmoid Fit Coefficients for 25% RAP Silo Storage Mixtures

	0 hrs	2.5 hrs	5 hrs	7.5 hrs	10 hrs
A	3.121866	3.450939	3.328481	3.262516	5.298032
B	0.494071	0.449584	0.444167	0.439491	0.444380
D	1.285849	1.025680	1.143004	1.224221	-0.810550
M	-1.916247	-2.666963	-2.819014	-2.768459	-3.946622
T	0.938351	0.867812	0.833286	0.790512	2.798376

Table 38: Root Mean Square (RMS) Errors of Sigmoidal Fit and Dynamic Modulus Data for Silo Storage Mixtures

	Virgin	25% RAP
0 hrs	1.59%	1.40%
2.5 hrs	2.78%	0.73%
5 hrs	2.44%	0.95%
7.5 hrs	0.85%	1.15%
10 hrs	-	0.26%

Table 39: Dynamic Modulus Sigmoid Fit Coefficients for Field Core Mixtures

	Virgin, PG 58-28	15% RAP, PG 58-28	25% RAP, PG 58-28	25% RAP, PG 52-34	30% RAP, PG 52-34	40% RAP, PG 52-34
A	1.199800	2.051638	1.377756	1.274178	1.214500	2.048376
B	0.554271	0.523765	0.549838	0.726528	0.492613	0.465359
D	3.089878	2.306319	2.893349	2.870898	3.048594	2.303675
M	0.241678	-0.792778	-0.034883	1.009928	0.424068	-0.559122
T	-0.079378	0.989724	-0.029867	0.946608	-0.071469	1.089041

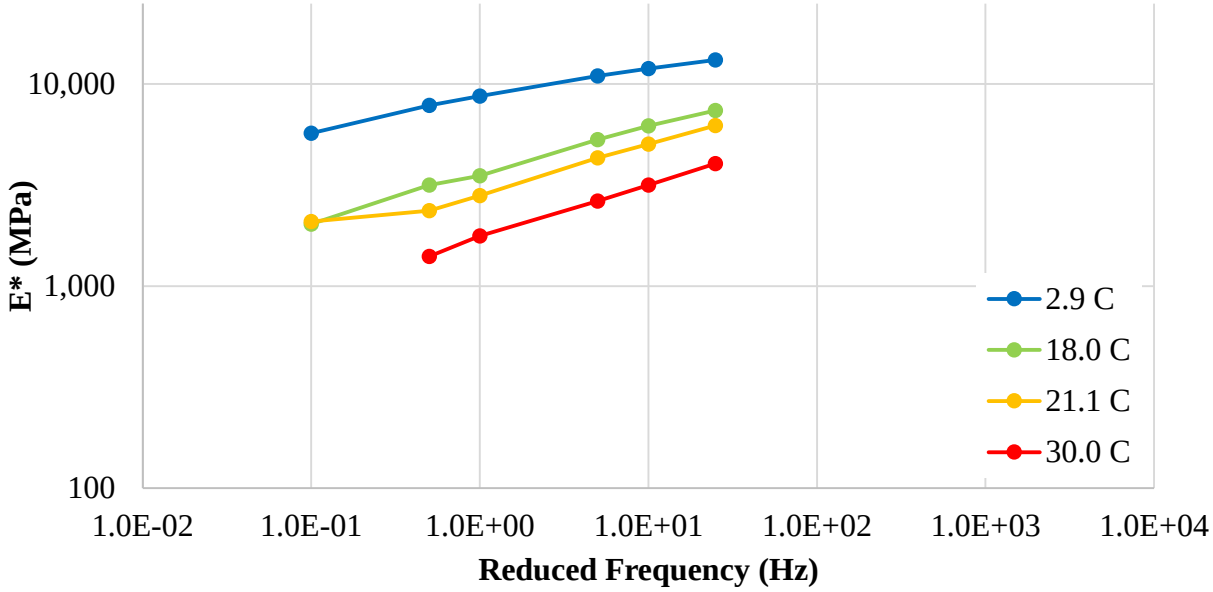

Figure 113: Example of Dynamic Modulus Isotherms before Fitting

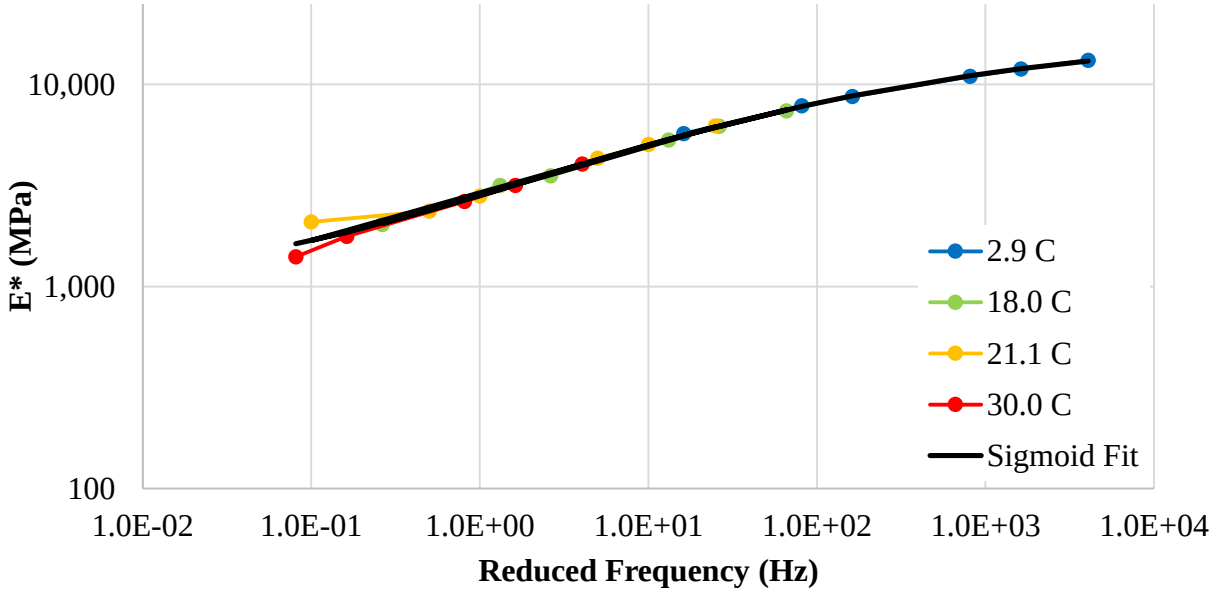

Figure 114: Example of Shifting Isotherms to Form Sigmoid Fit Master Curve

B.5 Dynamic Modulus T-Tests for Specimen Fabrications Study

Table 40: Statistical T-Test p-Values for Dynamic Modulus of PG 58-28 Field Core Mixtures

Comparison Group 1: Virgin, PG 58-28																							
Comparison Group 2	2.9° C						18.0° C						21.1° C						30.0° C				
	25 Hz	10 Hz	5 Hz	1 Hz	0.5 Hz	0.1 Hz	25 Hz	10 Hz	5 Hz	1 Hz	0.5 Hz	0.1 Hz	25 Hz	10 Hz	5 Hz	1 Hz	0.5 Hz	0.1 Hz	25 Hz	10 Hz	5 Hz	1 Hz	0.5 Hz
15% RAP, PG 58-28	0.021	0.011	0.004	0.003	0.001	0.001	0.433	0.459	0.359	0.187	0.262	0.995	0.085	0.095	0.126	0.146	0.172	0.555	0.926	0.892	0.880	0.792	0.565
25% RAP, PG 58-28	0.681	0.591	0.618	0.521	0.497	0.201	0.574	0.617	0.620	0.381	0.328	0.018	-	-	-	-	-	-	0.066	0.078	0.095	0.294	0.186
25% RAP, PG 52-34	0.013	0.010	0.008	0.007	0.006	0.012	-	-	-	-	-	-	0.027	0.040	0.054	0.086	0.305	-	-	-	-	-	-
30% RAP, PG 52-34	0.087	0.122	0.320	0.378	0.375	0.662	0.256	0.298	0.406	0.472	0.524	0.491	-	-	-	-	-	-	0.097	0.137	0.085	0.281	0.484
40% RAP, PG 52-34	0.677	0.638	0.605	0.611	0.691	0.897	0.150	0.155	0.174	0.218	0.257	0.691	0.550	0.764	0.952	0.734	0.599	0.394	0.064	0.073	0.089	0.134	0.353
Comparison Group 1: 15% RAP, PG 58-28																							
Comparison Group 2	2.9° C						18.0° C						21.1° C						30.0° C				
	25 Hz	10 Hz	5 Hz	1 Hz	0.5 Hz	0.1 Hz	25 Hz	10 Hz	5 Hz	1 Hz	0.5 Hz	0.1 Hz	25 Hz	10 Hz	5 Hz	1 Hz	0.5 Hz	0.1 Hz	25 Hz	10 Hz	5 Hz	1 Hz	0.5 Hz
Virgin, PG 58-28	0.021	0.011	0.004	0.003	0.001	0.001	0.433	0.459	0.359	0.187	0.262	0.995	0.085	0.095	0.126	0.146	0.172	0.555	0.926	0.892	0.880	0.792	0.565
25% RAP, PG 58-28	0.035	0.025	0.011	0.005	0.003	0.011	0.104	0.123	0.093	0.015	0.019	0.131	-	-	-	-	-	-	0.074	0.062	0.062	0.152	0.034
25% RAP, PG 52-34	0.001	0.001	0.001	0.001	0.000	0.001	0.025	0.037	0.033	0.020	0.021	0.300	0.005	0.006	0.007	0.014	0.071	0.243	0.085	0.083	0.091	0.105	0.110
30% RAP, PG 52-34	0.003	0.004	0.013	0.018	0.014	0.078	0.021	0.030	0.049	0.046	0.086	0.292	-	-	-	-	-	-	0.026	0.036	0.044	0.319	0.744
40% RAP, PG 52-34	0.044	0.034	0.028	0.031	0.080	0.133	0.009	0.012	0.010	0.006	0.012	0.774	0.022	0.038	0.154	0.275	0.359	0.325	0.016	0.017	0.022	0.052	0.059
Comparison Group 1: 25% RAP, PG 58-28																							
Comparison Group 2	2.9° C						18.0° C						21.1° C						30.0° C				
	25 Hz	10 Hz	5 Hz	1 Hz	0.5 Hz	0.1 Hz	25 Hz	10 Hz	5 Hz	1 Hz	0.5 Hz	0.1 Hz	25 Hz	10 Hz	5 Hz	1 Hz	0.5 Hz	0.1 Hz	25 Hz	10 Hz	5 Hz	1 Hz	0.5 Hz
Virgin, PG 58-28	0.681	0.591	0.618	0.521	0.497	0.201	0.574	0.617	0.620	0.381	0.328	0.018	-	-	-	-	-	-	0.066	0.078	0.095	0.294	0.186
15% RAP, PG 58-28	0.035	0.025	0.011	0.005	0.003	0.011	0.104	0.123	0.093	0.015	0.019	0.131	-	-	-	-	-	-	0.074	0.062	0.062	0.152	0.034
25% RAP, PG 52-34	0.010	0.008	0.008	0.005	0.005	0.006	0.165	0.189	0.200	0.136	0.185	0.422	-	-	-	-	-	-	0.025	0.034	0.053	0.340	0.241
30% RAP, PG 52-34	0.058	0.079	0.233	0.254	0.258	0.352	0.186	0.226	0.331	0.507	0.696	0.572	-	-	-	-	-	-	0.090	0.241	0.553	0.373	0.029
40% RAP, PG 52-34	0.501	0.442	0.450	0.433	0.514	0.593	0.306	0.325	0.399	0.677	0.957	0.005	-	-	-	-	-	-	0.032	0.054	0.110	0.587	0.899

Table 41: Statistical T-Test p-Values for Dynamic Modulus of PG 52-34 Field Core Mixtures

Comparison Group 1: 25% RAP, PG 52-34																							
Comparison Group 2	2.9° C						18.0° C						21.1° C						30.0° C				
	25 Hz	10 Hz	5 Hz	1 Hz	0.5 Hz	0.1 Hz	25 Hz	10 Hz	5 Hz	1 Hz	0.5 Hz	0.1 Hz	25 Hz	10 Hz	5 Hz	1 Hz	0.5 Hz	0.1 Hz	25 Hz	10 Hz	5 Hz	1 Hz	0.5 Hz
Virgin, PG 58-28	0.013	0.010	0.008	0.007	0.006	0.012	-	-	-	-	-	-	0.027	0.040	0.054	0.086	0.305	-	-	-	-	-	-
15% RAP, PG 58-28	0.001	0.001	0.001	0.001	0.000	0.001	0.025	0.037	0.033	0.020	0.021	0.300	0.005	0.006	0.007	0.014	0.071	0.243	0.085	0.083	0.091	0.105	0.110
25% RAP, PG 58-28	0.010	0.008	0.008	0.005	0.005	0.006	0.165	0.189	0.200	0.136	0.185	0.422	-	-	-	-	-	-	0.025	0.034	0.053	0.340	0.241
30% RAP, PG 52-34	0.062	0.072	0.101	0.091	0.086	0.120	0.541	0.572	0.621	0.580	0.607	0.668	-	-	-	-	-	-	0.226	0.210	0.077	0.086	0.112
40% RAP, PG 52-34	0.067	0.067	0.077	0.071	0.073	0.132	0.131	0.137	0.130	0.113	0.146	0.069	0.035	0.042	0.055	0.068	0.188	0.771	0.281	0.279	0.287	0.347	0.370
Comparison Group 1: 30% RAP, PG 52-34																							
Comparison Group 2	**2.9° C**						**18.0° C**						**21.1° C**						**30.0° C**				
	25 Hz	**10 Hz**	**5 Hz**	**1 Hz**	**0.5 Hz**	**0.1 Hz**	**25 Hz**	**10 Hz**	**5 Hz**	**1 Hz**	**0.5 Hz**	**0.1 Hz**	**25 Hz**	**10 Hz**	**5 Hz**	**1 Hz**	**0.5 Hz**	**0.1 Hz**	**25 Hz**	**10 Hz**	**5 Hz**	**1 Hz**	**0.5 Hz**
Virgin, PG 58-28	0.087	0.122	0.320	0.378	0.375	0.662	0.256	0.298	0.406	0.472	0.524	0.491	-	-	-	-	-	-	0.097	0.137	0.085	0.281	0.484
15% RAP, PG 58-28	0.003	0.004	0.013	0.018	0.014	0.078	0.021	0.030	0.049	0.046	0.086	0.292	-	-	-	-	-	-	0.026	0.036	0.044	0.319	0.744
25% RAP, PG 58-28	0.058	0.079	0.233	0.254	0.258	0.352	0.186	0.226	0.331	0.507	0.696	0.572	-	-	-	-	-	-	0.090	0.241	0.553	0.373	0.029
25% RAP, PG 52-34	0.062	0.072	0.101	0.091	0.086	0.120	0.541	0.572	0.621	0.580	0.607	0.668	-	-	-	-	-	-	0.226	0.210	0.077	0.086	0.112
40% RAP, PG 52-34	0.399	0.487	0.732	0.786	0.749	0.857	0.444	0.502	0.592	0.633	0.710	0.262	-	-	-	-	-	-	0.577	0.435	0.208	0.111	0.047
Comparison Group 1: 40% RAP, PG 52-34																							
Comparison Group 2	**2.9° C**						**18.0° C**						**21.1° C**						**30.0° C**				
	25 Hz	**10 Hz**	**5 Hz**	**1 Hz**	**0.5 Hz**	**0.1 Hz**	**25 Hz**	**10 Hz**	**5 Hz**	**1 Hz**	**0.5 Hz**	**0.1 Hz**	**25 Hz**	**10 Hz**	**5 Hz**	**1 Hz**	**0.5 Hz**	**0.1 Hz**	**25 Hz**	**10 Hz**	**5 Hz**	**1 Hz**	**0.5 Hz**
Virgin, PG 58-28	0.677	0.638	0.605	0.611	0.691	0.897	0.150	0.155	0.174	0.218	0.257	0.691	0.550	0.764	0.952	0.734	0.599	0.394	0.064	0.073	0.089	0.134	0.353
15% RAP, PG 58-28	0.044	0.034	0.028	0.031	0.080	0.133	0.009	0.012	0.010	0.006	0.012	0.774	0.022	0.038	0.154	0.275	0.359	0.325	0.016	0.017	0.022	0.052	0.059
25% RAP, PG 58-28	0.501	0.442	0.450	0.433	0.514	0.593	0.306	0.325	0.399	0.677	0.957	0.005	-	-	-	-	-	-	0.032	0.054	0.110	0.587	0.899
25% RAP, PG 52-34	0.067	0.067	0.077	0.071	0.073	0.132	0.131	0.137	0.130	0.113	0.146	0.069	0.035	0.042	0.055	0.068	0.188	0.771	0.281	0.279	0.287	0.347	0.370
30% RAP, PG 52-34	0.399	0.487	0.732	0.786	0.749	0.857	0.444	0.502	0.592	0.633	0.710	0.262	-	-	-	-	-	-	0.577	0.435	0.208	0.111	0.047

Table 42: Statistical T-Test p-Values for Phase Angles of PG 58-28 Field Core Mixtures

Comparison Group 1: Virgin, PG 58-28																							
Comparison Group 2	2.9° C						18.0° C						21.1° C						30.0° C				
	25 Hz	10 Hz	5 Hz	1 Hz	0.5 Hz	0.1 Hz	25 Hz	10 Hz	5 Hz	1 Hz	0.5 Hz	0.1 Hz	25 Hz	10 Hz	5 Hz	1 Hz	0.5 Hz	0.1 Hz	25 Hz	10 Hz	5 Hz	1 Hz	0.5 Hz
15% RAP, PG 58-28	0.928	0.600	0.900	0.609	0.678	0.397	0.727	0.624	0.745	0.760	0.882	0.787	0.220	0.685	0.421	0.581	0.701	0.926	0.184	0.951	0.868	0.929	1.000
25% RAP, PG 58-28	0.696	0.169	0.100	0.027	0.006	0.015	0.775	0.528	0.576	0.405	0.214	0.792	-	-	-	-	-	-	0.270	0.532	0.334	0.188	0.296
25% RAP, PG 52-34	0.224	0.062	0.096	0.319	0.288	0.453	-	-	-	-	-	-	0.176	0.797	0.845	0.672	0.970	-	-	-	-	-	-
30% RAP, PG 52-34	0.486	0.681	0.543	0.656	0.759	0.759	0.833	0.912	0.971	0.942	0.978	0.846	-	-	-	-	-	-	0.604	0.674	0.618	0.367	0.272
40% RAP, PG 52-34	0.138	0.470	0.538	0.971	0.931	0.570	0.959	0.960	0.953	0.787	0.761	0.969	0.310	0.734	0.768	0.572	0.607	0.835	0.546	0.259	0.266	0.161	0.538
Comparison Group 1: 15% RAP, PG 58-28																							
Comparison Group 2	2.9° C						18.0° C						21.1° C						30.0° C				
	25 Hz	10 Hz	5 Hz	1 Hz	0.5 Hz	0.1 Hz	25 Hz	10 Hz	5 Hz	1 Hz	0.5 Hz	0.1 Hz	25 Hz	10 Hz	5 Hz	1 Hz	0.5 Hz	0.1 Hz	25 Hz	10 Hz	5 Hz	1 Hz	0.5 Hz
Virgin, PG 58-28	0.928	0.600	0.900	0.609	0.678	0.397	0.727	0.624	0.745	0.760	0.882	0.787	0.220	0.685	0.421	0.581	0.701	0.926	0.184	0.951	0.868	0.929	1.000
25% RAP, PG 58-28	0.843	0.332	0.223	0.304	0.239	0.521	0.367	0.155	0.272	0.308	0.476	0.439	-	-	-	-	-	-	0.419	0.273	0.260	0.043	0.072
25% RAP, PG 52-34	0.346	0.025	0.106	0.241	0.275	0.259	0.727	0.560	0.717	0.689	0.716	0.411	0.406	0.781	0.501	0.818	0.795	0.684	0.667	0.635	0.742	0.929	0.433
30% RAP, PG 52-34	0.519	0.472	0.519	0.511	0.622	0.477	0.404	0.372	0.551	0.636	0.762	0.984	-	-	-	-	-	-	0.356	0.517	0.636	0.147	0.092
40% RAP, PG 52-34	0.218	0.230	0.514	0.734	0.744	0.336	0.548	0.491	0.712	0.867	0.977	0.664	0.633	0.916	0.656	0.957	0.966	0.938	0.399	0.339	0.243	0.358	0.399
Comparison Group 1: 25% RAP, PG 58-28																							
Comparison Group 2	2.9° C						18.0° C						21.1° C						30.0° C				
	25 Hz	10 Hz	5 Hz	1 Hz	0.5 Hz	0.1 Hz	25 Hz	10 Hz	5 Hz	1 Hz	0.5 Hz	0.1 Hz	25 Hz	10 Hz	5 Hz	1 Hz	0.5 Hz	0.1 Hz	25 Hz	10 Hz	5 Hz	1 Hz	0.5 Hz
Virgin, PG 58-28	0.696	0.169	0.100	0.027	0.006	0.015	0.775	0.528	0.576	0.405	0.214	0.792	-	-	-	-	-	-	0.270	0.532	0.334	0.188	0.296
15% RAP, PG 58-28	0.843	0.332	0.223	0.304	0.239	0.521	0.367	0.155	0.272	0.308	0.476	0.439	-	-	-	-	-	-	0.419	0.273	0.260	0.043	0.072
25% RAP, PG 52-34	0.139	0.003	0.022	0.057	0.053	0.092	0.775	0.637	0.623	0.622	0.921	0.772	-	-	-	-	-	-	0.529	0.343	0.274	0.188	0.487
30% RAP, PG 52-34	0.350	0.311	0.279	0.291	0.293	0.323	1.000	0.599	0.523	0.413	0.420	0.508	-	-	-	-	-	-	0.195	0.479	0.459	0.337	0.465
40% RAP, PG 52-34	0.094	0.054	0.171	0.283	0.215	0.151	0.847	0.664	0.538	0.293	0.142	0.739	-	-	-	-	-	-	0.212	0.075	0.024	0.007	0.034

Table 43: Statistical T-Test p-Values for Phase Angles of PG 52-34 Field Core Mixtures

Comparison Group 1: 25% RAP, PG 52-34																							
Comparison Group 2	2.9° C						18.0° C						21.1° C						30.0° C				
	25 Hz	10 Hz	5 Hz	1 Hz	0.5 Hz	0.1 Hz	25 Hz	10 Hz	5 Hz	1 Hz	0.5 Hz	0.1 Hz	25 Hz	10 Hz	5 Hz	1 Hz	0.5 Hz	0.1 Hz	25 Hz	10 Hz	5 Hz	1 Hz	0.5 Hz
Virgin, PG 58-28	0.224	0.062	0.096	0.319	0.288	0.453	-	-	-	-	-	-	0.176	0.797	0.845	0.672	0.970	-	-	-	-	-	-
15% RAP, PG 58-28	0.346	0.025	0.106	0.241	0.275	0.259	0.727	0.560	0.717	0.689	0.716	0.411	0.406	0.781	0.501	0.818	0.795	0.684	0.667	0.635	0.742	0.929	0.433
25% RAP, PG 58-28	0.139	0.003	0.022	0.057	0.053	0.092	0.775	0.637	0.623	0.622	0.921	0.772	-	-	-	-	-	-	0.529	0.343	0.274	0.188	0.487
30% RAP, PG 52-34	0.886	0.372	0.517	0.812	0.693	0.826	0.833	1.000	0.986	0.816	0.706	0.524	-	-	-	-	-	-	0.789	0.327	0.512	0.367	0.609
40% RAP, PG 52-34	0.504	0.183	0.403	0.488	0.479	0.944	0.959	0.980	0.925	0.694	0.451	0.625	0.687	0.855	0.882	0.844	0.727	0.587	0.833	0.942	0.427	0.161	0.197
Comparison Group 1: 30% RAP, PG 52-34																							
Comparison Group 2	2.9° C						18.0° C						21.1° C						30.0° C				
	25 Hz	10 Hz	5 Hz	1 Hz	0.5 Hz	0.1 Hz	25 Hz	10 Hz	5 Hz	1 Hz	0.5 Hz	0.1 Hz	25 Hz	10 Hz	5 Hz	1 Hz	0.5 Hz	0.1 Hz	25 Hz	10 Hz	5 Hz	1 Hz	0.5 Hz
Virgin, PG 58-28	0.486	0.681	0.543	0.656	0.759	0.759	0.833	0.912	0.971	0.942	0.978	0.846	-	-	-	-	-	-	0.604	0.674	0.618	0.367	0.272
15% RAP, PG 58-28	0.519	0.472	0.519	0.511	0.622	0.477	0.404	0.372	0.551	0.636	0.762	0.984	-	-	-	-	-	-	0.356	0.517	0.636	0.147	0.092
25% RAP, PG 58-28	0.350	0.311	0.279	0.291	0.293	0.323	1.000	0.599	0.523	0.413	0.420	0.508	-	-	-	-	-	-	0.195	0.479	0.459	0.337	0.465
25% RAP, PG 52-34	0.886	0.372	0.517	0.812	0.693	0.826	0.833	1.000	0.986	0.816	0.706	0.524	-	-	-	-	-	-	0.789	0.327	0.512	0.367	0.609
40% RAP, PG 52-34	0.566	0.954	0.933	0.731	0.833	0.883	0.859	0.965	0.884	0.723	0.653	0.717	-	-	-	-	-	-	0.917	0.079	0.094	0.027	0.031
Comparison Group 1: 40% RAP, PG 52-34																							
Comparison Group 2	2.9° C						18.0° C						21.1° C						30.0° C				
	25 Hz	10 Hz	5 Hz	1 Hz	0.5 Hz	0.1 Hz	25 Hz	10 Hz	5 Hz	1 Hz	0.5 Hz	0.1 Hz	25 Hz	10 Hz	5 Hz	1 Hz	0.5 Hz	0.1 Hz	25 Hz	10 Hz	5 Hz	1 Hz	0.5 Hz
Virgin, PG 58-28	0.138	0.470	0.538	0.971	0.931	0.570	0.959	0.960	0.953	0.787	0.761	0.969	0.310	0.734	0.768	0.572	0.607	0.835	0.546	0.259	0.266	0.161	0.538
15% RAP, PG 58-28	0.218	0.230	0.514	0.734	0.744	0.336	0.548	0.491	0.712	0.867	0.977	0.664	0.633	0.916	0.656	0.957	0.966	0.938	0.399	0.339	0.243	0.358	0.399
25% RAP, PG 58-28	0.094	0.054	0.171	0.283	0.215	0.151	0.847	0.664	0.538	0.293	0.142	0.739	-	-	-	-	-	-	0.212	0.075	0.024	0.007	0.034
25% RAP, PG 52-34	0.504	0.183	0.403	0.488	0.479	0.944	0.959	0.980	0.925	0.694	0.451	0.625	0.687	0.855	0.882	0.844	0.727	0.587	0.833	0.942	0.427	0.161	0.197
30% RAP, PG 52-34	0.566	0.954	0.933	0.731	0.833	0.883	0.859	0.965	0.884	0.723	0.653	0.717	-	-	-	-	-	-	0.917	0.079	0.094	0.027	0.031

Table 44: Statistical T-Test p-Values for Dynamic Modulus of PG 58-28 PMPC Mixtures

Comparison Group 1: Virgin, PG 58-28																		
Comparison Group 2	4.4° C						21.1° C						37.8° C					
	25 Hz	10 Hz	5 Hz	1 Hz	0.5 Hz	0.1 Hz	25 Hz	10 Hz	5 Hz	1 Hz	0.5 Hz	0.1 Hz	25 Hz	10 Hz	5 Hz	1 Hz	0.5 Hz	0.1 Hz
15% RAP, PG 58-28	0.251	0.272	0.333	0.323	0.304	0.211	0.105	0.145	0.226	0.407	0.450	0.893	0.863	0.705	0.603	0.612	0.584	0.501
25% RAP, PG 58-28	0.326	0.334	0.307	0.311	0.268	0.227	0.019	0.016	0.016	0.024	0.033	0.059	0.017	0.032	0.051	0.185	0.391	0.525
25% RAP, PG 52-34	0.610	0.539	0.481	0.418	0.368	0.361	0.063	0.066	0.075	0.168	0.293	0.493	0.928	0.526	0.328	0.239	0.487	0.583
30% RAP, PG 52-34	0.845	0.789	0.759	0.690	0.701	0.662	0.572	0.544	0.575	0.859	0.997	0.545	0.331	0.471	0.657	0.820	0.646	0.423
40% RAP, PG 52-34	0.949	0.980	0.982	0.884	0.823	0.829	0.925	0.914	0.897	0.624	0.401	0.290	0.226	0.329	0.444	0.486	0.382	0.404
Comparison Group 1: 15% RAP, PG 58-28																		
Comparison Group 2	4.4° C						21.1° C						37.8° C					
	25 Hz	10 Hz	5 Hz	1 Hz	0.5 Hz	0.1 Hz	25 Hz	10 Hz	5 Hz	1 Hz	0.5 Hz	0.1 Hz	25 Hz	10 Hz	5 Hz	1 Hz	0.5 Hz	0.1 Hz
Virgin, PG 58-28	0.251	0.272	0.333	0.323	0.304	0.211	0.105	0.145	0.226	0.407	0.450	0.893	0.863	0.705	0.603	0.612	0.584	0.501
25% RAP, PG 58-28	0.845	0.844	0.740	0.758	0.655	0.640	0.137	0.096	0.072	0.060	0.071	0.075	0.005	0.016	0.025	0.107	0.181	0.821
25% RAP, PG 52-34	0.028	0.022	0.016	0.013	0.009	0.017	0.011	0.011	0.014	0.036	0.065	0.409	0.662	0.226	0.131	0.092	0.130	0.447
30% RAP, PG 52-34	0.007	0.006	0.004	0.004	0.002	0.016	0.084	0.089	0.114	0.208	0.305	0.664	0.166	0.610	0.811	0.531	0.834	0.184
40% RAP, PG 52-34	0.003	0.004	0.005	0.002	0.001	0.020	0.315	0.359	0.455	0.899	0.669	0.315	0.121	0.378	0.702	0.745	0.507	0.140
Comparison Group 1: 25% RAP, PG 58-28																		
Comparison Group 2	4.4° C						21.1° C						37.8° C					
	25 Hz	10 Hz	5 Hz	1 Hz	0.5 Hz	0.1 Hz	25 Hz	10 Hz	5 Hz	1 Hz	0.5 Hz	0.1 Hz	25 Hz	10 Hz	5 Hz	1 Hz	0.5 Hz	0.1 Hz
Virgin, PG 58-28	0.326	0.334	0.307	0.311	0.268	0.227	0.019	0.016	0.016	0.024	0.033	0.059	0.017	0.032	0.051	0.185	0.391	0.525
15% RAP, PG 58-28	0.845	0.844	0.740	0.758	0.655	0.640	0.137	0.096	0.072	0.060	0.071	0.075	0.005	0.016	0.025	0.107	0.181	0.821
25% RAP, PG 52-34	0.125	0.106	0.085	0.080	0.071	0.065	0.004	0.002	0.001	0.001	0.002	0.006	0.006	0.042	0.141	0.575	0.693	0.651
30% RAP, PG 52-34	0.155	0.193	0.177	0.169	0.171	0.151	0.008	0.005	0.002	0.003	0.005	0.052	0.002	0.038	0.064	0.189	0.247	0.254
40% RAP, PG 52-34	0.271	0.261	0.243	0.217	0.194	0.178	0.075	0.067	0.072	0.151	0.510	0.865	0.002	0.010	0.021	0.094	0.128	0.198

Table 45: Statistical T-Test p-Values for Dynamic Modulus of PG 52-34 PMPC Mixtures

Comparison Group 1: 25% RAP, PG 52-34																		
Comparison Group 2	4.4° C						21.1° C						37.8° C					
	25 Hz	10 Hz	5 Hz	1 Hz	0.5 Hz	0.1 Hz	25 Hz	10 Hz	5 Hz	1 Hz	0.5 Hz	0.1 Hz	25 Hz	10 Hz	5 Hz	1 Hz	0.5 Hz	0.1 Hz
Virgin, PG 58-28	0.610	0.539	0.481	0.418	0.368	0.361	0.063	0.066	0.075	0.168	0.293	0.493	0.928	0.526	0.328	0.239	0.487	0.583
15% RAP, PG 58-28	0.028	0.022	0.016	0.013	0.009	0.017	0.011	0.011	0.014	0.036	0.065	0.409	0.662	0.226	0.131	0.092	0.130	0.447
25% RAP, PG 58-28	0.125	0.106	0.085	0.080	0.071	0.065	0.004	0.002	0.001	0.001	0.002	0.006	0.006	0.042	0.141	0.575	0.693	0.651
30% RAP, PG 52-34	0.525	0.468	0.381	0.375	0.276	0.342	0.071	0.060	0.019	0.031	0.061	0.071	0.069	0.098	0.121	0.167	0.123	0.159
40% RAP, PG 52-34	0.331	0.207	0.144	0.171	0.173	0.200	0.244	0.214	0.248	0.221	0.233	0.258	0.065	0.083	0.099	0.079	0.078	0.083
Comparison Group 1: 30% RAP, PG 52-34																		
Comparison Group 2	4.4° C						21.1° C						37.8° C					
	25 Hz	10 Hz	5 Hz	1 Hz	0.5 Hz	0.1 Hz	25 Hz	10 Hz	5 Hz	1 Hz	0.5 Hz	0.1 Hz	25 Hz	10 Hz	5 Hz	1 Hz	0.5 Hz	0.1 Hz
Virgin, PG 58-28	0.845	0.789	0.759	0.690	0.701	0.662	0.572	0.544	0.575	0.859	0.997	0.545	0.331	0.471	0.657	0.820	0.646	0.423
15% RAP, PG 58-28	0.007	0.006	0.004	0.004	0.002	0.016	0.084	0.089	0.114	0.208	0.305	0.664	0.166	0.610	0.811	0.531	0.834	0.184
25% RAP, PG 58-28	0.155	0.193	0.177	0.169	0.171	0.151	0.008	0.005	0.002	0.003	0.005	0.052	0.002	0.038	0.064	0.189	0.247	0.254
25% RAP, PG 52-34	0.525	0.468	0.381	0.375	0.276	0.342	0.071	0.060	0.019	0.031	0.061	0.071	0.069	0.098	0.121	0.167	0.123	0.159
40% RAP, PG 52-34	0.341	0.237	0.111	0.247	0.560	0.550	0.734	0.680	0.658	0.534	0.406	0.413	0.464	0.519	0.489	0.369	0.335	0.520
Comparison Group 1: 40% RAP, PG 52-34																		
Comparison Group 2	4.4° C						21.1° C						37.8° C					
	25 Hz	10 Hz	5 Hz	1 Hz	0.5 Hz	0.1 Hz	25 Hz	10 Hz	5 Hz	1 Hz	0.5 Hz	0.1 Hz	25 Hz	10 Hz	5 Hz	1 Hz	0.5 Hz	0.1 Hz
Virgin, PG 58-28	0.949	0.980	0.982	0.884	0.823	0.829	0.925	0.914	0.897	0.624	0.401	0.290	0.226	0.329	0.444	0.486	0.382	0.404
15% RAP, PG 58-28	0.003	0.004	0.005	0.002	0.001	0.020	0.315	0.359	0.455	0.899	0.669	0.315	0.121	0.378	0.702	0.745	0.507	0.140
25% RAP, PG 58-28	0.271	0.261	0.243	0.217	0.194	0.178	0.075	0.067	0.072	0.151	0.510	0.865	0.002	0.010	0.021	0.094	0.128	0.198
25% RAP, PG 52-34	0.331	0.207	0.144	0.171	0.173	0.200	0.244	0.214	0.248	0.221	0.233	0.258	0.065	0.083	0.099	0.079	0.078	0.083
30% RAP, PG 52-34	0.341	0.237	0.111	0.247	0.560	0.550	0.734	0.680	0.658	0.534	0.406	0.413	0.464	0.519	0.489	0.369	0.335	0.520

Table 46: Statistical T-Test p-Values for Phase Angles of PG 58-28 PMPC Mixtures

Comparison Group 1: Virgin, PG 58-28																		
Comparison Group 2	4.4° C						21.1° C						37.8° C					
	25 Hz	10 Hz	5 Hz	1 Hz	0.5 Hz	0.1 Hz	25 Hz	10 Hz	5 Hz	1 Hz	0.5 Hz	0.1 Hz	25 Hz	10 Hz	5 Hz	1 Hz	0.5 Hz	0.1 Hz
15% RAP, PG 58-28	0.851	0.563	0.364	0.461	0.405	0.391	0.610	0.271	0.161	0.223	0.424	0.352	0.722	0.457	0.700	0.273	0.055	0.198
25% RAP, PG 58-28	0.947	0.324	0.315	0.196	0.239	0.221	0.607	0.476	0.364	0.705	0.871	0.158	0.710	0.636	0.384	0.912	0.188	0.042
25% RAP, PG 52-34	0.179	0.919	0.431	0.281	0.134	0.090	0.361	0.449	0.289	0.158	0.189	0.213	0.238	0.529	0.855	0.037	0.404	0.038
30% RAP, PG 52-34	0.547	0.539	0.651	0.707	0.555	0.926	0.417	0.858	0.292	0.131	0.127	0.234	0.105	0.227	0.006	0.006	0.001	0.003
40% RAP, PG 52-34	0.221	0.163	0.145	0.201	0.182	0.484	0.509	0.549	0.305	0.270	0.798	0.919	0.490	0.203	0.550	0.584	0.302	0.059
Comparison Group 1: 15% RAP, PG 58-28																		
Comparison Group 2	**4.4° C**						**21.1° C**						**37.8° C**					
	25 Hz	**10 Hz**	**5 Hz**	**1 Hz**	**0.5 Hz**	**0.1 Hz**	**25 Hz**	**10 Hz**	**5 Hz**	**1 Hz**	**0.5 Hz**	**0.1 Hz**	**25 Hz**	**10 Hz**	**5 Hz**	**1 Hz**	**0.5 Hz**	**0.1 Hz**
Virgin, PG 58-28	0.851	0.563	0.364	0.461	0.405	0.391	0.610	0.271	0.161	0.223	0.424	0.352	0.722	0.457	0.700	0.273	0.055	0.198
25% RAP, PG 58-28	0.795	0.655	0.811	0.499	0.919	0.529	0.933	0.591	0.552	0.460	0.453	0.495	0.520	0.402	0.279	0.472	0.821	0.194
25% RAP, PG 52-34	0.325	0.396	0.697	0.836	0.698	0.221	0.140	0.852	0.892	0.473	0.329	0.110	0.361	0.753	0.932	0.096	0.955	0.159
30% RAP, PG 52-34	0.675	0.297	0.267	0.337	0.264	0.491	0.049	0.106	0.412	0.741	0.342	0.105	0.157	0.244	0.002	0.002	0.001	0.018
40% RAP, PG 52-34	0.323	0.066	0.069	0.092	0.087	0.209	0.206	0.540	0.700	0.699	0.941	0.763	0.727	0.471	0.665	0.990	0.875	0.333
Comparison Group 1: 25% RAP, PG 58-28																		
Comparison Group 2	**4.4° C**						**21.1° C**						**37.8° C**					
	25 Hz	**10 Hz**	**5 Hz**	**1 Hz**	**0.5 Hz**	**0.1 Hz**	**25 Hz**	**10 Hz**	**5 Hz**	**1 Hz**	**0.5 Hz**	**0.1 Hz**	**25 Hz**	**10 Hz**	**5 Hz**	**1 Hz**	**0.5 Hz**	**0.1 Hz**
Virgin, PG 58-28	0.947	0.324	0.315	0.196	0.239	0.221	0.607	0.476	0.364	0.705	0.871	0.158	0.710	0.636	0.384	0.912	0.188	0.042
15% RAP, PG 58-28	0.795	0.655	0.811	0.499	0.919	0.529	0.933	0.591	0.552	0.460	0.453	0.495	0.520	0.402	0.279	0.472	0.821	0.194
25% RAP, PG 52-34	0.199	0.142	0.715	0.390	0.459	0.269	0.324	0.852	0.743	0.258	0.197	0.068	0.212	0.435	0.551	0.073	0.885	0.845
30% RAP, PG 52-34	0.495	0.189	0.218	0.136	0.169	0.310	0.297	0.390	0.988	0.313	0.172	0.062	0.117	0.211	0.051	0.028	0.011	0.275
40% RAP, PG 52-34	0.170	0.031	0.098	0.034	0.089	0.184	0.578	0.907	0.859	0.404	0.751	0.523	0.374	0.212	0.267	0.588	0.797	0.619

Table 47: Statistical T-Test p-Values for Phase Angles of PG 52-34 PMPC Mixtures

Comparison Group 1: 25% RAP, PG 52-34																		
Comparison Group 2	4.4° C						21.1° C						37.8° C					
	25 Hz	10 Hz	5 Hz	1 Hz	0.5 Hz	0.1 Hz	25 Hz	10 Hz	5 Hz	1 Hz	0.5 Hz	0.1 Hz	25 Hz	10 Hz	5 Hz	1 Hz	0.5 Hz	0.1 Hz
Virgin, PG 58-28	0.179	0.919	0.431	0.281	0.134	0.090	0.361	0.449	0.289	0.158	0.189	0.213	0.238	0.529	0.855	0.037	0.404	0.038
15% RAP, PG 58-28	0.325	0.396	0.697	0.836	0.698	0.221	0.140	0.852	0.892	0.473	0.329	0.110	0.361	0.753	0.932	0.096	0.955	0.159
25% RAP, PG 58-28	0.199	0.142	0.715	0.390	0.459	0.269	0.324	0.852	0.743	0.258	0.197	0.068	0.212	0.435	0.551	0.073	0.885	0.845
30% RAP, PG 52-34	0.594	0.536	0.304	0.224	0.135	0.201	0.875	0.410	0.694	0.589	0.671	0.723	0.566	0.214	0.301	0.540	0.146	0.410
40% RAP, PG 52-34	0.606	0.119	0.063	0.054	0.033	0.080	0.389	0.786	0.863	0.809	0.473	0.416	0.527	0.886	0.915	0.199	0.948	0.500
Comparison Group 1: 30% RAP, PG 52-34																		
Comparison Group 2	**4.4° C**						**21.1° C**						**37.8° C**					
	25 Hz	**10 Hz**	**5 Hz**	**1 Hz**	**0.5 Hz**	**0.1 Hz**	**25 Hz**	**10 Hz**	**5 Hz**	**1 Hz**	**0.5 Hz**	**0.1 Hz**	**25 Hz**	**10 Hz**	**5 Hz**	**1 Hz**	**0.5 Hz**	**0.1 Hz**
Virgin, PG 58-28	0.547	0.539	0.651	0.707	0.555	0.926	0.417	0.858	0.292	0.131	0.127	0.234	0.105	0.227	0.006	0.006	0.001	0.003
15% RAP, PG 58-28	0.675	0.297	0.267	0.337	0.264	0.491	0.049	0.106	0.412	0.741	0.342	0.105	0.157	0.244	0.002	0.002	0.001	0.018
25% RAP, PG 58-28	0.495	0.189	0.218	0.136	0.169	0.310	0.297	0.390	0.988	0.313	0.172	0.062	0.117	0.211	0.051	0.028	0.011	0.275
25% RAP, PG 52-34	0.594	0.536	0.304	0.224	0.135	0.201	0.875	0.410	0.694	0.589	0.671	0.723	0.566	0.214	0.301	0.540	0.146	0.410
40% RAP, PG 52-34	0.655	0.524	0.307	0.370	0.524	0.614	0.151	0.510	0.815	0.838	0.601	0.511	0.232	0.275	0.080	0.091	0.173	0.090
Comparison Group 1: 40% RAP, PG 52-34																		
Comparison Group 2	**4.4° C**						**21.1° C**						**37.8° C**					
	25 Hz	**10 Hz**	**5 Hz**	**1 Hz**	**0.5 Hz**	**0.1 Hz**	**25 Hz**	**10 Hz**	**5 Hz**	**1 Hz**	**0.5 Hz**	**0.1 Hz**	**25 Hz**	**10 Hz**	**5 Hz**	**1 Hz**	**0.5 Hz**	**0.1 Hz**
Virgin, PG 58-28	0.221	0.163	0.145	0.201	0.182	0.484	0.509	0.549	0.305	0.270	0.798	0.919	0.490	0.203	0.550	0.584	0.302	0.059
15% RAP, PG 58-28	0.323	0.066	0.069	0.092	0.087	0.209	0.206	0.540	0.700	0.699	0.941	0.763	0.727	0.471	0.665	0.990	0.875	0.333
25% RAP, PG 58-28	0.170	0.031	0.098	0.034	0.089	0.184	0.578	0.907	0.859	0.404	0.751	0.523	0.374	0.212	0.267	0.588	0.797	0.619
25% RAP, PG 52-34	0.606	0.119	0.063	0.054	0.033	0.080	0.389	0.786	0.863	0.809	0.473	0.416	0.527	0.886	0.915	0.199	0.948	0.500
30% RAP, PG 52-34	0.655	0.524	0.307	0.370	0.524	0.614	0.151	0.510	0.815	0.838	0.601	0.511	0.232	0.275	0.080	0.091	0.173	0.090

Table 48: Statistical T-Test p-Values for Dynamic Modulus of PG 58-28 PMLC Mixtures

Comparison Group 1: Virgin, PG 58-28																		
Comparison Group 2	4.4° C						21.1° C						37.8° C					
	25 Hz	10 Hz	5 Hz	1 Hz	0.5 Hz	0.1 Hz	25 Hz	10 Hz	5 Hz	1 Hz	0.5 Hz	0.1 Hz	25 Hz	10 Hz	5 Hz	1 Hz	0.5 Hz	0.1 Hz
15% RAP, PG 58-28	0.018	0.057	0.050	0.030	0.028	0.000	0.037	0.037	0.009	0.001	0.001	0.002	0.001	0.003	0.008	0.726	0.169	0.008
25% RAP, PG 58-28	0.005	0.003	0.002	0.001	0.001	0.000	0.000	0.000	0.000	0.000	0.001	0.001	0.005	0.008	0.014	0.074	0.580	0.147
25% RAP, PG 52-34	0.037	0.014	0.013	0.015	0.021	0.038	0.013	0.012	0.016	0.031	0.057	0.129	0.345	0.503	0.608	0.868	0.964	0.915
30% RAP, PG 52-34	0.025	0.002	0.001	0.000	0.000	0.000	0.001	0.000	0.001	0.001	0.003	0.001	0.007	0.009	0.012	0.025	0.032	0.056
40% RAP, PG 52-34	0.001	0.000	0.000	0.000	0.000	0.000	0.000	0.003	0.003	0.000	0.000	0.000	0.076	0.337	0.842	0.143	0.042	0.009
Comparison Group 1: 15% RAP, PG 58-28																		
Comparison Group 2	**4.4° C**						**21.1° C**						**37.8° C**					
	25 Hz	**10 Hz**	**5 Hz**	**1 Hz**	**0.5 Hz**	**0.1 Hz**	**25 Hz**	**10 Hz**	**5 Hz**	**1 Hz**	**0.5 Hz**	**0.1 Hz**	**25 Hz**	**10 Hz**	**5 Hz**	**1 Hz**	**0.5 Hz**	**0.1 Hz**
Virgin, PG 58-28	0.018	0.057	0.050	0.030	0.028	0.000	0.037	0.037	0.009	0.001	0.001	0.002	0.001	0.003	0.008	0.726	0.169	0.008
25% RAP, PG 58-28	0.221	0.199	0.183	0.157	0.160	0.151	0.009	0.021	0.017	0.010	0.010	0.007	0.060	0.063	0.135	0.129	0.238	0.912
25% RAP, PG 52-34	0.139	0.070	0.057	0.024	0.023	0.003	0.060	0.039	0.041	0.006	0.012	0.030	0.011	0.027	0.099	0.934	0.175	0.008
30% RAP, PG 52-34	0.182	0.155	0.133	0.077	0.072	0.002	0.136	0.111	0.077	0.013	0.022	0.105	0.063	0.436	0.908	0.018	0.004	0.017
40% RAP, PG 52-34	0.114	0.087	0.066	0.028	0.018	0.007	0.014	0.024	0.017	0.009	0.007	0.008	0.489	0.238	0.146	0.101	0.087	0.271
Comparison Group 1: 25% RAP, PG 58-28																		
Comparison Group 2	**4.4° C**						**21.1° C**						**37.8° C**					
	25 Hz	**10 Hz**	**5 Hz**	**1 Hz**	**0.5 Hz**	**0.1 Hz**	**25 Hz**	**10 Hz**	**5 Hz**	**1 Hz**	**0.5 Hz**	**0.1 Hz**	**25 Hz**	**10 Hz**	**5 Hz**	**1 Hz**	**0.5 Hz**	**0.1 Hz**
Virgin, PG 58-28	0.005	0.003	0.002	0.001	0.001	0.000	0.000	0.000	0.000	0.000	0.001	0.001	0.005	0.008	0.014	0.074	0.580	0.147
15% RAP, PG 58-28	0.221	0.199	0.183	0.157	0.160	0.151	0.009	0.021	0.017	0.010	0.010	0.007	0.060	0.063	0.135	0.129	0.238	0.912
25% RAP, PG 52-34	0.008	0.007	0.005	0.003	0.004	0.001	0.000	0.000	0.000	0.001	0.002	0.002	0.010	0.016	0.023	0.092	0.599	0.150
30% RAP, PG 52-34	0.010	0.008	0.006	0.003	0.003	0.000	0.000	0.000	0.000	0.001	0.002	0.003	0.026	0.051	0.082	0.535	0.547	0.080
40% RAP, PG 52-34	0.837	0.726	0.608	0.266	0.153	0.025	0.748	0.926	0.858	0.497	0.324	0.103	0.073	0.048	0.041	0.032	0.054	0.437

Table 49: Statistical T-Test p-Values for Dynamic Modulus of PG 52-34 PMLC Mixtures

Comparison Group 1: 25% RAP, PG 52-34																		
Comparison Group 2	4.4° C						21.1° C						37.8° C					
	25 Hz	10 Hz	5 Hz	1 Hz	0.5 Hz	0.1 Hz	25 Hz	10 Hz	5 Hz	1 Hz	0.5 Hz	0.1 Hz	25 Hz	10 Hz	5 Hz	1 Hz	0.5 Hz	0.1 Hz
Virgin, PG 58-28	0.037	0.014	0.013	0.015	0.021	0.038	0.013	0.012	0.016	0.031	0.057	0.129	0.345	0.503	0.608	0.868	0.964	0.915
15% RAP, PG 58-28	0.139	0.070	0.057	0.024	0.023	0.003	0.060	0.039	0.041	0.006	0.012	0.030	0.011	0.027	0.099	0.934	0.175	0.008
25% RAP, PG 58-28	0.008	0.007	0.005	0.003	0.004	0.001	0.000	0.000	0.000	0.001	0.002	0.002	0.010	0.016	0.023	0.092	0.599	0.150
30% RAP, PG 52-34	0.252	0.316	0.350	0.364	0.412	0.384	0.381	0.269	0.184	0.116	0.192	0.128	0.054	0.054	0.054	0.045	0.041	0.035
40% RAP, PG 52-34	0.000	0.000	0.000	0.000	0.000	0.000	0.000	0.000	0.000	0.000	0.001	0.001	0.184	0.602	0.897	0.134	0.042	0.009
Comparison Group 1: 30% RAP, PG 52-34																		
Comparison Group 2	4.4° C						21.1° C						37.8° C					
	25 Hz	10 Hz	5 Hz	1 Hz	0.5 Hz	0.1 Hz	25 Hz	10 Hz	5 Hz	1 Hz	0.5 Hz	0.1 Hz	25 Hz	10 Hz	5 Hz	1 Hz	0.5 Hz	0.1 Hz
Virgin, PG 58-28	0.025	0.002	0.001	0.000	0.000	0.000	0.001	0.000	0.001	0.001	0.003	0.001	0.007	0.009	0.012	0.025	0.032	0.056
15% RAP, PG 58-28	0.182	0.155	0.133	0.077	0.072	0.002	0.136	0.111	0.077	0.013	0.022	0.105	0.063	0.436	0.908	0.018	0.004	0.017
25% RAP, PG 58-28	0.010	0.008	0.006	0.003	0.003	0.000	0.000	0.000	0.000	0.001	0.002	0.003	0.026	0.051	0.082	0.535	0.547	0.080
25% RAP, PG 52-34	0.252	0.316	0.350	0.364	0.412	0.384	0.381	0.269	0.184	0.116	0.192	0.128	0.054	0.054	0.054	0.045	0.041	0.035
40% RAP, PG 52-34	0.000	0.000	0.000	0.000	0.002	0.000	0.006	0.004	0.000	0.000	0.001	0.001	0.894	0.344	0.149	0.024	0.012	0.005
Comparison Group 1: 40% RAP, PG 52-34																		
Comparison Group 2	4.4° C						21.1° C						37.8° C					
	25 Hz	10 Hz	5 Hz	1 Hz	0.5 Hz	0.1 Hz	25 Hz	10 Hz	5 Hz	1 Hz	0.5 Hz	0.1 Hz	25 Hz	10 Hz	5 Hz	1 Hz	0.5 Hz	0.1 Hz
Virgin, PG 58-28	0.001	0.000	0.000	0.000	0.000	0.000	0.000	0.003	0.003	0.000	0.000	0.000	0.076	0.337	0.842	0.143	0.042	0.009
15% RAP, PG 58-28	0.114	0.087	0.066	0.028	0.018	0.007	0.014	0.024	0.017	0.009	0.007	0.008	0.489	0.238	0.146	0.101	0.087	0.271
25% RAP, PG 58-28	0.837	0.726	0.608	0.266	0.153	0.025	0.748	0.926	0.858	0.497	0.324	0.103	0.073	0.048	0.041	0.032	0.054	0.437
25% RAP, PG 52-34	0.000	0.000	0.000	0.000	0.000	0.000	0.000	0.000	0.000	0.000	0.001	0.001	0.184	0.602	0.897	0.134	0.042	0.009
30% RAP, PG 52-34	0.000	0.000	0.000	0.000	0.002	0.000	0.006	0.004	0.000	0.000	0.001	0.001	0.894	0.344	0.149	0.024	0.012	0.005

Table 50: Statistical T-Test p-Values for Phase Angles of PG 58-28 PMLC Mixtures

Comparison Group 1: Virgin, PG 58-28																		
Comparison Group 2	4.4° C						21.1° C						37.8° C					
	25 Hz	10 Hz	5 Hz	1 Hz	0.5 Hz	0.1 Hz	25 Hz	10 Hz	5 Hz	1 Hz	0.5 Hz	0.1 Hz	25 Hz	10 Hz	5 Hz	1 Hz	0.5 Hz	0.1 Hz
15% RAP, PG 58-28	0.648	0.004	0.014	0.019	0.009	0.076	0.042	0.024	0.020	0.011	0.028	0.048	0.100	0.267	0.703	0.391	0.426	0.622
25% RAP, PG 58-28	0.810	0.101	0.091	0.021	0.050	0.005	0.028	0.001	0.029	0.005	0.012	0.006	0.115	0.078	0.142	0.435	0.671	0.723
25% RAP, PG 52-34	0.148	0.882	0.898	0.973	0.943	0.993	0.537	0.749	0.758	0.856	0.976	0.897	0.084	0.043	0.043	0.035	0.010	0.010
30% RAP, PG 52-34	0.184	0.569	0.567	0.386	0.281	0.150	0.002	0.007	0.014	0.098	0.257	0.278	0.047	0.177	0.666	0.267	0.062	0.040
40% RAP, PG 52-34	0.022	0.058	0.104	0.092	0.089	0.057	0.017	0.000	0.001	0.001	0.005	0.014	0.146	0.056	0.911	0.523	0.975	0.149
Comparison Group 1: 15% RAP, PG 58-28																		
Comparison Group 2	**4.4° C**						**21.1° C**						**37.8° C**					
	25 Hz	**10 Hz**	**5 Hz**	**1 Hz**	**0.5 Hz**	**0.1 Hz**	**25 Hz**	**10 Hz**	**5 Hz**	**1 Hz**	**0.5 Hz**	**0.1 Hz**	**25 Hz**	**10 Hz**	**5 Hz**	**1 Hz**	**0.5 Hz**	**0.1 Hz**
Virgin, PG 58-28	0.648	0.004	0.014	0.019	0.009	0.076	0.042	0.024	0.020	0.011	0.028	0.048	0.100	0.267	0.703	0.391	0.426	0.622
25% RAP, PG 58-28	0.557	0.684	0.959	0.861	0.399	0.526	0.306	0.183	0.155	0.363	0.351	0.597	0.604	0.172	0.175	0.230	0.421	0.571
25% RAP, PG 52-34	0.183	0.002	0.013	0.018	0.009	0.077	0.044	0.025	0.021	0.045	0.025	0.095	0.075	0.155	0.417	0.643	0.764	0.892
30% RAP, PG 52-34	0.222	0.005	0.017	0.024	0.012	0.097	0.056	0.032	0.077	0.059	0.089	0.129	0.152	0.382	0.751	0.483	0.653	0.812
40% RAP, PG 52-34	0.122	0.079	0.223	0.248	0.239	0.542	0.466	0.987	0.854	0.863	0.723	0.527	0.305	0.458	0.717	0.521	0.476	0.229
Comparison Group 1: 25% RAP, PG 58-28																		
Comparison Group 2	**4.4° C**						**21.1° C**						**37.8° C**					
	25 Hz	**10 Hz**	**5 Hz**	**1 Hz**	**0.5 Hz**	**0.1 Hz**	**25 Hz**	**10 Hz**	**5 Hz**	**1 Hz**	**0.5 Hz**	**0.1 Hz**	**25 Hz**	**10 Hz**	**5 Hz**	**1 Hz**	**0.5 Hz**	**0.1 Hz**
Virgin, PG 58-28	0.810	0.101	0.091	0.021	0.050	0.005	0.028	0.001	0.029	0.005	0.012	0.006	0.115	0.078	0.142	0.435	0.671	0.723
15% RAP, PG 58-28	0.557	0.684	0.959	0.861	0.399	0.526	0.306	0.183	0.155	0.363	0.351	0.597	0.604	0.172	0.175	0.230	0.421	0.571
25% RAP, PG 52-34	0.229	0.096	0.093	0.020	0.052	0.026	0.031	0.001	0.031	0.024	0.029	0.026	0.098	0.060	0.112	0.302	0.488	0.604
30% RAP, PG 52-34	0.240	0.118	0.101	0.027	0.060	0.033	0.049	0.016	0.050	0.037	0.048	0.035	0.140	0.086	0.147	0.360	0.531	0.636
40% RAP, PG 52-34	0.021	0.209	0.250	0.220	0.496	0.925	0.035	0.007	0.028	0.126	0.108	0.828	0.147	0.094	0.140	0.316	0.656	0.926

Table 51: Statistical T-Test p-Values for Phase Angles of PG 52-34 PMLC Mixtures

Comparison Group 1: 25% RAP, PG 52-34																		
Comparison Group 2	4.4° C						21.1° C						37.8° C					
	25 Hz	10 Hz	5 Hz	1 Hz	0.5 Hz	0.1 Hz	25 Hz	10 Hz	5 Hz	1 Hz	0.5 Hz	0.1 Hz	25 Hz	10 Hz	5 Hz	1 Hz	0.5 Hz	0.1 Hz
Virgin, PG 58-28	0.148	0.882	0.898	0.973	0.943	0.993	0.537	0.749	0.758	0.856	0.976	0.897	0.084	0.043	0.043	0.035	0.010	0.010
15% RAP, PG 58-28	0.183	0.002	0.013	0.018	0.009	0.077	0.044	0.025	0.021	0.045	0.025	0.095	0.075	0.155	0.417	0.643	0.764	0.892
25% RAP, PG 58-28	0.229	0.096	0.093	0.020	0.052	0.026	0.031	0.001	0.031	0.024	0.029	0.026	0.098	0.060	0.112	0.302	0.488	0.604
30% RAP, PG 52-34	0.222	0.405	0.401	0.304	0.255	0.122	0.024	0.013	0.012	0.006	0.035	0.003	0.019	0.032	0.082	0.278	0.357	0.320
40% RAP, PG 52-34	0.003	0.059	0.104	0.093	0.090	0.057	0.016	0.000	0.001	0.000	0.004	0.047	0.044	0.016	0.189	0.587	0.340	0.067
Comparison Group 1: 30% RAP, PG 52-34																		
Comparison Group 2	**4.4° C**						**21.1° C**						**37.8° C**					
	25 Hz	**10 Hz**	**5 Hz**	**1 Hz**	**0.5 Hz**	**0.1 Hz**	**25 Hz**	**10 Hz**	**5 Hz**	**1 Hz**	**0.5 Hz**	**0.1 Hz**	**25 Hz**	**10 Hz**	**5 Hz**	**1 Hz**	**0.5 Hz**	**0.1 Hz**
Virgin, PG 58-28	0.184	0.569	0.567	0.386	0.281	0.150	0.002	0.007	0.014	0.098	0.257	0.278	0.047	0.177	0.666	0.267	0.062	0.040
15% RAP, PG 58-28	0.222	0.005	0.017	0.024	0.012	0.097	0.056	0.032	0.077	0.059	0.089	0.129	0.152	0.382	0.751	0.483	0.653	0.812
25% RAP, PG 58-28	0.240	0.118	0.101	0.027	0.060	0.033	0.049	0.016	0.050	0.037	0.048	0.035	0.140	0.086	0.147	0.360	0.531	0.636
25% RAP, PG 52-34	0.222	0.405	0.401	0.304	0.255	0.122	0.024	0.013	0.012	0.006	0.035	0.003	0.019	0.032	0.082	0.278	0.357	0.320
40% RAP, PG 52-34	0.004	0.061	0.109	0.100	0.099	0.070	0.020	0.006	0.001	0.001	0.030	0.060	0.257	0.538	0.871	0.959	0.484	0.084
Comparison Group 1: 40% RAP, PG 52-34																		
Comparison Group 2	**4.4° C**						**21.1° C**						**37.8° C**					
	25 Hz	**10 Hz**	**5 Hz**	**1 Hz**	**0.5 Hz**	**0.1 Hz**	**25 Hz**	**10 Hz**	**5 Hz**	**1 Hz**	**0.5 Hz**	**0.1 Hz**	**25 Hz**	**10 Hz**	**5 Hz**	**1 Hz**	**0.5 Hz**	**0.1 Hz**
Virgin, PG 58-28	0.022	0.058	0.104	0.092	0.089	0.057	0.017	0.000	0.001	0.001	0.005	0.014	0.146	0.056	0.911	0.523	0.975	0.149
15% RAP, PG 58-28	0.122	0.079	0.223	0.248	0.239	0.542	0.466	0.987	0.854	0.863	0.723	0.527	0.305	0.458	0.717	0.521	0.476	0.229
25% RAP, PG 58-28	0.021	0.209	0.250	0.220	0.496	0.925	0.035	0.007	0.028	0.126	0.108	0.828	0.147	0.094	0.140	0.316	0.656	0.926
25% RAP, PG 52-34	0.003	0.059	0.104	0.093	0.090	0.057	0.016	0.000	0.001	0.000	0.004	0.047	0.044	0.016	0.189	0.587	0.340	0.067
30% RAP, PG 52-34	0.004	0.061	0.109	0.100	0.099	0.070	0.020	0.006	0.001	0.001	0.030	0.060	0.257	0.538	0.871	0.959	0.484	0.084

Table 52: Statistical T-Test p-Values of PMPC vs. PMLC Mixtures

Dynamic Modulus																		
Mix Types	4.4° C						21.1° C						37.8° C					
	25 Hz	10 Hz	5 Hz	1 Hz	0.5 Hz	0.1 Hz	25 Hz	10 Hz	5 Hz	1 Hz	0.5 Hz	0.1 Hz	25 Hz	10 Hz	5 Hz	1 Hz	0.5 Hz	0.1 Hz
Virgin, PG 58-28	0.006	0.038	0.044	0.036	0.033	0.022	0.000	0.002	0.002	0.000	0.000	0.002	0.000	0.000	0.000	0.008	0.234	0.393
15% RAP, PG 58-28	0.187	0.195	0.206	0.116	0.127	0.157	0.003	0.005	0.004	0.001	0.001	0.001	0.000	0.000	0.002	0.000	0.004	0.491
25% RAP, PG 58-28	0.754	0.698	0.579	0.708	0.679	0.709	0.649	0.614	0.518	0.575	0.556	0.751	0.922	0.893	0.996	0.672	0.678	0.926
25% RAP, PG 52-34	0.001	0.001	0.001	0.001	0.001	0.000	0.000	0.000	0.000	0.000	0.000	0.000	0.000	0.001	0.002	0.048	0.569	0.115
30% RAP, PG 52-34	0.000	0.000	0.000	0.000	0.000	0.000	0.000	0.000	0.000	0.000	0.000	0.000	0.000	0.000	0.000	0.001	0.090	0.008
40% RAP, PG 52-34	0.045	0.013	0.014	0.011	0.020	0.141	0.035	0.040	0.042	0.053	0.122	0.258	0.002	0.002	0.002	0.005	0.007	0.017
Phase Angle																		
Mix Types	4.4° C						21.1° C						37.8° C					
	25 Hz	10 Hz	5 Hz	1 Hz	0.5 Hz	0.1 Hz	25 Hz	10 Hz	5 Hz	1 Hz	0.5 Hz	0.1 Hz	25 Hz	10 Hz	5 Hz	1 Hz	0.5 Hz	0.1 Hz
Virgin, PG 58-28	0.420	0.071	0.037	0.046	0.035	0.037	0.979	0.073	0.038	0.002	0.003	0.005	0.110	0.005	0.630	0.566	0.790	0.082
15% RAP, PG 58-28	0.522	0.174	0.382	0.299	0.310	0.214	0.288	0.235	0.208	0.386	0.476	0.437	0.451	0.819	0.728	0.723	0.601	0.377
25% RAP, PG 58-28	0.382	0.342	0.082	0.265	0.418	0.571	0.936	0.429	0.375	0.429	0.301	0.324	0.576	0.343	0.427	0.428	0.281	0.326
25% RAP, PG 52-34	0.001	0.023	0.027	0.003	0.003	0.007	0.046	0.076	0.114	0.185	0.420	0.282	0.571	0.682	0.917	0.061	0.529	0.269
30% RAP, PG 52-34	0.143	0.035	0.019	0.022	0.024	0.045	0.010	0.018	0.019	0.010	0.136	0.210	0.294	0.266	0.001	0.000	0.000	0.002
40% RAP, PG 52-34	0.336	0.069	0.127	0.154	0.100	0.123	0.094	0.265	0.202	0.230	0.519	0.811	0.893	0.686	0.667	0.495	0.278	0.225

B.6 Shifted Phase Angle Isotherms with High Temperature Results for Field Core Mixtures

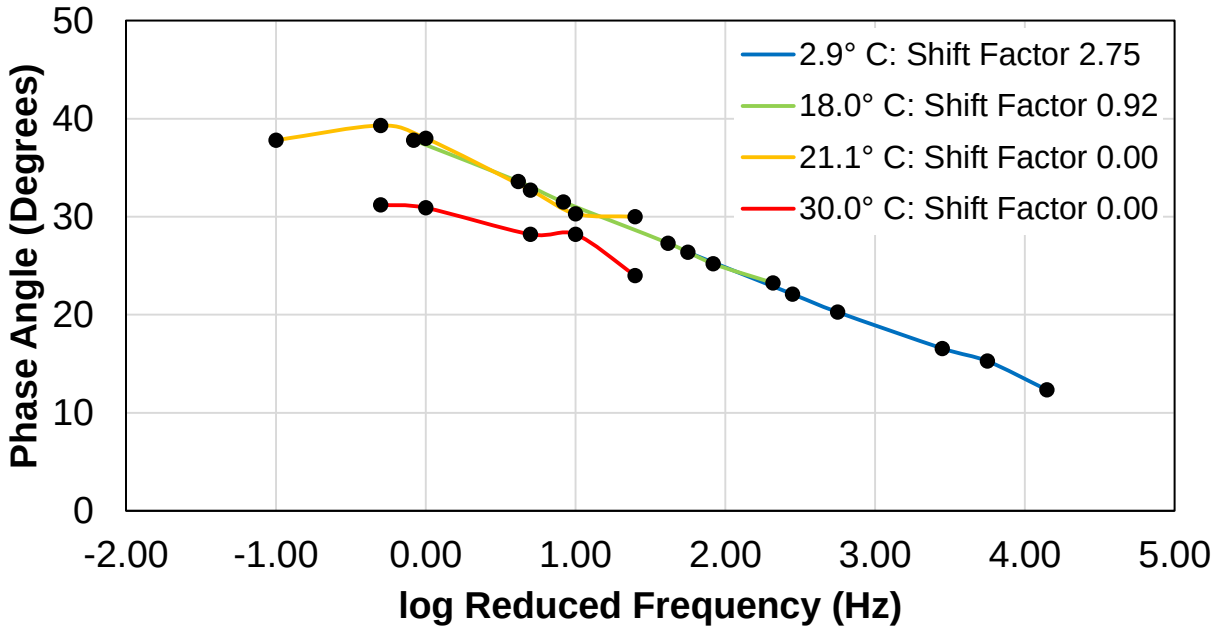

Figure 115: Shifted Phase Angle Isotherms for Virgin, PG 58-28 Field Core Mixture

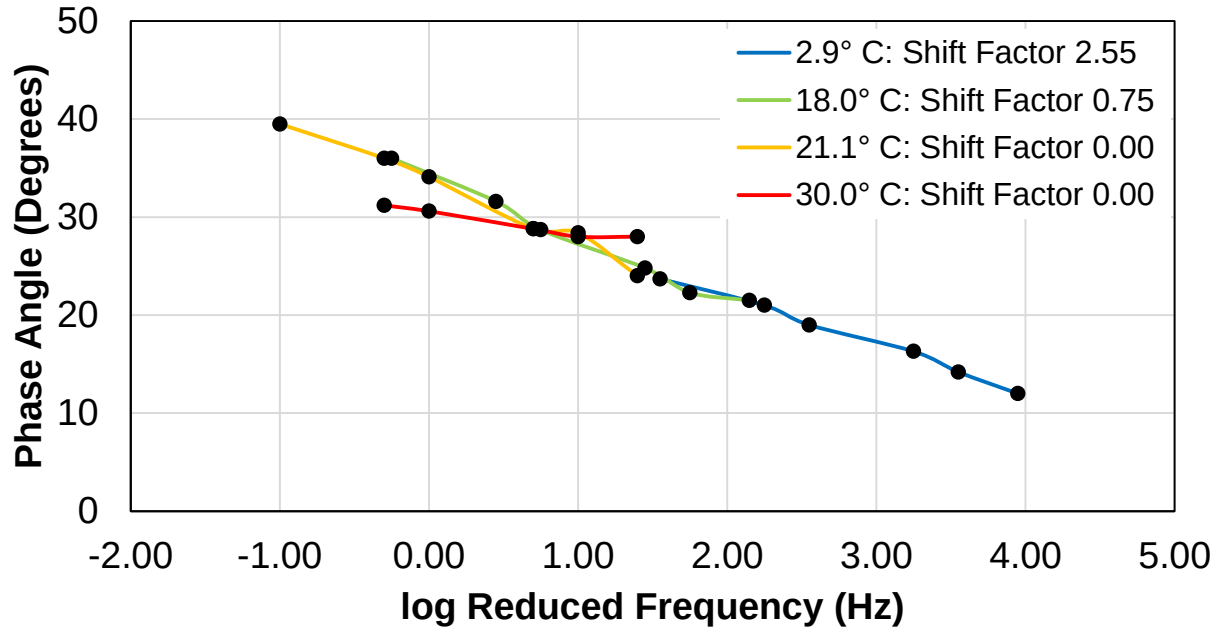

Figure 116: Shifted Phase Angle Isotherms for 15% RAP, PG 58-28 Field Core Mixture

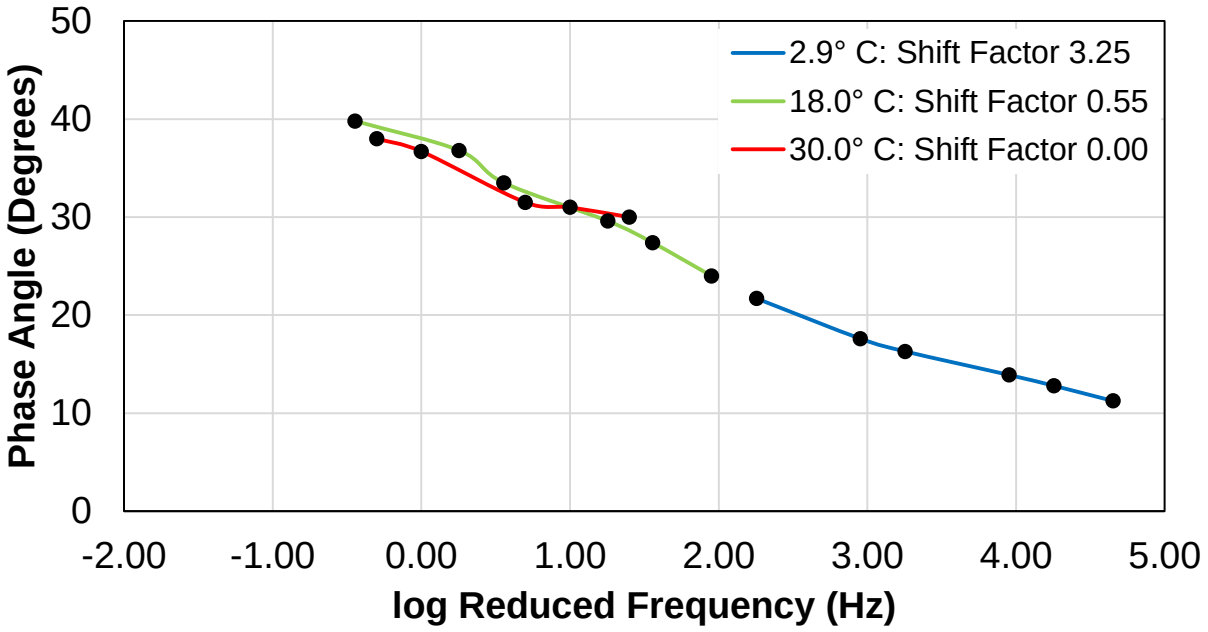

Figure 117: Shifted Phase Angle Isotherms for 25% RAP, PG 58-28 Field Core Mixture

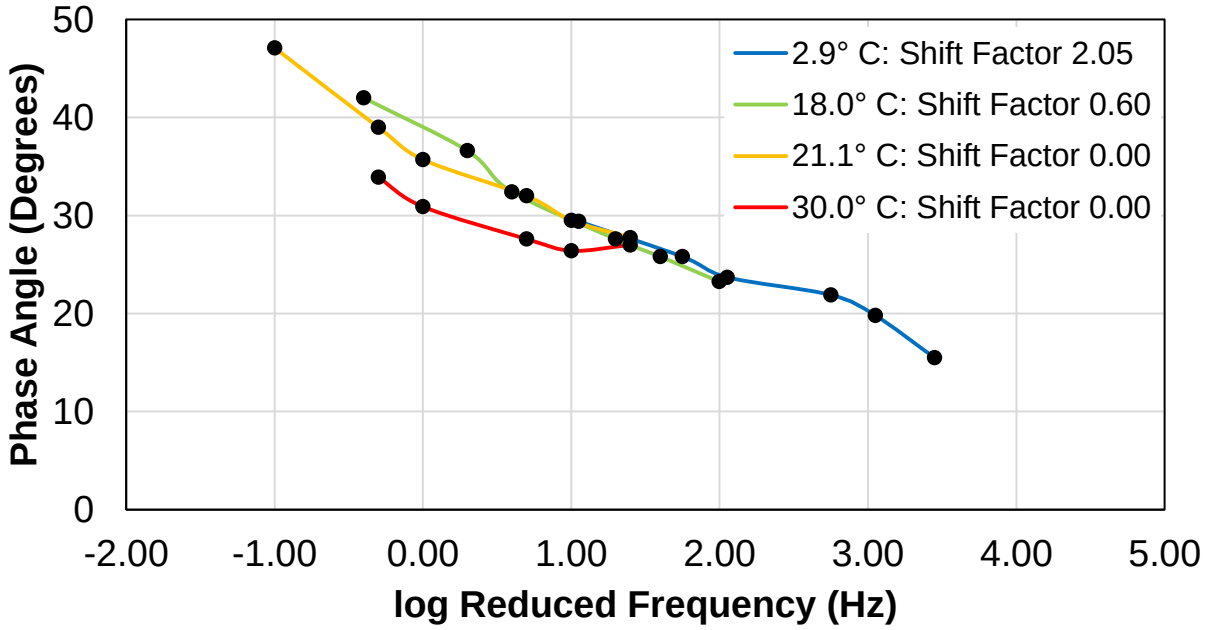

Figure 118: Shifted Phase Angle Isotherms for 25% RAP, PG 52-34 Field Core Mixture

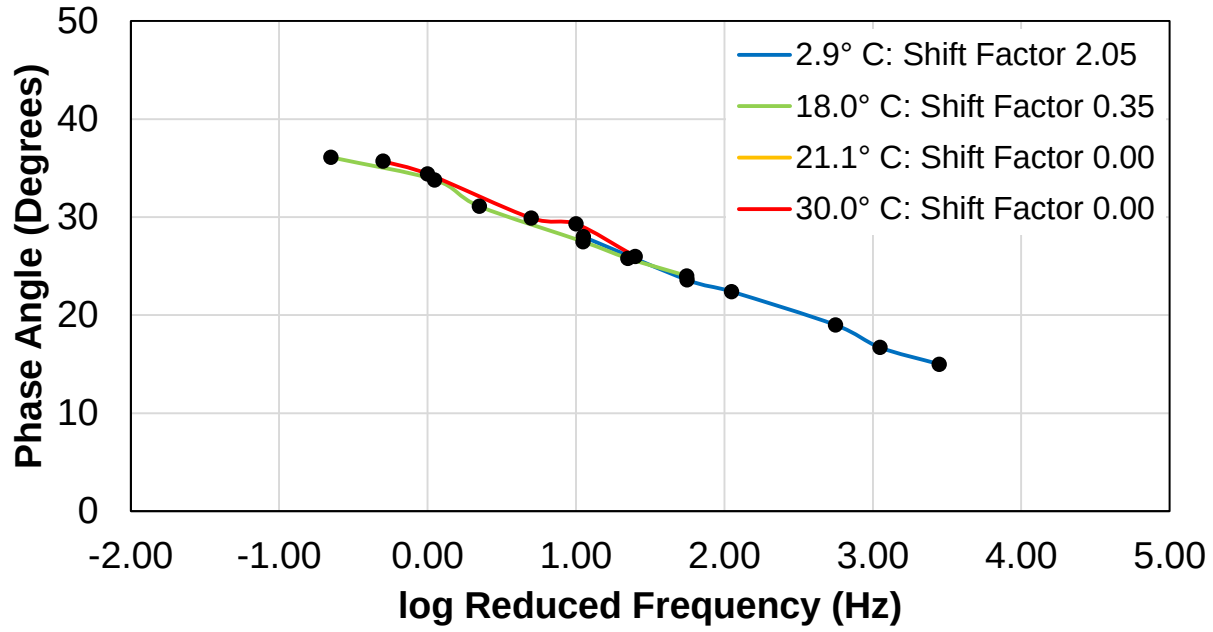

Figure 119: Shifted Phase Angle Isotherms for 30% RAP, PG 52-34 Field Core Mixture

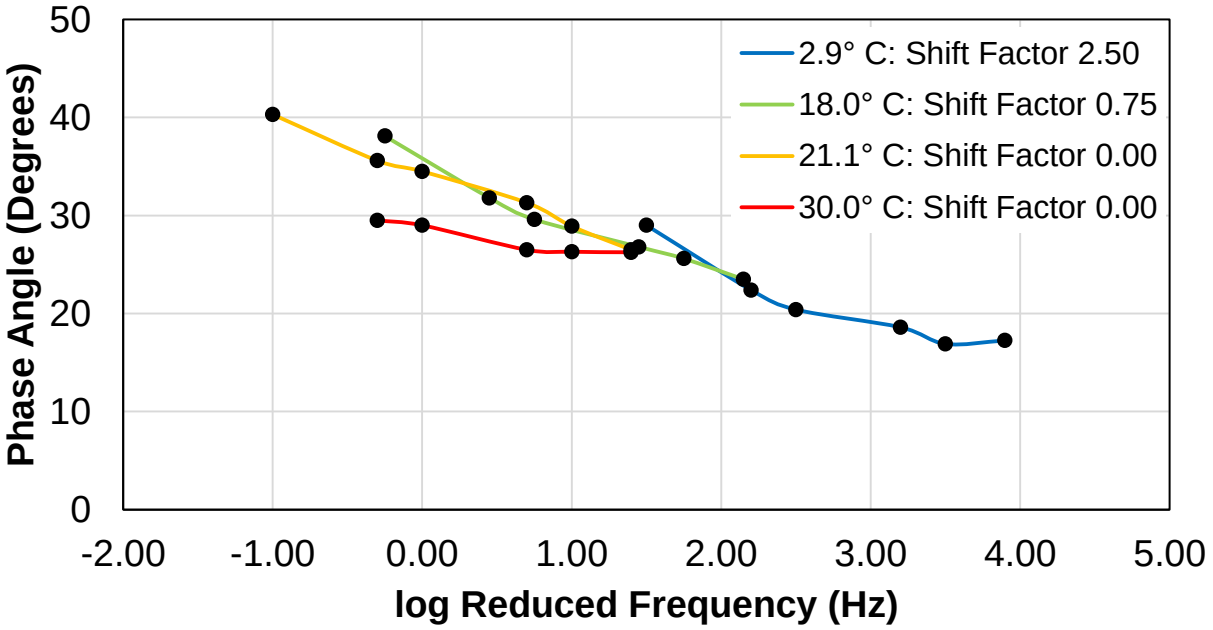

Figure 120: Shifted Phase Angle Isotherms for 40% RAP, PG 52-34 Field Core Mixture

B.7 S-VECD Fatigue Data

Table 53: S-VECD Fatigue Test Results for Virgin Silo Storage Mixtures

Silo Storage Time	Replicate #	Temperature (° C)	Frequency (Hz)	$\|E^*\|_{fingerprint}$ (MPa)	N_f	G^R
0 hrs	1	20	10	6858	21798	5.43E+01
	2	20	10	7727	5215	4.39E+02
	3	20	10	6072	7535	1.71E+02
	4	20	10	7119	47685	1.63E+01
2.5 hrs	1	20	10	7316	42390	1.97E+01
	2	20	10	7950	5095	3.87E+02
	3	20	10	7460	15955	8.95E+01
	4	20	10	7860	4375	7.18E+02
5 hrs	1	20	10	8449	38464	2.28E+01
	2	20	10	7190	13476	3.87E+01
	3	20	10	7755	18225	5.73E+01
	4	20	10	7492	6295	3.11E+02
7.5 hrs	1	20	10	8947	12419	1.26E+02
	2	20	10	8837	6615	3.05E+02
	3	20	10	8389	40483	1.94E+01

Table 54: Power Equation Coefficients of G^R-N_f Results for Virgin Silo Storage Mixtures

Silo Storage Time	Coefficients in $y = ax^b$		N_f at G^R=100
	a	b	
0 hrs	5.92E+07	-1.401	13223
2.5 hrs	1.75E+08	-1.501	14439
5 hrs	3.58E+07	-1.372	11149
7.5 hrs	2.16E+08	-1.528	13987

Table 55: S-VECD Fatigue Test Results for Field Core Mixtures

	Replicate #	Temperature (° C)	Frequency (Hz)	$\|E^*\|_{fingerprint}$ (MPa)	N_f	G^R
Virgin, PG 58-28	1	15	10	6648	14777	6.25E+01
	2	15	10	7250	5015	1.89E+02
	3	15	10	6353	24899	1.58E+01
	4	15	10	7723	10543	2.05E+01
15% RAP, PG 58-28	1	15	10	8204	8155	1.58E+02
	2	15	10	7420	17140	2.78E+01
	4	15.1	10	6563	15873	3.70E+01
	5	15	10	5957	5775	1.46E+02
25% RAP, PG 58-28	1	15	10	8746	2615	2.76E+02
	2	15	10	8240	11857	5.41E+01
	4	15	10	6880	32655	5.01E+00
25% RAP, PG 52-34	2	15	10	5166	9875	3.96E+01
	3	15	10	5753	72542	3.81E+00
	4	15	10	4682	21247	4.15E+01
30% RAP, PG 52-34	1	15.1	10	3795	18412	9.06E+01
	3	15	10	5222	90399	3.36E+00
	4	15	10	6848	3015	2.34E+02
40% RAP, PG 52-34	1	15	10	5663	16369	7.72E+01
	2	15	10	4870	1355	5.24E+02
	4	15	10	5445	1255	6.98E+02

Table 56: Power Equation Coefficients of G^R-N_f Results for Field Core Mixtures

Mix	Coefficients in $y = ax^b$		N_f at G^R=100
	a	b	
Virgin, PG 58-28	1.61E+07	-1.366	6494
15% RAP, PG 58-28	2.77E+08	-1.639	854
25% RAP, PG 58-28	6.60E+07	-1.548	5746
25% RAP, PG 52-34	5.50E+06	-1.246	6378
30% RAP, PG 52-34	6.77E+06	-1.231	8372
40% RAP, PG 52-34	2.10E+05	-0.815	11875

B.8 S-VECD Fatigue Damage Characteristic Curves of Individual Replicates

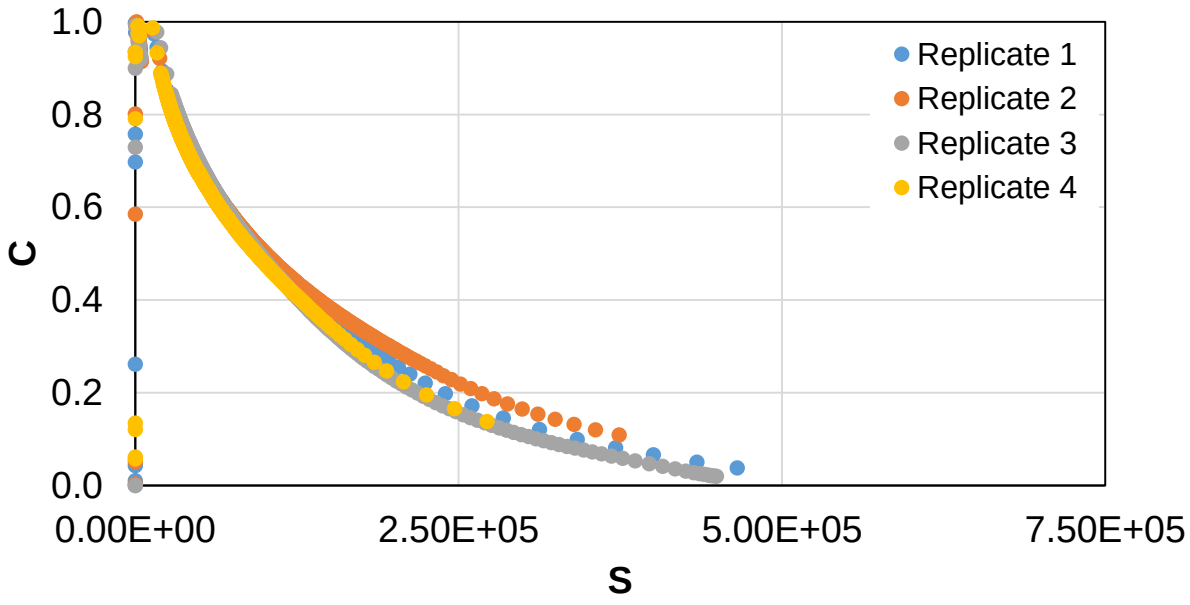

Figure 121: S-VECD Fatigue Damage Characteristic Curves for 0 Hours Virgin Silo Storage Individual Replicates

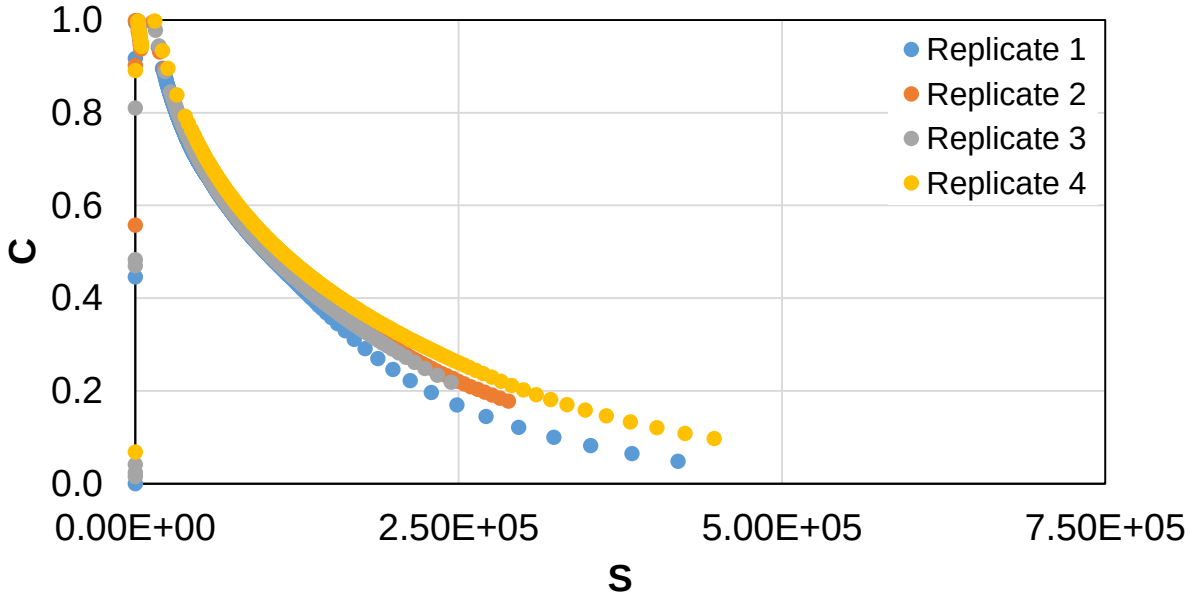

Figure 122: S-VECD Fatigue Damage Characteristic Curves for 2.5 Hours Virgin Silo Storage Individual Replicates

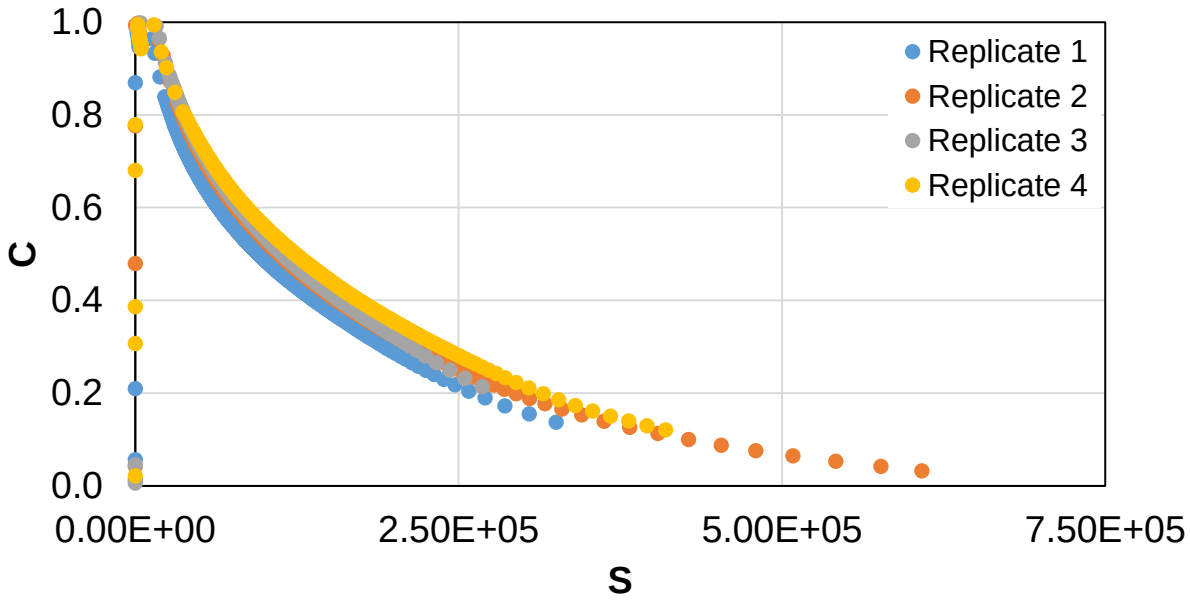

Figure 123: S-VECD Fatigue Damage Characteristic Curves for 5 Hours Virgin Silo Storage Individual Replicates

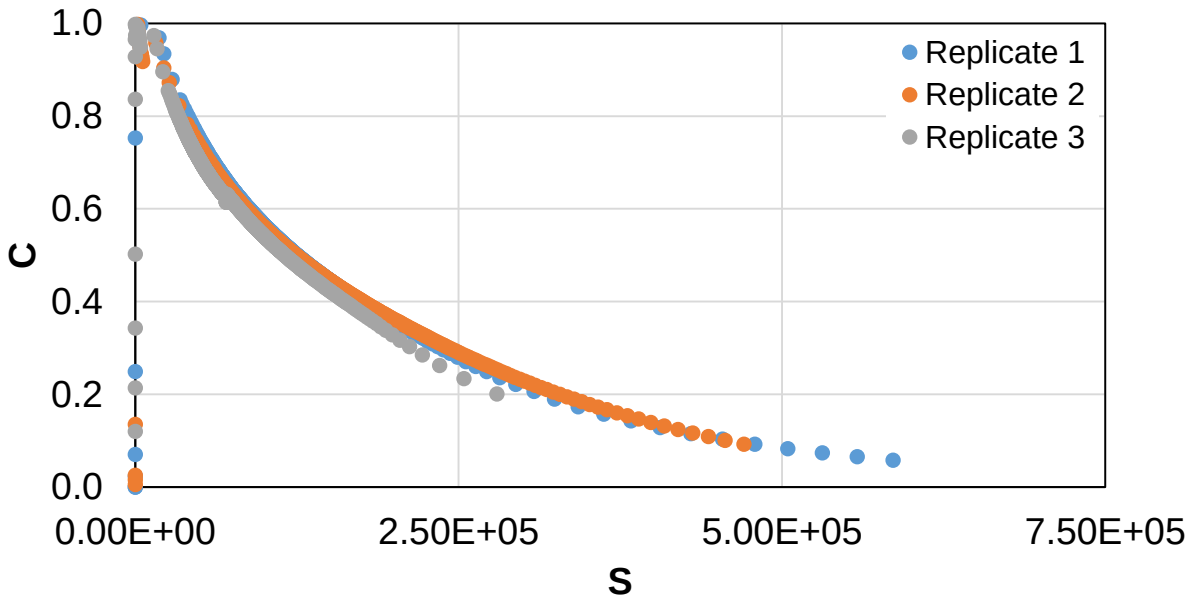

Figure 124: S-VECD Fatigue Damage Characteristic Curves for 7.5 Hours Virgin Silo Storage Individual Replicates

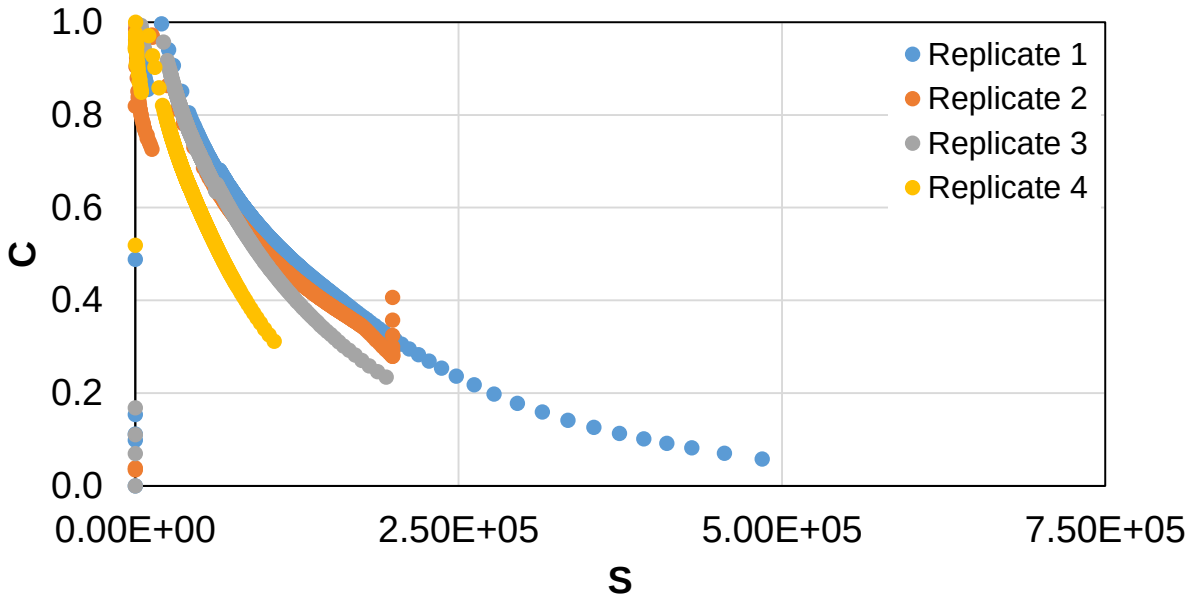

Figure 125: S-VECD Fatigue Damage Characteristic Curves for Virgin, PG 58-28 Field Core Individual Replicates

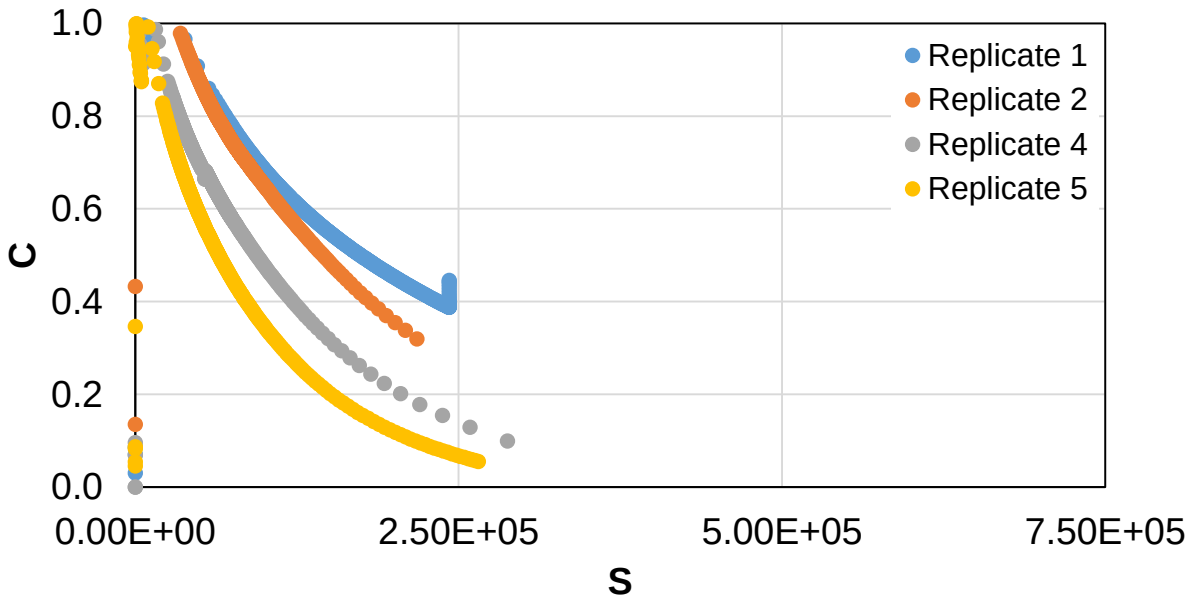

Figure 126: S-VECD Fatigue Damage Characteristic Curves for 15% RAP, PG 58-28 Field Core Individual Replicates

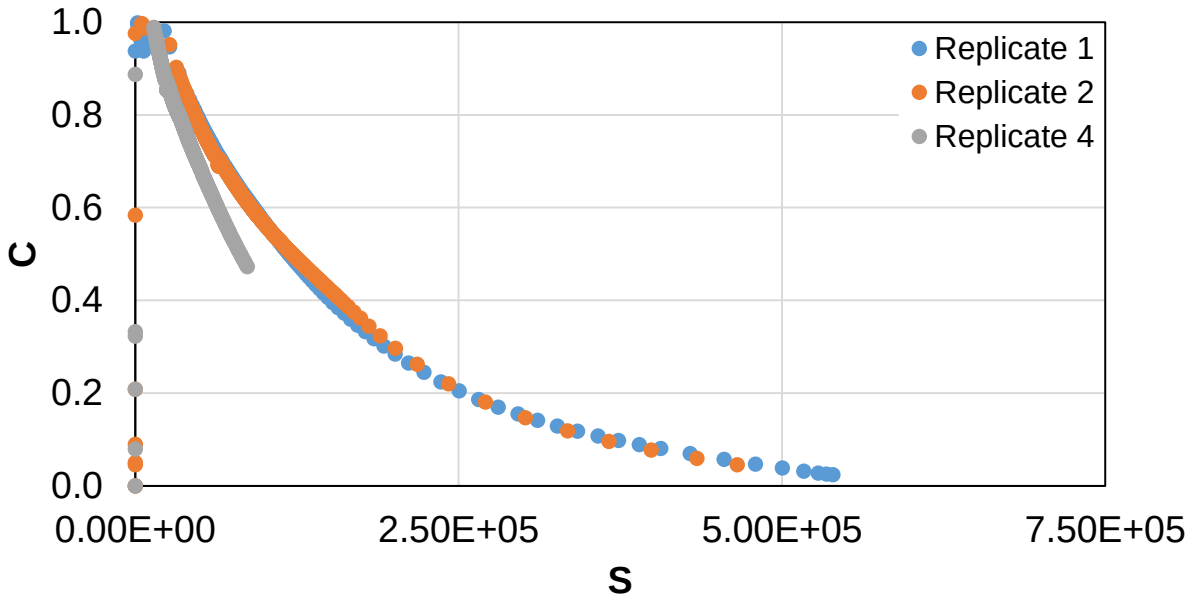

Figure 127: S-VECD Fatigue Damage Characteristic Curves for 25% RAP, PG 58-28 Field Core Individual Replicates

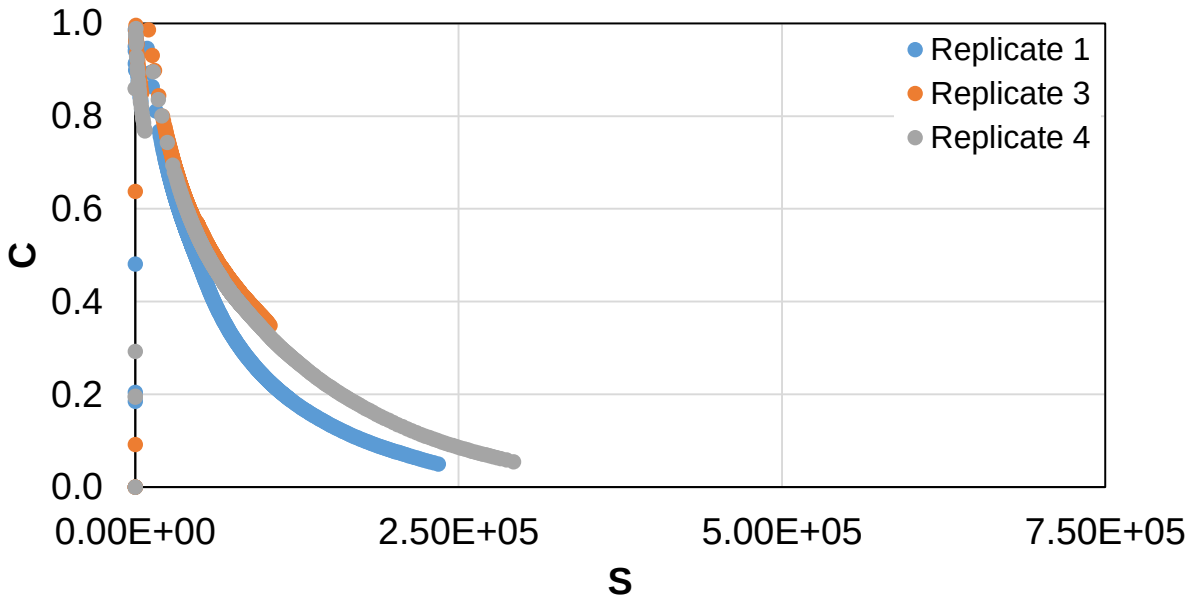

Figure 128: S-VECD Fatigue Damage Characteristic Curves for 25% RAP, PG 52-34 Field Core Individual Replicates

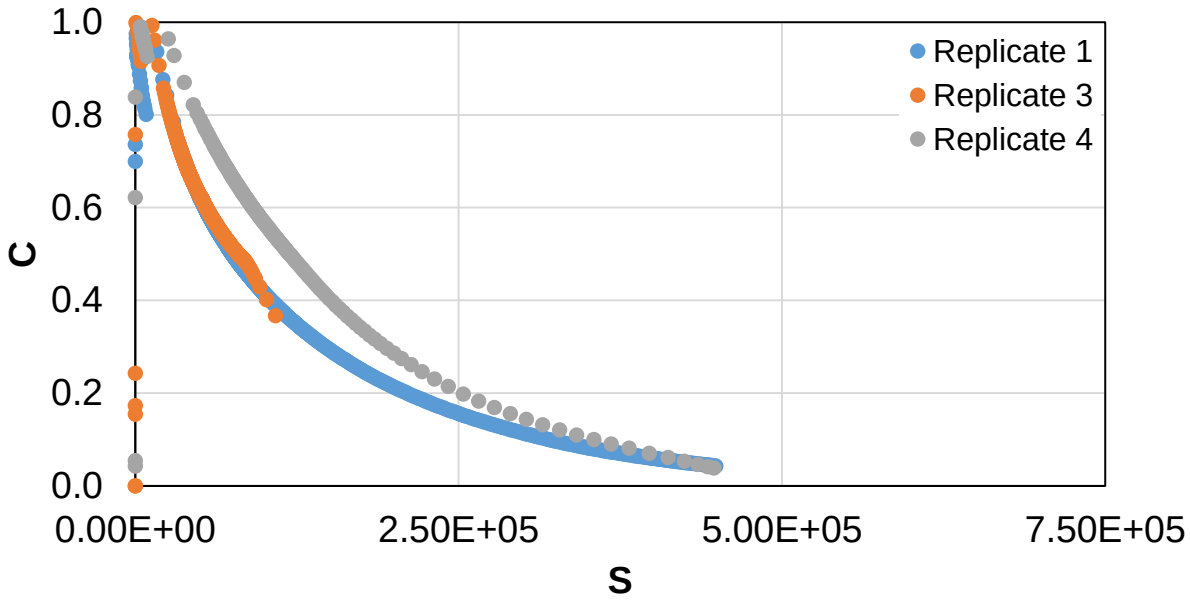

Figure 129: S-VECD Fatigue Damage Characteristic Curves for 30% RAP, PG 52-34 Field Core Individual Replicates

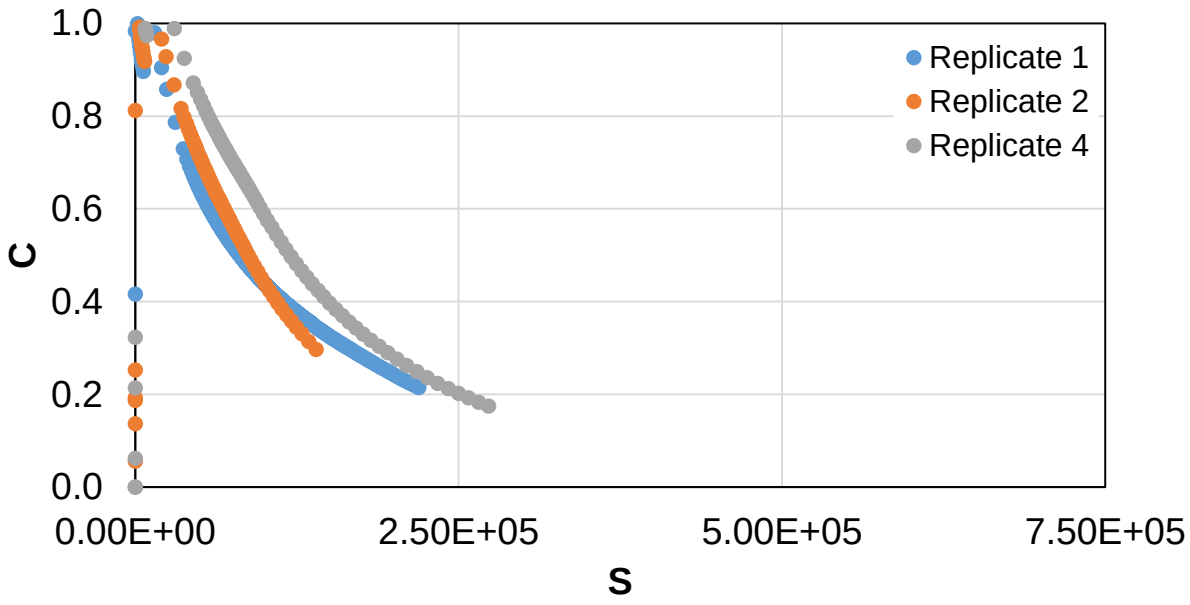

Figure 130: S-VECD Fatigue Damage Characteristic Curves for 40% RAP, PG 52-34 Field Core Individual Replicates

B.9 LVECD Contours

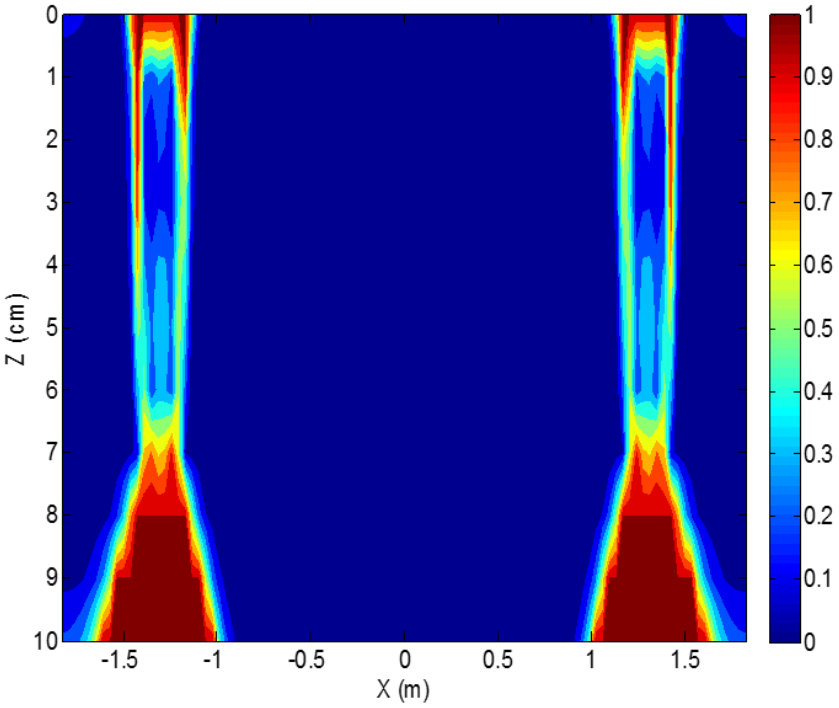

Figure 131: LVECD Damage Contours in Boston, MA Climate for 0 Hours Virgin Silo Storage Mixture

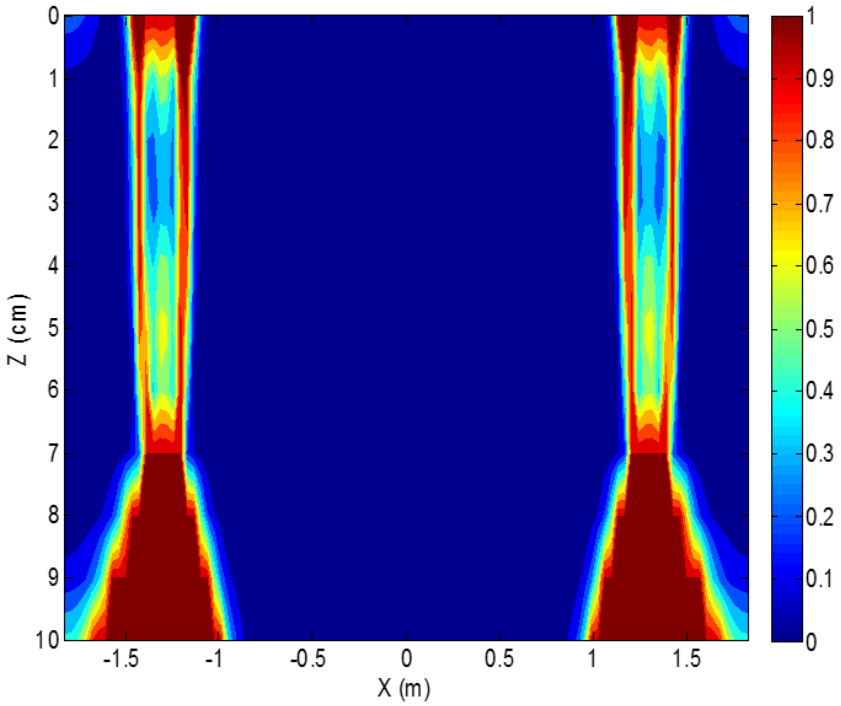

Figure 132: LVECD Damage Contours in Boston, MA Climate for 2.5 Hours Virgin Silo Storage Mixture

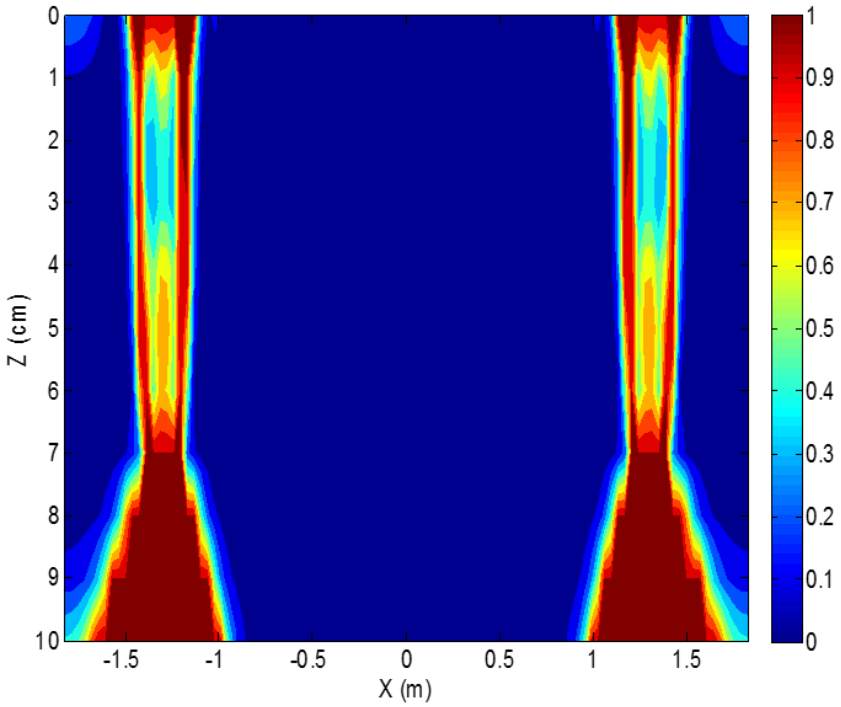

Figure 133: LVECD Damage Contours in Boston, MA Climate for 5 Hours Virgin Silo Storage Mixture

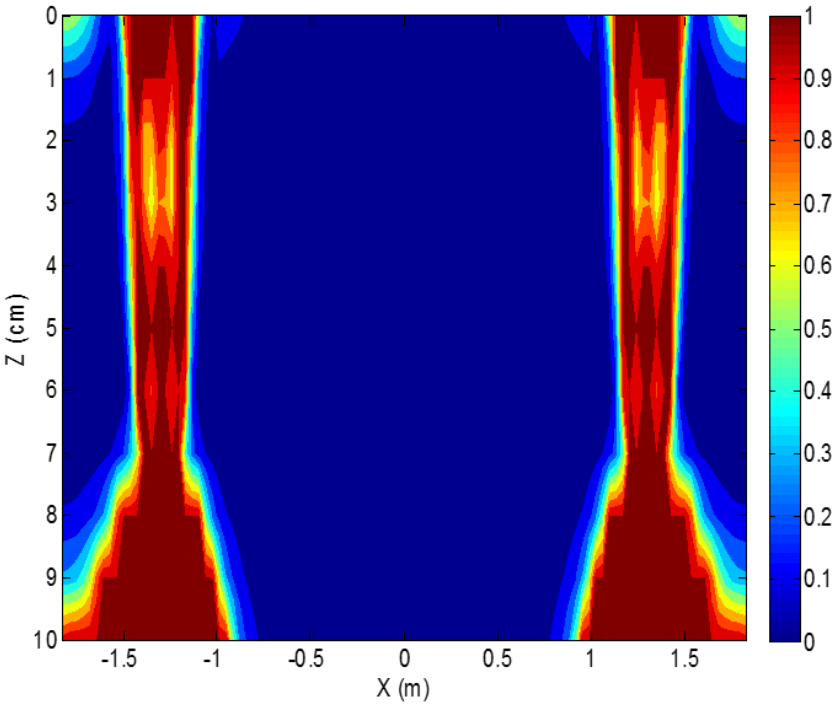

Figure 134: LVECD Damage Contours in Boston, MA Climate for 7.5 Hours Virgin Silo Storage Mixture

APPENDIX C: "EFFECT OF SILO STORAGE TIME ON THE CHARACTERISTICS OF VIRGIN AND RAP ASPHALT MIXTURES" BY JACQUES ET AL.

EFFECT OF SILO STORAGE TIME ON THE CHARACTERISTICS OF VIRGIN AND RAP ASPHALT MIXTURES

Christopher Jacques
Graduate Research Assistant, University of New Hampshire
W183 Kingsbury Hall, Durham, NH 03824
Tel: 207-240-0177; Email: cds43@wildcats.unh.edu

Jo Sias Daniel, Ph.D., Corresponding Author
Professor, University of New Hampshire
Tel: 603-862-3277; Fax: 603-862-2364; Email: jo.daniel@unh.edu

Thomas Bennert, Ph.D.
Research Professor, Rutgers University
Center for Advanced Infrastructure and Transportation (CAIT)
100 Brett Road, Piscataway, NJ 08854
Tel: 609-213-3312; Fax: 848-445-0577; Email: bennert@rci.rutgers.edu

Gerald Reinke
President, MTE Services, Inc.
915 Commercial Ct., Onalaska, WI 54650
Tel: 608-779-6304; Fax: 608-781-4694; Email: gerald.reinke@mteservices.com

AmirHossein Norouzi
Graduate Research Assistant, Ph.D. Candidate, North Carolina State University
Tel: 919-607-8467; Email: anorouz2@ncsu.edu

Christopher Ericson, M.S.
Research Engineer, Rutgers University
Center for Advanced Infrastructure and Transportation (CAIT)
Tel: 848-445-0579; Fax: 848-445-0577; Email: cericson@gmail.com

Walaa Mogawer, Ph.D., P.E., F. ASCE
Director, Highway Sustainability Research Center, University of Massachusetts
151 Martine Street - Room 131, Fall River, MA 02723
Tel: 508-910-9824; Fax: 508-999-9120; Email: wmogawer@umassd.edu

Y. Richard Kim, Ph.D., P.E., F. ASCE
Distinguished University Professor, North Carolina State University
Campus Box 7908, Raleigh, NC 27695
Tel: 919-515-7758; Fax: 919-515-7908; Email: kim@ncsu.edu

Word Count: 7,458 (5,708 words for text, 1 table, and 6 figures)

Submission Date: November 15, 2015

ABSTRACT
Many hot mix asphalt plants store material in heated silos before they are ready to be transported to construction sites. The time that material is stored in the silo is not controlled and is widely variable, depending on several factors. As the material is exposed to elevated temperatures, short-term aging of the binder may occur. Another important consideration is the interaction between reclaimed asphalt pavement (RAP) and virgin binders, as blending or diffusion could occur between the binders. In this study, a virgin and 25% RAP mixture were sampled at incremental silo storage times up to 10 hours. Characterization testing included performance grading, rheological indices, Glover-Rowe parameter evaluation, and Rolling Thin-Film Oven (RTFO) aging on the binders; and complex modulus, simplified viscoelastic continuum damage model (S-VECD) for fatigue, and thermal stress restrained specimen testing of the mixtures. Simulations using the layered viscoelastic critical distresses pavement analysis to predict fatigue behavior from the S-VECD model, is utilized to show the potential effects silo storage time has on pavement life. Results from all tests indicated that mixtures age with an increase in silo storage time. RAP materials experienced a greater effect, which may be a function of the air void content or indication of blending/diffusion in the silo. RTFO aging showed that current laboratory conditioning methods do not necessarily simulate asphalt plant production. It was apparent that production parameters, such as silo storage time, have a significant impact on mixture performance.

Keywords: Silo storage, asphalt mixtures, reclaimed asphalt pavement, short-term aging, cracking

INTRODUCTION

At many hot mix asphalt (HMA) plants, the loose asphalt mixture is stored in silos before trucks are ready to transport it to the construction site. The asphalt materials are stored at or near mixing temperature and some silos are heated to help maintain workability of the mixture. As the material is exposed to elevated temperatures, additional aging of the asphalt binder may occur. Aging causes the asphalt binder to become stiffer and more brittle, which will affect its service performance. The length of storage time in the silos could therefore have a significant effect. Storage time is typically not controlled or recorded and can vary widely based on construction region, silo type, mix size, and truck schedules. It is important to gain a better understanding of the impact of mixture production parameters on the performance of the mixture in the field.

The use of reclaimed asphalt pavement (RAP) in mixtures is common practice due to its economic and environmental benefits. While most agencies are comfortable using 15-20% of RAP in mixtures, there is a desire to use higher percentages. Sabouri et al. (*1*) showed that higher percentages of RAP were tolerable with increased asphalt layer thicknesses. It was demonstrated that fatigue resistance deteriorated in all cases where rutting resistance improved, but a balance could be obtained that produced an economical and well-performing mixture. Daniel et al. (*2*) showed that the stiffening of RAP mixtures occurs at a much slower rate than virgin mixtures, likely because of the presence of already-aged binder. The fatigue performance showed widely varying results under stress and strain-controlled evaluations. This highlights the importance of integrating mixture and pavement design, as mixtures can perform differently depending on their location within a pavement structure.

It is important to understand the effect of silo storage on both virgin mixtures and those including RAP. At elevated temperatures, the interaction of the RAP and virgin binders needs to be considered. Several recent studies have attempted to characterize the interaction that occurs between virgin and RAP binders, which is a complex chemical process. Huang et al. (*3*) suggests that mechanical blending affects only a small portion of the aged RAP binder and instead forms a stiffer composite layer system. The two major processes that occur in the virgin-RAP binder interaction are mixing, or contact between the binders, and blending/diffusion after contact (*4*). The key mechanism is the diffusion process. Kriz et al. (*4*) conducted dynamic shear rheometer (DSR) simulations to understand the diffusion process and degree of blending in thick and thin binder layers. It was concluded that the diffusion process is completed (100% blending) within minutes of mixing for thinner binder layers, and only about 90% degree of blending completed after typical production stages for thicker binder layers. The degree of blending was analyzed using typical mixing, storage, transportation, and placement times. In this study, it is interesting to note that the assumed storage time was 60 minutes and that the majority of blending in thick binder layers occurred during the storage stage. As the storage time continues past one hour, it is hypothesized that the diffusion or blending could continue between the binders and that this phenomenon may have an appreciable impact on mixture performance. The storage time could have an effect on the short-term aging of the overall mixture and/or an effect on the blending between RAP and virgin binders.

Zhao et al. (*5*) also conducted research into blending between RAP and virgin binder, questioning the full mobilization assumption. The binder mobilization rate was found to be close to 100% for 10-20% RAP mixtures and approximately 75% for 25% RAP, which suggests that the 25% RAP binder could potentially mobilize further during longer silo storage times. In the study by Zhao et al., it was concluded that HMA containing higher amounts of RAP may affect the cracking resistance due not only to increased stiffness from the RAP materials, but also from

an under-asphalted mixture or heterogeneous blending from the lower mobilization rate. An under-asphalted mixture could result in a pavement structure more prone to cracking (*6*).

Other studies utilized Bonaquist's approach of comparing the overlap of measured dynamic modulus master curves with those predicted from recovered binder testing to assess binder blending (*7, 8*). The main conclusions were that plant production practices, which are commonly ignored in their relation to mixture performance, will have an impact on mixture performance, and different contractors achieved various degrees of blending, including poor blending. Rad et al. (*9*) also suggests that the temperature of conditioning be controlled in the production stage to achieve full blending of the binders. It is also important to note that different virgin and RAP binders will cause different interactions among each other and varying stiffening effects can occur (*10*).

Another production parameter in the same family as silo storage time is haul distance or haul time. This parameter is also not typically documented or strictly limited, and additional short-term aging or embrittlement could occur during this time that the mix is kept at elevated temperatures. Howard et al. (*11*) investigated haul time effects on HMA and also explored using warm-mix technologies to facilitate long haul distances. They found no significant changes in binder properties for haul distances up to 8 hours. It appeared that continuous binder grades became warmer with longer haul times, but these increases were considered comparable with normal HMA production and placement.

Production parameters, such as silo storage time and haul time, among others, are important to consider. Mix designers do not have control over these parameters, and the potential effects on mixture performance are not taken into account. The objective of this paper is to gain a better understanding of the effect of silo storage time, a key production parameter, as it relates to asphalt binder and mixture performance. Silo storage time is evaluated for virgin and RAP mixtures to measure the short-term aging effect and determine if blending/diffusion occurs in the silo with the RAP mixture.

MATERIALS AND METHODS

Mixture Information

A virgin mixture and 25% RAP mixture with 12.5 mm nominal maximum aggregate size were evaluated in this study at incremental silo storage times. The virgin mixture used a PG 64-22 binder and included material sampled after silo storage times of 0, 2.5, 5, and 7.5 hours after production began. The 25% (by total mass) RAP mixture used a PG 64-22 binder and was sampled at 0, 2.5, 5, 7.5, and 10 hours. The RAP mixture was used for an active paving job and the material was sampled at the different times during production; therefore, the reported storage times are approximate. Specimens were produced by immediately compacting loose mix sampled from the plant without reheating the material. The target asphalt content of the mixtures was 5.4%. Mixture discharge temperatures were approximately 175°C, which is not unusual during shoulder seasons in the Northeast.

Binder Testing and Analysis

The asphalt binders were extracted and recovered from loose mix sampled from the asphalt plant in accordance with AASHTO T164 using tri-chlorethylene as the solvent. After the recovery process, the asphalt binder was tested for the respective high temperature PG grade, in accordance with AASHTO M320. The recovered asphalt binder was treated as an RTFO-aged

(Rolling Thin Film Oven) asphalt binder. Virgin binder was also conditioned in the RTFO at five conditioning times (45, 85, 135, 170, and 300 minutes) to evaluate how well RTFO aging simulated the plant production and storage time associated with the virgin mixture in this study.

Master stiffness curves for the recovered binders were generated using the dynamic shear rheometer results at varying temperatures (95, 80, 70, 60, 45, 35, 25, 15, 5, -5 and -15°C) and loading frequencies within a strain range of 0.005 to 0.02. Data quality checks and analysis were conducted using the software package RHEA™.

Anderson et al. (*12*) identified the difference between the bending beam rheometer (BBR) stiffness (S) and m-slope critical low temperature as a means of indexing the non-load associated cracking potential of asphalt binders. Asphalt binders that exhibit a greater difference between the S and m-slope low temperature have been recognized as being prone to non-load associated cracking. The parameter, defined as ΔT_{cr}, is shown in Equation 1:

$$\Delta T_{cr} = T_{cr(Stiffness)} - T_{cr(m-slope)} \quad (1)$$

where,

ΔT_{cr} = Difference in critical low temperature PG grade

$T_{cr\ (Stiffness)}$ = Critical low temperature grade predicted using the BBR Stiffness (S)

$T_{cr\ (m\text{-}slope)}$ = Critical low temperature grade predicted using the BBR m-slope

In Equation 1, as the ΔT_{cr} decreases, the asphalt binder is considered to be more prone to non-load associated cracking. Initially, Anderson et al. (*12*) set a limit of $\Delta T_{cr} \leq -2.5$°C for when there is an identifiable risk of cracking and preventative action should be considered. Rowe (*13*) recommended that at a $\Delta T_{cr} \leq -5$ºC immediate remediation should be considered.

Glover et al. (*14*) proposed the rheological parameter, G'/(η'/ G'), as an indicator of ductility based on a derivation of a mechanical analog to represent the ductility test consisting of springs and dashpots. Rowe (*13*) re-defined the Glover parameter in terms of |G*| and δ based on analysis of a Black Space diagram and suggested use of the parameter $|G^*|\cdot(\cos\delta)^2/\sin\delta$, termed the Glover-Rowe (G-R) parameter, in place of the original Glover parameter.

Rowe proposed measuring the G-R parameter based on construction of a master curve from frequency sweep testing at 5°C, 15°C, and 25°C in the DSR and interpolating to find the value of G-R at 15°C and 0.005 rad/sec to assess binder brittleness (*15*). A higher G-R value indicates increased brittleness. It has been proposed that a G-R parameter value of 180 kPa corresponds to damage onset whereas a G-R value exceeding 450 kPa corresponds to significant cracking based on a study relating binder ductility to field block cracking and surface raveling by Anderson et al. (*12*). The test results generated during the master stiffness curve analysis was utilized to determine the G-R parameter.

The Christensen-Anderson-Marasteanu Model (CAM) master curve parameters (ω_o, R, and T_d) have specific physical significance. As crossover frequency, ω_o, increases, the hardness of the binder decreases, which indicates lower degrees of aging. The rheological index, R-value, is defined as the difference between the log of the glassy modulus and the log of the dynamic modulus at the crossover frequency. As R-value increases, the master curve becomes flatter indicating a more gradual transition from elastic behavior to steady-state flow. Normally, R-value is higher for oxidized/aged asphalt (*16*). Mogawer et al. (*17*) demonstrated that by plotting the crossover frequency vs. R-value, the relative change in aging, or rejuvenating, can be tracked.

Therefore, the use of the crossover frequency – R-value space can allow for an evaluation of aging occurring due to silo storage time.

Mixture Testing and Analysis

Dynamic Modulus

The Asphalt Mixture Performance Tester (AMPT) was used to perform dynamic modulus testing in unconfined uniaxial compression. Three replicate specimens were tested for each condition. These specimens were tested at target temperatures of 4.4°C, 21.1°C, and 37.8°C and standard frequencies of 25, 10, 5, 1, 0.5, and 0.1 Hz. The dimensions of the tested specimens were 100 mm in diameter by 150 mm tall with a 70 mm gauge length. Load levels were determined so that the resulting strain amplitudes were between 35 and 75 microstrain. Data was obtained from the final six cycles of each loading series.

The average dynamic modulus isotherms were shifted to a generalized logistic function (Equation 2) to construct the master curve at a reference temperature of 21.1°C. The time-temperature shift factors were allowed to free-shift, meaning no underlying shape of the shift factor versus temperature curve was assumed.

$$\log|E^*| = \delta + \frac{\alpha}{[1+\lambda(\exp^{\beta+\gamma(\log\omega_r)})]^{1/\lambda}} \quad (2)$$

where,

$|E^*|$ = Dynamic Modulus
ω_r = reduced frequency
$\alpha, \beta, \gamma, \delta, \lambda$ = fitting parameters

S-VECD Fatigue Cracking

Fatigue testing was performed in uniaxial tension on the AMPT. Specimens were cut to dimensions of 100 mm in diameter by 130 mm tall and glued to end platens that were fixed in the AMPT. Air void content, determined by AASHTO T166, was 7.0±0.5%. Testing was performed at 20.0°C and 10 Hz. The virgin mixtures were tested with four replicate specimens (three for 7.5 hours) at varying microstrain levels ranging from 300 to 450 microstrain to cover a range of numbers of cycles to failure. Fatigue testing was not performed on the 25% RAP mixtures due to a lack of available specimens.

Analysis on the fatigue results was performed using the simplified viscoelastic continuum damage (S-VECD) model developed by Underwood et al. (*18*). S-VECD is a mode-of-loading independent, mechanistic model that allows the prediction of fatigue cracking performance under various stress/strain amplitudes at different temperatures from only a few tests. The S-VECD model is composed of two material properties, the damage characteristic curve and the energy-based failure criterion. The damage characteristic curve defines how fatigue damage evolves in a mixture and is developed by plotting two calculated parameters at each loading cycle, the secant pseudo-stiffness (C) and the damage parameter (S). The exponential form shown in Equation 3 was used to fit the damage characteristic curves.

$$C = e^{aS^b} \quad (3)$$

where,

a, b = Damage model coefficients

The S-VECD fatigue failure criterion, called the G^R method, involves the released pseudo strain energy. This concept focuses on the dissipated energy that is related to energy release from damage evolution only and is fully compatible and predictable using the S-VECD model. The G^R characterizes the overall rate of damage accumulation during fatigue testing. A characteristic relationship, which is found to exist in both RAP and non-RAP mixtures, can be derived between the rate of change of the averaged released pseudo strain energy during fatigue testing (G^R) and the final fatigue life or number of cycles to failure (N_f). The equation to calculate G^R is as follows:

$$G^R = \frac{\frac{1}{2}\int_0^{N_f} \left(\varepsilon^R{}_{0,ta}\right)_i^2 (1-F_i)}{N_f{}^2} \quad (4)$$

where,

$(\varepsilon^R{}_{0,ta})_i$ = pseudo strain amplitude at cycle *i*
F_i = pseudo stiffness at cycle *i*

Pavement Fatigue Life Evaluation

The layered viscoelastic critical distresses (LVECD) program was used to predict the long-term fatigue performance of pavements under traffic loading. Eslaminia et al. (*19*) developed the layered viscoelastic structural program with the material level continuum damage model to calculate the required stresses and strains for the fatigue behavior prediction using three-dimensional viscoelastic calculations under moving loads. The LVECD simulations were performed for both thin and thick pavement structures using the required parameters including design time, structural layout, traffic, and climate. The thin pavement structure had an asphalt layer of 100 mm and aggregate base of 200 mm; the thick pavement had an asphalt layer of 300 mm with the same base. The aggregate base and the subgrade were modeled using the linear elastic properties with the modulus values of 350 MPa and 100 MPa, respectively.

Two climates were evaluated: Boston, Massachusetts and Raleigh, North Carolina using pavement temperatures obtained from the Enhanced Integrated Climate Model (EICM). Also, a single tire with the standard loading of 80 kN at the center of pavement was utilized. The average annual daily truck traffic (AADTT) was assumed to be 2,000.

For fatigue cracking resistance evaluation, LVECD calculates the damage growth and the damage factor based on Miner's law (Equation 5). If the damage factor is equal to zero, the element does not experience any damage, while a damage factor of one indicates total failure of the element.

$$\sum_{i=1}^{T} D_i = \frac{N_i}{N_{fi}} \quad (5)$$

where,

D = damage
T = total number of periods
N_i = traffic for period *i*
N_{fi} = allowable failure repetitions under the conditions that prevail in period *i*

TSRST

In order to assess the low temperature cracking susceptibility, each mixture was tested in the Thermal Stress Restrained Specimen Test (TSRST) device in accordance with AASHTO TP10-93. TSRST testing was performed on loose mixture that was reheated in the laboratory. Three replicate gyratory specimens 150 mm in diameter by 185 mm tall were fabricated for the virgin and RAP mixtures. Specimens were then cored and cut to 54 mm in diameter by 160 mm tall. The air voids of the final cut specimens were 6.5±1.0%.

RESULTS AND DISCUSSION

Binder Testing

Performance Grading

The general trend in PG grade results (Table 1) shows an increase in high temperature PG grade of 0.39°C/hr and 0.53°C/hr of silo storage time for the binder extracted and recovered from the virgin and RAP mixes, respectively. An increase in intermediate temperature PG grade of 0.20°C/hr was observed for the virgin mix while the RAP mix had no measurable trend. The low temperature PG grade increased 0.14°C/hr and 0.21°C/hr for virgin and RAP mixtures, respectively, with the low temperature grade being m-slope dependent for both. The results also show a general trend of the BBR ΔT_{cr} remaining relatively constant and then negatively increasing (i.e. greater difference between S and m-slope critical low temperature) after 5 hours of storage time. The recovered binder from the virgin mixture consistently has a smaller ΔT_{cr} than the 25% RAP mixture, indicating that the virgin asphalt binder has undergone less aging.

TABLE 1 Performance grade results for extracted/recovered asphalt binders.

Virgin Mix										
Silo Storage Time (Hrs)	Performance Grade (^{o}C)					Rheological Indices				
	High Temp (RTFO)	Intermediate Temp	Low Temperature			R-value	Crossover Fequency	Glover-Rowe Analysis (15° C, 0.005 rad/s)		
			Stiffness (S)	m-slope	BBR ΔT_{crit}			G* (Pa)	δ (degrees)	G-R (kPa)
0 Hrs	72.1	22.7	-25.1	-24.8	-0.3	1.732	149.1	8.78E+04	71.1	9.8
2.5 Hrs	73.8	23.3	-25.0	-24.6	-0.4	1.808	123.4	9.84E+04	69.8	12.5
5 Hrs	73.4	24.1	-24.9	-24.7	-0.2	1.784	105.5	1.22E+05	69.5	16.0
7.5 Hrs	75.5	24.1	-25.1	-23.6	-1.5	1.866	101.2	1.43E+05	68.9	19.8

25% RAP Mix										
Silo Storage Time (Hrs)	Performance Grade (^{o}C)					Rheological Indices				
	High Temp (RTFO)	Intermediate Temp	Low Temperature			R-value	Crossover Fequency	Glover-Rowe Analysis (15° C, 0.005 rad/s)		
			Stiffness (S)	m-slope	BBR ΔT_{crit}			G* (Pa)	δ (degrees)	G-R (kPa)
0 Hrs	73.9	24.6	-25.9	-24.9	-1.0	1.977	100.2	1.83E+05	66.8	31.0
2.5 Hrs	76.2	22.6	-25.4	-22.8	-2.6	2.002	74.2	2.20E+05	65.8	40.7
5 Hrs	77.9	24.5	-24.9	-23.4	-1.5	2.094	43.5	3.19E+05	63.6	70.2
7.5 Hrs	77.3	23.6	-25.2	-22.7	-2.5	2.070	52.6	2.77E+05	64.3	58.0
10 Hrs	80.0	24.1	-24.8	-22.3	-2.5	2.150	29.0	3.78E+05	62.2	93.1

Glover-Rowe Parameter and Rheological Indices

The Glover-Rowe Parameter analysis, shown in Figure 1(a), illustrates that as silo storage time increases, the extracted asphalt binder becomes more aged and migrates to areas where potential, non-load associated cracking is a concern. The results also show that the 25% RAP mixture initiates and moves closer to the threshold values than the asphalt binder from the virgin mixture. The measured crossover frequency and R-value shown in Figure 1(b) clearly indicates that a change in the CAM rheological indices occurs due to longer silo storage times, indicating that aging is occurring over time. The binder extracted from the RAP mixture shows larger changes than the extracted virgin binder.

The results of the RTFO aging for various times are also shown in Figure 1. These results indicate that using the specified time of 85 minutes in the RTFO does not simulate the aging that occurred during plant production and silo storage for the virgin mixtures. In fact, it can be seen that RTFO conditioning does not show similar stiffness (G* and δ) and CAM rheological indices to 0 hours of silo storage time until approximately 170 minutes, which is twice the amount specified in AASHTO T240. This clearly indicates that current laboratory conditioning methods do not necessarily simulate asphalt plant production. The large differences in this case are likely a result of the relatively high (175°C) production temperatures that would have aged the asphalt binder, especially under extended silo storage times.

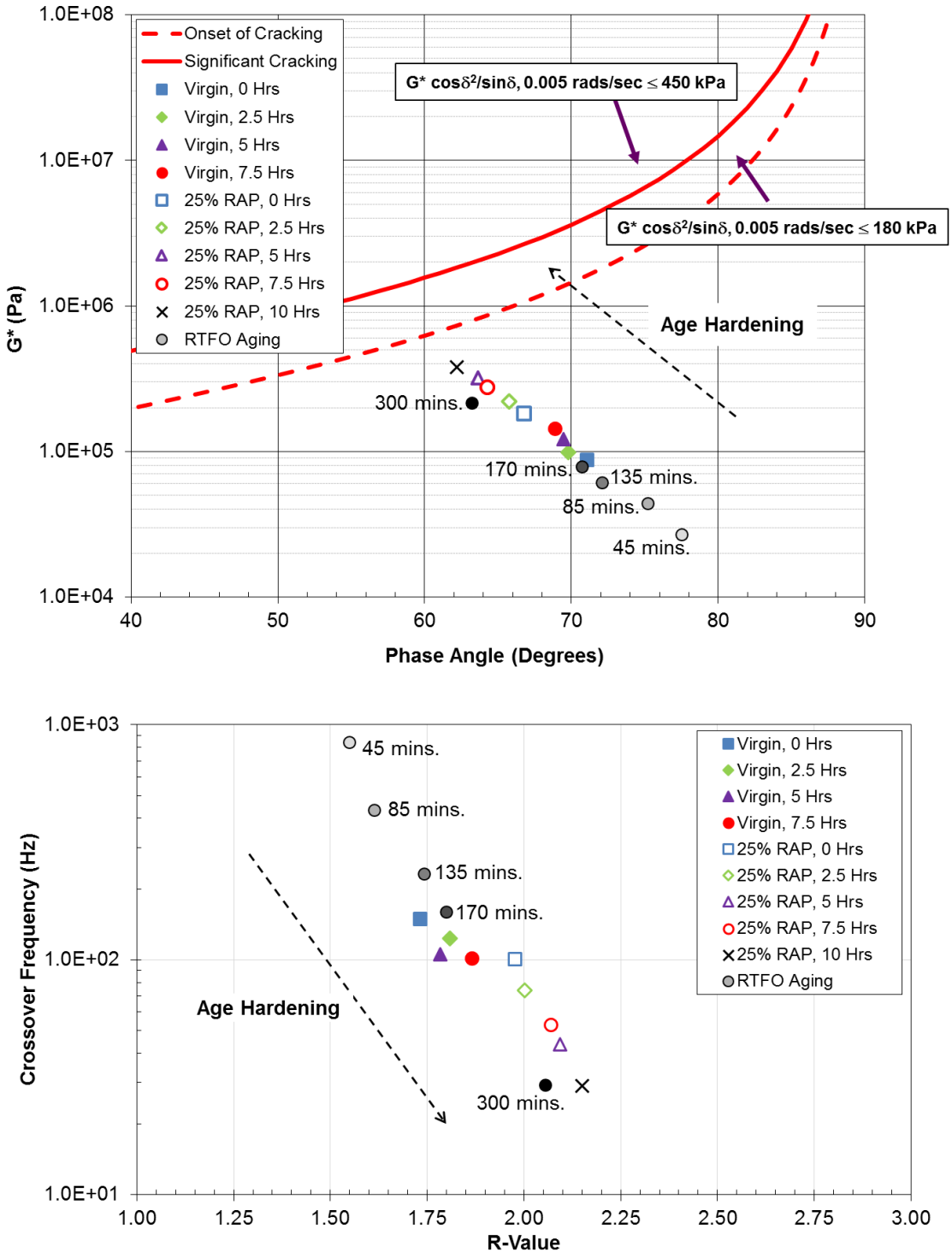

FIGURE 1 Effect of silo storage time and RTFO conditioning on retained asphalt binder: a) Black Space plot and b) Crossover frequency – R-value space.

Mixture Testing

Dynamic Modulus

Dynamic modulus master curves were constructed for varying silo storage times as shown in Figure 2(a) and (b) for the virgin and 25% RAP mixtures, respectively. Average air void content of the test specimens, determined in accordance with AASHTO T166, is also shown. Each master curve represents the fitted sigmoidal function from the average of three replicate specimens. Both the virgin and RAP mixtures show an increase in dynamic modulus as the mixtures remain in the silo for longer periods. The RAP mixture shows greater increases with storage time than the virgin mixtures.

Figure 2(c) and (d) shows Black Space plots for the virgin and RAP mixtures. In Black Space, lower phase angles at similar modulus values indicate that the mixture may be more prone to cracking. At higher stiffness values, the silo storage time has little effect on the phase angle for both mixtures. At lower stiffness values and near the inflection point, there is a decrease in phase angle with longer storage times. The virgin mixture shows larger differences near the inflection point and the RAP mixture shows larger differences at the low stiffness values.

A statistical analysis was also conducted on the raw data using independent sample t-tests with a confidence interval of 95%. Statistically, the 0, 2.5, and 5 hours mixtures are all similar for the virgin material. The 7.5 hours virgin mixture is statistically different from the 0 and 2.5 hours storage times. The RAP mixture at 7.5 and 10 hours shows significant differences from 0 hours. Phase angle results generally show little statistical significance.

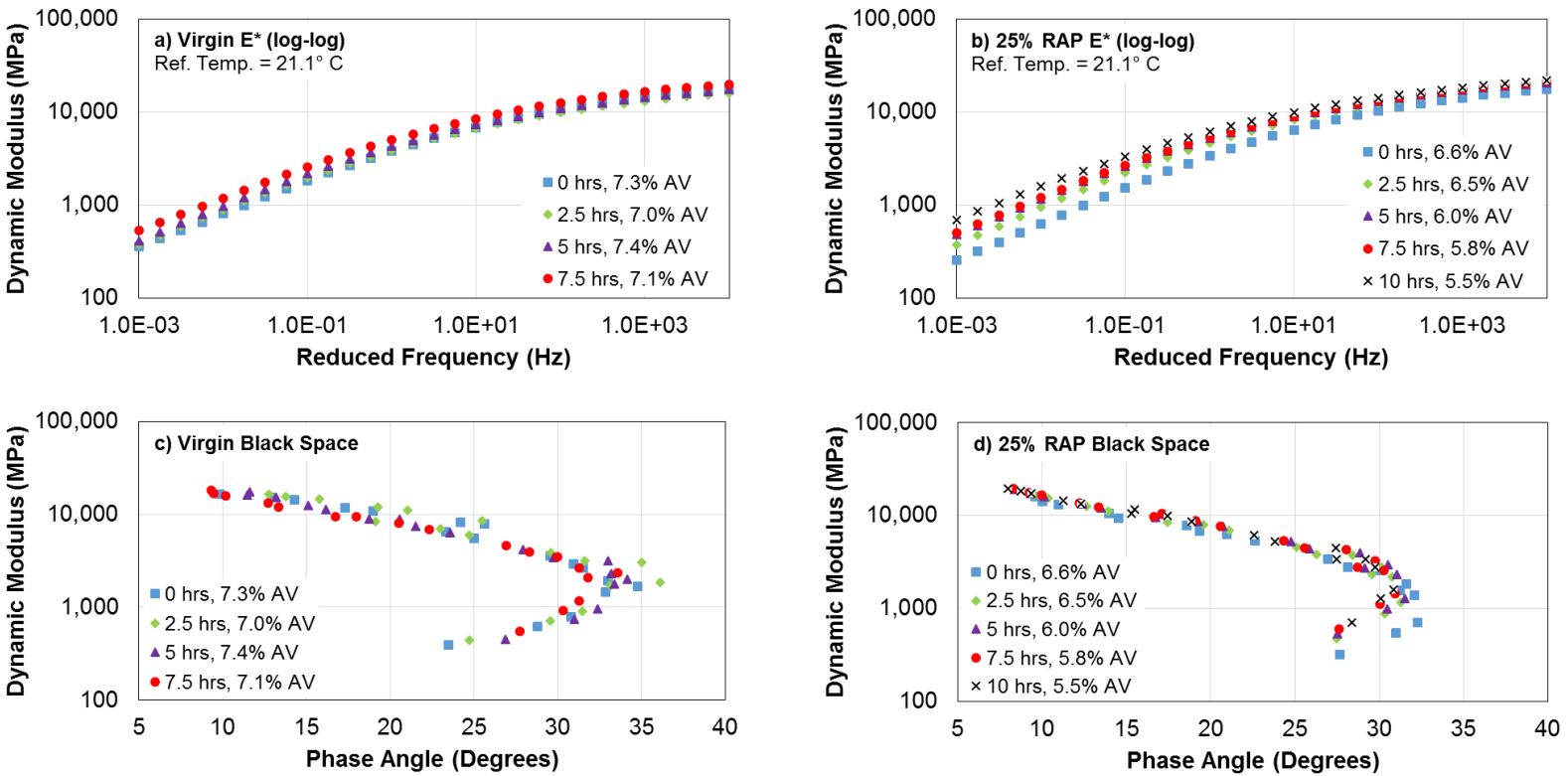

FIGURE 2 Complex modulus testing results: Dynamic modulus master curves (a, b) and Black Space plots (c, d) for virgin and 25% RAP mixtures.

Using the sigmoidal fit master curves, dynamic modulus ratios were calculated comparing each mixture to its respective 0 hours value. Figure 3(a) shows the ratio of dynamic modulus values with respect to the 0 hours master curve across all frequencies. The average of all these values are then summarized in Figure 3(b). The virgin mixtures show a slightly higher ratio in the lower frequencies, and the ratio increases with storage time. On average, the 7.5 hours virgin mixture is approximately 1.3 times stiffer than the 0 hours mixture. Stiffening of the virgin mixtures implies that there is short-term aging or additional binder absorption occurring within the silo, particularly at longer storage times such as 7.5 hours.

The RAP mixtures show higher ratios and larger differences across the frequency range than the virgin mixtures. The RAP mixture at 2.5 hours has a similar ratio to the virgin mixture at 7.5 hours. It is clear that the RAP mixture experiences greater stiffness changes than the virgin mixture as silo storage time increases. This could imply that there is blending or diffusion between RAP and virgin binders in the silo, in addition to short-term aging that is experienced with the virgin mixture. The differences in air void contents could also be contributing to some of the stiffening observed.

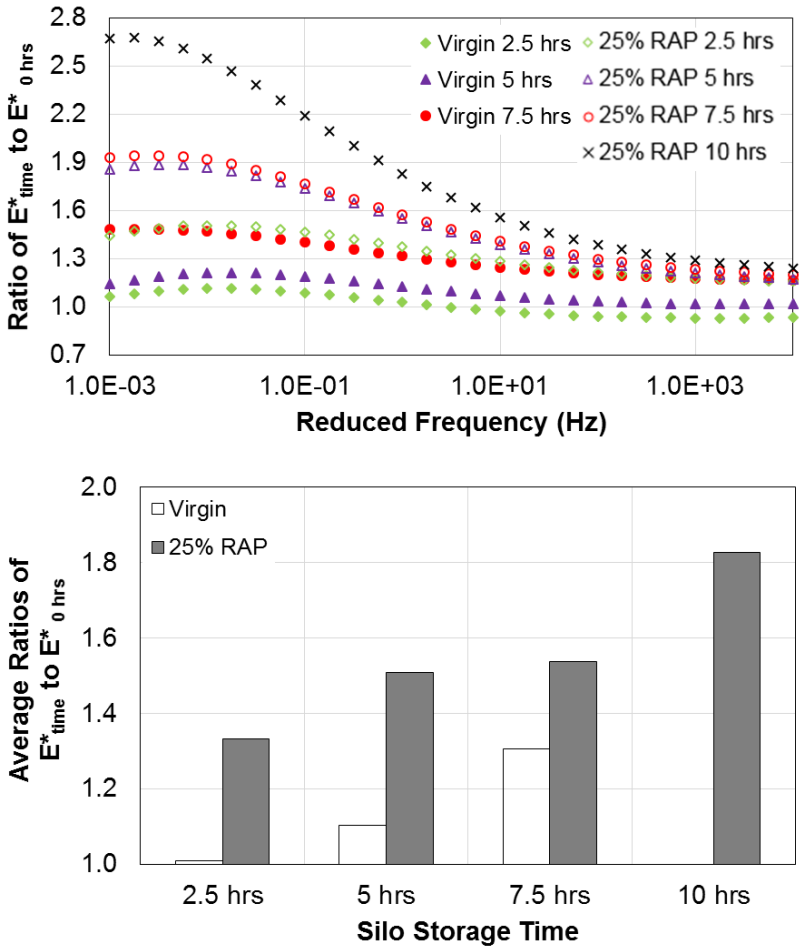

FIGURE 3 Dynamic modulus ratios for a) all frequencies and b) overall average.

S-VECD Fatigue Cracking

The results from the S-VECD testing and analysis on the virgin mixtures are shown in Figure 4. Fatigue data for the 25% RAP mixtures was not available due to lack of materials. For the damage characteristic curves shown in Figure 4 (a), a clear increase in pseudo-stiffness is observed with an increase in silo storage time. Figure 4 (b) shows the relationship between the failure criterion G^R, a parameter that characterizes damage accumulation, and number of cycles to failure, N_f. Typically, mixtures with similar slopes and that are closer to the upper right corner of G^R-N_f space indicate better fatigue resistance. There appears to be little distinction between the mixtures, but it is observed that the 7.5 hours mixture has the largest slope (-1.528) which may indicate more susceptibility to fatigue cracking. It is important to keep in mind that the fatigue performance in the field also depends on the location within the pavement structure and loading conditions.

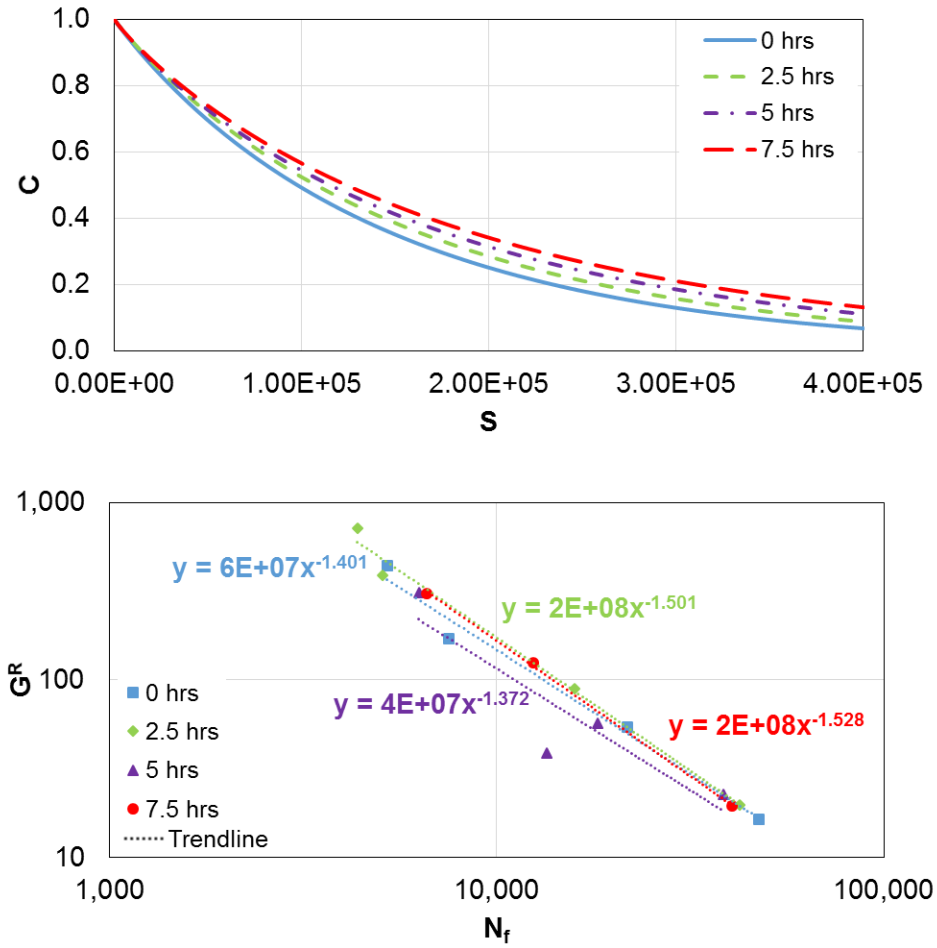

FIGURE 4 S-VECD virgin mixture results: a) damage characteristic curves and b) fatigue failure criterion.

Pavement Fatigue Life Evaluation

Figure 5 presents the results from LVECD analysis for virgin mixtures among two climate conditions for thin and thick pavements. Although LVECD was verified by several researchers (*20, 21*) for various conditions, this software has not been fully calibrated, and the transfer

function to convert the predicted damage obtained from LVECD to cracking area in the field is still under development. Therefore, predictions presented in this paper are for relative comparisons; they use the number of elements that experienced more than 20% damage ($N/N_f > 0.20$) to evaluate the relative effects of silo storage time on the pavement performance. Figure 5 shows that an increase in silo storage time causes increases in fatigue damage for both types of pavements and climates, with increases of approximately 40% from 0 to 7.5 hours storage times for the thin pavements and tripling of the damage for thick pavements (although magnitude of damage in thick pavements is much lower).

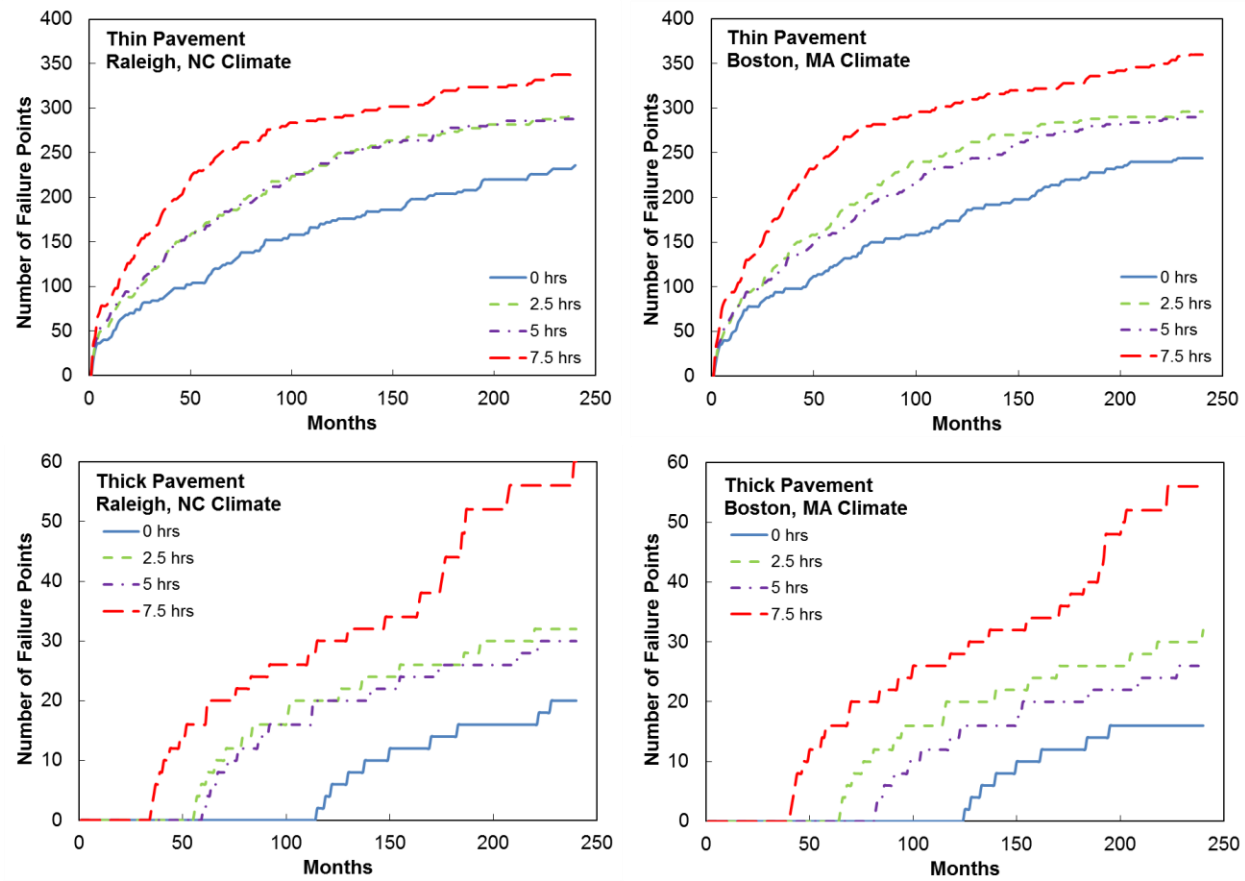

FIGURE 5 Comparison of fatigue resistance for virgin mixture using LVECD thick/thin pavements and two climate conditions.

TSRST

Results from the thermal stress restrained specimen test (TSRST) are shown in Figure 6. Error bars represent one standard deviation from the mean. Warmer critical cracking temperatures from TSRST results can indicate susceptibility to thermal cracking. While most results are within a few degrees of each other, warmer temperatures were observed with statistical significance for the virgin mixture at 5 hours and for the RAP mixture at 7.5 hours.

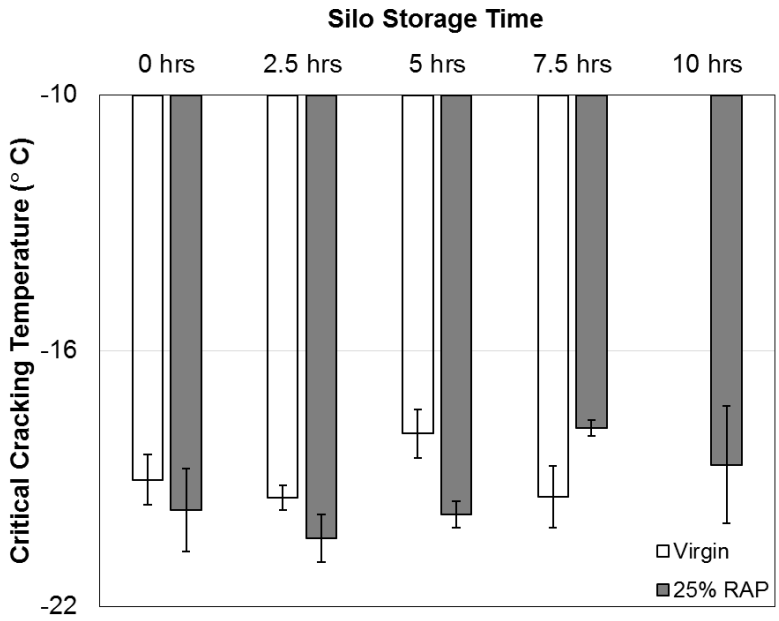

FIGURE 6 Critical cracking temperatures (TSRST) among virgin and RAP mixtures.

SUMMARY AND CONCLUSIONS

In this study, the effect of silo storage time on virgin and RAP mixtures was evaluated. Binders were evaluated using performance grading, rheological indices, and the Glover-Rowe parameter. Mixtures were evaluated with complex modulus, S-VECD fatigue, pavement life evaluation with LVECD, and TSRST. Testing was performed at incremental silo storage times up to 7.5 hours for the virgin mixture and 10 hours for the 25% RAP mixture. The following observations were made based on the results and analysis:

- Binder results showed an increase in both high and low grades with longer silo storage times. Larger increases were observed for the high temperatures and in the RAP mixtures. ΔT_{cr} analysis showed that the binders became more m-controlled as silo storage time increased, particularly after 5 hours, and the RAP mixtures experienced greater increases.
- Recovered binders showed a clear change in rheological indices (CAM model) and in the Glover-Rowe parameter. The binders of the virgin and RAP mixtures experienced trends associated with age hardening as silo storage increased, indicating short-term aging occurring within the silo.
- RTFO aging of the virgin tank binder showed that current laboratory conditioning times do not necessarily simulate asphalt plant production. In this study, it was not until 170 minutes of RTFO conditioning that properties similar to the 0 hours extracted virgin binder were obtained.
- Dynamic modulus testing on the mixtures showed that an increase in silo storage time caused an increase in stiffness for both virgin and RAP mixtures, and this difference was statistically significant at a storage time of 7.5 hours. The RAP material clearly experienced a greater increase in stiffness with storage time than the virgin mixture. This may be a result of the decreasing air void content of the RAP mixture or an indication of blending/diffusion within the silo.

- S-VECD fatigue testing was only performed for the virgin mixtures. An increase in silo storage time resulted in an increase in pseudo-stiffness using the damage characteristic curve. Analysis in the G^R-N_f plot showed little distinction between storage times, but identified 7.5 hours as the most susceptible to fatigue cracking.
- Fatigue life evaluation using the LVECD analysis showed that the 7.5 hours virgin mixture was much more susceptible to fatigue cracking than the 0 hours mixture, while the 2.5 and 5 hours mixtures were similar. This fatigue life evaluation showed similar trends among thin and thick pavements and in two different climates.
- TSRST results indicated warmer critical cracking temperatures for the 5 hours virgin mixture and 7.5 hours RAP mixture, but there were no other statistically significant differences

Results from several tests clearly indicate that the mixtures undergo stiffening, likely due to aging, as silo storage time increases. Both virgin and RAP mixtures experienced changes as a result of being stored in the silo, but the RAP mixture may have experienced larger changes. This indicates that there may be a combination of short-term aging within the silo and a blending or diffusion process occurring with the RAP mixture. The larger changes among the RAP mixture may also have been affected by the decreasing air void content.

The primary objective of this study was to gain a better understanding of the relation between production parameters, particularly silo storage time, and mixture performance. This study indicates that silo storage time can have a significant impact on field performance. RTFO aging also showed that current laboratory conditioning methods do not necessarily simulate plant production. Similar to other production parameters, the length of silo storage time is not typically controlled and depends on several factors. There are many situations whereby plants will need to vary production parameters, such as temperature and silo storage times. It is important to recognize that control of these parameters is currently not practical and existing laboratory conditioning methods may not accurately capture what occurs in the field. However, it is also important to understand the impacts of plant production variations on the properties of the asphalt mixture.

Future work is needed to gain a more complete understanding of production variations and silo storage time in particular. Different PG grades and RAP contents, binder absorption, and other material properties should be explored in future testing. The relation to haul time must also be considered as both processes expose the mixtures to elevated temperatures for relatively long durations. Additional work would be beneficial to further explore the effects of production parameters mixture properties.

ACKNOWLEDGEMENTS

The authors would like to acknowledge the participating agencies in TPF 5(230) “Evaluation of Plant-Produced High-Percentage RAP Mixtures in the Northeast”: FHWA, New Hampshire, Maryland, New Jersey, New York, Pennsylvania, Rhode Island, and Virginia for funding this work. Thanks also to Cindy LaFleur at Old Castle Materials for supplying the mixtures and production information.

REFERENCES

1. Sabouri, M., T. Bennert, J.S. Daniel, and Y.R. Kim. Evaluating Laboratory-Produced Asphalt Mixtures with RAP in Terms of Rutting, Fatigue, Predictive Capabilities, and High RAP Content Potential. *Transportation Research Record: Journal of the Transportation Research Board*, Transportation Research Board of the National Academics, Washington, D.C., 2015, in press.
2. Daniel, J.S., N. Gibson, S. Tarbox, A. Copeland, and A. Andriescu. Effect of Long-Term Aging on RAP Mixtures: Laboratory Evaluation of Plant Produced Mixtures. *Journal of the Association of Asphalt Paving Technologists*, Vol. 82, 2013, pp. 327-365.
3. Huang, B., G. Li, D. Vukosavljevic, X. Shu, and B. Egan. Laboratory Investigation of Mixing Hot-Mix Asphalt with Reclaimed Asphalt Pavement. *Transportation Research Record: Journal of the Transportation Research Board*, *No. 1929*, Transportation Research Board of the National Academics, Washington, D.C., 2005, pp. 37-45.
4. Kriz, P., D. Grant, B. Veloza, M. Gale, A. Blahey, J. Brownie, R. Shirts, and S. Maccarrone. Blending and Diffusion of Reclaimed Asphalt Pavement and Virgin Asphalt Binders. *Journal of the Association of Asphalt Paving Technologists*, Vol. 83, 2014, pp. 225-270.
5. Zhao, S., B. Huang, X. Shu, and M. Woods. Quantitative Characterization of Binder Blending: How Much RAP/RAS Binder is Mobilized During Mixing. *Transportation Research Record: Journal of the Transportation Research Board*, Transportation Research Board of the National Academics, Washington, D.C., 2015, in press.
6. Mensching, D., J.S. Daniel, T. Bennert, M. Mederios Jr., M. Elwardany, W. Mogawer, E. Hajj, and M. Alavi. Low Temperature Properties of Plant-Produced RAP Mixtures in the Northeast. *Journal of the Association of Asphalt Paving Technologists*, Vol. 83, 2014, pp. 37-79.
7. Mogawer, M., T. Bennert, J.S. Daniel, R. Bonaquist, A. Austerman, and A. Booshehrian. Performance Characteristics of Plant-Produced High RAP Mixtures. *Journal of the Association of Asphalt Paving Technologists*, Vol. 81, 2012, pp. 403-439.
8. McDaniel, R., A. Shah, G. Huber, and A. Copeland. Effects of Reclaimed Asphalt Pavement Content and Virgin Binder Grade on Properties of Plant Produced Mixtures. *Journal of the Association of Asphalt Paving Technologists*, Vol. 81, 2012, pp. 369-401.
9. Rad, F.Y., N.R. Sefidmazgi, and H. Bahia. Application of Diffusion Mechanism to Study the Degree of Blending Between Fresh and RAP Binder in the DSR. *Transportation Research Record: Journal of the Transportation Research Board*, *No. 2444*, Transportation Research Board of the National Academics, Washington, D.C., 2014, pp. 71-77.
10. Huang, S.C., A. Pauli, R.W. Grimes, and F. Turner. Aging Characteristics of RAP Binder Blends- What Types of RAP Binders Are Suitable for Multiple Recycling? *Journal of the Association of Asphalt Paving Technologists*, Vol. 83, 2014, pp. 297-343.
11. Howard, I., G. Baumgardner, W. Jordan III, A. Menapace, W. Mogawer, and J. Hemsley, Jr. Haul Time Effects on Unmodified, Foamed, and Additive-Modified Binders Used in Hot-Mix Asphalt. *Transportation Research Record: Journal of the Transportation Research Board*, *No. 2347*, Transportation Research Board of the National Academics, Washington, D.C., 2013, pp. 88-95.

12. Anderson, M., G. King, D. Hanson, and P. Blankenship. Evaluation of the Relationship Between Asphalt Binder Properties and Non-Load Related Cracking. *Journal of the Association of Asphalt Paving Technologists*, Vol. 80, 2011, pp. 615-661.
13. Rowe, G.M. Prepared Discussion for the AAPT paper by Anderson et al.: Evaluation of the Relationship between Asphalt Binder Properties and Non-Load Related Cracking. *Journal of the Association of Asphalt Paving Technologists*, Vol. 80, 2011, pp. 649-662.
14. Glover, C., R. Davison, C. Domke, Y. Ruan, P. Juristyarini, D. Knorr, and S. Jung. *Development of a New Method for Assessing Asphalt Binder Durability with Field Evaluation.* Publication FHWA-TX-05-1872-2. National Research Council, Washington, D.C, 2005.
15. Rowe, G.M., G. King, and M. Anderson. The Influence of Binder Rheology on the Cracking of Asphalt Mixes on Airport and Highway Projects. *ASTM Journal of Testing and Evaluation*, 42(5), 2014.
16. Christensen, D. W., and D. A. Anderson. Interpretation of Dynamic Mechanical Test Data for Paving Grade Asphalt Cements. *Journal of the Association of Asphalt Paving Technologists,* Vol. 61, 1992, pp. 67-116.
17. Mogawer, W., T. Bennert, A. Austerman, and C. Ericson. Investigating the Aging Mitigation Capabilities of Rejuvenators in High RAP Mixtures Using Black Space Diagrams, Binder Rheology and Mixture Tests. Accepted for publication in the *Journal of the Association of Asphalt Paving Technologists,* Vol. 85, 2015, in press.
18. Underwood, B.S., and Y.R. Kim. Improved Calculation Method of Damage Parameter in Viscoelastic Continuum Damage Model. *International Journal of Pavement Engineering*, Vol. 11, 2010, pp. 459-476.
19. Eslaminia, M., S. Thirunavukkarasu, M. N. Guddati, and Y. R. Kim. Accelerated Pavement Performance Modeling Using Layered Viscoelastic Analysis. *Proceedings of the 7th International RILEM Conference on Cracking in Pavements*, Delft, Netherlands, 2012, pp. 20-22.
20. Park, H.J., and Y.R. Kim. Investigation into Top-Down Cracking of Asphalt Pavements in North Carolina. *Transportation Research Record: Journal of the Transportation Research Board*, *No. 2368*, Transportation Research Board of the National Academics, Washington, D.C., 2013, pp. 45-55.
21. Norouzi, A., and Y. R. Kim. Mechanistic Evaluation of the Fatigue Cracking in Asphalt Pavements. *International Journal of Pavement Engineering*, 2015, in press.